Identification and functional analysis of new factors that mediate *tramtrack's* function during *Drosophila* tracheal system development

(Identificación y análisis funcional de nuevos factores que median la función de tramtrack durante el desarrollo del sistema traqueal de Drosophila)

Bárbara Rotstein Bajo

"Identification and functional analysis of new factors that mediate *tramtrack's* function during *Drosophila* tracheal system development"

(Identificación y análisis funcional de nuevos factores que median la función de tramtrack durante el desarrollo del sistema traqueal de Drosophila)

Bárbara Rotstein Bajo

PhD Thesis, 2013

Departamento de Genética
Programa de Doctorado de Genética
Facultad de Biología
Universidad de Barcelona

"Identification and functional analysis of new factors that mediate *tramtrack's* function during *Drosophila* tracheal system development"
(Identificación y análisis funcional de nuevos factores que median la función de *tramtrack* durante el desarrollo del sistema traqueal de *Drosophila*)

Memoria presentada por

Bárbara Rotstein Bajo

Para optar al grado de

Doctor por la Universidad de Barcelona

Esta Tesis Doctoral ha sido realizada en el Departamento de Biología del Desarrollo del Instituto de Biología Molecular de Barcelona (IBMB), perteneciente al Consejo Superior de Investigaciones Científicas (CSIC), Parc Científic de Barcelona (PCB), bajo la supervisión de la Dra. Marta Llimargas

El director   El alumno   El tutor

Dra. Marta Llimargas   Bárbara Rotstein Bajo   Dra. Montserrat Corominas

Table of contents

5.1. Crosses performed to generate recombinants flies to be transcriptionally compared

5.1.1. *ttk* recombinant line

5.1.2. UAS *ttk 69* recombinant line

5.2. Embryo collection

5.3. Embryo sorting

5.4. Cell disruption

5.5. Cell isolation study

5.6. RNA extraction

5.7. Microarray hybridization

6. COMPUTATINAL ANALYSIS

7. QUANTITATIVE REAL TIME qPCR

7.1. Stage-specific qPCR

8.Tube length measurements

9. GENERATION OF AN ANTIBODY AGAINST CG13188 IN *DROSOPHILA*

9.1. Plasmid construction

9.2. Preparation of recombinant proteins and antibody generation

RESULTS

Chapter I: Identification of genes that mediate *Tramtrack's* function during *Drosophila* tracheal development

1. GENOME-WIDE ANALYSIS TO IDENTIFY TTK DEPENDENT TRANSCRIPTIONAL REGULATORS

1.1. Generation of the genetic fly lines to be transcriptionally compared

1.2. Validation of the genetic fly lines to be transcriptionally compared

1.3. Sorting of the different populations to be transcriptionally compared

1.3.1. Isolation of specific embryonic population

1.3.2. Isolation of specific cell population

1.4. Isolation of RNA and microarrays hybridisation

2. BIOINFORMATIC ANALYSIS OF MICROARRAY EXPERIMENTS

3. MICROARRAY DATA ANALYSIS

3.1. The in vivo transcriptome confirms in vitro results and is backed by known biology

Introduction

INTRODUCTION

1. TUBULAR ORGANS

Many organs that carry out important physiological functions, such as gas and liquid exchange, are composed of a complex network of tubules. Examples of tube-based organs are the lung, kidney, neural tube and mammary gland in mammals, as well as the trachea and salivary gland in *Drosophila melanogaster* (Gumbiner, 1992; Affolter et al., 2003).
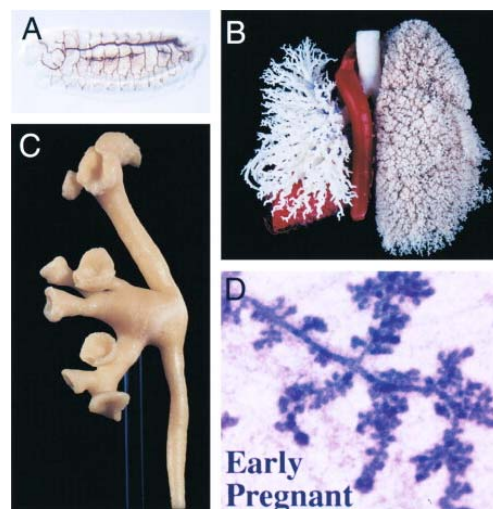
Figure 1. Examples of branched tubular organs. (**A**) *Drosophila melanogaster* tracheal system of a stage 15 embryo, visualised with a luminal antibody, 2A12. (**B**) Adult human lung filled with acryl polyester. In red, the descending aorta is visible; (**C**) Adult human kidney filled with a coloured polyester; (**D**) Mammary gland of a mouse in early pregnancy (Adapted from Affolter et al., 2003).

One of the fundamental aspects of Developmental Biology is to understand how cells organise into tissues and organs during embryonic development. Increasing our understanding about the basic mechanisms of tubulogenesis (morphogenesis of branched tubular structures) will help to better understand the mechanisms of morphogenesis. In addition, it might also have important implications for comprehending some human pathologies, since defects in the formation or size of tubular structures can lead to organ failure, as is evident in devastating human diseases such as polycystic kidney disease and neonatal respiratory distress syndrome (O'Brodovich, 1996; Lubarsky and Krasnow, 2003). Furthermore, the identification of the molecular networks that underlie tubule formation should lead to the development of new methods for diagnosis and treatment of such disorders.

2. MECHANISMS OF TUBULOGENESIS

The branched tubular structure is a good transport system because it maximizes the surface area, within a constrained volume, used for physiological exchanges with surroundings tissues. A uniform shape and distinct tube diameter determines the flow rate of the transported fluids through each organ. Thus, the acquisition of the proper tube dimensions is critical for organ function.

Although the final shape, size and function of different tube-based organs vary between organisms, many of the cellular and molecular mechanisms underlying their development are evolutionarily conserved (Metzger and Krasnow, 1999; Gjorevski and Nelson, 2010).

2.1. Morphogenetic mechanisms

There are several strategies by which different types of tubes develop and can be classified according to whether the participating cells already have apical–basal polarity or whether such polarity is acquired in response to local cues. Thus, tubes are assembled through diverse morphogenetic mechanisms such as wrapping and budding (where the tube arises from a polarized epithelium) or by cavitation, cord hollowing, cell hollowing (where the tube arises from cells that are not epithelial and the cells polarize as the tube forms) (Hogan and Kolodziej, 2002; Lubarsky and Krasnow, 2003; Chung and Andrew, 2008). Interestingly, two novel mechanisms have been described recently as cell wrapping and cell assembly (Medioni et al., 2008; Santiago-Martinez et al., 2008) (Figure 2).

2.1.1. Wrapping: During this process a lumen is formed by folding a flat polarised epithelial sheet. One of the cellular mechanisms known to induce wrapping is apical constriction although others might also be required. This process has been described during neural tube formation in vertebrates (Colas and Schoenwolf, 2001; Haigo et al., 2003; Lubarsky and Krasnow, 2003; Baer et al., 2009) (Figure 2A).

2.1.2. Budding: By this mechanism, a group of cells in an existing polarised epithelial sheet or tube migrates out and forms a new tube as the bud extends. This process has been described during branching morphogenesis of many organs, including the lung and kidney in mammals and the salivary glands and main branches of the tracheal system in *Drosophila* (Metzger and Krasnow, 1999; Hogan and Kolodziej,

2002; Lubarsky and Krasnow, 2003) (Figure 2B).

2.1.3. Cavitation: In this process, a group of cells organized in a cylinder create a central cavity (lumen) by eliminating the cells in the centre by apoptosis and autophagy. This mechanism is observed during mammalian salivary gland morphogenesis (Huang and Strasser, 2000; Melnick and Jaskoll, 2000; Lubarsky and Krasnow, 2003) (Figure 2C).

2.1.4. Cord hollowing: During this process, cells are positioned in a cylindrical cord and an open-space between the cells that faces the future luminal side is formed. Therefore, the tissue requires the establishment of a new apico-basal polarity. Cord hollowing has been observed in zebrafish gut, vasculature and nervous system development (Lubarsky and Krasnow, 2003; Chung and Andrew, 2008) (Figure 2D).

2.1.5. Cell hollowing: By this mechanism, a lumen is formed within the cytoplasm of a single cell, across its length. It has been described during *Caenorhabditis elegans* excretory cell and *Drosophila* tracheal terminal cell development (Buechner, 2002; Lubarsky and Krasnow, 2003; Baer et al., 2009) (Figure 2E).

2.1.6. Cell assembly: During this process, two bilateral rows of cells that are lined up along the midline migrate to each other to come progressively into contact. Subsequently, cell shape remodelling and membrane extension processes are required to join cells on either side of the midline, first at the dorsal-most and then at the ventral-most regions between cells. Resultant junctions allow to enclosed tube by creating an internal lumen between the apical surfaces of the contra-lateral cells. It has been observed during *Drosophila* heart tube development (Medioni et al., 2008; Santiago-Martinez et al., 2008) (Figure 2G).

2.1.7. Cell wrapping: By this mechanism, cells remodel their shapes (by wrapping around the future lumen) and apical junctions, fuse with themselves, becoming donut-shaped single-cell tubes. It has been described in *Caenorhabditis elegans* digestive's tract (Rasmussen et al., 2008) (Figure 2F).
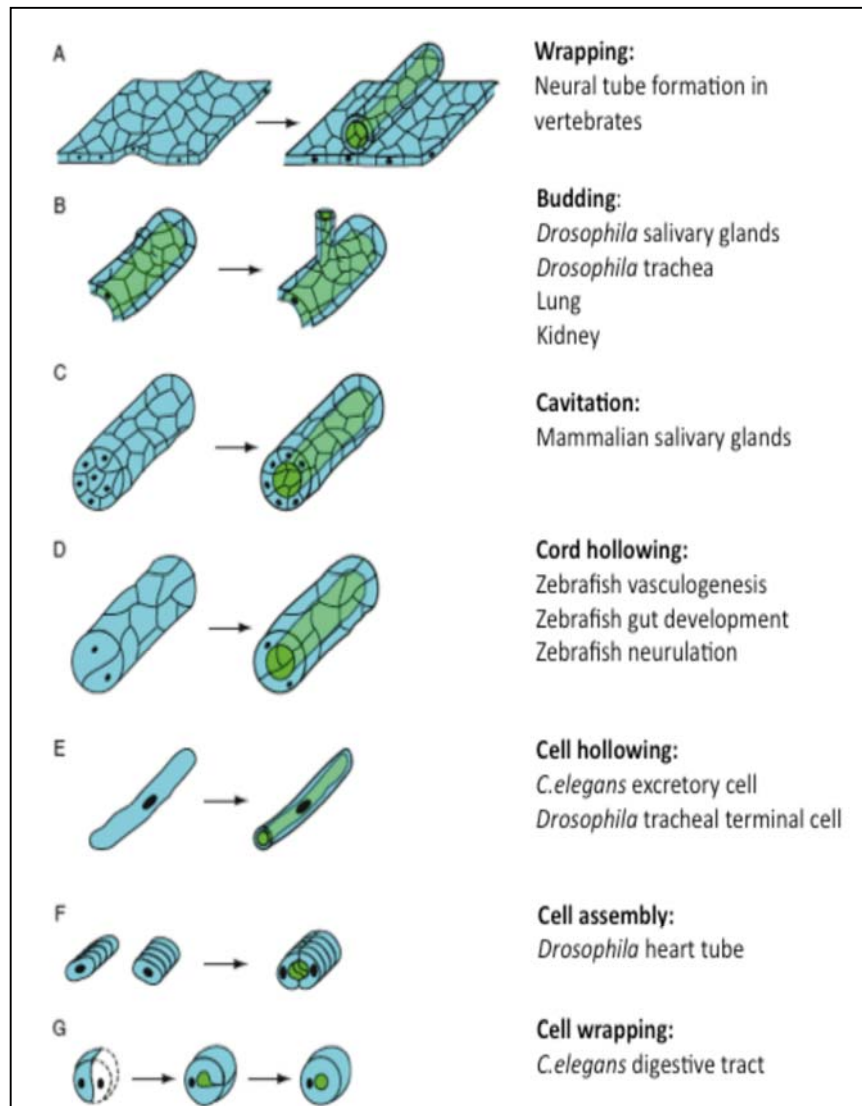
Figure 2. Different morphogenetic mechanisms to generate a tubular structure. Scheme representing the ''starting point'' and the ''final form'' of each listed mechanism: (**A**) Wrapping: an epithelial sheet folds and seals to form a tube. (**B**) Budding: a group of cells from an existing epithelial sheet or tube migrates out or extends to form a new branch. (**C**) Cavitation: a tube is formed by the elimination of cells in the centre of a cylindrical cell mass. (**D**) Cord hollowing: in a solid cord-like structure, the lumen is formed by the generation of open space and remodelling of the apical surface of the cells facing the future lumen. (**E**) Cell hollowing: the lumen forms within a single cell, spanning its length. (**F**) Cell assembly: tube formation results from cell migration and cell shape changes, accompanied by specification of a luminal domain; and (**G**) Cell wrapping: a cell wraps around the future lumen and fuses with itself. Note that the apical (luminal) surface is marked in green (Adapted from Baer et al., 2009).

3. *DROSOPHILA MELANOGASTER* TRACHEAL SYSTEM AS A MODEL TO STUDY TUBULOGENESIS

Although *in vitro* tube formation assays are simplistic (and so not perfect) representations of *in vivo* developmental process, they are starting to be more frequently used to identify basic principles underlying the formation of diverse types of tubular organs. Unfortunately, it is still very challenging to extrapolate the results back to the biology of the whole organism.

Many aspects of tubular morphogenesis can not be addressed suitably by studying mammalian organs because they are structurally complex and moreover, systematic analyses of genetic and cellular programs guiding the development are difficult due to technical problems (Buechner, 2002). In order to identify the mechanisms that regulate tube formation and size control, it is advantageous to use simpler model systems that are genetically accessible, such as the respiratory organ of the fruit fly *Drosophila melanogaster*.

Several features of the *Drosophila* tracheal system make it an excellent model to study the mechanisms of tubulogenesis and tube size control. First, *Drosophila* tracheal system consists of a network of structurally simple tubes. In contrast to most vertebrates, it is an epithelial monolayer (lacking the complexity introduced by the multilayer structure of most vertebrate tubes including blood vessels and the bronchial tubes of the lungs), whose development does not involve cell proliferation but it mainly relies on cell migration and changes in cell shape and cellular junctions (Beitel and Krasnow, 2000; Samakovlis et al., 1996a). Interestingly, although it was thought that the tracheal system does not employ apoptotic processes to remove damaged or undesired cells, it has been recently shown that cell death contributes to determine the final number of cells in specific types of tracheal branches, in which extensive cell rearrangements are needed for its formation (Baer et al., 2010).

Second, *Drosophila melanogaster* is a very convenient model system as it adds many advantages. It is a small insect that has a short generation time (it takes approximately 10 days at 25°C). *Drosophila melanogaster* life cycle (Figure 3) includes three distinct developmental phases (egg, larva and pupa) before reaching the adult stage.
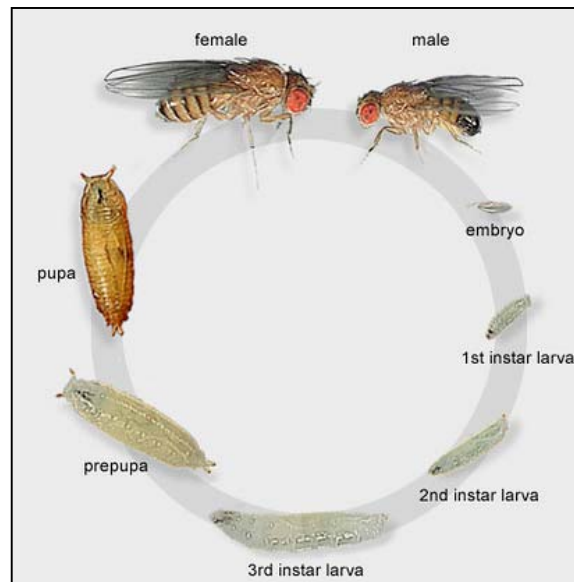
Figure 3. ***Drosophila melanogaster* life cycle.** It takes around 10 days at 25ºC and it consists in different developmental stages, embryo, larva, pupa and adult (Adapted from FlyMove. Weigmann et al., 2003).

Embryonic development lasts about 22–24 hours, after which a larva hatches from the egg. After hatching, larvae undergo three successive larval stages (L1, L2 and, L3, which last for about 24 hr, 24 hr, and 48 hr, respectively). At the end of this period, an L3 larva begins pupariation. Over the next four days, metamorphosis takes place. Pupae and adult tissues generated by imaginal cells (tissue-specific progenitors that remain quiescent during embryonic and larval life) replace larval tissues. Interestingly, organs that are functional throughout life, such as the trachea, the epidermis and muscles, undergo extensive remodelling. In contrast, organs that are exclusively functional in the adult, such as the wings and legs, are generated *de novo* during pupariation. After this process a fly ecloses from its pupal case. This newly emerged fly becomes fertile after about 4 hours, being capable of entering again in a new life cycle.

In addition to its small size and short developmental cycle, *Drosophila* has been so successful as a model organism because it offers powerful genetics, molecular and cellular tools for research. *Drosophila* has been used as a model organism for more than 100 years. So, accumulated information, together with integrated on-line genetic and genomic resources, as well as stock centres provide valuable experimental tools, facilitating handling to study flies in the laboratory (Golic and Golic, 1996; St Johnston, 2002; Ryder et al., 2007).

Thus, *Drosophila* tracheal system is well suited for revealing the cellular, molecular and genetic mechanisms underlying epithelial tube morphogenesis.

14

3.1. General features

The tracheal system is the respiratory system in *Drosophila*. The final pattern and size of tracheal tubes are critical for their physiological activity, and therefore these features are strictly controlled.

The *Drosophila* embryonic, larval, pupa and adult tracheal system follows the same general structure, which consists on a stereotyped and ramified tubular network, that expands to the whole organism (Figure 4).
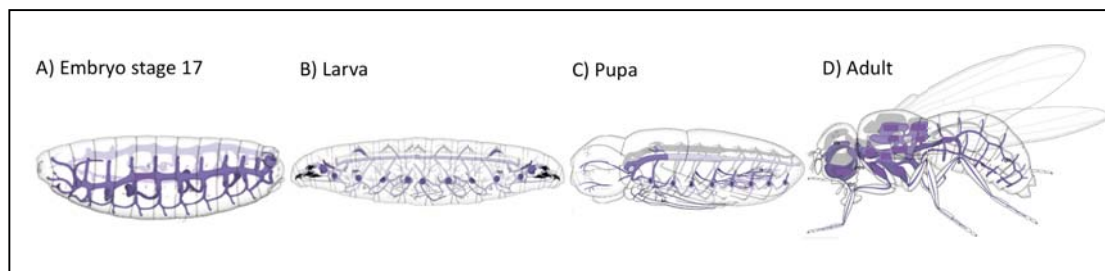
Figure 4. Structure of *Drosophila melanogaster* tracheal system at different stages. A scheme showing the branched tubular tracheal network, which ramifies extensively through the body, at embryonic stage 17 **(A)**, larva **(B)**, pupa **(C)** and adult **(D).** Note that tracheal system is coloured in purple (Adapted from Hartestein, 1993).

The adult airway is remodelled during metamorphosis by different populations of imaginal tracheoblasts located at various positions along the larval body. Moreover, the head and thoracic tracheal system undergo dramatic remodelling that results in dilated structures called air sacs, which supply oxygen to the brain and to the flight muscles, respectively. The larval tracheal system is structurally similar in all three instars, being the main difference, the increasing number of smaller tracheal branches or tracheoles in the successive stages. The embryonic tracheal system follows a stereotyped pattern of branching, which becomes functional by the end of embryogenesis (Manning and Krasnow, 1993; Cabernard and Affolter, 2005; Guha and Kornberg, 2005; Weaver and Krasnow, 2008).

3.2. Tracheal system function

The tracheal system is a tubular network of ectoderm-derived epithelial tubes that supplies oxygen to the internal tissues (Ghabrial et al., 2003). In *Drosophila* and other small insects, gas exchange occurs by simple diffusion, exchanging oxygen and carbon dioxide between their tissues and the air. Oxygen enters from the outside through specialized openings called spiracles. Then, oxygen is transported into the different tracheal branches until it finally reaches specialised capillary-like tubules with blind ends that facilitate gas exchange with the surrounding target tissues.

Drosophila avoids the dehydration risk by covering the tracheal tubes with a luminal or apical cuticle lining (that also provides a barrier against infection) and by controlling the size of the spiracle openings to match the need of oxygen (Lehmann, 2001; Uv et al., 2003).

Interestingly, besides its primary gas transport function, the tracheal system may also provide an endoskeleton-like structural support and guidance for neuronal pathfinding (Chapman, 1982; Giniger et al., 1993; Manning and Krasnow, 1993; Younossi-Hartenstein and Hartenstein, 1993).

3.3. *Drosophila* tracheal epithelium

Drosophila tracheal tubes consist of an epithelial monolayer composed of approximately 1600 cells. The specialized functions of epithelial tissues depend, in part, on the apico-basal polarity of their cells. The tracheal epithelium, like other epithelia, is connected by junctional complexes, which contain transmembrane proteins that interact with cytoplasmic components to mediate anchoring to the cytoskeleton, intracellular signal transduction and intercellular cell adhesion.

In some tubular organs such as the tracheal system, the apical domain faces the lumen, where an apical extracellular matrix assembles (aECM); the lateral domain contacts neighbouring cells within the epithelial layer, and the basal domain is in contact with the basal ECM (bECM). The lateral membrane of epithelial cells in *Drosophila* is subdivided into three domains, which are, from apical to basal: Sub-Apical Region (SAR), Adherens Junction (AJ) and Septate Junction (SJ) (Tepass et al., 2001; Knust, 2002) (Figure 5).
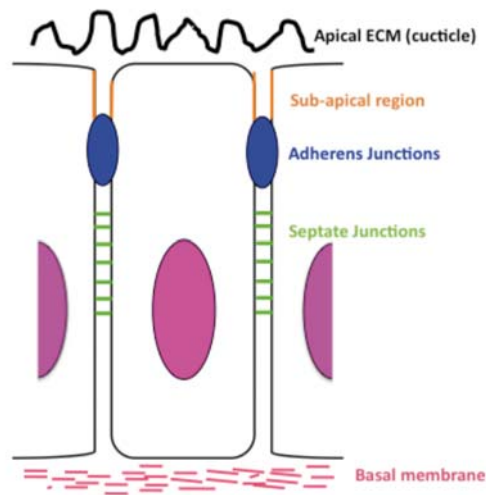
Figure 5. *Drosophila* **tracheal epithelial cells.** A scheme representing the typical structure of an epithelial cell: Sub-apical region (orange), Adherens junctions (blue) and Septate junctions (green). Note that the cell is apically in contact with the aECM and basally with the bECM (Adapted from Tepass et al., 2001).

a) Apical extracellular matrix: Tracheal tubes need to be rigid enough to ensure continuous air transport, but also, flexible enough along their axis to prevent breaks of the tubular system when body segments move relative to each other. This capacity is mainly ensured by the tracheal cuticle, which is an ECM secreted by the tracheal epithelium that covers the whole apical surface of tracheal tubes (Manning and Krasnow, 1993).

The cuticle has a stratified structure with different chemical composition and properties (Locke, 2001; Moussian et al., 2005) (Figure 6).
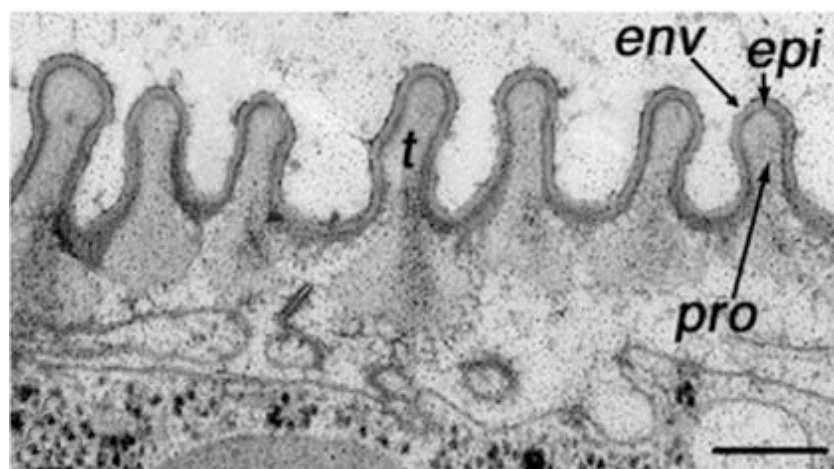
Figure 6. Stratified structure of the cuticle. Transmission electron microscopy reveals three layers of cuticle in wild-type embryos: the envelope layer (env), the proteinaceous epicuticle (epi) and the chitin-rich procuticle (pro). Anterior is to the left and dorsal is up in all pictures. Scale bar 1μm (Adapted from Araújo et al., 2005).

17

The envelope is the outermost protective layer. It is composed of lipids that provide hydrophobicity. Basal to the envelope there is the epicuticle, a chitin-free and protein-rich layer responsible for the cuticle stiffness. The most internal and thicker layer is the procuticle. It is assembled at the cell surface and directly in contact with the tracheal apical epithelium. Chitin fibres with parallel orientation and cuticular proteins, which confer stability and elasticity to the cuticle, compose the procuticle.

Tracheal cuticle forms prominent ridges called taenidial folds that are projected inside the lumen, reinforcing the tube and preventing it from collapsing. The pattern of taenidial folds is defined by the actin cytoskeleton, which organises a network of actin that runs in parallel bundles that are perpendicular to the tube axis. The size of the taenidial folds is proportional to the diameter of the tubes (Matusek et al., 2005; Tonning et al., 2005; Luschinig et al., 2006; Wang et al., 2006) (Figure 7).
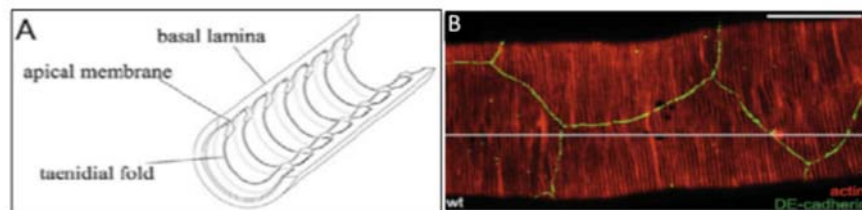
Figure 7. Tracheal cuticle presents taenidial folds. (**A**) Schematic drawing of a wild-type airway showing that the tracheal cuticle is laid down on the inner apical surface of tracheal cells. (**B**) In tracheal tubes, actin runs in parallel bundles (red) that are perpendicular to the tube axis, and located at the level of the AJ (green). Scale bar 50 μm (Adapted from Matusek et al., 2005; Moussian et al., 2005).

Besides this apical ECM, a second type of apical ECM is assembled transiently inside the luminal space of the growing tracheal tubes from stage 14 until stage 17. This transient matrix consists of chitin fibres that, running along the length of the tubes, form a chitin filament whose assembly and modifications guarantee the acquisition of the proper tube size (Tonning et al., 2005; Luschnig et al., 2006). At the end of embryogenesis, these fibres and all the luminal content is eliminated by endocytosis, allowing the trachea to fill with air (Tsarouhas et al., 2007).

b) Sub-apical region: It is required to establish and maintain the apico-basal polarity in epithelial cells. It contains several polarity regulators that form two complexes: Crumbs (Crb) and Par complex (Tepass et al., 2001; Knust and Bossinger, 2002). During *Drosophila* tracheal system morphogenesis Crb is required for different tracheal events, such as apical constriction, ordered invagination (Laprise et al., 2010; Letizia et al., 2010).

c) Adherens junctions: Adherens junctions (AJs) are located apically just under the sub-apical region. The key component of the AJ is E-cadherin (E-cad), a transmembrane molecule that mediates homophilic adhesion between neighbouring cells in a Ca^{2+}-dependent manner. AJs play a role in cell adhesion, intracellular signalling and the attachment of the actin cytoskeleton to the plasma membrane (Tepass et al., 2001). During *Drosophila* tracheal development E-cad levels are dynamically regulated by trafficking, and such regulation, among others, modulates intercalation, a fundamental mechanism that underlie the elongation of epithelial cells (See section 4.2.3) (Shaye et al., 2008).

d) Septate junctions: Sepate junctions (SJ) lie basal to the AJ. SJs are composed of protein complexes, including Neurexin IV, Sodium potassium ATPase, Coracle, Claudins and other components (Tepass et al., 2001). SJs have been shown to play key roles in tracheal epithelial morphogenesis such as the maintenance of the transepithelial diffusion barrier, tissue integrity and tube size control (Wu and Beitel, 2004; Swanson and Beitel, 2006; Laprise et al., 2010).

e) Basal membrane: The basal membrane, a highly specialized region at the basal side of polarized epithelial cells, is composed of the secreted glycoproteins Laminin, Collagen IV and the heparan sulfate proteoglycan Perlecan (Tepass et al., 2001). It provides mechanical continuity between emerging tissues and it has been implicated in many processes such as cell differentiation, shape, adhesion and migration (Martin et al., 1999; Urbano et al., 2009). In particular, during tracheal morphogenesis it has been shown to be required for dorsal trunk and visceral branch migration (Boube et al., 2001).

3.4. Tracheal metameric structure

Drosophila tracheal system has a highly stereotyped metameric structure immediately evidenced at embryonic stages. Ten tracheal metameres (named Tr1-Tr10) begin their development as ten independent groups of tracheal cells on each side of the embryo, which undergo different cellular processes to form an interconnected structure at the end of embryogenesis.

The typical metameric pattern, which is shown in figure 8, persists during larval stages, until being the tracheal system extensively modified at metamorphosis to form the pupal and adult organ (Manning and Krasnow, 1993).
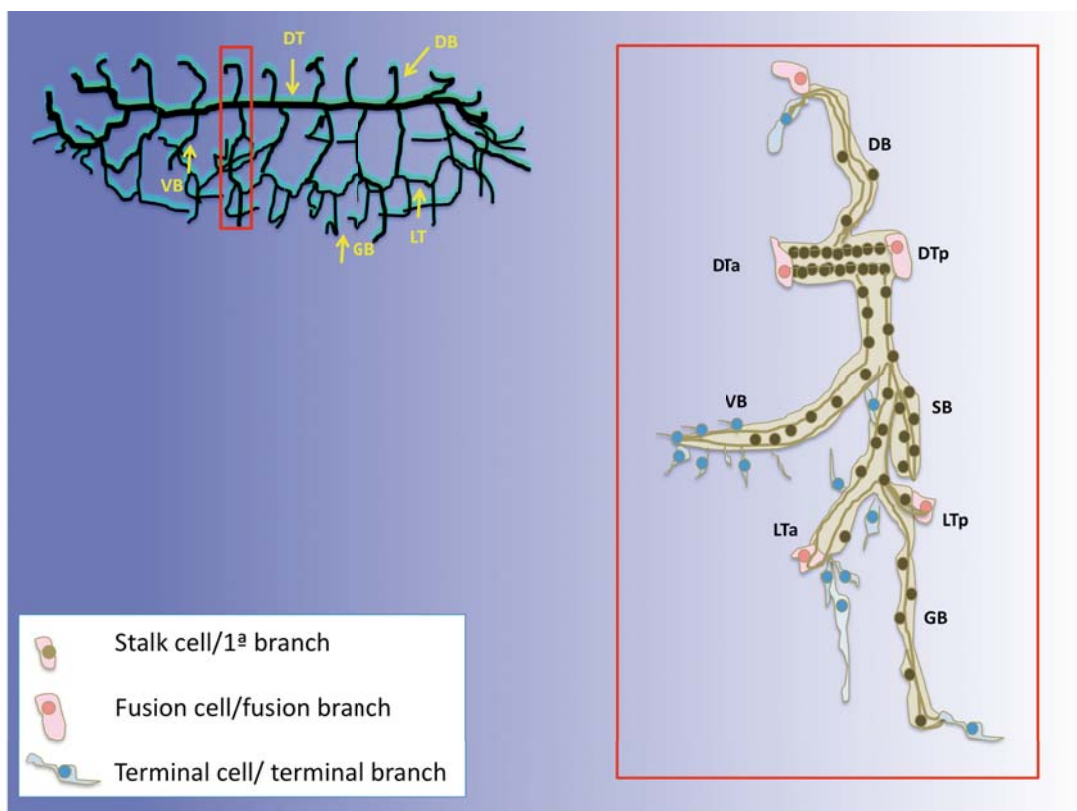
Figure 8. Structure of a typical tracheal metamere. A) Lateral view of the embryonic tracheal system of *Drosophila*. The tracheal branches are visualized by antibody staining against a luminal antigen and one typical metamere is highlighted in yellow. (**B**) A schematic representation of a single tracheal metamere. The main branches are indicated: the dorsal trunk (DT); dorsal branch (DB); transverse connective (TC); visceral branch (VB); lateral trunk anterior (LTa); posterior lateral trunk/ganglionic branch (LTp/GB); spiracular branch (SB) (Adapted from Uv et al., 2003).

The thicker branch in the system is the dorsal trunk (DT). The transverse connective (TC) is the branch that grows perpendicular to DT and contacts with the lateral trunk (LT) branch, which is divided in lateral trunk anterior (LTa) and lateral trunk posterior (LTp).

From the DT, dorsal branches (DB) grow dorsally and connect to the DB on the opposite side of the embryo through a process of dorsal anastomosis. From the TC, visceral branches (VB) extend inward and towards the gut. The spiracular branches (SB) extend toward the epidermis to connect with the lateral spiracles. The ganglionic branches (GB) grow ventrally from the TC and target the central nervous system (CNS). The cerebral branch (CB) and pharyngeal branch (PB) grow antero-dorsally, in the most anterior segment.

3.5. *Drosophila* tracheal tubes

All branches at the end of embryogenesis are composed of fixed number of cells and have particular growth rates and tubular dimensions. According to their features, tracheal branches can be classified under three different types of tubes: (Figure 9).
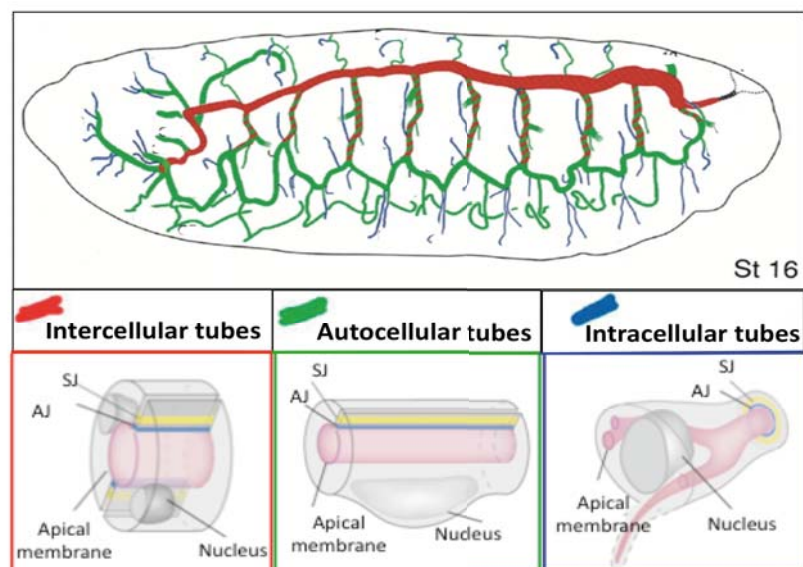
Figure 9. Types of tracheal tubes: "**Intercellular tubes**": Multicellular tubes built by wedge-shaped cells in which two to five cells compose the lumen circumference; "**Autocellular tubes**:" Multicellular tubes built by cells lying in a row that form intercellular junctions with proximal and distal cells within the branch. Single cells with autocellular junctions encircle de lumen; "**Intracellular tubes:**" They are composed of tubular protrusions from single cells without autocellular junctions. They are found in terminal branches (Adapted from Uv et al., 2003 and Ribeiro et al., 2004).

a) <u>Intercellular tubes:</u> Multicellular tubes constituted for several flattened, wedge-shaped cells connected by intercellular junctions that surround a lumen. This type of tube is found in the DT branch, and parts of the TC.

b) <u>Autocellular tubes:</u> These are narrower multicellular tubes formed by interconnected cells lying in a row. A single tube-shaped cell that is folded over itself and sealed by autocellular junctions makes the luminal circumference. This type of tube is found in DB, LT, VB and GB.

c) <u>Intracellular tubes:</u> These tubes are formed by single cells that form an intracellular lumen that is not sealed by junctional complexes. This type of tube is found in the terminal branches, intracellular seamless capillaries specialized to mediate gas exchange with target tissues (Samakovlis et al., 1996; Uv et al., 2003; Kerman et al., 2006; Baer et al., 2009).

Interestingly, the fusion anastomoses tubes, which interconnect tubes from adjacent metameres to ensure a continuous network, are heterogeneous in their composition. The main part of the fusion branch is an extracellular tube and the minor part of the branch is a seamless intracellular tube (Gervais et al., 2012).

3.6. Tracheal cell types

The tracheal cells can be grouped into three genetically and morphologically distinct cell types (Figure 8): Stalk cells (brown cells in the figure) constitute the main branches, fusion cells (pink cells in the figure) connect the metameres to each other to generate a continuous network and terminal cells (blue cells in the figure) mediate gas exchange with target tissues (Uv et al., 2003).

4. MORPHOGENESIS OF *DROSOPHILA* EMBRYONIC TRACHEAL SYSTEM

4.1. General features

  Drosophila embryonic tracheal morphogenesis relies on a number of different cellular processes that includes changes in cell shape, cell migration, intercalation, branch fusion and tubule maturation. Remarkably, the entire tracheal branching process takes place in the absence of cell divisions (Samakovlis et al., 1996).

4.2. *Drosophila* embryonic tracheal system morphogenesis

  Tracheal development begins around 6 hours AEL (after egg laying) from mid-embryogenesis (stage10) and lasts until 17 hours AEL (stage 17) (all embryonic stages and times are according to Campos-Ortega and Hartenstein, 1985). Tracheal development can be divided into different consecutive steps (Figure 10), each of which uses distinct genetic, cellular and molecular mechanisms. However, it has been shown that these different steps are genetically coupled, so that the genes that control a specific morphological event also control the genes required for the next step (Samakovlis et al., 1996; Ghabrial et al., 2003).
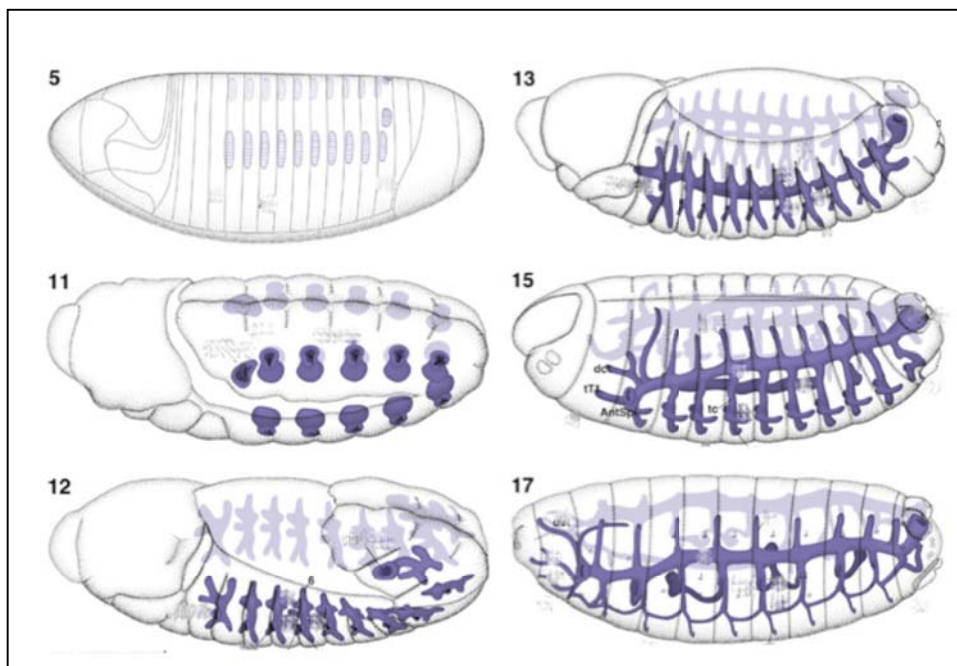
Figure 10. Developmental stages during embryonic tracheal system development in *Drosophila melanogaster.* Lateral view of *Drosophila's* embryonic tracheal development. During stage 11, ten tracheal placodes on either side of the embryo can be detected. During stage 12, the tracheal cells start to migrate into diverse directions and form finger-like structures called primary branches. By stage 15, the dorsal trunk anterior and dorsal trunk posteriors of adjacent metameres have fused to form a continuous dorsal trunk. Finally, at stage 17, the terminal branches have sprouted from the interconnected tracheal branches and spread through target tissues. Tracheal system is marked in purple (Hartestein, 1993).

4.2.1. Tracheal induction: At stage10, 20 groups of ectodermal cells, ten on each side of the embryo from the second thoracic segment (T2) to the eighth abdominal segment (A8), adopt a specific morphology and differentiate from their neighbours. These groups of cells form the tracheal placodes.

The early-expressed tracheal transcription factors *trachealess* (*trh*) and *ventral veinless (vvl),* are essential for tracheal cell fate specification as they activate a number of downstream genes, although it is known that other factors are also required for tracheal induction (de Celis et al., 1995; Isaac and Andrew, 1996; Kuhnlein and Schuh, 1996; Wilk et al., 1996; Llimargas and Casanova, 1997; Boube et al., 2000; Brown et al., 2001; Chen et al., 2002; Chung et al., 2011).

4.2.2. Invagination: At stage 11, a group of tracheal cells positioned in the dorso-central part of the tracheal placode, constrict their apical surface (Figure 11A) and start invaginating into the underlying tissues in an ordered manner (Figure 11B). Next, the cells of the dorsal side of the placode rotate completely around their axis and internalise, while ventral cells gradually slide beneath. As a result, a finger-like structure is formed (Figure 11C). After invagination, the tracheal cells remain connected to the epidermis through the cells of the spiracular branch.
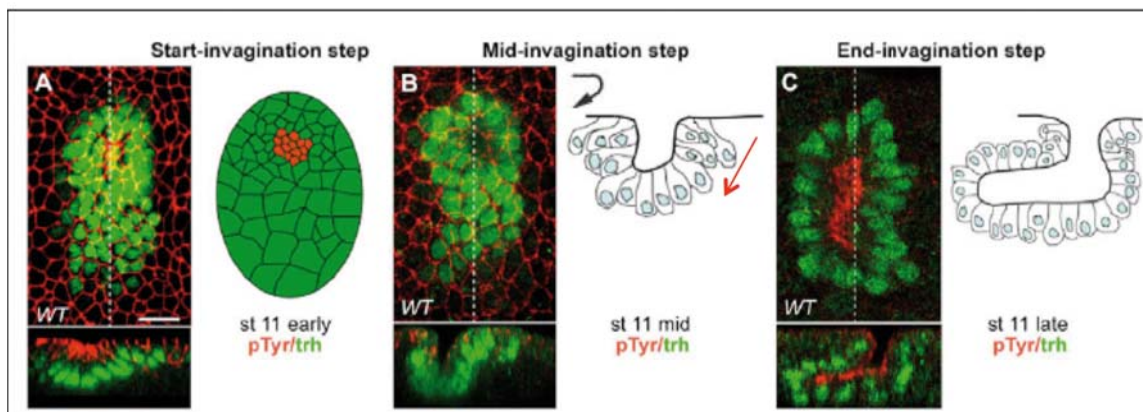
Figure 11. Sequences of cell shape changes during tracheal invagination. Confocal sections showing a single tracheal embryonic metamere stained to visualise the tracheal cells (marked with *phosphotyrosine (pTyr)*, to visualise the apical surface and the nuclear tracheal marker (*trh*)). For each placode scanned in the *X–Y* axis, reconstruction of a *Z*-section (indicated by the dotted line) is shown below. To the side, a schematic representation of cell shape changes during invagination. (**A**) At the onset of invagination at early stage 11, a small group of cells has reduced its apical perimeter, and the epithelium begins to bend. (**B**) As invagination proceeds during mid stage 11, cells of the dorsal side of the placode internalise, rotating dorsally around their axis (black arrow), while ventral cells slide beneath (red arrow), leading to the formation of a finger-like structure (**C**) (Adapted from Letizia et al., 2010).

Both *trh* and *vvl* regulate Epithelial Growth Factor (EGF) pathway, whose activation is crucial for correct tracheal invagination, as it directs the formation of an apical acto-myosin complex that facilitates localised apical cell constriction. Moreover, it has been shown that the apical determinant protein Crumbs (Crb) is required for proper invagination, apical cell constriction and acto-myosin complex organisation, acting in parallel of the EGF pathway (Llimargas and Casanova, 1999; Brodu and Casanova, 2006; Nishimura et al., 2007; Letizia et al., 2010).

4.2.3. Primary branching: Six primary branches (termed dorsal trunk anterior (DTa), dorsal trunk posterior (DTp), dorsal branch, visceral branch, lateral trunk anterior (LTa) and lateral trunk posterior/ganglionic branch) bud from the tracheal sac after invagination. The elongation of these branches relies on directed cell migration and cell rearrangements (such as changes in cell contacts and shapes). There are three signalling pathways that determine the direction of migration and the particular features of each branch:

a) Breathless (Btl), the Fibroblast Growth Factor Receptor (FGFr), is expressed in all tracheal cells from stage 11 of development. Its ligand, Branchless (Bnl), is expressed in groups of ectodermal and mesodermal cells located near the tracheal cells. Bnl encodes a chemoattractant that guides primary branch outgrowth (Figure 12).
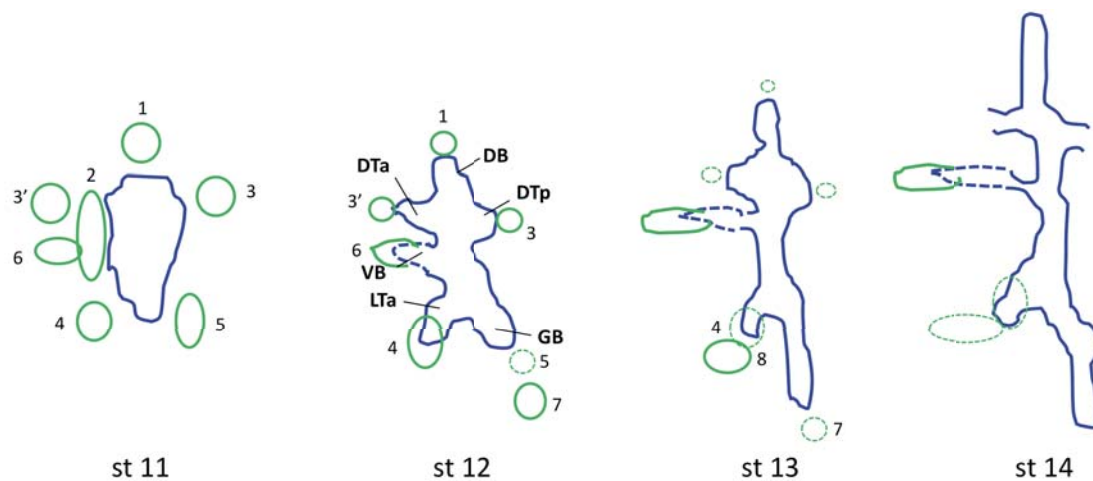
Figure 12. Summary of *bnl* expression in a typical hemisegment. Solid blue, outline regions of *bnl* RNA expression; dotted blue shows regions of weaker or variable expression. Green, outlines the developing tracheal system (Adapted from Sutherland et al., 1996).

At stage 11, just before tracheal branching begins, *bnl* expression appears in five small clusters of epidermal cells surrounding the tracheal sac, at the positions where the five primary tracheal branches will bud. Another cluster (sixth) of mesodermal cells also starts to express *bnl* at around the same time, near the position where the sixth primary branch will form. As the primary branches grow (stages 12 and 13), *bnl* expression in the clusters decreases in a specific spatial pattern: the *bnl*-expressing cells closest to or contacting the growing tracheal branches lose expression first, continuing to migrate toward the remaining *bnl*-expressing cells. Then, two more clusters of cells (seventh and eighth) begin to express *bnl* whereas its expression in the other clusters turns off, predicting thereby, the subsequent outgrowth of specific branches.

bnl also has a second patterning function. It activates later programs of tracheal gene expression, which lead to second and terminal branch formation. Thus, FGF-signalling pathway controls tracheal branching formation, whereas the expression of its ligand, *bnl,* encodes branch-patterning information. Thereby, mutants for *bnl* or *btl*, only form rudimentary primary branches (Figure 13A and 13C, in comparison to 13B and 13D) (Sutherland et al., 1996).
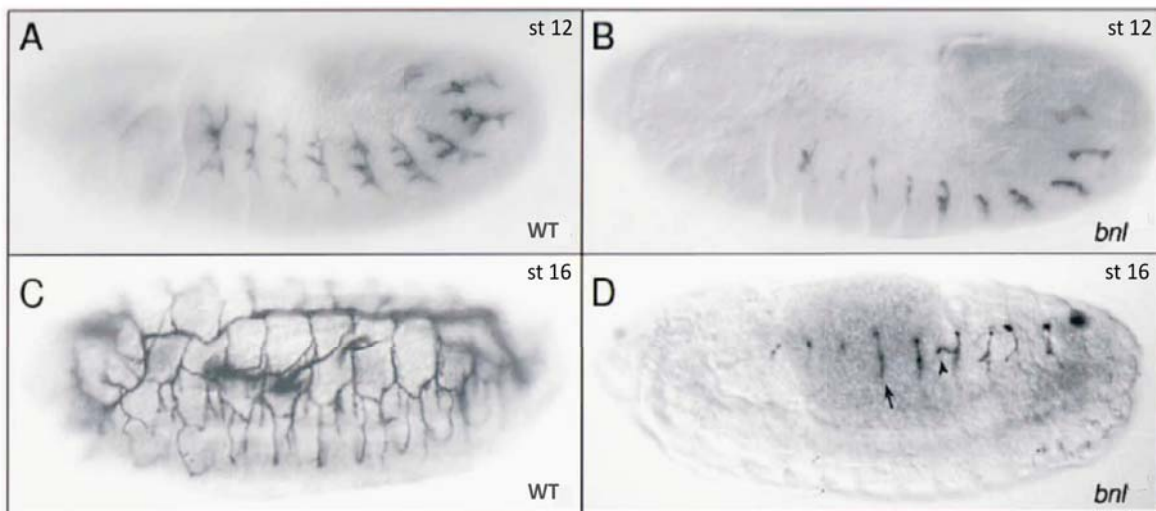
Figure 13. Tracheal phenotype of *bnl* mutants. Lateral view of wild-type (A and C) and *bnl* mutant (B and D) embryos at different developmental stages stained with a tracheal luminal marker. **(A)** Wild-type stage 12 embryo where primary branches have begun to grow out. **(B)** In *bnl* mutants, primary branches do not grow out. **(C)** Wild-type stage 16 embryo showing the tracheal lumen along the tracheal tree. **(D)** In *bnl* mutants, the tracheal metameres remain as unbranched elongate sacs (arrow) except for an occasional rudimentary branch (arrowhead) (Adapted from Sutherland et al., 1996).

b) Decapentaplegic (Dpp), the *Drosophila* homolog of the vertebrate Bone Morphogenetic Proteins (BMPs), which are members of the Transforming Growth Factor beta (TGF-β) family, is secreted from ectodermal stripes dorsal and ventral to the tracheal placode. In *Drosophila*, Dpp signals through the type II receptor, Punt, and the type I receptors, Thickveins (Tkv) and Saxophone (Sax). This pathway, during tracheal morphogenesis, allows the migration of tracheal cells in the dorso-ventral axis, and is therefore required for the formation of the dorsal and ventral branches (Vincent et al., 1997; Chen et al., 1998). Thereby, mutants in Dpp pathway lead to a disrupted formation of the branches that migrate along the dorso-ventral axis such as the DB, LT and GB. Moreover, the presumptive lost cells become integrated into the DT (Figure 14B). On the other hand, when the Dpp pathway or its targets, *kni* and *knrl*, are ectopically expressed, DT and VB fail to migrate in the antero-posterior direction and instead, migrate in the dorso-ventral direction. Moreover, the prospective DT and VB cells are recruited into the DB (Figure 14D).
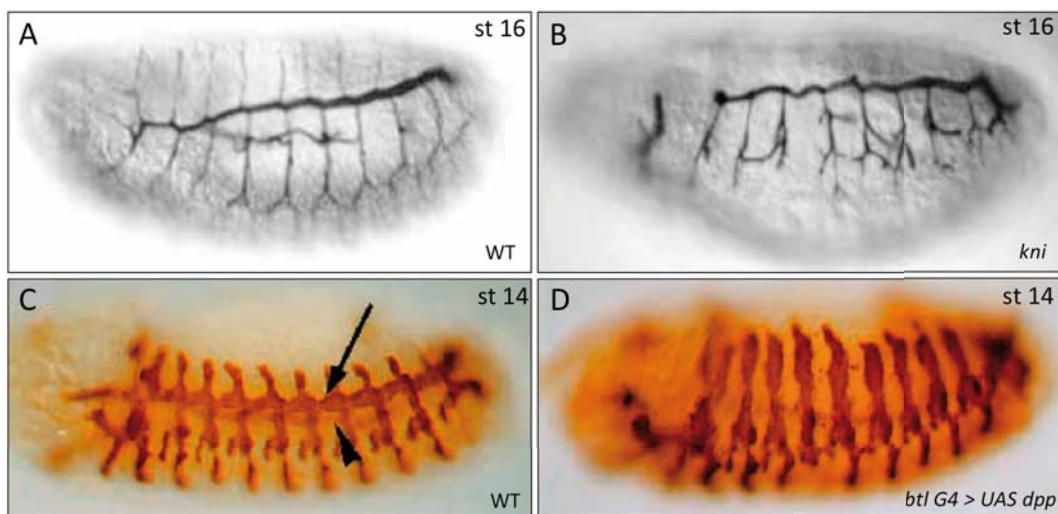
Figure 14. Dpp signalling pathway mutants show tracheal embryonic defects. (A-B) Lateral view of stage 16 wild-type (**A**) and *kni* mutant (**B**) embryos, stained with a luminal marker. (**B**) *kni* mutant embryos show disrupted formation of DB, LT and GB, as compared to wild-type (**A**). **(C-D)** Lateral view of stage 14 wild-type (**C**) and btlG4>UAS *dpp* (D) embryos stained with a luminal marker. (**D**) Ectopic activation of *dpp* in the tracheal cells, inhibit the development of all anteriorly growing branches (DT, arrowhead; VB, arrow), as compared to wild-type. Notice that in (**D**) the prospective DT and VB cells are recruited into the DB (Adapted from Vincent et al., 1997; Chen et al., 1998).

c) The activation of the Wingless (Wg) pathway is required for the migration of the DT along the antero-posterior axis, for the specification of the fusion cells, as well as for the guidance of the GB (Llimargas, 2000). Wg pathway regulates DT formation by controlling the expression of *spalt* (*sal*) and *spalt related* (*salr*), two partially redundant zinc-finger transcription factors, in the DB and the DT cells (Chihara and Hayashi, 2000; Llimargas, 2000; Llimargas and Lawrence, 2001). Thus, mutants for the Wg/Wnt pathway present a discontinuous DT branch and although some fragments of DT are often fused (black arrows in Figure 15B), they also display defects on branch fusion (white asterisk in Figure 15B).
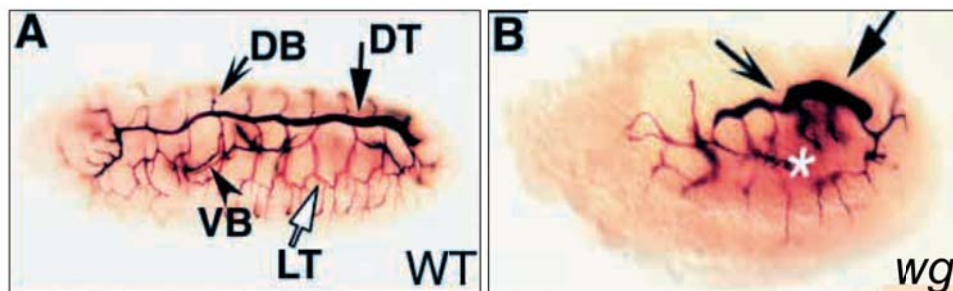
Figure 15. Wg pathway requirement during tracheal development. (A-B) Lateral view of late stage embryos stained with a luminal marker. (**A**) Wild-type embryo with the different tracheal branches (DB, DT, VB and LT) indicated by distinct arrows and arrowheads. (**B**) In null *wg* mutant, DT is disrupted and branch fusions are impaired (white asterix in B) (Adapted from Llimargas, 2000).

Interestingly, the morphogenesis of the transverse connective branch does not require either the Dpp or the Wg/Wnt pathway. Therefore, this structure has been considered as a basal state for the tracheal tree as many primitive insects have a rudimentary tracheal system that lacks longitudinal trunks connecting adjacent segments and connections with the opposite segmental side (Franch-Marro and Casanova, 2002).

4.2.3.1. Branch elongation

During primary branching tracheal tubes must extend considerably maintaining their cell number. There are two critical mechanisms to achieve branch extension: cell intercalation and directed cell migration.

Cell intercalation represents a particular type of polarised cell rearrangement that encompasses tube elongation. During the process, most tracheal branches (DB, GB and VB) undergo a transformation to substitute intercellular AJ into autocellular AJ. In contrast, the DT does not undergo this type of rearrangement. Affolter and colleagues analysed the process at cell resolution level, proposing a model that is divided in four key morphological steps (Ribeiro et al., 2004) (Figure 16).
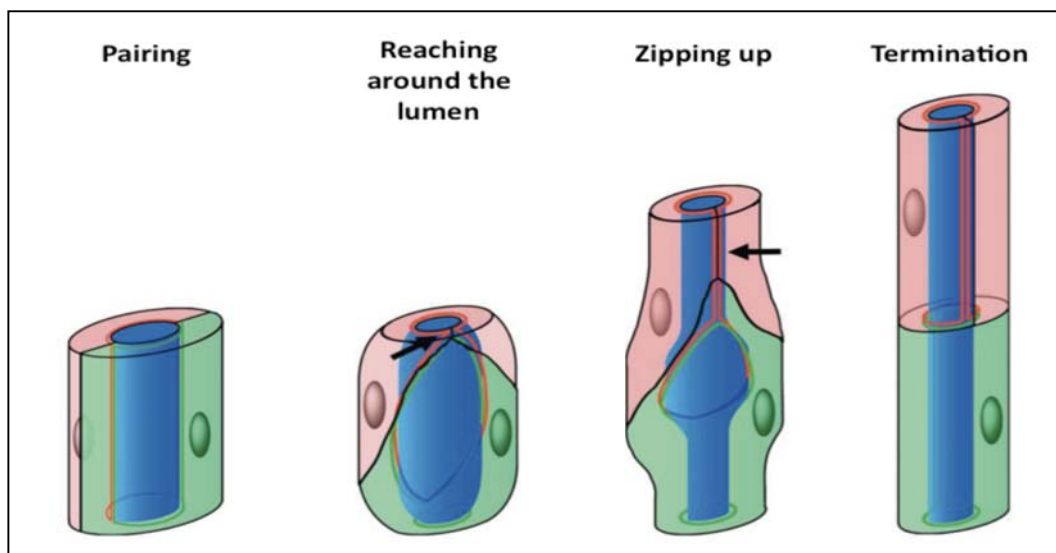
Figure 16. Schematic representation of the intercalation process. Neighbouring cells are side-by-side arranged. Then, one cell (marked in red) reaches around the lumen (blue) by displacing the other cell (green), leading to the first contact between the AJs of a single cell at the proximal or distal end. The third step is called "zipping up", and consists in the conversion of intercellular AJ into autocellular AJ, leading two cells connected by small AJ rings (Adapted from Ribeiro et al., 2004).

They described the following steps:

1.- Pairing: Initially, neighbouring cells are aligned side-by-side

2.-Reaching around the lumen: The side-by-side alignment becomes destabilized, possibly by the pulling force generated by the dorsal movement of the leading cells toward Bnl/FGF, forcing the cells to intercalate, shifting their relative position and forming the first autocellular AJ.

3.- Zipping up: Intercalation is accompanied by individual cells (marked in red in the figure) reaching around the entire lumen (blue) by displacing the other cell (green). During this step, as the cells move dorsally and elongate, intercellular AJs of adjacent cells are successively replaced by autocellular AJs.

4.- Termination: The elongated cells adopt an end-to-end arrangement. Small rings of E-cad marker around the luminal space represent the intercellular AJs that connect individual tube cells.

Dpp and Wg/Wnt signalling pathways control cell intercalation. Wg signalling is required for the expression of Sal in the DT, which inhibits intercalation in this branch. Dpp signalling in the dorsal-most cells, as mentioned above, is required for *kni* and *knrl* activity, which suppresses *sal* transcription, allowing intercalation in the dorsal and ventral branches of the tracheal system. Moreover, it has been demonstrated that differences in adhesion molecules' trafficking in different tracheal branches, such as E-cad, are crucial to promote or inhibit intercalation. So, it has been shown that enhanced Rab11 accumulation, which correlates with *sal* activity, is required to inhibit intercalation in the DT, whereas low levels of Rab11-mediated trafficking are needed to promote intercalation in the DB (Shaye et al., 2008) (Figure 17).
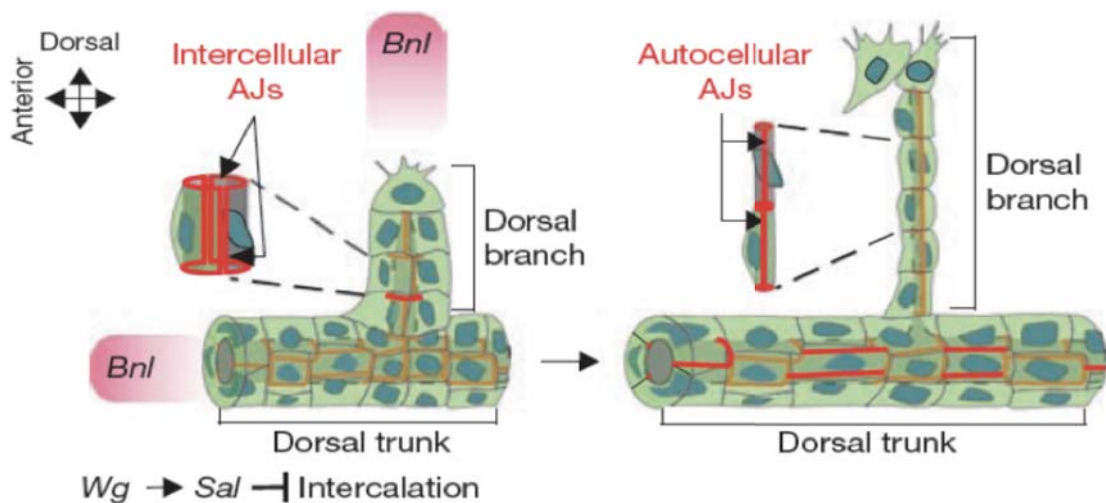
Figure 17. Diagram showing the regulation of the tracheal intercalation process. Bnl/FGF-induced pulling forces lead to the outgrowth of an initial bud. Intercalation process is controlled by Dpp and Wg signalling pathways. It is inhibited in the DT by *sal*; the expression of which requires Wg signalling. *kni* expression is induced by Dpp signalling in the dorsal-most cells and suppresses *sal* transcription, thereby allowing intercalation and the formation of autocellular AJs (Adapted from Shaye et al., 2008).

4.2.4. Secondary branching: At stage 13 of development, secondary branches arise at the tip of all primary branches (except for the DT). Secondary branches are characterized by their unicellular nature and follow, similar to primary branching, a stereotypical pattern that is regulated by FGF activity (Scholz et al., 1993; Hacohen et al., 1998). However, different sets of genes are activated. Cells generating secondary branches express markers called Pantip, such as Pointed (Pnt) (Samakovlis et al.; 1996a). When *bnl* is ectopically expressed, *pnt* and other secondary genes are induced, resulting in ectopic secondary branches (Sutherland et al., 1996). Interestingly, FGF signalling activates a Pantip marker called Sprouty (Spry), which inhibits secondary branching in neighbouring cells. When Spry function is absent, the secondary branch genes are not inhibited, and ectopic secondary branches are formed (Hacohen et al., 1998).

4.2.5. Terminal branching: From stage 16, most secondary branches generate hundreds of fine terminal branches that permeate the whole embryo (Figure 18). Terminal branches are seamless intracellular capillaries constituted of a single tracheal cell, in stereotyped embryonic positions although their growth depends on the oxygen needs of the tissue at larval stages (Jarecki et al., 1999). Embryonic terminal branch formation is controlled by *dsrf* (*Drosophila* homolog of *serum response factor*) expression, which is triggered by *bnl* signalling (Affolter et al., 1994; Guillemin et al., 1996; Sutherland et al., 1996). It has been shown recently that *bnl* triggers terminal branching initiation by a *dsrf*-independent mechanism, being the *dsrf* transcription induced by *bnl* signalling, required to maintain terminal branch elongation (Gervais and Casanova, 2011).
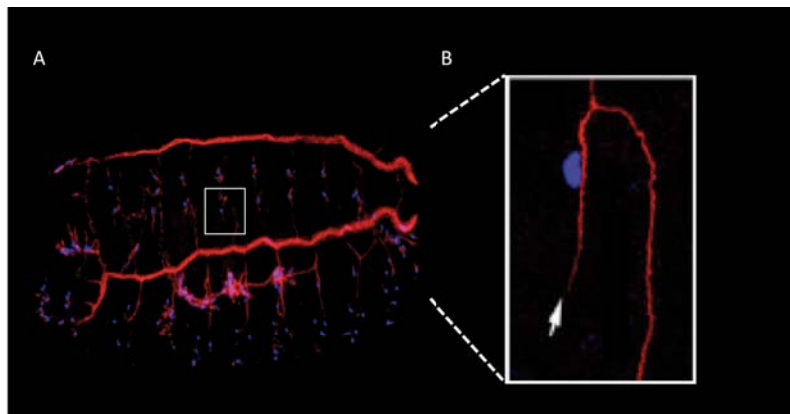
Figure 18. Tracheal terminal branches. (**A**) Tracheal system at late embryogenesis. (**B**) Higher magnification of the marked region in A. Dorsal branch showing DSRF-positive cells (blue) and terminal branches (arrow) detected using the luminal marker chitin-binding probe (CBP, in red).

4.2.6. Branch fusion: While most tracheal branches during embryogenesis continue forming new branches, five branches in each metamere cease branching and grow towards to fuse adjacent branches to interconnect the tracheal network. A specialized cell at the tip of each fusion branch changes its morphology, polarity and adhesion features and mediates each fusion event. There are two main types of fusion events: the one that links up adjacent tracheal metameres (called dorsal and lateral trunk fusion), and the one that connects the two sides of the tracheal system (called dorsal and ventral anastomosis).

4.2.6.1. Cellular dynamics of a tracheal fusion event

Samakovlis' and Hayashi's labs described in detail the cellular dynamics of an embryonic tracheal fusion event in *Drosophila,* which requires target recognition, actin cytoskeleton remodelling and intracellular tube formation (Samakovlis et al., 1996b; Tanaka-Matakatsu et al., 1996; Tanaka et al., 2004). In summary, at embryonic stage 14 the fusion process starts by each fusion cell emitting filopodia toward each other at the place and in the direction in which fusion cells will meet (arrowhead in Figure 19A). At this time, there is a deposition of E-cad at the contact point between the two fusion partners (Tanaka-Matakatsu et al., 1996; Lee et al., 2003). During this process, an actin track that associates with E-cad dependent contacts, play crucial roles in the change of fusion cell shape and in lumen formation (Lee and Kolodziej, 2002; Lee et al., 2003;
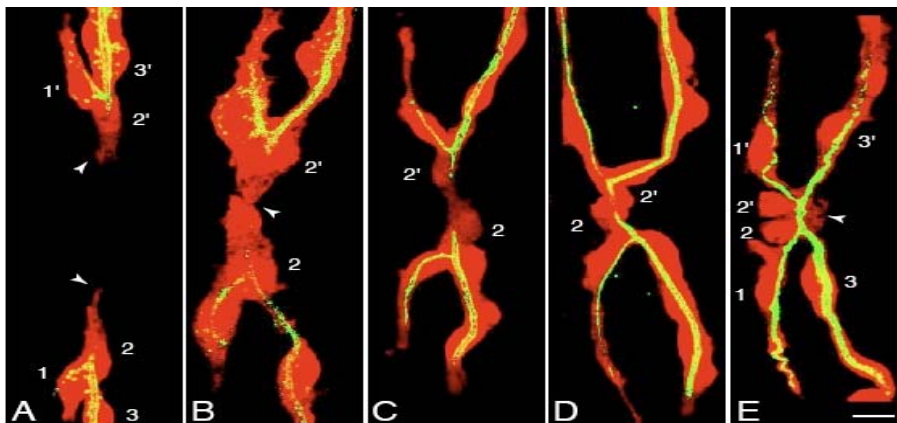
Figure 19. Cell dynamics of dorsal branch fusion cells forming a dorsal anastomosis. Dorsal view of tracheal cells that are marked in red and the lumen in green. The cell bodies of the DB1, 2 and 3 cells in the two dorsal branches are labelled (1, 2, 3 and 1', 2', 3'). Each fusion cell (2 and 2') extends a filopodia towards its partner (arrowheads in **A**). After the contact (arrowhead in **B**), their cell bodies move toward each other (**C, D**) and a lumen extends through each cell and connects to the lumen of its partner (**E**). The lumen expands slightly at the fusion point and the expansion persists afterwards (arrowhead in **E**). Scale bar, 5 μm (Adapted from Samakovlis et al, 1996b).

Tanaka et al., 2004). Then, the cell bodies begin to elongate until the two fusion cells meet (Figure 19B). While the cells adopt a doughnut shaped configuration, the lumen extends in parallel to the movement of the fusion cells (Figure 19C and 19D) to establish the connection between the branches (Figure 19E) (Samakovlis, et al., 1996b; Gervais et al., 2012).

4.2.6.2. Signalling pathways that restrict fusion cell fate

As branch development proceeds, several signalling pathways act to restrict fusion cell fate. It has been shown that localized expression of *bnl* and *wg* in tracheal surrounding tissues provides combinatorial cues that induce the expression of the fusion marker *escargot* (*esg)* in individual cells at the tips of primary branches. In addition, Dpp signalling pathway triggers *delta* (*dl*) expression in the potential fusion cell, which in turn, activates *Notch* (N) but represses *esg* in neighbouring cells. This regulatory mechanism, called lateral inhibition, ensures that only a single cell containing the highest initial level of *esg* and *dl* becomes the fusion cell at the end of each primary branch (Samakovlis et al., 1996b; Tanaka-Matakatsu et al., 1996; Ikeya and Hayashi, 1999; Llimargas, 1999; Steneberg et al., 1999; Chihara and Hayashi, 2000; Kerman et al., 2006). Moreover, *esg* also induces the expression of other fusion genes such as *shotgun* (*shg*), *members only* (*mbo), headcase* (hdc) and *dysfusion* (*dys*) (Tanaka-Matakatsu et al., 1996; Steneberg et al., 1998; Jiang and Crews, 2003). Recently, it has been shown that fusion cell number is regulated by Equinoid protein, which acts as a positive regulator of Notch activity (Laplante et al., 2010).

4.2.7. Tubule maturation: Although early stages of *Drosophila* tracheal system development has been well characterised, less is understood about the tubule maturation process that takes place at late embryogenesis. Samakovlis and colleagues proposed a model for tubule maturation describing different events such as, tube size determination, protein secretion, protein clearance and the transition from liquid-to-air-filled tubes (Tsarouhas et al., 2007).

Due to the complexity and relevance of the process, by which tubes acquire their optimal dimensions during development and become physiologically functional, these aspects will be introduced in more detail in the next section.

5. TRACHEAL TUBULE MATURATION

In parallel to the correct establishment of the tracheal pattern, tracheal tubes undergo a process of tube maturation to become physiologically functional. The work of Samakovlis' lab has start to elucidate the genetic programs that underlie tube maturation. They described a model for tracheal tube maturation that consists in various sequential and interdependent steps. In summary, the process involves a secretion burst followed by tube expansion, the clearance of a solid luminal material and the replacement of luminal liquid by gas (Tsarouhas et al., 2007).

5.1. Apical secretion and tube size expansion

Each tracheal branch must acquire specific tubular dimensions to accommodate specific transport demands. Thus, tube length and diameter growth control are indispensable for correct organ function. Remarkably, diameter and length are independently regulated processes (Beitel and Krasnow, 2000). Lumen diameter expansion occurs within a defined time interval from embryonic stage 13 until stage 16, whereas tube elongation is a continuous process during tracheal development (Beitel and Krasnow, 2000). It has been shown that the control of tube dimensions depend on the apical secretion of chitin and other luminal proteins, the assembly of a transient chitin extracellular matrix inside the lumen of all growing tracheal tubes, cell shape changes, and the growth of apical membrane (Hemphala et al., 2003; Tonning et al., 2005).

At embryonic stage 13, a burst of apical secretion of chitin and other proteins is initiated. It continues as a massive secretory pulse through stage 14, to deliver material into the lumen of the developing tracheal branches. Chitin is the principal component of this secreted apical extracellular matrix.

Chitin is a linear polymer composed of N-acetylglucosamines (GlcNAc), whose biosynthesis is divided in three main steps. First, polymerization in the cytoplasm requires chitin synthase enzymes, such as *mummy (mmy)* and *krotzkopf verkehrt* (*kkv*) and UDP-N-acetylglucosamines as a substrate (Araújo et al., 2005; Devine et al., 2005; Moussian et al., 2006). Then, the nascent polymer is transported across the membrane to the extracellular space. Once there, chitin-organizing factors inserted in the apical plasma membrane, such as Knickkopf (Knk) and Retroactive (Rtv), assemble the singles polymers into microfibrils of different diameters and lengths (Devine et al.,

2005; Moussian et al., 2006). This chitin luminal matrix first promotes and coordinates radial tube expansion, and then, its modification by the secreted chitin deacetylases *Serpentine (Serp)* and *Vermiform (Verm)*, restrict the length of the tube by modifying the assembled luminal matrix (Luschnig et al., 2006; Wang et al., 2006). Accordingly, mutants in genes involved in chitin biogenesis or assembly (such as *cystic, mmy*, *kkv*, *knk*, *rtv*) results in tracheal tubes of irregular diameter and lengths (Araújo et al., 2005; Devine et al., 2005; Moussian et al., 2006; Tonning et al., 2006). On the other hand, mutants for chitin binding proteins, such as the chitin deacetylases Verm and Serp, show only expanded tubes in comparison to WT (Figure 20) (Luschnig et al., 2006).
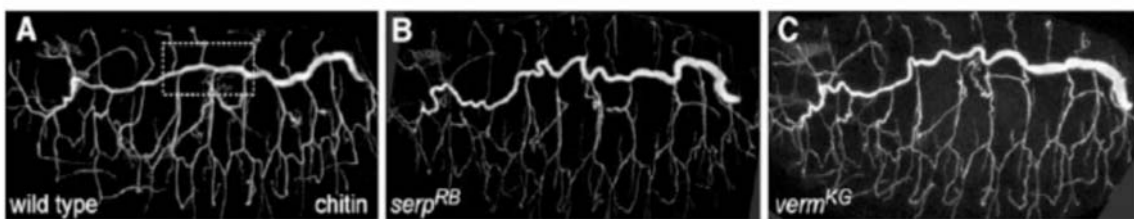
Figure 20. Effects of *serp* and *verm* mutations on tracheal tube structure. (A–C) Stage-16 embryos of the indicated homozygous genotypes immunostained with a fluorescent chitin binding probe (CBP) to show the tracheal lumen. Note that tracheal tubes in *serp* (**B**) and *verm* (**C**) mutants are elongated and convoluted compared to wt (**A**) (Adapted from Luschnig et al., 2006).

Chitin and luminal proteins need to be efficiently transported into the lumen. The general secretory pathway is required for such transport. Secretion begins with the synthesis of proteins in the ribosomes in the cytosol. Then, the proteins are delivered to specific locations depending on the sorting signal contained in their amino acid sequence (Bradshaw, 1989). Proteins are commonly direct to the endoplasmic reticulum (ER), where they are translocated into ER's lumen. In the lumen, proteins are glycosylated and folded. Misfolded proteins are identified and retrotranslocated to the cytosol to be degraded. Vesicles containing properly folded proteins enter the Golgi apparatus. In the Golgi, glycosylation and further posttranslational modifications occur. The coating protein complex–II (COP-II) mediates the transport from ER to the Golgi complex, while COP-I is involved in intra-Golgi transport, as well as in transport from Golgi to the ER (Jayaram et al., 2008). COP-II components are the small Ras-like GTPase Sar1, the Sec23/Sec24 subcomplex and the Sec13/Sec31 subcomplex. Once the proteins reach the trans-Golgi, they are sorted into different types of vesicles, each containing a different set of cargos, and trafficked by a distinct mechanism to their final

destination in the membrane. Mutants in genes involved in vesicular transport between cellular compartments (For instance the COPII components: *sar1*, *sec13*, *sec23* and *sec24*) have been shown to cause tube dilation and tracheal apical extracellular matrix secretion defects (Tsarouhas et al., 2007; Forster et al., 2010) (Figure 21).
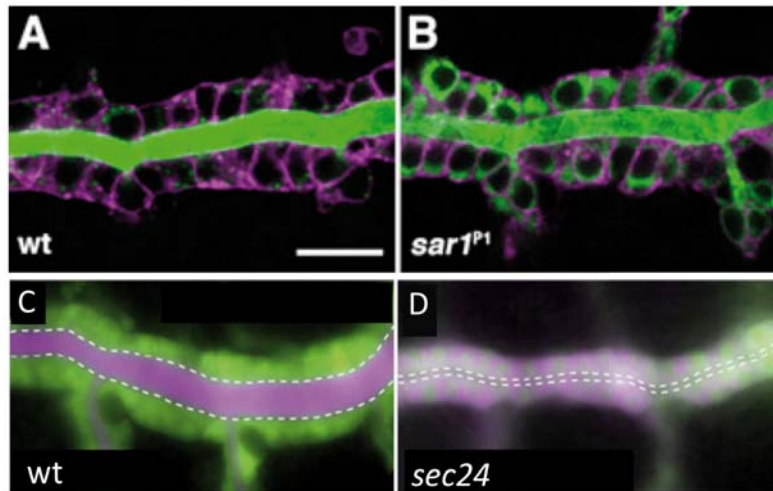
Figure 21. Efficient vesicular transport is required for tracheal maturation. (**A-B**) Late stage embryos express btl > GFP-CAAX (magenta) and were stained for the luminal Gasp protein (green); *sar^{1P1}* mutant embryos show strong intracellular retention of luminal markers (**B**) in comparison to wt (**A**). (**C-D**) Late stage embryos express GFP (green) and Vermiform-RFP (Verm-RFP) (magenta) in tracheal cells under the control of *btl* Gal4. *sec24* mutant show defects in secretion, tracheal tube expansion and tracheal cell morphology (**D**), Verm-RFP is secreted into the tracheal lumen in wild-type embryos (**C**) but accumulates in tracheal cells in *sec24* mutants (**D**). The dorsal trunk (DT) lumen (dashed lines) is dilated in stage 16 wt embryos (C) but remains narrow in *sec24* mutants (D) (Adapted from Tsarouhas et al., 2007; Forster et al., 2010).

Besides the chitin-based apical extracellular matrix, other factors have been shown to play a role in tube size control. On one hand, apical membrane biogenesis regulates tube growth as inferred from the defects observed in mutants for apical proteins (Laprise et al., 2010). In this respect, it has been shown that mutants for the transcription factor *grainy head* (*grh*) produce excessive apical membrane, resulting in elongated and convoluted tubes (Hempala et al., 2003). On the other hand, a role of an actin/myosin-dependent apical membrane trafficking pathway has been proposed. In this case, the protein Diaphanous (Dia) and its regulators Rho1 and Rho-GEFs, promote the formation of polarized actin cables that allow efficient trafficking of secretory vesicles toward the apical membrane. When *rho1, rho-GEFs or dia* are mutated, secretion of luminal markers, such as 2A12, is blocked, resulting in convoluted and longer tubes (Massarwa et al., 2009). Furthermore, of particular interest is the role of SJ components in tube size control. Mutants in SJ components or SJ-associated proteins

(α/β subunits of the Na+/K+ ATPase, *coracle, crumbs, disc large (dlg), gliotactin, lachesin, neurexin IV, neuroglian, scribble (scrib), varicose (vari)* and *yurt*) develop convoluted and longer tracheal tubes in comparison with wild-type, demonstrating a role in tube size independent of its function in the establishment of the diffusion barrier (Beitel and Krasnow, 2000; Hemphala et al., 2003; Paul et al., 2003; Llimargas et al., 2004; Wu and Beitel, 2004; Paul et al., 2007; Bachmann et al., 2008; Laprise et al., 2010). The extra-long tube phenotypes caused by the mutation of some of these genes are shown in figure 22.
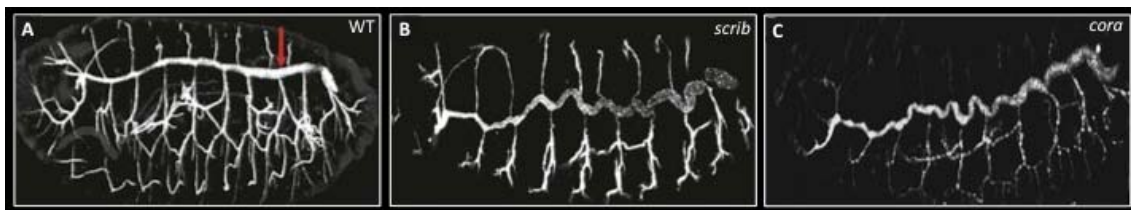
Figure 22. Effects of epithelia polarity proteins in tracheal tube size. (**A–C**) Stage16 embryos of the indicated homozygous genotypes immunostained with the tracheal luminal antigen 2A12 to show the tracheal tree. Note that tracheal tubes in *scribble* (**B**), *coracle* mutants are elongated and convoluted compared to wild-type (**A**) (Adapted from Laprise et al., 2010).

In addition, mutants for the claudins *megatrachea*, *sinuous* (*sinu*) and *kune-kune (kune)*, which are required for SJ organization and promote luminal secretion of Serp and Verm, showed longer and convoluted tubes in comparison to wild type (Behr et al., 2003; Wu et al., 2004; Nelson et al., 2010). Finally, it has recently been shown that the tyrosine kinase Src42A-dependent recycling of E-Cad at AJ is required specifically for the elongation of intercellular tracheal tubes (DT) by orienting the expansion of the cell surface (Forster and Luschnig, 2012).

Moreover, it is proposed that the lumen is initially filled with liquid during embryonic stages, which helps to keep the lumen opened (Manning and Krasnow, 1993).

5.2. Protein clearance and tracheal filling

Little is known about how morphological and physiological maturation events are coordinated (Behr et al., 2007). It has been demonstrated that the tracheal tubes, in order to become physiologically functional, need to clear the lumen by degrading the chitin filament and the liquid contained. How these processes occur is not well understood.

Interestingly, in other tubular organs such as the mammalian lung, immature tubes are also filled with liquid before becoming functional. Defects in this process are evident in the human neonatal respiratory distress syndrome, where premature infants retain liquid in their lungs (which after birth, are still structurally immature) impairing blood oxygenation. This data suggests that liquid secretion and removal are essential and evolutionary conserved steps in airway maturation (O'Brodovich, 1996; Lubarsky and Krasnow, 2003; Wu and Beitel, 2004).

5.2.1. Protein clearance

At the end of embryogenesis, by stage 17, luminal proteins (such as Gasp and Verm) and the chitinous cable are cleared, leaving the lumen filled with liquid. It has been described that a massive wave of endocytosis is activated in the tracheal epithelium to perform this role (Tsarouhas et al., 2007).

Endocytosis mediated by Clathrin requires the transmembrane protein Wurst. *wurst* encodes a protein containing six putative transmembrane domains, a type 1 Clathrin binding motif and a carboxy-terminal cytoplasmic J-domain, which bind to the heat shock protein (Hsc70) family as co-chaperones and stimulate their ATPase activity. It has been proposed that Wurst recruits Hsc70-4 and Clathrin to the apical membrane and coordinates the early steps of Clathrin-mediated endocytosis (Wingen et al.; 2009). Shibire (Shi) and Rab5 act at later stages in the pathway (Figure 23).
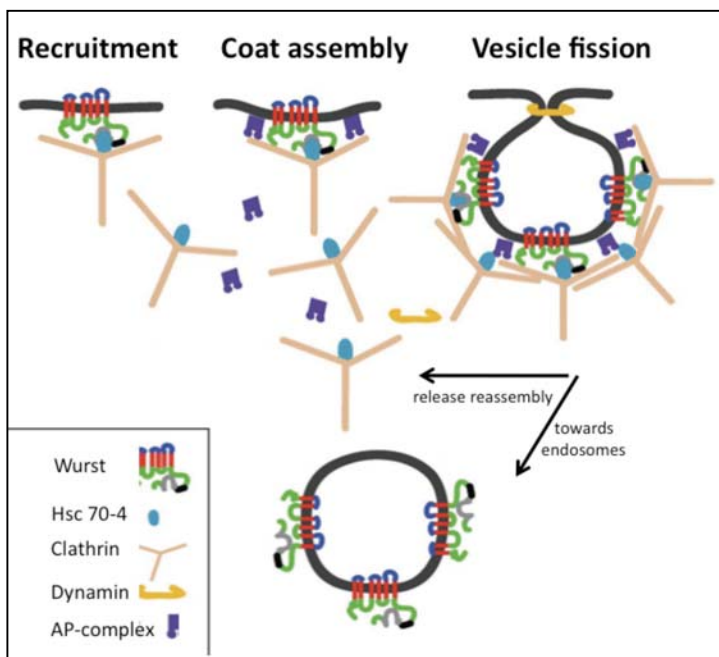
Figure 23. Wurst is involved in endocytosis. Wurst interacts via its C-terminal Clathrin binding motif type 1 and the J-domain with Clathrin and Hsc70-4, respectively, and recruits both to the membrane at early steps of endocytosis. After endocytosis, Wurst remains inside the vesicle. In contrast, Clathrin and Hsc70-4 are released and recycled. Abbreviations: AP, Adaptor protein complex (Adapted from Wingen et al., 2009).

wurst mutation results in a tube elongation phenotype, due to defective ECM organization in the tracheal tubes, as well as the absence of luminal protein clearance that impairs gas filling (Behr et al., 2007; Wingen et al., 2010). In addition, mutants for *clathrin*, *rab5* and *dynamin* also retain chitin and proteins inside the tracheal tubes, as the endocytosis is impaired (Figure 24) (Tsarouhas et al., 2007).
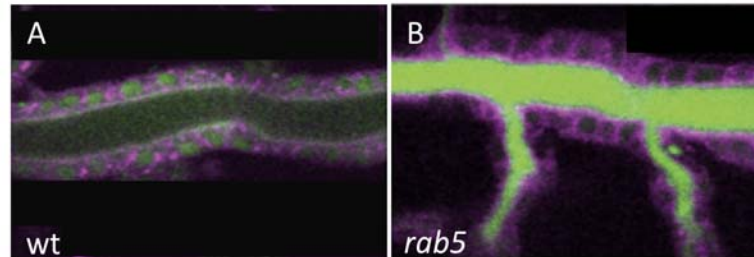
Figure 24. Mutant embryos for *rab5* are defective in luminal protein clearance. The membrane of DT tracheal cells were marked by btl > myr-mRFP (magenta). (**A**) Wild-type embryos clear ANF-GFP (green) from the lumen while *rab5* embryos retain it (**B**). Abbreviations: myr, Myristoylation (Adapted from Tsarouhas et al., 2007).

5.2.2. Tracheal filling

Tracheal filling, which occurs after protein clearance, has been divided in two phases: liquid removal from the lumen (liquid absorption) and its replacement with gas (gas filling) (Buck and Keister, 1955).

5.2.2.1. Liquid absorption

It is still unclear how liquid is cleared from the lumen. Before the clearance, and in order to prevent the tubes from collapsing, a rigid cuticle is laid down (Manning and Krasnow, 1993).

The most accepted mechanism of liquid removal is the "absorption theory". It points out that liquid is actively transported for its elimination. This active transport is achieved by variations in the osmotic gradient between the trachea and hemocoel, which might require epithelial ion channels (Liu et al., 2003; Foster and Wood, 2012). Different genes, encoding a variety of protein transport families, have been described to affect liquid absorption. For instance, *pickpocket* (*ppk*) protein family genes encoding epithelial Na+ channels (ENaCs) (Liu et al., 2003) or *congested like tracheae* (*colt*) encoding for a carnitine acylcarnitine translocase, required for long chain fatty acids

(acyl-CoAs) transport across the mitochondrial membrane, display liquid clearance defects (Hartestein et al., 1997) (Figure 25).
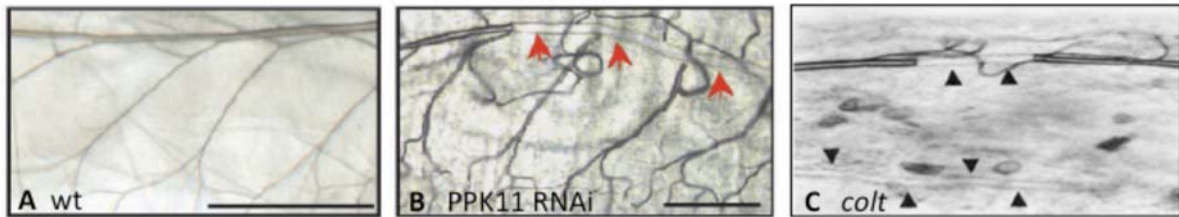
Figure 25. Gas filling defects. Defective gas filling of tracheal system in *PPK11* (**B**) and *colt* (**C**) mutant embryos. Note the refringence resulting from gas filling of the tracheal trunks and branches in wild-type (**A**); whereas those in *PPK11* and *colt* mutants are only partially filled with gas (red and black arrowheads, respectively) Scale bar 100 mm (Adapted from Hartestein et al, 1997; Liu et al., 2003).

5.2.2.2. Gas filling

In a standardised chain of events a bubble of unknown gas (as its composition has never been analysed) and origin, appears in one of DT branches between metameres 4 to 6. This gas bubble quickly expands through the DT (Figure 26A), first posteriorly (Figure 26B) and then anteriorly. The bubble then spreads through the posterior anastomosis to the contra-lateral DT (Figure 26C). Within 10 minutes, the entire tracheal network is filled with gas (Figure 26D) (Tsarouhas et al., 2007).
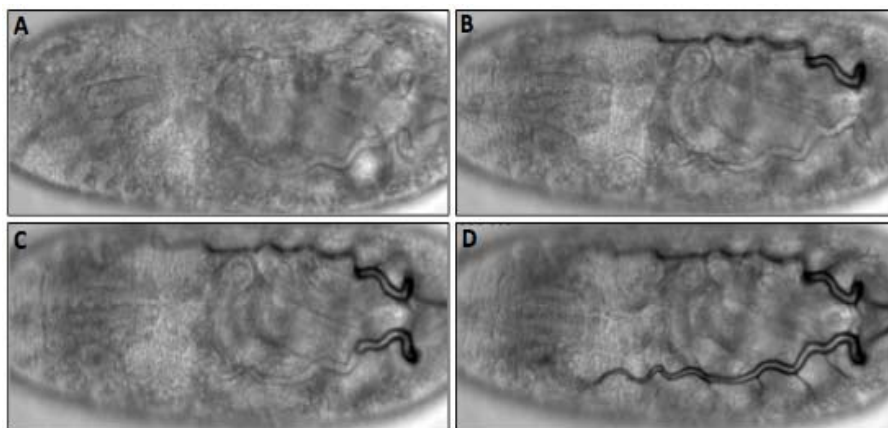
Figure 26. Gas filling process. Wild-type embryo showing the liquid clearance/gas filling process. The initiation of gas filling is shown in (**A**), and its completion, when all tracheal branches are gas filled in (**D**) (Adapted from Tsarouhas et al., 2007).

Mutant larvae for *uninflatable* (*uif*), a gene that encodes an apically localized transmembrane protein, have crushed tracheal tubes that are defective in gas filling, although their tracheal patterning and maturation appear normal during embryogenesis (Figure 27) (Zhang and Ward, 2010).
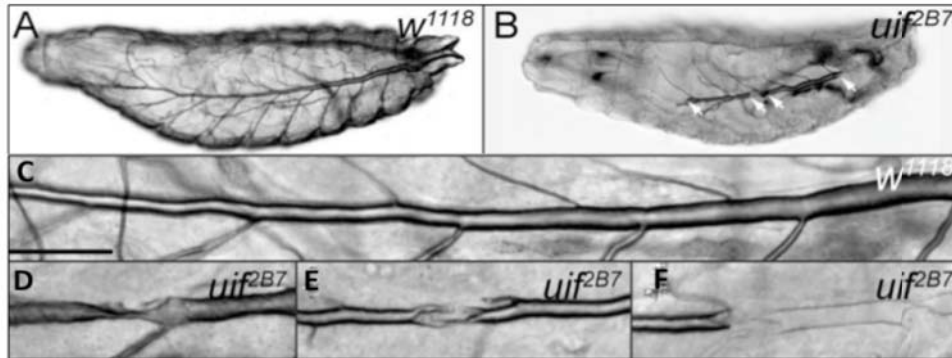
Figure 27. *vif* mutant first instar larvae have defects in tracheal inflation and damaged tracheal tubes. The tracheae of *uif* mutant animals are partially to completely uninflated (white arrows) (**B**) in comparison to wild-type,(**A**). (**C-F**) Differential interference contrast micrographs of dorsal tracheal trunks in wild type (**C**) and *vif* mutants (**D-F**) newly hatched first instar larvae. Note the regular diameter of the inflated dorsal trunk in the wild type larvae that contrast to *uif* mutant tracheae, which appeared crushed and showed discontinuous regions that are uninflated (Adapted from Zhang and Ward, 2009).

Based on the previous observations, Samakovlis and colleagues proposed the following model of tube maturation (Tsarouhas et al., 2007) (Figure 28).
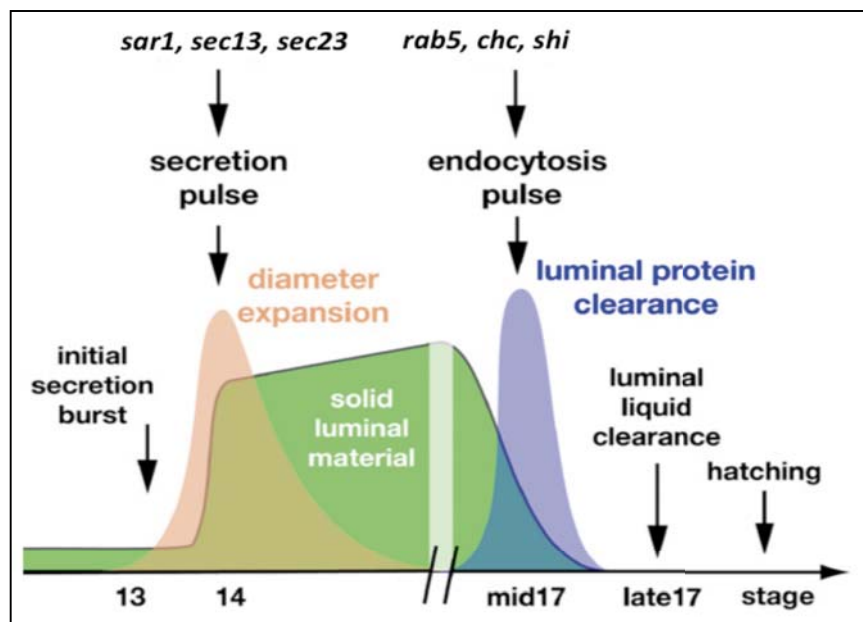
Figure 28. Schematic model of airway maturation. The initial secretion burst (green) extends into a massive, continued secretion pulse (orange) of chitin-binding proteins that fill the lumen. The COPII-dependent secretion pulse is essential for luminal matrix assembly and tube diameter expansion. At early stage 17, the tracheal epithelium activates a pulse of endocytic activity (blue) that internalizes and removes solid contents from the lumen. The endocytosis pulse requires the function of Rab5, Clathrin, and Dynamin (Adapted from Tsarouhas et al., 2007).

41

6. TRAMTRACK HAS MULTIPLE REGULATORY FUNCTIONS IN *DROSOPHILA* EMBRYOGENESIS

6.1. General features

Ttk was first characterised in a screen aimed to identify new genes involved in the *Drosophila* embryonic segmentation process, with a particular interest in transcriptional regulators of the pair-rule gene *fushi-tarazu* (*ftz*) (Harrison and Travers, 1990).

Drosophila ttk gene is one of the founder members of the Broad complex/ Tramtrack/Bric-a-brac/Pox virus and zinc finger (BTB/POZ) gene family, containing a protein-protein interaction domain (Bardwell and Treisman, 1994; Zollman et al., 1994) with an evolutionary conserved structure and function (Bardwell and Treisman, 1994; Wen et al, 2000). Although the general property of the BTB domain is to mediate homomeric dimerisation, it has also been shown to be involved in heteromeric interactions (Dhorian et al., 1997).

The *ttk* locus encodes, by alternatively spliced mRNAs, two proteins (Ttk-69 and Ttk-88) that share a common N-terminus but differ on the C-terminus and zinc finger motifs, suggesting that each Ttk protein may regulate different target genes. Consistent with this, Ttk-69 and Ttk-88 have been shown to have distinct DNA-binding specificities *in vitro* (Harrison and Travers, 1990; Brown et al., 1991; Read and Manley, 1992). These differences in DNA-binding specificities raise the issue of whether the proteins have different roles *in vivo*.

According to developmental studies, both Ttk isoforms function as transcriptional repressors (Harrison and Travers, 1990; Read et al., 1992; Xiong and Montell, 1993). Interestingly, the BTB domain has been reported to be capable of mediating transcriptional activation as well (Kaplan and Calame, 1997; Kobayashi et al., 2000).

6.2. Temporal and spatial regulation of embryonic *ttk* expression

Throughout early developmental stages, the *ttk* RNA expression pattern is homogeneously distributed throughout the embryo, presumably due to a strong maternal contribution. The first zygotic expression of *ttk* is detected at embryonic stage 7 in the anterior midgut primordium (Figure 29A), and then at stages 8 and 9 it is expressed on the mesodermal surface of the yolk space. Subsequently, it is observed at stage 11 in the

posterior midgut primordium, tracheal and salivary gland placodes and in the head region (Figure 29B). By the time of germband retraction, there is strong staining in the visceral mesoderm and weaker staining in the ectoderm (Figure 29C). Its expression starts to be more homogeneous at stage 13, when germband retraction has been completed, and after dorsal closure (stage 13) (Figure 29D), the epidermal expression intensifies and becomes almost ubiquitous throughout the epidermis (Harrison and Travers, 1990).
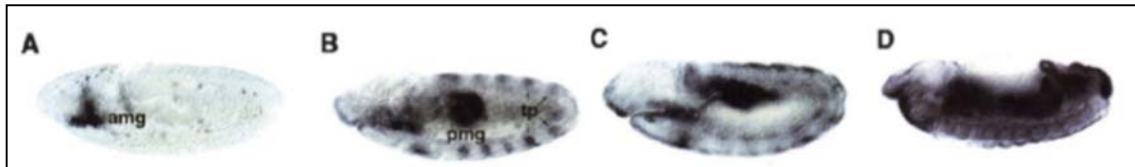
Figure 29. *ttk* embryonic expression pattern. (**A**) *ttk* is first detected in the anterior midgut precursors (amg). (**B**) Subsequently, the domain of expression expands to include the tracheal pits (tp) and posterior midgut invagination (pmg). (**C**) During invagination of the midgut precursors, it is observed in clusters of cells in the ectoderm and mesoderm. (**D**) Midgut expression persists until fusion, after which it decays. At this stage Ttk is also detected in the oesophagus and surrounding cells and posterior spiracles while the epidermal staining intensifies and becomes almost ubiquitous, being maintained until after dorsal closure (Adapted from Badenhorst et al, 1996).

The distribution of *ttk* RNA observed during embryogenesis is similar to the distribution of Ttk protein (Read and Manley, 1992). Its complex temporal and spatial expression in late embryos suggests that *ttk* has multiple regulatory functions in *Drosophila* embryogenesis.

6.3. Tramtrack's function in *Drosophila* development

Ttk is a widely expressed transcription factor whose function has been analysed extensively during development. For instance, Ttk is required in the CNS for glial development (Salzberg et al., 1994; Giesen et al., 1997; Badenhorst et al., 2001). Interestingly, it is also needed in cell fate determination of sensory organs during asymmetric divisions in *Drosophila* peripheral nervous system (Guo et al., 1995; Ramaekers et al., 1997). Moreover, it regulates the pattern of several pair-rule genes (Brown et al., 1991; Read and Manley, 1992). In addition, a role for Ttk in cell cycle and oogenesis has also been proposed (Badenhorst et al., 2001; Baonza et al., 2002; Althauser et al., 2005; Audibert et al., 2005).

6.3.1. Tramtrack regulates different morphogenetic events during *Drosophila* tracheal development

It was previously described that Ttk plays critical roles in the specification of different adult and embryonic tissues. However, no major roles for Ttk after cell fate determination were known. Our lab showed that Ttk acts downstream of cell fate specification controlling a range of cellular processes. In fact, our lab described a key role for Ttk in tracheal development (Araújo et al., 2007). In particular, our work identified different Ttk-69 requirements during tracheal development by the analysis of *ttk* $^{D2-50}$ mutant amorphic allele. We showed that Ttk is required for the following different steps:

6.3.1.1. Specification and establishment of the primary branching

The first detectable tracheal defects in *ttk*$^{D2-50}$ mutants are at stage 13, when visceral branches are often reduced or when present have fewer cells. Interestingly, the TC contains more cells, suggesting that the TCs are probably incorporating the VB cells. In fact, from stage 12-13, *bnl* expression is almost lost from the visceral mesoderm, which is presumably responsible for VB formation (Figure 30) (Araújo et al., 2007).
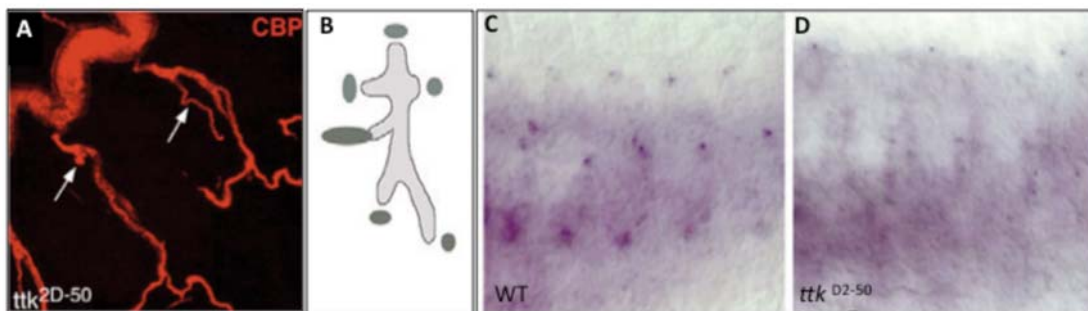
Figure 30. Ttk specifies different tracheal cell identities and the establishment of the primary branching. (**A**) Details of two tracheal metameres, showing the absence or reduction (arrows) of visceral branches (VBs) in a *ttk*$^{D2-50}$ mutant. (**B**) Schematic representation of wild-type *bnl* expression (dark grey) at stage 13. (**C, D**) Expression of *bnl* at stage 13. Note the reduction in size and number of *bnl* spots in the *ttk* mutant (**D**) (Adapted from Aráujo et al., 2007).

6.3.1.2. Specification of fusion fate requires N mediated regulation of Ttk levels

Expression of the fusion markers *esg* and *dys* is not detected in embryos over-expressing *ttk*69 in the tracheal system (Figure 31B) in comparison to wild type (Figure 31A). These results reveal that tracheal cells failed to acquire the fusion identity, resulting in an absence of branch fusions (Araújo et al., 2007).
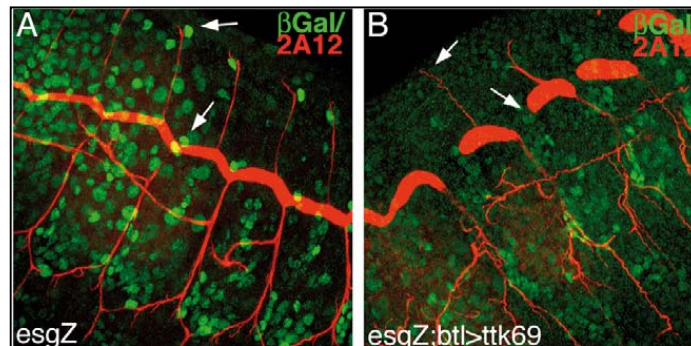
Figure 31. Stage 15 embryos labelled to highlight Esg-positive fusion cells (arrows in **A**). Tracheal over-expression of *ttk69* (**B**) blocks fusion fate acquisition (arrows) and branch fusions (Adapted from Araújo et al., 2007).

It has been described that Ttk acts as an effector of N signal during several developmental contexts (Guo et al., 1996; Jordan et al., 2006; Okabe et al., 2001). The fusion phenotype of *ttk* over-expression (Figure 32A) resembles that of constitutive activation of the N pathway, which also blocks fusion (Figure 32B) (Ikeya and Hayashi, 1999; Llimargas, 2000; Steneberg et al., 1999), suggesting regulatory activities of these genes during tracheal development.
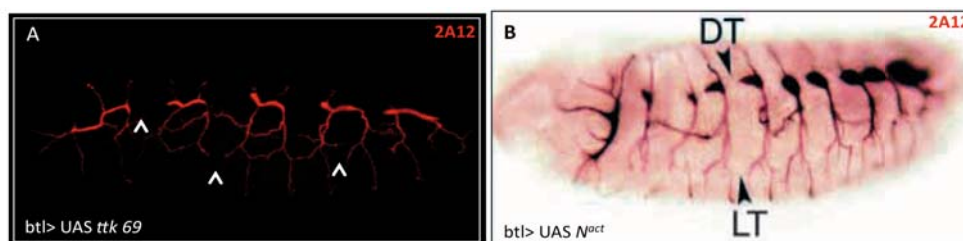
Figure 32. (**A, B**) Late stage embryos stained with Ab-2A12 to show the tracheal lumen. (**A**) Fluorescent staining of late stage embryo over-expressing *ttk69* the tracheal system. (**B**) Staining of late stage embryo over-expressing in the tracheal system *N*. Arrowheads mark the un-fused dorsal trunk (DT) and lateral trunk (LT) in both panels. Note the similarity of the phenotypes (Adapted from Llimargas, 2000).

Actually, we showed that Ttk acts as a downstream effectors of N during fusion cell type specification (Araújo et al., 2007).

6.3.1.3. Ttk as a positive regulator of tracheal cell intercalation

At late embryogenesis, ttk^{D2-50} mutant embryos show intercalation defects, evidenced by the presence of intercellular AJs between cells in branches where autocellular AJs should be present (Figure 33) (Araújo et al., 2007).
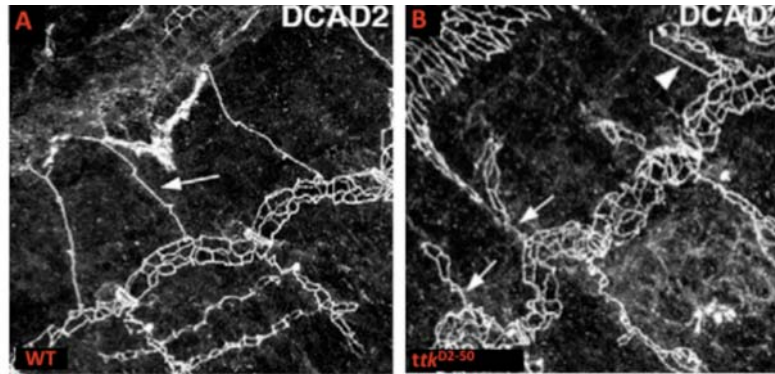
Figure 33. *Ttk* is required during tracheal cell intercalation. Projections of confocal sections showing details of stage 16 embryos focused at the dorsal trunk (DT) and dorsal branches (DBs). Accumulation of DE-cad (labelled with DCAD2) shows the presence of autocellular adherens junctions (arrow in A) in wild type (**A**). (**B**) ttk^{D2-50} embryos exhibit mainly intercellular AJs (arrowhead) and only occasional short stretches of autocellular ones (arrows) (Adapted from Aráujo et al., 2007).

Several DBs with no signs of autocellular AJs (Figure 33A, arrowhead), and others with short stretches of autocellular AJs followed by long stretches of intercellular ones (visualised as a mesh-like structure, Figure 33, arrows) were found. *In vivo* analyses indicated that ttk^{D2-50} mutant tracheal cells remain cuboidal and positioned side-by-side without elongating the DB branches (Figure 33B). Moreover, this defect was not caused by cell fate misspecification because in ttk^{D2-50} mutants the primary branching markers, such as Sal and Kni, were correctly accumulated. It was neither produced by defects in other tissues since the phenotype was rescued by tracheal-specific expression of *ttk*, indicating an autonomous requirement for Ttk during intercalation (Araújo et al., 2007). Interestingly, it has been shown that the intercalation phenotype observed in ttk^{D2-50} mutant is due to impairment in the reaching around the lumen step and the zipping up step (Araújo et al., 2007).

6.3.1.4. Positive regulator of intracellular lumen formation

Terminal cell identity is specified in ttk^{D2-50} mutants as visualised by the presence of the terminal cell marker DSRF, but interestingly and contrary to wt, terminal branches do not extend (Figure 34B arrow).
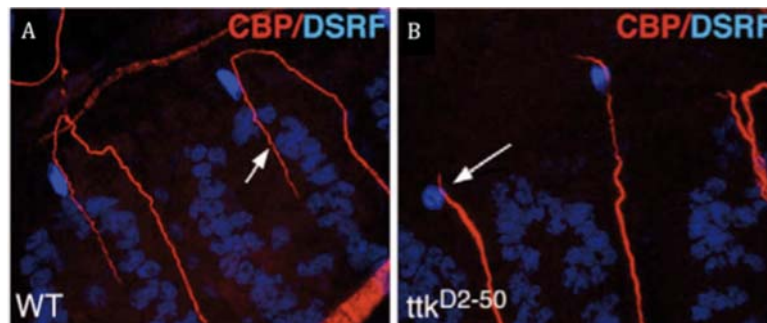
Figure 34. *Ttk* **is involved in the formation of terminal branches.** (**A**) DBs showing DSRF-positive cells and terminal branches (arrow in A) in wt. (**B**) Notice the absence of terminal branches (arrow in B) in spite of DSRF expression in ttk^{D2-50} mutants (B) (Adapted from Aráujo et al., 2007).

6.3.1.5. Control of tracheal tube size

ttk^{D2-50} mutants (Figure 365) had, in comparison to wt (Figure 35A), longer and wider tubes. When stained for markers to detect the intraluminal chitin matrix, such as CBP or 2A12, ttk^{D2-50} mutant embryos showed decreased chitin protein levels, an amorphous and disorganised chitin filament, as well as convoluted appearance of the DT (Figure 35D). In addition, the expression of the chitin synthase enzyme *mmy* was increased in *ttk* embryos, at stages in which chitin is being synthesised, and lowers when *ttk* is over-expressed, identifying *mmy* as a target of Ttk. Furthermore, the expression of *serp* and *verm*, whose secretion depends on SJ activity and are required to assemble the chitin filament, was decreased in ttk^{D2-50} mutants.
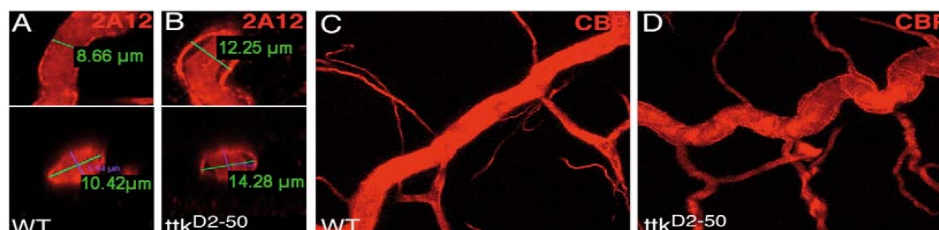
Figure 35. ttk^{D2-50} **controls tracheal tube size.** (**A**, **B**) Portions of DT in longitudinal views (upper panels) or in cross-sections (lower panels) of wt (**A**) and ttk^{D2-50} mutants (**B**). Thickness of the tubes is measured. (**C**, **D**) Stage 16 embryos showing accumulation of CBP in the DT. ttk^{D2-50} mutants show an abnormal intraluminal chitin filament (Adapted from Araújo et al., 2007).

47

In further confirmation of the role of Ttk on SJ orchestration, loss of the trans-epithelial diffusion barrier in *ttk* mutants was also observed (Figure 36).
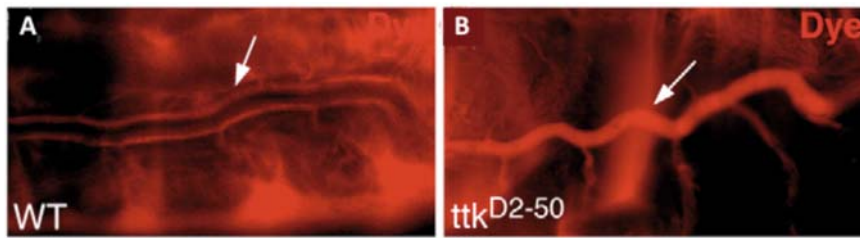
Figure 36. *ttk^{D2-50}* mutants are defective in trans-epithelial diffusion barrier. *Drosophila* embryos at stage 16 trachea-injected with a rhodamine-labelled dye. *ttk^{D2-50}* embryos (**B**) are permeable to the dye, which fills the tracheal lumen (arrows), whereas the wt trachea are impermeable (**A**).

Altogether, indicates that Ttk controls tube size by regulating the formation of the chitin filament and its proper assembly via SJ activity (Araújo et al., 2007).

In this section, we have introduced not only the relevance of using *Drosophila's* tracheal system development as a suitable model for tubulogenesis and size control but, highlighted the significance of Ttk as a key factor during tracheal system morphogenesis. Thus, the importance of gaining insights into the mechanisms underlying Ttk's tracheal specific functions has been suggested.

Objectives

AIMS OF THE THESIS

The aim of this Thesis was to identify new factors that, acting downstream of the transcription factor Ttk, mediate Ttk's multiple functions during tracheal development. In particular, tube size and intracellular lumen formation. To address this main objective and identify the transcriptional profile of Ttk modulation, we undertook a Microarray analysis after Ttk loss- and gain-of-function conditions, both in whole embryos and in cell populations enriched for tracheal cells.

Specific objectives were:

1.- Generation of fly lines to be transcriptionally compared.

2.- Sorting out of the different genetic cell populations to be transcriptionally compared.

3.- Microarray analysis using Affymetrix *Drosophila* Genome 2.0 Arrays.

4.- Bioinformatics analysis of microarray experiments.

5.- Validation of the method.

6.- Functional analysis of microarray experiments.

7.- Selection of Ttk targets based on expression pattern and molecule nature criteria.

Materials and methods

1. FLY HUSBANDRY

The different *Drosophila* stocks and crosses were kept on standard conditions at 25°C. Over-expression experiments were conducted at 29°C. Flies were kept in plastic vials of various sizes, which are filled with a rich culture medium composed by flour, glucose, agar, fresh yeast and propionic acid as a preservative. The lay-plates where the females lay embryos contain a gelatinous medium composed by juice, bacteriological agar, yeast extract and propionic acid (Ashburner, 1989).

1.1. *Drosophila* stocks

All the *Drosophila* stocks used in this Thesis, except those specifically generated for our experiments, (see bellow) are described in Fly Base (http://flybase.org/) and Vienna *Drosophila* RNAi Centre (http://stockcenter.vdrc.at/control/main).

All the ectopic and/or over-expression experiments were performed using the UAS/Gal4 system (Brand and Perrimon, 1993). This system allows the ectopic expression/over-expression of the interested gene in the expression domain of another gene. It requires two transgenic lines: one encodes the Gal4 protein under the control of the promoter of a gene with a pattern of interest, and the second one contains the gene of interest under the control of UAS (Upstream Activation Sequence) sequences.

Fly stocks used to generate the different *ttk* mutant recombinant lines (*bt*l RFP moe *ttk* /TM3 twi GFP and UAS *ttk 69* btl RFP moe):

- *btl* RFP moe: This construct enables the visualization of the shape (due to moesin (moe), which interacts with actin) of all tracheal cells (due to *btl* promoter) *"in vivo"* (due to the RFP).

- *ttk*$^{D2-50}$/ TM3 twi GFP: The allele *ttk*$^{D2-50}$ is homozygous lethal so we had this stock balanced with a standard balancer chromosome (TM3). In our case the TM3 chromosome includes the molecular marker twi-GFP (twist, twi; GFP, green fluorescent protein), allowing the detection of mutant embryos *"in vivo"* and also in fixed and stained tissue by the absence of GFP.

- Adv/Cyo; UAS *ttk 69*: This line carries in the third chromosome, in homozygosis, the UAS *ttk 69* construct that is expressed under the control of UAS regulatory sequence (Generated by M.Llimargas).

Fly stocks used to measure the tracheal dorsal trunk branch length:

- CG10725: RNAi 37868, 37869 and 100225.

- *Cht2*: RNAi 7609, 44917 and 102249.

- *Idgf5*: RNAi 16795 and 100977.

- *Idgf3*: RNAi 12423 and 12422.

- *Lcp1*: RNAi 30792 and 30793.

- Ccp84Ac: RNAi 31086 and 102212.

- Cpr11A: RNAi 14895 and 103321.

- Cpr11B: RNAi 102554.

- Cpr30B: RNAi 37983 and 37984.

- Cpr49Ah: RNAi 23183 and 23185.

- Cpr62Bb: RNAi 43849, 50394, 50807 and 107973.

- Cpr73D: RNAi 23720.

- Cpr78Cb: RNAi 31058, 31060 and 107767.

- Cpr60D: RNAi 17896, 19482, 39687 and 102601.

- Cpr47Eg: RNAi 3262, 3263 and 104519.

- Cpr65Av: RNAi 23328, 23331 and 104058.

- *Punch*: RNAi 33923.

- *Shavenoid*: RNAi 36512.

- *Bursicon*: RNAi 26719.

- *Tantalus*: RNAi 27671.

- *Papillote*: RNAi 8316.

- CG7715: RNAi 38215.

- Cpr65Eb: RNAi 35992.

- *Discs large* RNAi 1076, 1365, 1694 and 1736.

- *varicose* mutant allele *vari*[3953]: This allele is embryonic lethal due to a P-element insertion in the chromosomal region 38A6-39E1 that corresponds to the varicose locus (Beitel and Krasnow, 2000).

Fly stocks used to study the role of CG13188 gene:

-   CG13188: RNAi 32152, 32153 and 102370.

Other fly lines used:

- *btl* Gal4 UAS src GFP: This line has been used for tracheal specific expression achieved with the UAS/Gal4 system (Brand and Perrimon, 1993), as the *btl* Gal4 line (Shiga et al., 1996) drives the expression of UAS constructs in all tracheal cells after the invagination step. It allows the visualisation of cell shape thanks to GFP expression in the pattern of src ()

- *btl* Gal4 UAS tau GFP/ Cyo wg z: This in another *btl* Gal4 line used for tracheal specific expression. It also allows cell body visualisation due to GFP expressed according to tau pattern ()

- LP39 Gal 4/ Cyo wg z; UAS GFP: This Gal 4 line (provided by M. Calleja and G. Morata) drives the expression of the UAS construct in a *spalt* pattern of expression.

2. FIXATION OF EMBRYOS

Embryos were staged according to Campos-Ortega and Hartenstein (Campos-Ortega and Hartenstein, 1985) and stained following standard protocols. Immunostainings were performed on fixed embryos. First the collected embryos were washed with water to get rid of the yeast and then dechorionated with 50% bleach for 2 minutes. To stop dechorionation, the embryos were rinsed several times with water. Subsequently, the embryos were collected in a nylon membrane basket and transferred to a vial with 0.250 ml formaldehyde 37%, 2 ml heptane and 2 ml PBS. The embryos were fixed on a rotator for 20 minutes (except for anti-DEcad, for which they were fixed for 10 minutes). The lower phase (the fixative) was removed, and methanol was added to the heptane in a 1:1 ratio. Vials were shacked vigorously to devitellinise embryos. Embryos were washed several times with methanol and kept in Eppendorf

tubes at -20°C for long-term storage or used for fluorescent immunostaining.

3. FLUORESCENT IMMUNOSTAINING OF EMBRYOS

Fixed embryos were washed 3x 20 minutes with 1ml PBT-BSA (PBS 1X, Triton 0.1% y BSA 0.3%) and incubated in 300μl of PBT-BSA with the primary antibody overnight at 4°C (Ashburner, 1989). The following day, embryos were washed 3x 20 minutes with PBT-BSA to get rid of unbound primary antibody. Subsequently, the embryos were incubated with the secondary antibody in PBT-BSA for 2 hours at room temperature. The embryos were washed 3x 10 minutes with 1ml PBT (PBS 1X, Triton 0.1%) to remove unbound secondary antibody, and mounted using the standard fluorescent medium Fluoromount-G (Southern Biotech).

The following primary antibodies were used: anti-GFP, 1:600 (Molecular Probes and Roche); anti-ßGal, 1:600 (Cappel and Promega); anti-Trh, 1:600 (made by N. Martín in the laboratory of J. Casanova); anti-DEcad (DCAD2), 1:100 (Developmental Studies Hybridoma Bank); anti-Serp, 1:300; anti-Verm, 1:300 (S. Luschnig, University of Bayreuth, Germany); anti-DSRF, 1:500 (Cold Spring Harbor Laboratory, CSHL); anti-Knk, 1:500 (B.Moussian, Tuebingen, Germany). Chitin was visualised with CBP at 1:500 (New England Biolabs), mAb2A12 at 1:10 (Developmental Studies Hybridoma Bank) and WGA at 1:100 (Molecular Probes). Primary antibodies were detected by using secondary Cy3-, Cy2- and Cy5-conjugated antibodies used at 1:300 (Jackson ImmunoResearch).

4. IMAGING

Confocal images from fluorescent stainings were obtained with a Leica TCS-SPE system. TIFF images were post-processed digitally with ImageJ software. Unless otherwise stated, images are maximum intensity projections of several confocal z-sections; and in the panels labelled 'GFP' the embryos carried *btl*Gal4 driving GFP-fusion protein.

Photographs of live embryos were captured on a Nikon Eclipse 80i microscope by a digital camera Nikon DXM 1200F.

5. MICROARRAY ANALYSIS

This analysis is a multi-step process as schematised in figure 37. The first step consisted in generating the appropriate fly lines that allowed distinguishing the *ttk* mutant or *ttk 69* over-expression homozygous embryos from the rest of the population.
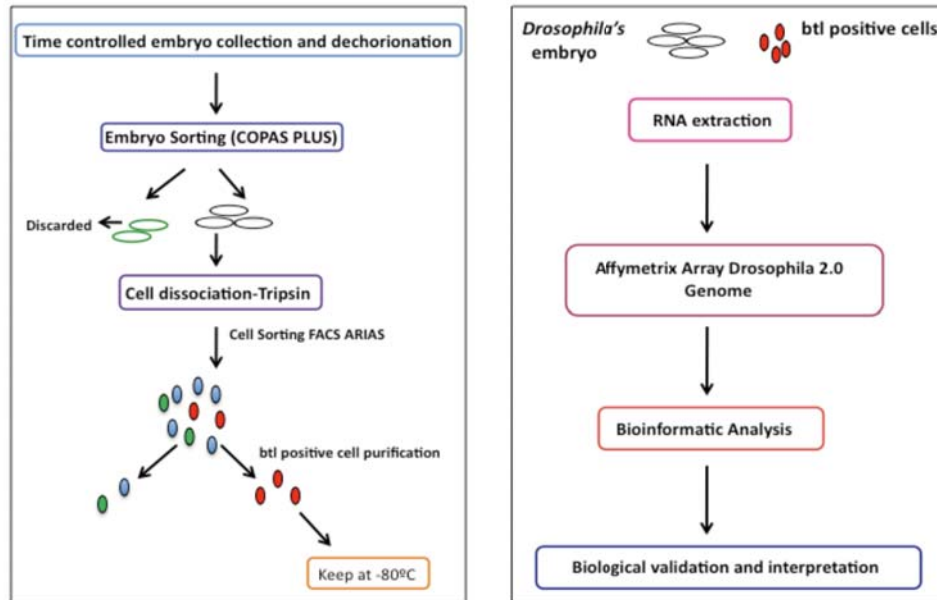
Figure 37. Schemes showing the Microarray multi-step process performed. Note that the different steps are interdependent in a sequential manner. Efficient embryo sorting is a prerequisite for the tissue disgregation. Similarly, efficient cell sorting is a condition for RNA isolation.

5.1. Crosses to generate the recombinant lines

5.1.1. Crosses to generate the *ttk* mutant recombinant line

F0) ♂ yw; *btl* RFP moe X ♀ w-; *ttk*$^{D2-50}$/TM3 twi-GFP

F1) ♀ w/yw; *btl* RFP moe/ *ttk*$^{D2-50}$ X ♂ w-; ttk^{D2-50} / TM3 ftz lacZ

F2) Individual crosses of ♂ yw or w; *btl* RFP moe (*ttk*$^{D2-50}$?)/TM3 ftz lacZ X ♀ w-; *ttk*$^{D2-50}$ /TM3 twi-GFP

We first selected potential recombinant males by the presence of *btl RFP moe*, detected by an eye colour marker (mini-white (w^+); generating orange eyes). To determine if these males were also carrying the *ttk*$^{D2-50}$ allele and were therefore recombinants, a lethality complementation test was carried out. Individual males were crossed to *ttk*$^{D2-50}$/ TM3 females.

Recombinant *btl RFP moe* ttk^D2-50 chromosomes were identified due to their lethality over the *ttk*^D2-50 chromosome of females (as *ttk*^D2-50 is homozygous lethal).

Non-recombinant *btl RFP moe* chromosomes were identified by their viability over the *ttk*^D2-50 chromosome of females. These non-recombinant lines underwent the same scheme of crosses as the recombinants, making their genetic backgrounds as similar as possible to that of the recombinants, and were therefore used as control lines.

5.1.2. Crosses to generate the UAS *ttk* 69 recombinant line

F0) ♂ yw; *btl* RFP moe   X   ♀   Adv/Cyo; UAS *ttk* 69

F1) ♀ yw; Adv or Cyo; *btl* RFP moe/ UAS *ttk* 69   X   ♂ w-; Ly/ TM3 lac Z

F2) Individual crosses of ♂ w-; *btl* RFP moe (UAS *ttk* 69?)/ TM3 or Ly   X   ♀ *ttk*^D2-50 /TM3 twi-GFP

We detected recombination by a strong orange-red eye colour in comparison to each individual line, as both lines carry the *w*^+ transgene. We established the "UAS *ttk* 69 *btl* RFP moe/TM3 twi-GFP" line, which is homozygous viable.

We then crossed male "UAS *ttk* 69 *btl* RFP moe/ TM3 twi GFP" recombinants to females "w-; *btl* Gal4 UAS tau GFP/ Cyo z", in order to over-express *ttk* 69 under the control of the *btl* promoter and check the presence of all transgenes. As control embryos, we used those from the cross that carried the "UAS *ttk* 69 *btl* RFP moe" line.

5.2. Embryo collection

To collect embryos with developing trachea (from st.11 to st.17), we allowed the flies to lay for 07:40 hr at 25ºC and then let the embryos age 05:20 hr more at 25ºC. (Figure 38).
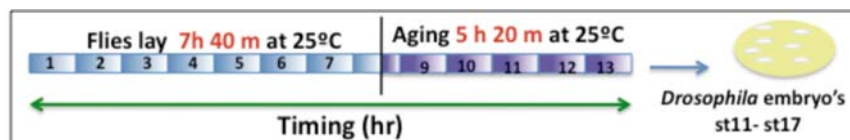
Figure 38. **Schematic representation of the strategy used to collect *Drosophila's* embryos from stage 11 to stage 17 in development.**

60

5.3. Embryo sorting

To sort embryos by the absence or presence of the GFP tagged markers, we used the embryo sorting technique using COPAS PLUS system. As the system had not been previously used to segregate *Drosophila* embryos, we set up and optimised the technique in the Facility. We manually separated 300 twi-GFP negative embryos (homozygous) and 300 twi-GFP positive embryos (heterozygous) from the control condition (*btl* RFP moe/ TM3 twi GFP) under a fluorescence microscope, and passed them through the COPAS embryo sorter. This allowed us to identify the region where our embryos of interest (non twi-GFP expressing) were distributed. Then, we ran a negative control population (yellow-white (yw^+) embryos that do not expressed twi-GFP marker) to check this defined region (Figure 40).
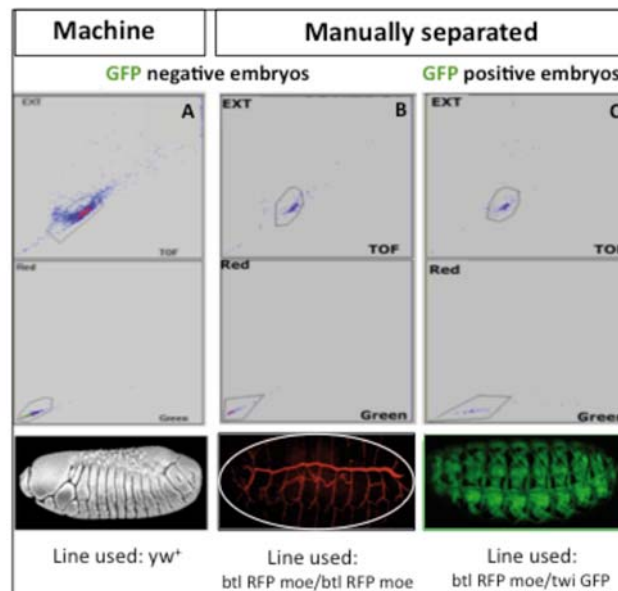
Figure 40. (**A-C**) **Modified dot plots histograms from the COPAS PLUS embryo sorting that show the defined regions to isolate GFP negative embryos.** Note that the GFP negative region is distributed similarly in the control line used (**B**) and in the external negative control population yw^+ (**A**), as compared with GFP positive embryos (**C**).

Once the sorting region was set around that population of interest, we passed a mixed population, of GFP expressing and non-expressing embryos from the control and *ttk*^D2-50 mutant situation through the machine to fine-tune the machine parameters (pressure, size of the collecting drop, time of flow sample, etc) (Figure 41).
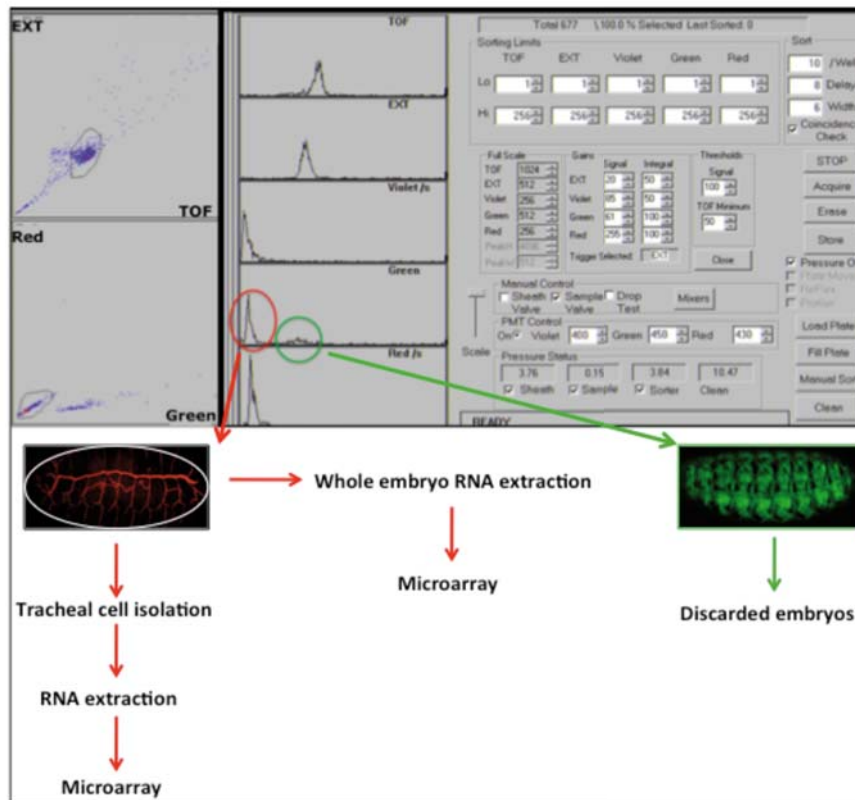
Figure 41. Modified figures from the COPAS PLUS embryo sorting. These images showed two populations (red and green circles in figures), of embryos in both genetic backgrounds (control and ttk^{D2-50} mutant). Also, we can visualize a polygonal region positioned around the No twi-GFP embryos that were successfully isolated from both control and ttk^{D2-50} mutant population.

These tests ensured that the machine selected and dispensed only embryos within the selected region, with purity greater than 98%, and with the expected ratio of 75% GFP-positive, which were discarded into the waste container, and 25% GFP negative embryos, which were dispensed into the collection chamber.

It was not necessary to sort out embryos from the over-expression of *ttk 69* because the generated mutant recombinant line (UAS *ttk* 69 *btl* RFP moe) is homozygous viable as well as the *btl* Gal4 UAS tau GFP line used. Thus, all embryos resulting from the cross between these two lines were used because all of them were over-expressing *ttk 69* in the tracheal system. The control line for the over-expression experiments was the "UAS *ttk* 69 *btl* RFP moe" line.

5.4. Cell disruption

For several rounds, pools of 600–1000 sorted embryos from all the genotypes were homogenised in cold S2 medium in a crystal douncer (KONTES Gerresheimer) with three strokes without rotating the pestle (mechanical cell disruption). Thereafter, 60 ml of trypsin-EDTA 9X (SIGMA) was added to 1.5 ml of S2 medium and shaken for 15 minutes at room temperature to the homogenised embryonic sample (enzymatic cell disruption). 5 ml of Hoechst-33342 nuclear marker per 600–1000 embryos was added to the trypsinisation reaction. Subsequently, the reaction was stopped with a 1:1 PBS:BSA buffer, obtaining a heterogynous cell lysate populations of each condition.

5.5. Cell isolation study

We used a Fluorescence Activated Cell Sorter (FACS Aria SORP sorter; Beckton Dickinson, San Jose, California) to isolate tracheal cells from the previous heterogynous cell lysate populations from each condition.

Flow cytometry FACS cell sorting is a powerful technique that allows the researcher to measure the fluorescence emission of individual cells, at multiple wavelengths, in populations of thousands of cells, using fluorescent affinity markers placed on the marked experimental cells to isolate specific cell types by measuring not only the relative fluorescence, but also size, DNA content and complexity among other properties. So, specific marked cell populations can be physically sorted, and then used in diverse biochemical assays, such as microarray analysis, as it is our case.

There are two main flow cytometric parameters: the forward scatter (FSC) and the side scatter (SSC). The FSC parameter shows the light intensity of a particle in solution measured by the difference between the refractive index of the medium and the cell. To detect the FSC, samples were excited using a 488nm laser that corresponds to the blue-green region of the visible spectrum. The SSC parameter detects the scattered light in a perpendicular direction to the laser axis, adding discrimination among cell types in a heterogeneous sample. So, tracheal cells were clearly discriminated in the scatter plot of FSC versus SSC (Figure 42A, Panel 1). Setting the gate based on these two parameters, and in order to identify living cells in G0/G1 cell cycle phase (as there is no cell division at these stages of development in the tracheal cells) and reduce cell aggregates, we were able to draw a gate according to the expression profile of the nuclear marker

Hoechst-33342 (Figure 42A, Panel 2) and select cells with these features. Samples were excited with a UV laser for Hoechst-33342. Among the cell population we isolated the fraction enriched for RFP-positive expression (detected by the presence of the "*btl*/RFP moe" marker), by exciting the sample with a 532 nm laser, to select entire living tracheal cells (Figure 42A, Panel 3), discarding the auto-fluorescence (AF) and the rest of entire living cells. Thus, living tracheal cells were isolated by their RFP fluorescence, AF, FSC, SSC and Hoechst-33342 expression intensities, being summarised the gating strategy in figure 42.

To check the distribution of the isolated pure tracheal cell population, we also re-passed them through the FACS ARIAS cell sorting, observing that they behave as one population and are separated inside the "red separation region" (Figure 42B), showing a complementary plot to an isolated negative control cell population (Figure 42 C).
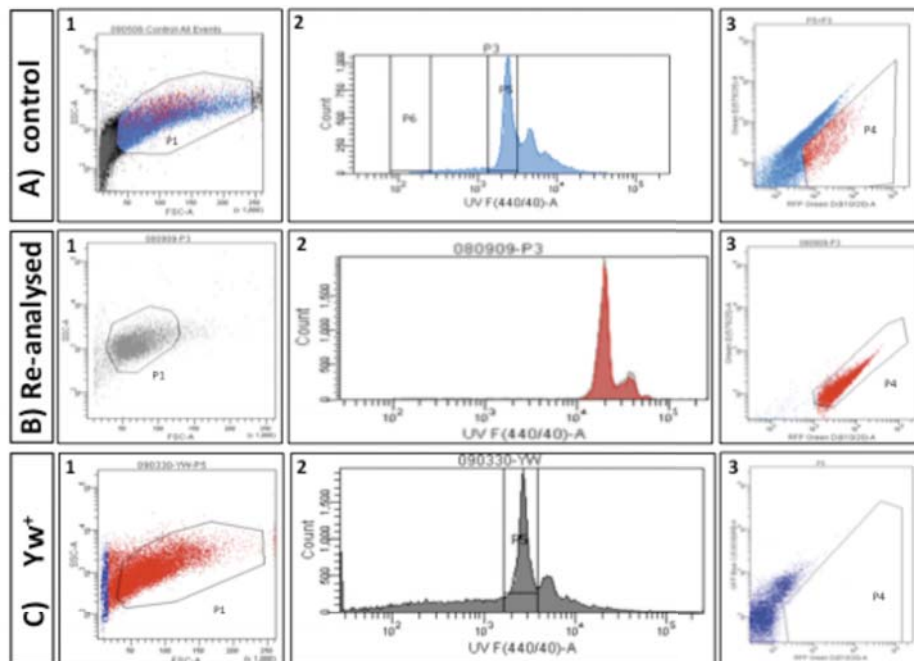
Figure 42. Gating strategy for FACS-assisted RFP positive cell sorting. Regions are drawn to include the population of interest. (**Panel A**) Data for mutant control cell suspension. (**1A**) Region in A is drawn and placed to include most of the events that exhibit similar SSC and FSC values. (**1B**) P5 region is drawn and placed to include live cells with only 2C DNA content, which are the cells at G0/G1 cell cycle phase. (**1C**) P4 region is drawn and placed to distinguish RFP-positive from RFP-negative cells with respect to relative cell size and fluorescence. (**Panel B**) Red positive isolated in Panel A, were re-analysed through the machine, behaving as a unique population (**Panel C**) Negative control embryonic population, that alter applying the same parameters as Panel A, **1C** showed a complementary plot 3 respect to 1A3.

Once the FACS ARIAS cell-sorting technique was set up and optimised, ensuring that we could work with a high efficiency of isolation, we were able to isolate, in a single cell sorting experiment, an average of 25,000-100,000 tracheal cells from the conditions analysed (Figure 43).
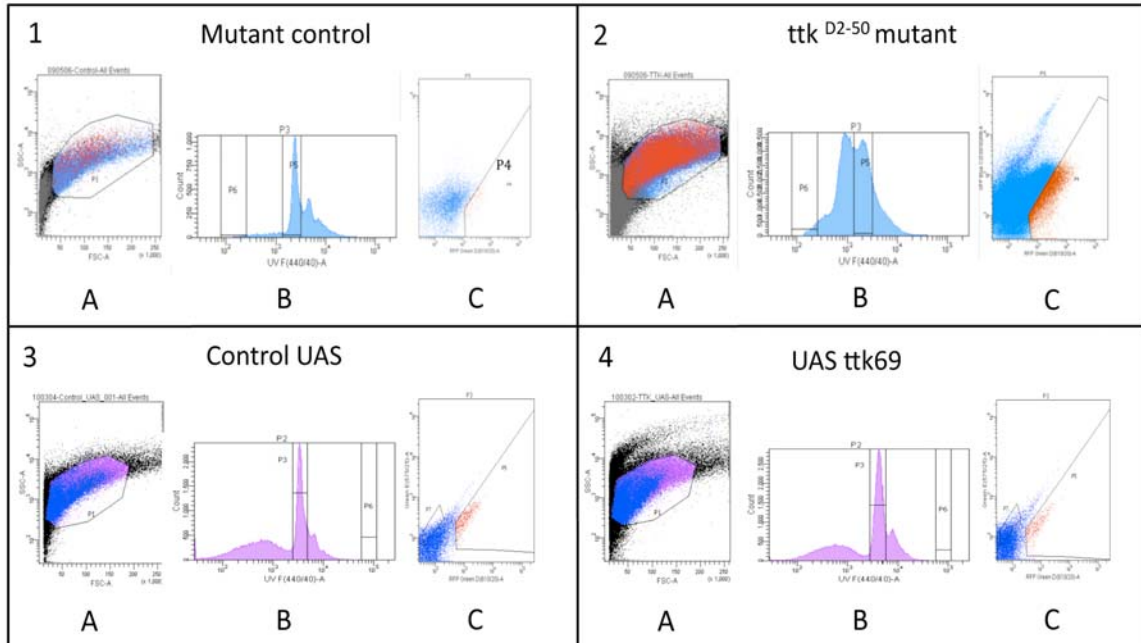
Figure 43. The same gating strategy for FACS-assisted RFP positive cell sorting as panel above, showing equivalent plots. Panel 1: data for mutant control cell suspension. Panel 2: Data for ttk^{D2-50} mutant cell condition. Panel 3: Data for control UAS-experiment cell condition. Panel4: Data for UAS-$ttk69$ cell condition.

We kept the material from each sorting frozen at -80ºC, until the number of cells required to extract sufficient RNA for each condition (and for each replicate) was obtained.

5.6. RNA extraction

Total RNA from pools of about 1,000 embryos from the four genotypes (control, ttk^{D2-50} mutant, over-expression control and over-expression ttk 69 mutant was extracted using the GibcoBRL Trizol protocol.

RNA extraction from all purified cell samples from the four genotypes were performed using the RNeasy QIAGEN RNA Extraction Kit, starting with 100,000 isolated cells of each condition. RNA was quantified using the Nanodrop ND-1000 spectrophotometer (Fisher Scientific) and integrity was evaluated on the Bioanalyzer 2100 (Agilent) using the RNA 6000 Nano Kit.

5.7. Microarray Hybridization

We used the IRB Functional Genomics Core Facility to perform a microarray analysis. We pooled multiple RNA collections from different cell sorting runs from the same week to minimise the variation inherent among collections and to obtain adequate RNA from each genotype. 5 ng total RNA per sample was processed using the isothermal amplification SPIA Biotin System (NuGEN Technologies, Inc.). 2.2 mg of cDNA from each genotype and for each sample condition were hybridized to GeneChip 2.0 *Drosophila* Genome Arrays (Affymetrix, Santa Clara, CA) in triplicate. The Facility provided all the reagents, equipment and expertise for hybridisation and scanning. Raw microarray data has been deposited in the MIAME compliant GEO database, series GSE30239.

6. COMPUTATIONAL ANALYSIS

We established collaboration with Dr. Adryan, a bio-informatician group leader at the Cambridge Systems Biology Centre, for the computational analysis of our data. He used R and Bioconductor programs (Wang et al., 2002; Gentleman et al., 2004) to process our raw microarray data. For further details on normalisation and scaling see GEO data series GSE30239 (Barrett et al., 2011). All other data analysis was performed using custom-written Perl scripts, using BDGP gene expression database (March 2007) (Tomancak et al., 2007) and BioGrid genetic interactions (Stark et al., 2011) for comparison. Gene lists were managed in FlyMine (Lyne et al., 2007) and analysed for Gene Ontology-enrichment using their implementation of the hypergeometric test with Benjamini-Hochberg multiple testing correction. The Ttk chromatin immunopurification data was obtained from the modENCODE website and visualised using the Integrated Genome Browser (http://bioviz.org/igb/).

7. QUANTITATIVE REAL TIME qPCR

We used equal amounts of total RNA of embryos at stages 11 to 16 from each condition and genotype to synthesise complementary cDNA by random-hexamer-priming (RevertAid H Minus First Strand cDNA Synthesis FERMENTAS Kit) in triplicate. A LightCycler 480 Real-Time PCR System with 50 amplification cycles and the SYBR Green PCR Master Mix (Roche) were used to amplify cDNAs. Relative quantities were normalized to expression of CG13167, a mitochondrial ATPase that showed stable expression throughout all experimental conditions. All PCR reactions were carried out in triplicate in 20 ml reaction volumes containing 2 ml cDNA template. Samples were analyzed using the LightCycler 480 Real-Time PCR System software (Roche). All PCR primers were designed using the MacVector 11.1 software, aimed to amplify a product size of 75–150 bp, and are listed in Table 1.

Real-time qPCR primer sequences				
Gene name	Gene symbol	FlyBase ID	Forward primer 5'-3'	Reverse primer 5'-3'
Chitinase 2	*Cht2*	CG2054	AACTATCCCCTTCTGCGGACC	GAATCTCGTTCTCGGAGTCATCC
Cht5	*Cht5*	CG9307	ATCGGTCGCTATGGATTGGAG	AAACTTGCTGAAGCCACCCTG
Chitin deacetylase -like4	*Cda4*	CG32499	TCACACATTGCCAACGGTAACT Ac	TGGACAGCGGTTCAAATACGG
Cuticular protein 78Cb	*Cpr78Cb*	CG7663	GCAAGTGTCCGTGAAGAAGGC	AGGGCAAGAAACATTTGGGC
Imaginal disc growth factor 3	*Idgf3*	CG4559	GCTCCTGGAATCGGGACAAC	GCGTGGCTTATTTCTGGGAAG
Cht9	*Cht9*	CG10531	ACTCGCTGTCCTCTGCCTTAGC	AACTTGCCATTGCCGCTGC
CG7715	*CG7715*	CG7715	TACTATGTGTGCCCGAGCGTC	TCTGGAGGACAAAGGTGAAGAC C
CG8460	*CG8460*	CG8460	CGATTTGTTTTTGTGCGATTTAT G	CAGTAGAAGCAGGAGAGCGACG
Imaginal disc growth factor 1	*Idgf1*	CG4472	AGTTGTCGCAGAACGCATCC	CCATACGCCAAAATCTCCATTAT C
discs large 1	*dlg1*	CG1725	CATGCGCATCGAATCGGACAC	AGTCTGGGACCCGCTCCTCGA
scribbled	*scrib*	CG42614	CAGTTGCTGTATCTGCCCTACT CG	ACACCTGTTCGCCCGTTTCC
varicose	*vari*	CG9326	CCAGAAACAACAAAGTGAATGG C	CATCGTGGTCGGATAGGTCAGTC
headcase	*hdc*	CG15532	TTCTTCAGGCGTCCTAATGGC	CCAGTTTGCGACAGTCTCCG
scute	*sc*	CG3827	GCAATCAAAATCAACCCGCTG	TGGTCAGTGCCATACCCCTTG
achaete	*ac*	CG3796	GCAATCTCCAACTGGCAGCAC	CGGTAGTCTTCAAAACTGGCTTC C
Hairless	*H*	CG5460	CGGTTAGCGATGATAGCGAGT C	CATTCGTGATTCTGGGCAGC
CG13167	*CG13167*	CG13167	CCTGCCCATCTTTCCATCCC	TTCCGCTTGAGGAGACCCAC
CG13188	*CG13188*	CG13188	ATTGGACTGTGCGGCTTCG	GGATGAGGATGTTCCCAGCG

Table 1. Primer sequences used for qPCR. Notice that expression changes were deemed significant at p $\leq$ 0.05.

7.1. Stage-specific qPCR

To compare the expression profile of embryos at different stages, we collected embryos at stages 11 to 13 and embryos at stages 14 to 16. For the collection of the younger embryos we allowed flies to lay eggs for 5,20 hr at 25ºC and subsequently allowed embryos to develop for another 5 hr at 25ºC. For the older embryo collection we allowed flies to lay eggs for 5,20 hr at 25ºC and subsequently allowed embryos to develop for another 10,20 hr at 25ºC.

Embryos were dechorionated and sorted by presence or absence of GFP using the COPAS PLUS Sorter to obtain the homozygous mutants and control embryos. Total RNA from pools of about 1,000 embryos from each genotype (control and ttk [D2-50] mutant) at each developmental stage was extracted using the GibcoBRL Trizol standard protocol. RNA was quantified using the Nanodrop ND-1000 spectrophotometer (Fisher Scientific). Equal amounts of total RNA were used to synthesise complementary cDNA by random-hexamer-priming (RevertAid H Minus First Strand cDNA Synthesis FERMENTAS Kit) in triplicate, to perform and analyse the qPCR experiments as we describe above.

8. TUBE LENGTH MEASUREMENTS

We stained embryos with CBP to visualise their tracheal system. Digital micrographs of dorsal trunks of embryos at stage 16 and 17 were used to measure their length by adapting a previously published method (Laplante et al., 2010). The length of the DT was obtained by the difference of two types of measurements between the third and eight tracheal metameres. We first measured the length of a line traced following the path of the dorsal trunk between the selected points (Figure 44, Panels A, blue line) using ImageJ. To check that the extra-long trachea phenotype is not due to a decrease body size, we also measured in ImageJ the length of a straight line drawn between the same selected points of the same embryos (Figure 44, Panels B, yellow line).
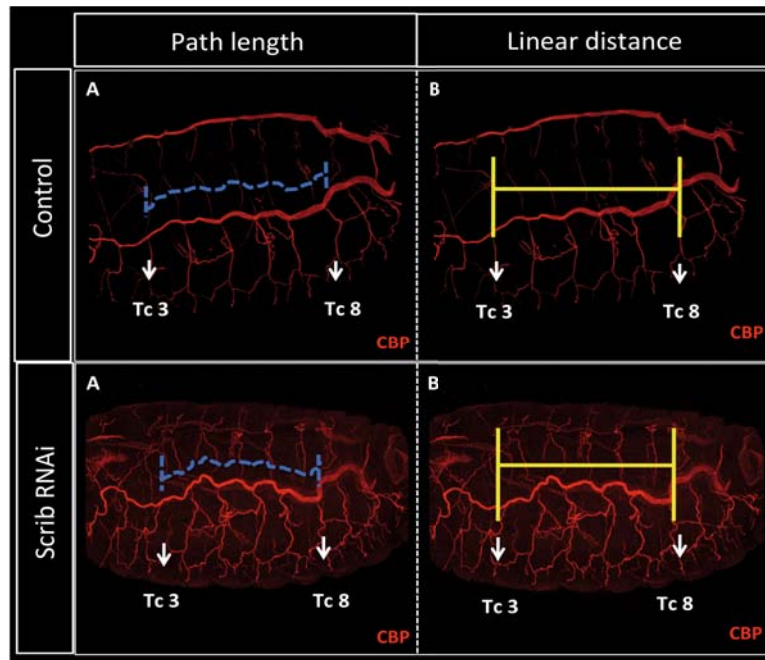
Figure 44. Example of dorsal trunk length comparison. The path length described by the DT between the TC of tracheal segments three to eight was measured by tracing a line through the tube following the three-dimensional aspects of the dorsal trunk (blue line). The distance between the transverse connectives of tracheal segments three to eight was measured by tracing a straight line between the start and finish point of the path (yellow line) (**A**, control; **B**, mutant for *scribble*).

The significance of tracheal length differences between controls, RNAi knockdown mutants and the available loss-of-function alleles used, were determined using the statistical Wilcoxon's test in R, and considered significative with a p-value <0.05.

9. GENERATION OF AN ANTIBODY AGAINST CG13188 IN *DROSOPHILA*

The antibody was generated with the valuable technical help of N. Martin, a research assistant in Dr. Casanova's group (IRB).

9.1. Plasmid construction

A DNA fragment of 1542 base pairs (bp) that encodes the N-terminal region of CG13188-RB was amplified by PCR in standard conditions, with a melting temperature of 62ºC and 90 seconds of extending with the primer pair:

NdeI: CATATGGTGTCGCGTCGAAAAATT

XhoI: CTCGAGTCAGTCCCATTCCCCGAT

The PCR product for CG13188-N was cloned in the pGEMT-easy expression vector, which is a convenient system to clone PCR product. We checked the cloning by digesting with *NdeI* and *XhoI* and obtaining the correspondent agarose gel size band. The DNA was purified from the gel band following a standard protocol (Illustra^{TM} GFX^{TM} PCR DNA Gel purification Kit), and ligated with the expression vector pET28a (Novagen), which carries an N-terminal His tag, that was previously digested with *NdeI* and *XhoI*.

9.2. Preparation of recombinant proteins and antibody generation

The resulting positive clone was used to transform BL21 (DE3) cells (Novagen) for protein expression. Four colonies were selected to perform a protein expression test: Bacteria were grown at 37ºC in LB media (1% Bacto tryptone, 0'5% Bacto yeast extract, 171 mM NaCl, 50 µg/mL carbenicillin, 50 µg/mL kanamycin). Cells were induced with 1 mM IPTG, and protein was expressed at 37ºC during 2 hours.

The positive clones were selected and the recombinant protein (63 KDa) fused with a His tag to its N-terminal, was purified through a column of nickel (Qiagen) in denaturalise conditions (8M urea).

Purified recombinant protein, used as antigen to immunise rats according to the protocol of "Antibodies: a laboratory manual (Ed Harlow and David Lane)", was sent to the Animal House IBMB Facility for producing the CG13188 polyclonal rat antiserum.

Results

Chapter I: Identification of genes that mediate *ttk's* function during *Drosophila* tracheal deveolopment

1. GENOME-WIDE ANALYSIS TO IDENTIFY TTK DEPENDENT TRANSCRIPTIONAL REGULATORS

Ttk, as a transcription factor, might regulate the spatio-temporal expression of thousands of different genes that contribute to the proper development and functioning of the organism. It is implicated in a wide range of developmental decisions, ranging from early embryonic patterning to differentiation processes in organogenesis (Harrison and Travers, 1990; Read and Manley, 1992; Guo et al., 1995; Badenhorst, 2001; Araújo et al., 2007). Specifically, we are interested in Ttk as a key player during tracheal development as it is involved in the establishment of tracheal identities, tracheal cell rearrangements, branch fusion, intracellular tube formation and control of tube size (Araújo et al., 2007).

In order to separate specifically the tracheal action of Ttk from its action on other tissues and identify direct or indirect Ttk target genes that could explain the diverse tracheal phenotypes seen in mutant embryos, we combined genome-wide approaches with cell type specific isolation. To this end, we pursued whole-embryo microarray transcriptome profiling on homozygous embryos for the ttk^{D2-50} mutant allele and control embryos at developmental stages 11 to 16. Furthermore, we profiled embryos of the same age range that over-express *ttk* in the domain of *btl* GAL4 driver line, which includes the tracheal system and the midline, together with controls. Whole-embryo expression profiles were combined with transcription profiles of embryonic cell isolates enriched for tracheal cells, and separated by fluorescence-activated cell sorting (FACS).

This analysis provided an *in vivo* census of genes, whose transcription responds to Ttk loss-of-function and misexpression, revealing insights into the mechanisms of *ttk's* function.

1.1 Generation of the genetic fly lines to be transcriptionally compared

We firstly generated the appropriate recombinant fly lines (See materials and methods for further details), which were:

Mutant line: *btl* RFP moe *ttk*$^{D2-50}$ /TM3 twi-GFP

Control line for the mutant experiments: *btl* RFP moe/TM3 twi-GFP.

The control and mutant fly lines generated carried a green fluorescent (GFP)-marked balancer on the third chromosome, which allowed distinguishing the homozygous control or mutant embryos (by the absence of GFP expression) from the heterozygote ones, using the flow cytometer COPAS embryo sorter.

Stocks used to over-express ttk69: "*btl* RFP moe UAS *ttk* 69" x "*btl* Gal4 UAS tau GFP".

The gain-of-function experiment was performed using the Gal4/UAS system (Brand and Perrimon, 1993). In particular, we used the homozygous viable "*btl* Gal4 UAS tau GFP" line to drive the expression of the UAS *ttk* 69 construct in the tracheal system as the *btl* Gal4 line is expressed mainly in the tracheal cells throughout development. Tau is a microtubule-associated protein and is ideal to show the cell morphology (Butner and Kirschner 1991); Callahan and Thomas 1994). Moreover, this construct has Tau protein fused to GFP, which allowed us to detect the over-expression by the presence of GFP in the tracheal cells.

Control line for the over-expression experiments: *btl* RFP moe UAS *ttk* 69.

As control line for this experiment we used the recombinant line generated (*btl* RFP moe UAS *ttk* 69) without crossing it with the *btl* Gal4 line.

In addition, all the generated lines also expressed a membrane tethered red fluorescent protein (RFP)-moesin (moe) under the control of the *btl* enhancer construct (*btl* Gal4 RFP moe) (See materials and methods for details). This allowed to isolated the *btl* positive cells using the FACS technique.

1.2. Validation of the genetic fly lines to be transcriptionally compared

After obtaining the different lines, we examined them *"in vivo"* under a fluorescence microscope, in order to verify that we detected the *btl* positive cells in red (due to the "*btl* Gal4 RFP moe") and that we distinguished the homozygous from heterozygous embryos (by the absence or presence of GFP from the chromosome balancer).

Additionally, we checked that the generated mutants stocks carried the desired mutations. To that end, we immunostained stage 16 embryos for CBP to visualise their tracheal pattern by the accumulation of chitin in the lumen, and for GFP (data not shown) (Figure 44).
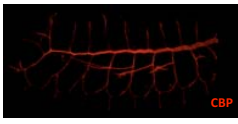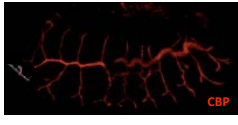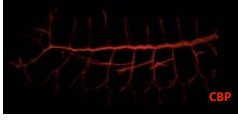
Condition	Fly Stock	Genotype	Tracheal phenotype
Control mutant	btl RFP moe / TM3 twi GFP	btl RFP moe / btl RFP moe	
mutant	btl RFP moe ttk^{D2-50} / TM3 twi GFP	btl RFP moe ttk^{D2-50} / btl RFP moe ttk^{D2-50}	
Control UAS	btl RFP moe UAS ttk69	btl RFP moe UAS ttk 69	
UAS TTK 69	♀ btl Gal4 UAS tau GFP X ♂ btl RFP moe UAS ttk69	btl Gal4 UAS tau GFP / btl RFP moe UAS ttk69	

Figure 44. Experimental conditions, fly stocks and genotypes transcriptionally analysed. The sample genotype and tracheal phenotype refer to the experimental condition that were analysed by microarray gene expression profiling. The tracheal pattern was visualised by the accumulation of chitin in the lumen using CBP (in red). Immunostainings show projections of confocal sections of embryos of the indicated genotypes at embryonic stage 16 in lateral views. Scale bar 100 mm.

Using this test, we observed that the mutant embryos displayed the *ttk* mutant tracheal phenotype (longer tubes manifested in its convoluted aspect and defects in fusion and terminal branch formation (Figure 44) (Araújo et al., 2007), confirming that the lines carried the desired mutant allele. The over-expression of *ttk69* in the tracheal system

also showed the previously characterised phenotype, consisting of a lack of branch fusions (Figure 44) (Araújo et al., 2007).

1.3. Sorting of the different populations to be transcriptionally compared

1.3.1. Isolation of specific embryonic population

To compare the gene expression profile of wild-type embryos with different *ttk* mutants (loss- and gain-of-function) in the two studied conditions (whole embryos and tracheal enriched cell population), we first isolated the homozygous embryos from control and *ttk* mutant (control: "*btl* RFPmoe/ TM3 twi-GFP"; *ttk* mutant: "*btl* RFP moe *ttk*$^{D2-50}$/ TM3 twi-GFP") separated by the absence of GFP. In order to acquire the samples in a massive and automated way, we used the COPAS PLUS embryo sorting technique (See Materials and Methods).

It was not necessary to separate embryos for the over-expression condition, as flies carrying the "*btl* RFP moe UAS ttk69" and the "*btl* GAL4 UAS tau GFP" driver are both homozygous viable.

1.4. Isolation of RNA and microarrays hybridisation

Subsequently, "*btl* RFF moe" positive cells were isolated from selected embryos of all the conditions by FACS ARIAS cell sorting technique. The tracheal system consists of approximately 1600 cells per embryo, however using the protocol that had been previously successfully used in other systems, we were initially only able to isolate a small percentage of the total number of tracheal cells per sorting. It was therefore necessary to set up and optimise the efficiency of the FACS ARIA cell sorting protocol to maximise the number of tracheal cells isolated from each embryo (See Materials and Methods).

1.4. Isolation of RNA and microarrays hybridisation

RNA was extracted in three biological replicates, with the exception of the experiments on the sorted cell populations in the over-expression group, where only two replicates were performed. The samples were hybridized to Affymetrix *Drosophila* Genome 2.0 Arrays (See Materials and Methods).

2. BIOINFORMATIC ANALYSIS OF MICROARRAY EXPERIMENTS

In order to check the quality of our microarray experiment several statistical and bioinformatics analyses were performed. We normalized the data to avoid technological variations and tested the robustness and reproducibility of the arrays. Thus, we normalised the microarray data with genes grouped under two biological processes whose expression is not changed under the conditions studied: oxido-phosphorylation and glycolysis (Table 2).

Glycolisis genes	Oxido-phosporylation genes
CG6058	CG17903
CG17654	CG13240
CG12055	CG7803
CG8893	CG3161
CG3001	CG17369
CG10160	CG11154
CG4001	CG8210
CG8251	CG8996
CG7070	CG6105
CG11661	CG3612
CG17645	CG8764
CG1721	CG9160
CG7010	CG9762
CG7024	CG34073
CG9961	CG34072
CG2964	CG34067
CG5362	CG34069
CG13334	CG34074
CG33791	CG34063
CG10748	CG34085
CG10749	CG34086
CG12229	CG34083
CG11249	CG3283
CG7362	CG9032
CG7998	CG14028
CG7069	CG1088
CG7059	CG4412
CG5432	CG6030
CG1544	CG4307
CG32849	CG2286
CG33102	CG3944
CG3127	CG14724
	CG8189
	CG6343
	CG7610

Table 2. The table showed the group of genes used to normalize the microarray data.

After data normalization (Figure 45) one array experiment from the embryo control, one from embryo mutant and one from cell mutant were behaving differently, being identified as replicates outliers (Figure 45, upper panels). In order to eliminate the significant effect they could have on the data, we filtered them out by excluding them for further analysis. Thus, the remaining arrays were comparable within groups. All experiments for the over-expression situation could be used (Figure 45, above panels). Remarkably, these arrays showed comparable similarity within and between groups to the arrays in the mutant experiments. The complete list of the microarray expression dataset can be accessed at the Gene Expression Omnibus database under the accession number GSE30239 (http://www.ncbi.nlm.nih.gov/geo/).
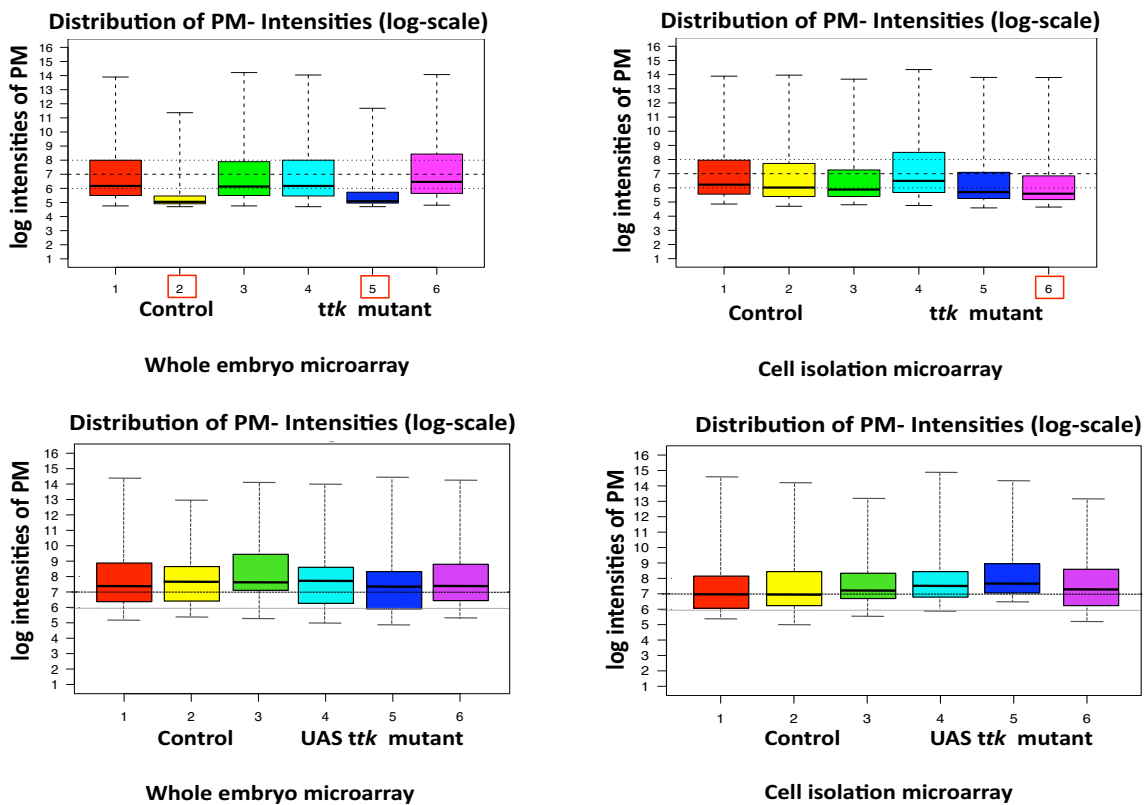
Figure 45. Microarray quality control plots for all the conditions analysed. Notice that even though the data were normalized, some replicate outliers (mark in red in the figure) were present in some array samples.

After data normalization, it is important to highlight that there is not a standard and unique way to analyse the processed data in order to extract the most biologically relevant information out of the microarray data. In our analysis, two parameters primarily determine the potentially significant changes and biological robustness of the

candidate genes that we could obtain: the expected expression change (as indicated by the fold change in signal) and the reliability of the observation (implied in the p-value). So, we defined candidate genes as those with a logFC ≥ 1 (translating to an at least two-fold expression change) at a p-value ≤ 0.05. The analysis with this parameter set identified 761 genes, whose expression were modified (positively or negatively) in response to *ttk* in the cell type specific experiment; and 676 in the mutant embryo experiment, with an overlap between the mutant conditions of 182 genes (positively or negatively) that corresponds to a 24%. An identical parameter set was used for the over-expression experiment, identifying 322 genes, that exhibited either increase or decrease significative changes in the over-expression cells condition, and 397 genes in embryos, with an overlap between experiments of 72 genes (22%) (Figure 46).
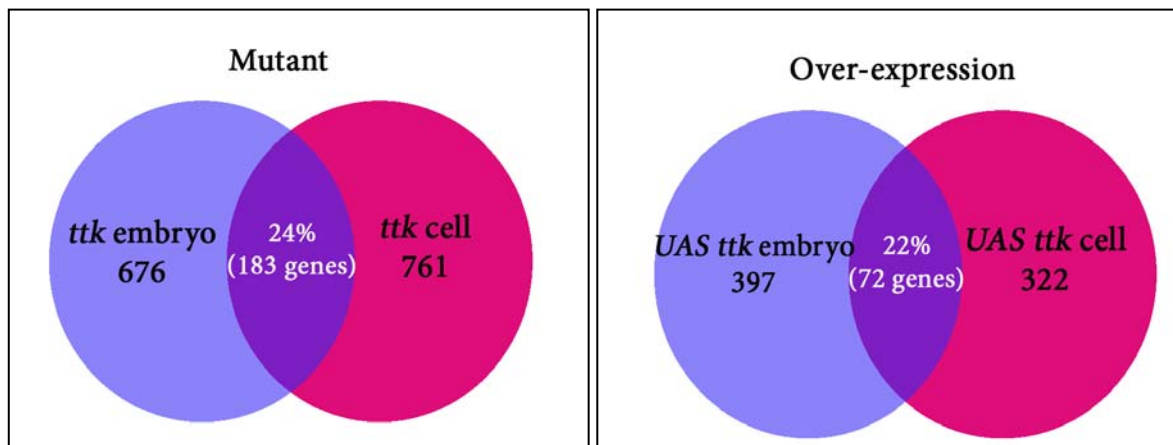
Figure 46. Numbers of genes differentially expressed: Diagram showing the numbers of transcripts that were differentially expressed at the significance level of p<0.05, in the different *ttk* mutant conditions (loss-of-function, left panel; and gain-of-function, right panel) in both conditions studied (whole-embryo, in blue; and cell specific, in red). Note the overlap that the comparison between whole-embryo and cell specific microarrays gave (pink).

Using our criteria for candidate genes (logFC ≥ 1 and p-value ≤ 0.05), we represented in a simply diagram the number of genes differentially expressed in both analysed conditions (Figure 46). The immediate expected reduction in the number of differentially expressed genes obtained through the cell sorting technique in comparison to the whole-embryo arrays does not seem apparent (Figure 46, pink circles vs. purple circles in both panels). In order to see whether the representation of the results by these numerical data graphics were masking Ttk tracheal signature or were the reflection of its multiple functions, we faced the data validation by different methods.

To better detect the Ttk tracheal specific signature, we evaluated the effectiveness of the cell specific strategy by a computational approach, making use of the high-throughput *in situ* hybridisation database at the Berkeley *Drosophila* Genome Project (BDGP). So far, the expression of 6138 genes has been reported during *Drosophila* embryogenesis (Tomancak et al., 2007). The computational approach we undertook consisted in classify the signal intensity data registered in the control cell specific microarrays (from the mutant and over-expression conditions) in steps of approximately 0.5 arbitrary intensity units, covering the embryonic developmental stages of 0 to16 of the microarray. Then, for each signal group, we determined, according to BDGP available expression information, how many genes were expressed in the tracheal system or midline (as the *btl* Gal4 driver used is expressed under those domains), ubiquitously expressed, expressed elsewhere in the embryo or not expressed (Figure 47).
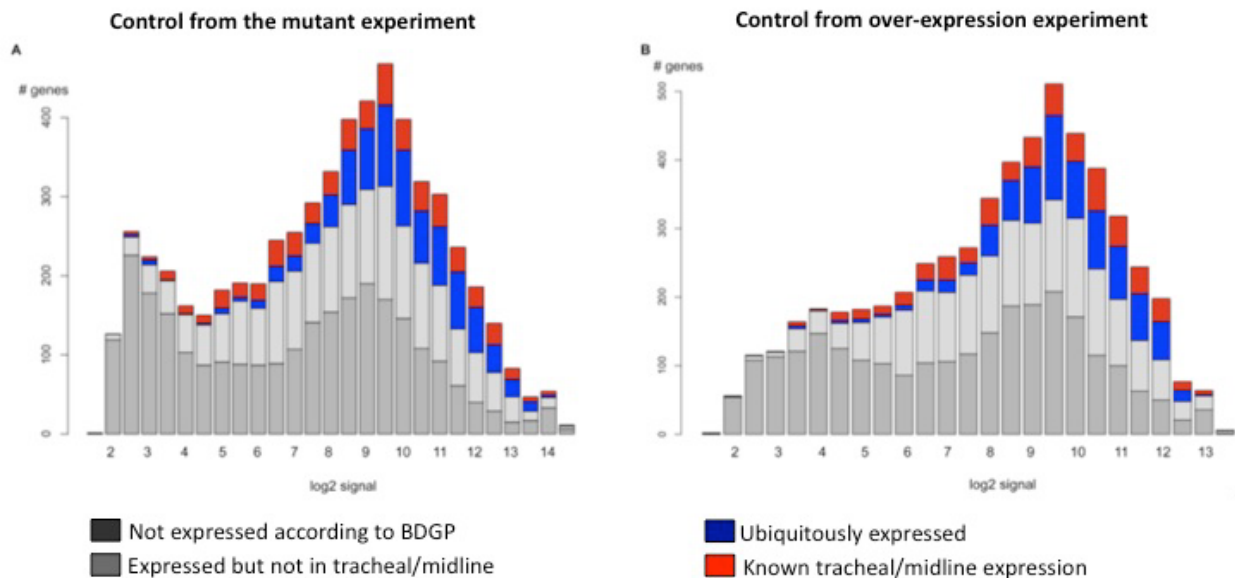
Figure 47. Histogram representing the spatial gene expression pattern in different microarray signal strength categories. Gene expression profiles from enriched cell populations for the control group in the (**A**) mutant and (**B**) over-expression are shown. Within the signal intensity histogram (x-axis: bins of $\log_2$ signal strength, y-axis: number of genes), the proportion of genes falling into one of four different spatial gene expression categories is shown: genes with tracheal or midline expression (red), genes with ubiquitous expression (blue), genes with expression elsewhere (light gray), genes not expressed according to the BDGP *in situ* database (dark gray).

Surprisingly, we found a large number of genes expressed in the purified cell population, that according to the BDGP gene expression database should not be expressed in the embryo (Figure 47, dark grey bars), accounting for almost half of the genes detected in the sorted cell population. Of the group of genes known to be

expressed during the relevant stages of embryogenesis, about half are specific for the midline and/or trachea (Figure 47, red bars), as expected because the *btl* driver its known to be expressed in those tissues, while the other half, should not be present if the preparations were pure (Figure 47, light gray bars).

Although false-negatives annotations from BDGP and technical aspects (such sample acquisition or data processing) could explain the results, the expression domain of the driver used must also be considered. Its known that the *btl* gene is expressed both in the tracheal system and in the ventral midline (Glazer and Shilo, 1991), but manual inspection of the *btl* RFP moe construct further confirmed detectable levels of expression in various other cell types during tracheal developmental stages (For instance, lateral ectoderm, endoderm, amnioserosa, others) (Figure 48).
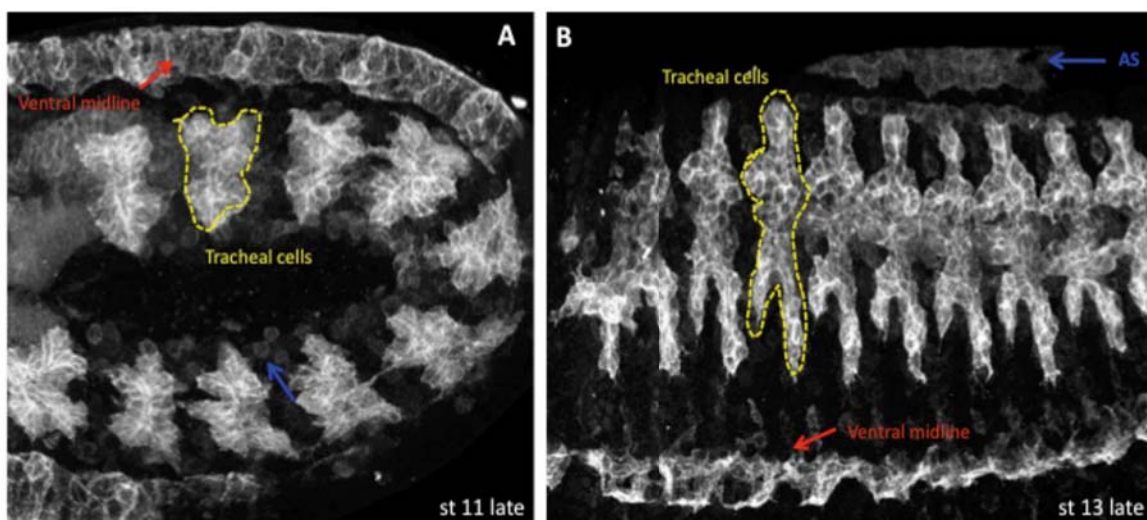
Figure 48. Developmental profile of *btl*Gal4 expression in *Drosophila* embryos. Note the expression of *btl* in the tracheal cells (marked in yellow), ventral midline (red arrows), amnioserosa (AS, blue arrows) and other cells (blue arrows) at early (**A**) and late (**B**) embryonic stages.

To further confirm the reliability of Ttk tracheal signature obtained in the cell type microarrays, we determined the contribution of tracheal genes in the sorted cell population by checking whether these arrays were more enriched in tracheal genes in comparison to the whole-embryo ones (Table 3, upper).

Comparison of gene expression values of sorted cell vs. whole embryos in **mutant experiments:**

Symbol	ID / function	Embryo	Cell	Diff.
trh	FBgn0003749 / key regulator of tracheal development	9,1	11,3	2,2
btl	FBgn0005592 / receptor in trachea and midline	7,7	9,4	1,7
dys	FBgn0039411 / specifically expressed in fusion cells	4,3	5,5	1,2
ttk	FBgn0003870 / expressed in trachea and most of the re	9,9	11,2	1,3
sim	FBgn0004666 / key regulator of the midline	7,4	8,7	1,3
twi	FBgn0003900 / key regulator of the mesoderm	8,7	7,1	-1,6
Mef2	FBgn0011656 / key regulator of muscle development	10,2	10,9	0,7
Srp	FBgn0003507 / broad mesodermal, a fatbody marker	8,1	11,1	3,0
Adp	FBgn0000057 / a fatbody/yolk marker	8,3	8,6	0,4

Comparison of gene expression values of sorted cell vs. whole embryos in **over-expression:**

Symbol	ID / function	Embryo	Cell	Diff.
trh	FBgn0003749 / key regulator of tracheal development	11,4	13,7	2,3
btl	FBgn0005592 / receptor in trachea and midline	9,5	12,2	2,7
sim	FBgn0004666 / key regulator of the midline	9,1	11,5	2,4
twi	FBgn0003900 / key regulator of the mesoderm	9,4	7,2	-2,2
Mef2	FBgn0011656 / key regulator of muscle development	8,4	7,1	-1,3
Srp	FBgn0003507 / broad mesodermal, a fatbody marker	10,5	12,5	2,0

Table 3. Raw signal intensities for embryos or sorted cells from *ttk* mutant experiments (upper panel) and *ttk* over-expression experiments (lower panel) are shown for selected marker genes. The difference reflects the enrichment of the marker in comparison to entire embryos. It is noteworthy that these values are from a log2 scale, meaning that a difference of 2 refers to an actual increase of 4-fold

We found by this analysis that the master tracheal gene *trh* shows a two-fold enrichment in the sorted cell population in comparison to whole embryos in both conditions analysed. Moreover, other tracheal genes such as *btl* and *dys*, were also enriched in the cell microarray (Tables 3, marked in red). In addition, the expression of other tissue markers, such as mesodermal, muscle or yolk markers was highly reduced in the sorted cell population in comparison to whole embryos in both conditions studied (Tables 3, marked in purple).

All these different tests emphasise the merit of the cell enrichment strategy as a powerful tool in the search for transcription factor targets because, while still not possible to isolate a pure population of embryonic tracheal cells, it was clearly confirmed the significance of the dataset. Moreover, it provides entry points for the investigation of the targets of Ttk regulation in further processes.

3. MICROARRAY DATA ANALYSIS

3.1. The *in vivo* transcriptome confirms *in vitro* results and is backed by known biology

In the course of our study, Reddy and colleagues published an *in vitro* expression profile on S2 *Drosophila* cell line after *ttk* knockdown by RNAi (Reddy et al., 2010). Using our criteria for candidate genes (logFC $\geq$ 1 at a p-value $\leq$ 0.05), their screen produced 1380 candidate genes. Although the absolute overlap between their candidate gene list and our lists is small, the degree of overlap between those experiments were statistically significant (Table 4) indicating that similar trends were detected in both datasets.

		S2 mutant		UAS, cells		UAS, embryos		mutant, cells		mutant, embryos	
		down	up	down	up	down	up	down	up	down	up
	FlyMine genes	620	760	96	246	73	326	254	515	220	422
S2 cells	down	-	1	1	22 (9.7×10⁻⁴)	3	7	21 (3.3×10⁻³)	14	16 (2.5×10⁻³)	18
	up	-	-	5	12	2	9	10	79 (<10⁻¹⁶)	13	35 (8.4×10⁻³)
UAS, cells	down	-	-	-	0 (<10⁻¹⁶)	21 (<10⁻¹⁶)	2	7 (4.5×10⁻⁴)	13 (1.6×10⁻⁵)	4 (2.0×10⁻²)	7 (1.0×10⁻³)
	up	-	-	-	-	0	51 (<10⁻¹⁶)	17 (9.4×10⁻⁷)	30 (4.7×10⁻⁶)	14 (1.2×10⁻⁵)	21 (9.6×10⁻⁶)
UAS, embryos	down	-	-	-	-	-	0	4 (1.2×10⁻²)	10 (9.3×10⁻⁵)	1	2
	up	-	-	-	-	-	-	18 (1.3×10⁻⁵)	23 (1.6×10⁻⁵)	10 (1.8×10⁻²)	7
mutant, cells	down	-	-	-	-	-	-	-	0	35 (<10⁻¹⁶)	0
	up	-	-	-	-	-	-	-	-	4	143 (<10⁻¹⁶)
mutant, embryos	down	-	-	-	-	-	-	-	-	-	0
	up	-	-	-	-	-	-	-	-	-	-

Table 4. Overlap in candidate gene lists from different transcriptomes. The table shows the number of candidate genes observed under each experimental condition. The degree of overlap is shown in absolute numbers, overlaps with statistically significant p-values are highlighted in bold.

3.2. Genome-wide functional analysis

We were also interested in genome-wide functional analysis to find sets of clustered genes, which in single-gene analysis may be missed, with important effects on general processes. To that purpose, we took advantage of the Gene Ontology (GO) annotations that describe gene products in terms of their associated biological processes, cellular components and molecular functions, aiming to highlight the most representative biological functional aspects of our dataset. Consistent with Ttk being a transcription factor involved in a wide range of biological processes, the GO analysis classified our dataset under diverse functional categories. Thus, several previously known Ttk requirements were found in different biological process (Figure 49).
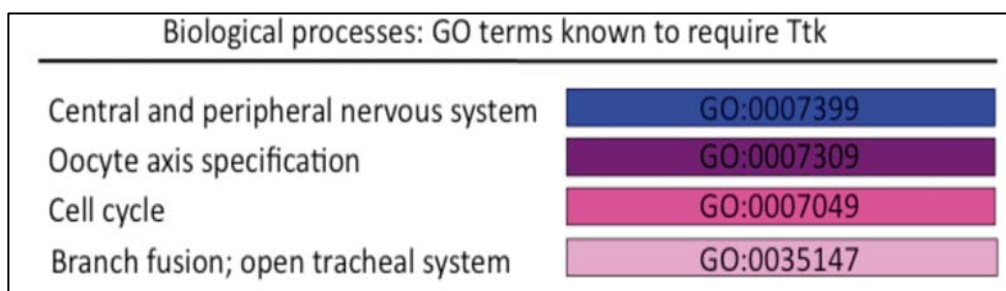
Figure 49. Gene Ontology categories regarding biological process previously known to require Ttk

Ttk was first described in the nervous system (Salzberg et al. 1994; Giesen et al. 1997; Badenhorst et al., 2001) and accordingly, a large variety of GO terms implicated in "central and peripheral nervous system development" (GO:0007399) were found (Figure 49, blue bar). It is also known that Ttk is required in oogenesis and cell cycle (Badenhorst, 2001; Baonza et al., 2002; Althauser et al., 2005; Audibert et al., 2005), so we also found several genes classified under the term "oocyte axis specification" (GO:0007309) (Figure 49, purple bar) and "cell cycle" (GO:0007049) (Figure 49, dark pink bar). Moreover, previous work from our lab indicated that Ttk plays multiple relevant roles in the formation of the *Drosophila* tracheal system (Araújo et al., 2007). Accordingly, the GO "branch fusion; open tracheal system" (GO:0035147) terms appeared significantly changed in our dataset (Figure 49, light pink bar).

3.3. Identification of putative Ttk target genes involved in chitin metabolism

Interestingly, as our work had previously implied a connection between Ttk function and cuticle formation (Araújo et al., 2007), we found in the course of GO analysis, a interesting range of GO terms involved in 'chitin metabolic process' being over-represented (GO0006030) in our dataset (Figure 50, yellow bar).

Figure 50. The figure shows the three most over-represented Gene ontology metabolic process

Our microarray results connect Ttk regulation not only to several downstream genes classified under the GO term "chitin metabolism", but also to "septate junction organization" (GO:0005918), both gene groups might be involved in the control of tube size as previously reported (Wu and Beitel, 2004; Schottenfeld et al., 2010). Moreover, it is known that *ttk* regulates tracheal tube extent (Araújo et al., 2007). As we were particularly interested in genes involved in the tracheal system, genes annotated under these categories came to our immediate attention, because in many cases they show inverse regulation in the mutant and over-expression situation. Thus, for further functional analysis we selected genes differentially expressed in our *ttk* experimental assays that participate in chitin metabolism and SJ organization, as they might be mediating Ttk's tube size control function.

3.4. Chitin metabolic genes show tube length phenotypes consistent with *ttk* mis-expression

Among all the genes differentially expressed in our microarray data that were classified under chitin metabolism, cuticle development and septate junction component categories, we selected for further analysis 11genes that are summarized in Table 5.

Selected downstream t*tk* targets for further analysis	
Chitin metabolisim	Cht9
	Cht5
	Cht2
	Cda4
	Idgf5
	Idgf3
	CG7715
Cuticle development	Cuticular protein (Cpr) 78Cb
SJ components	dlg
	Scrib
	Vari

Table 5. Selected downstream targets of *ttk* for further functional analysis. Note that they are classified under three GO terms: chitin metabolism, cuticle development and septate junction components.

We first validated the expression changes of these putative *ttk* targets obtained in the microarray experiment by performing quantitative real-time polymerase chain reaction (qPCR) analysis (Table 6).

	Gene name	ttk^{D2-50} embryos				ttk over-expression embryos			
		Microarray log FC	p-value	qPCR FC	p-value	Microarray log FC	p-value	qPCR FC	p-value
Chitinases	Cht2	−1.47 ↓	1.65E^{-01}	−5.5 ↓	<0.05	0.22	2.53E^{-02}	2.4 ↑	<0.05
	Cht5	−1.27 ↓	2.64E^{-02}	−10.0 ↓	<0.05	0.85 ↑	1.60E^{-04}	2.1 ↑	<0.05
	Cda4	−2.03 ↓	1.59E^{-01}	−5.3 ↓	<0.05	−0.02	9.36E^{-01}	−1.5 ↓	<0.05
	Idgf3	−1.96 ↓	2.53E^{-02}	−2.5 ↓	<0.05	0.29	5.91E^{-01}	ND	
	Cht9	−0.61	2.58E^{-01}	ND		2.41 ↑	0.00E^{+00}	4.7 ↑	<0.05
	CG7715	−1.46 ↓	2.68E^{-01}	−15.6 ↓	<0.05	1.42 ↑	4.44E^{-02}	2.9 ↑	<0.05
	CG8460	1.67 ↑	1.79E^{-02}	5.4 ↑	<0.05	0.18	8.11^{-02}	ND	
	Idgf1	−0.70	2.83E^{-01}	−9.00 ↓	<0.05	2.00 ↑	2.83E^{-02}	10.0 ↑	<0.05
Cpr	Cpr78Cb	−2.08 ↓	3.20E^{-02}	−15.0 ↓	<0.05	0.65	3.37E^{-01}	ND	
SJ	dlg1	1.57 ↑	9.15E^{-03}	1.61 ↑	<0.05	−0.015	1.03E^{-01}	ND	
	Scrib	0.50	5.00E^{-01}	ND		1.57 ↑	3.35E^{-03}	1.3 ↑	<0.05
	vari	−1.35 ↓	4.91E^{-02}	−6.6 ↓	<0.05	−0.015	2.32E^{-01}	ND	

Table 6. Validation of microarray candidates by quantitative PCR. Values obtained in the microarray and qPCR validation experiments performed on selected genes identified by microarray analysis in *ttk* mutant and *ttk* over-expression in whole embryo conditions, at developmental stages 11–16. Note the correlation in the levels and direction of change between the two experiments. Abbreviation: ND: Not analysed; SJ: Septate junctions; Cpr: Cuticular protein

We analyzed eight genes assigned to the GO term 'chitin metabolism'. We confirmed the expected gain or loss of RNA abundance in seven candidate genes in mutant embryo conditions. Furthermore, we validated the directional change of five of them in *ttk* over-expression experiments. Remarkably, our qPCR experiments confirmed minor transcriptional changes (absolute logFC<1) for several candidate *ttk* target genes (For instance, Idgf1 and Cda4). One gene annotated with "cuticular protein" was also analyzed and validated (Cpr78Cb). Moreover, three genes annotated with 'septate junction' were also analyzed by qPCR. Also in this case, the qPCR results confirmed the transcriptional changes and the direction in the change that were observed in the microarray analysis. This established that our microarray data could be used as a reliable platform for further analysis.

To understand whether these *ttk* targets can mediate, at least in part, the function of *ttk* in tube size regulation we performed a functional analysis. The approach we undertook consisted in the analysis of the length of the dorsal trunk of mutant embryos for the selected genes and compared it to an internal control. We used either loss-of-function alleles, when available, or express UAS-RNA interference (RNAi) (Kennerdell and Carthew, 1998; Misquitta and Paterson, 1999) in the tracheal system using the *btl*-GAL4 driver to down-regulate their activity. We stained embryos with CBP to visualise the luminal chitin filament and calculated their tube size by adapting a previous

published protocol (Laplante et al., 2010). Normalized measures of dorsal trunk length were obtained and statistically compared (See Material and Methods). Interestingly, five out of the eleven genes tested exhibited a tube size phenotype (Figure 51B-F in comparison to 51A).

Figure 51. Analysis of the effect of putative *ttk* targets on tube length. (**A–F**) Projections of confocal sections showing dorso-lateral views of embryos at embryonic stage 16, labeled to visualize the chitin filament with CBP. Anterior is to the left and dorsal is up in all panels. The RNAi lines or loss-of-function alleles used were the following: (**B**) Cpr78Cb: RNAi 107767; (**C**) vari3953; (**D**) Scrib RNAi; (**E**) Cda4: RNAi 36106; (**F**) dlg1: RNAi 1076. RNAi lines were driven with btl-GAL4 UAS-tau-GFP. Note the enlarged DTs in embryos from B to F as compared to **A** (control); (**G**) Histogram showing tracheal tube lengths. For each gene we compared the experimental situation that we called E to its internal control that we called C. E corresponds to the loss-of-function situation, either RNAi expressed with btl-GAL4 UAS-tau-GFP, or the homozygote mutant in the case of loss-of-function alleles; C corresponds to heterozygote embryos in the case of loss-of-function alleles or to the RNAi line alone. n indicates the number of embryos that were measured. The differences in length between the experimental and control conditions are significant at $p<0.05$. Scale bar 100 mm.

Among them, *vari* and *disc large* (*dlg1)* loss-of-function mutant alleles and four out of ten candidates tested by RNAi expression produced a tube size phenotype. *Vari, Scrib and dlg*1, which encode for SJ proteins, were expected (Figure 51C, 51D and 51F) (Jiang et al., 2010) but the Cpr78Cb and *Cda4* (Figure 51B and 51E) were genes not previously described in controlling tracheal tube growth. The down-regulation in the trachea by RNAi of the other six candidate genes did not result in tube size defects. These results indicated that either the down-regulation of the genes do not affect the control of tube size (because the gene is not required or due to functional redundancy),

or that the strength of the interfering lines is not sufficient to generate a visible effect. That is the case for instance of Cht2, which has been shown to generate tube size defects upon over-expression (Tonning et al., 2005). Nevertheless, the fact that some RNAi lines produce extra-long tracheal tubes already establish a link between Ttk and tracheal tube size genes.

3.5. Tramtrack feeds into various developmental programs in the tracheal system

We showed in our previous work that Ttk regulates different morphogenetic events during *Drosophila* tracheal development (Araújo et al., 2007). One of the tracheal functions known to require Ttk is the fusion process. Thus, we examined genes with described functions in this process for transcriptional changes in our microarray dataset. As expected, we found that several genes implicated in the fusion process were differentially expressed. For instance, the key transcription factor gene *escargot*, *headcase* (*hdc*) and CG15252 fusion genes showed a significant transcriptional response in the enriched cell population after *ttk* over-expression. Moreover, we validated by qPCR the transcriptional changes observed in the microarray (Table 7).

On the other hand, an interaction between Notch and Ttk in the tracheal system has been previously reported (Araújo et al., 2007). So, we checked in our dataset for Notch pathway components or interactors. We found differentially expressed several genes that are either targets of the Notch downstream effectors Su(H) (*HLHmdelta*, *scute (sc)*, *achaete (ac)*, *E(spl)*, *HLHm4*) or known interactors of the transcription complex (Hairless) (H), or factors downstream of H function (for instance, *Bearded*). Importantly, many of these genes showed significantly decreased expression in the over-expression situation, and increased expression in the mutant situation. We confirmed also by qPCR the changes observed (Table 7).

Gene name	$ttk^{\Delta2-50}$ embryos				ttk over-expression embryos			
	Microarray log FC	p-value	qPCR FC	p-value	Microarray log FC	p-value	qPCR FC	p-value
Hdc	2.55 ↑	$3.78E^{-04}$	10.0 ↑	<0.05	0.25	$1.00E^{-01}$	ND	
sc	1.86 ↑	$9.75E^{-02}$	1.6 ↑	<0.05	−1.29 ↓	$4.36E^{-02}$	−2.8 ↓	<0.05
ac	1.21 ↑	$3.12E^{-01}$	−2.6 ↓	<0.05	−1.80 ↓	$4.88E^{-02}$	−2.0 ↓	<0.05
H	2.27 ↑	$4.83E^{-02}$	1.5 ↑	<0.05	−0.15	$2.34E^{-01}$	ND	

Table 7. Validation of microarray candidates by quantitative PCR. Values obtained in the microarray and qPCR validation experiments performed on selected genes identified by microarray analysis in *ttk* mutant and *ttk* over-expression in whole embryo conditions, at developmental stages 11–16. Note the correlation in the levels and direction of change between the two experiments. ND: Not analysed.

While the role and mechanism of Ttk in the regulation of these Notch target genes is not clear, these results may provide a first explanation of our previous observation.

Finally, during the GO analysis we noticed an enrichment of different GO categories, which could potentially be involved in tracheal development (Figure 52).
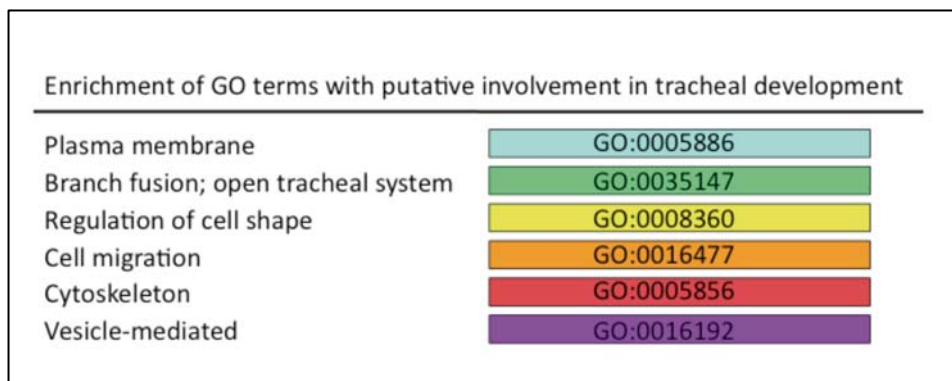
Figure 52. Selected GO terms with putative involvement in tracheal development.

These results confirmed the requirement of Ttk in various developmental programs during tracheal system development.

3.6. Stage-specific effects of Ttk regulation

Our microarray analysis and the validations of several candidates by qPCR generated results not always easy to interpret. Many genes showed unidirectional transcriptional responses (either up or down) to Ttk mis-expression conditions (either mutant or over-expression). For instance, the expression of Cda4 gene goes down in both mutant and over-expression conditions. But, interestingly, we found also some inconsistencies in the mode of transcriptional regulation (either up or down) between the microarray data and the qPCR experiments, as in the case of *acchaete* (*ac*) (Table 7). These results could be explained considering that Ttk itself exhibits different time-specific roles (For instance, first activating, then repressing), which cannot be resolved in our samples because microarrays were performed on samples comprising wide ranges of embryonic developmental stages from stage 11 to stage 16. Therefore, we selected three genes (*bnl*, *Cda4* and *ac*) to probe their expression profile on *ttk* mutant embryos

(in comparison to their controls) at stages 11 to 13 and at stages 14 to 16 by stage-specific qPCR (Table 8).

Gene symbol	Microarray logFC (stage 11-16)	p-value	qPCR (stage 11-13)	p-value	qPCR (stage 14-16)	p-value
ac	1.21	3.12E^{-01}	-5.20	<0,05	3.83	<0,05
bnl	-0.27	1.82 E^{-01}	-1.62	<0,05	-2.32	<0,05
Cda4	-2.03	1.59 E^{-01}	-1.19	<0,05	-1.30	<0,05

Table 8. Analysis of stage-specific regulation by quantitative PCR. The table shows the values obtained in the microarray (embryos at stages 11-16) and in the stage-controlled qPCR experiments (embryos at stages 11-13 and at stages 14-16). The analysis was performed on selected genes in whole embryo conditions in *ttk* mutants vs. control. Note the resolution of the stage-specific qPCR experiments.

A down-regulation of *Cda4* and *bnl* at the different stages tested were observed. Note that although by microarrays the significative expression changes of the expected Ttk's target *bnl* was not corroborated, we confirmed it by qPCR (Table 8). Moreover, we found that Ttk regulates *ac* differently at early or late embryonic stages (promoting or inhibiting its expression), indicating that Ttk can exert different stage-specific modes of action.

3.7. Tramtrack might directly regulate the expression of tracheal target genes

The broad range of biological functions could be either direct or indirect consequences of Ttk's role as a transcription factor. As an initial step towards asserting this question, we performed an *in silico* approach to detect putative direct targets of Ttk. The approach consisted in searching, among the selected genes, binding sites for Ttk. The modENCODE project has recently published such data for *Drosophila* embryos between stages 1-15, thereby capturing a significant proportion of tracheal development. Manual inspection of our candidate genes suggests that the majority of them possess significant Ttk binding (Figure 53).
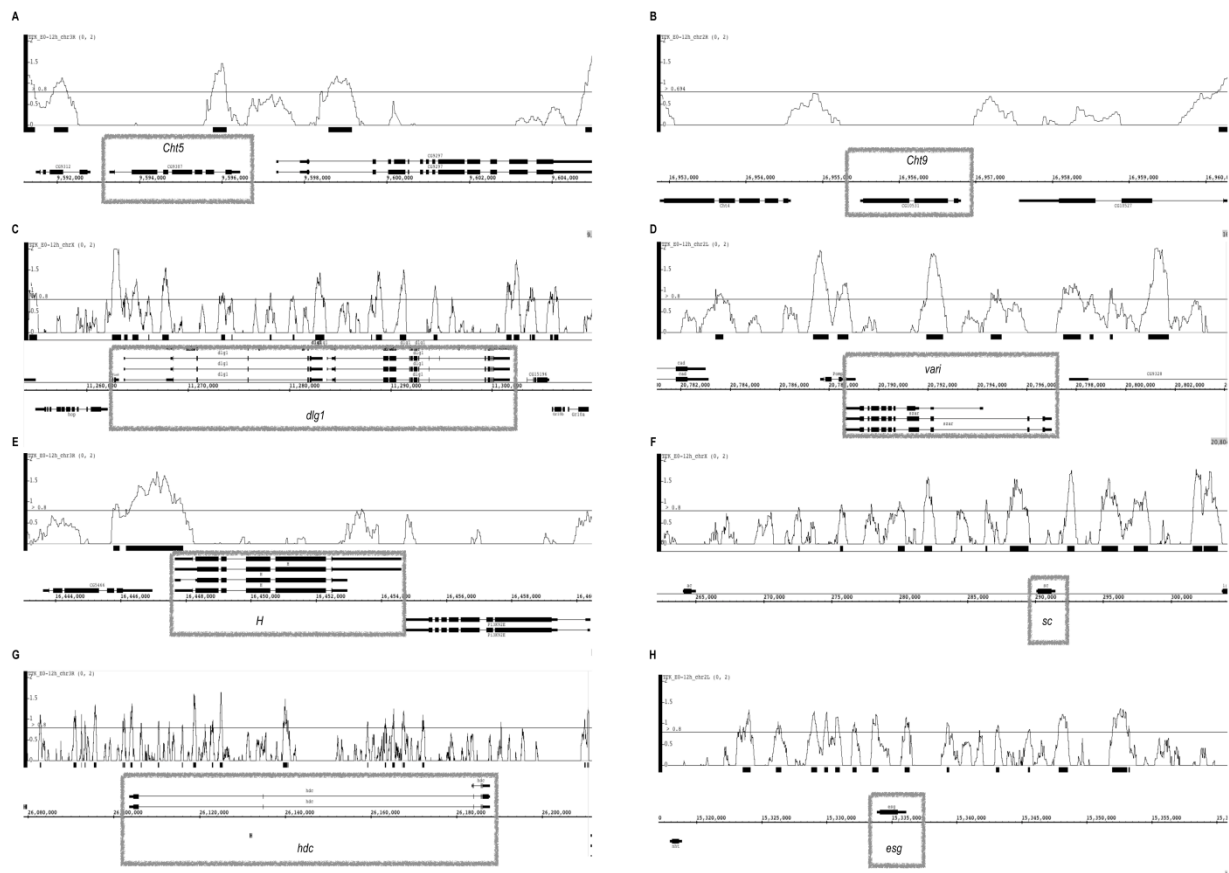
Figure 53. Chromatin immunoprecipitation (ChIP) enrichment for Ttk as determined by modENCODE. Panels (**A–H**) show ChIP profiles along the chromosomal axis for candidate genes (boxed) obtained by gene expression profiling. We assume measurable enrichment at log2(0.8), or 1.5-fold enrichment over background levels (indicated by the gray horizontal line. Genes plotted above the coordinate line are encoded on the plusstrand, and those below the coordinate line are on the minus-strand. It is noteworthy that Ttk enrichment does not necessarily occur near the 5'-end of these genes, but can also occur in intronic regions as frequently seen also for transcription factors.

This direct input from Ttk concerns genes involved in chitin metabolism (Figure 53A), septate junction formation (Figure 53C and 53D), Notch signalling (Figure 53E and 53F), and fusion cell fate (Figure 53G and 53H). It is noteworthy that Ttk binding is not a default, and that some of our candidate genes do not show significant binding during embryonic development, for instance: Cht9 (Figure 53B).

Regarding the apparent importance of Ttk in the regulation of genes involved in chitin metabolism, we performed a global analysis of Ttk binding using the modENCODE project data. This project performed Chromatin immunoprecipitation (ChIP) assay to probe different protein-DNA interactions. Therefore, they have identified specific genome regions that are associated with a particular protein, for instance Ttk (Figure

54).
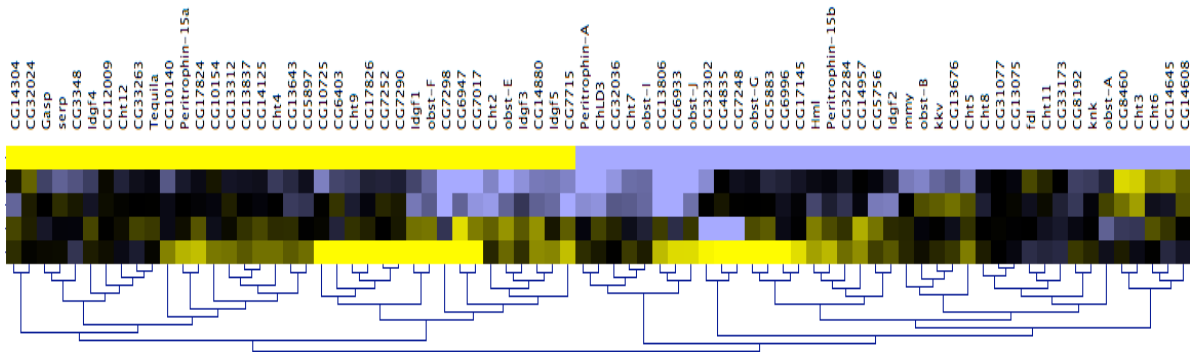
Figure 54. Cluster diagram of genes involved in chitin metabolic processes. Genes are clustered according to the gene expression changes in response to Ttk-mis-expression (from bottom to top: over-expression in cells, over-expression in embryos, mutant cells and mutant embryos) as well as Ttk binding sites according to modENCODE dataset (blue indicates significative presence of binding sites and yellow not significative presence of binding sites).

We found that 40 of 77 chitin metabolic genes showed significant Ttk ChIP enrichment. Within this group of genes with Ttk enrichment (Figure 54, marked in blue), there are a higher proportion of genes with absolute logFC $\geq$ 1 as transcriptional response in at least one of the experimental conditions probed with our microarrays (70% versus 51%), although this difference is not statistically significant (χ^2 test, p = 0.11).

The observation that about half of the genes without Ttk enrichment (Figure 54, marked in yellow) showed a transcriptional response, suggests that Ttk may indirectly moderate their expression via yet unknown additional regulators. However, the result of many target genes having Ttk binding sites (Figure 54, marked in blue) also suggests that Ttk mediates its function not only as a coordinator of other transcriptional regulators, but feeds in directly to the target genes immediately involved in the cellular response. It remains to be shown whether this role requires additional cofactors, or is primarily dependent on Ttk binding.

4. MICROARRAY CANDIDATE GENE APPROACH

We focused on a candidate gene approach as an attempt to identify new genes that mediate *Ttk'*s function during *Drosophila* tracheal system development. To that end, we grouped interesting putative candidate target genes in a new sub-list by selecting those genes differentially expressed in *ttk* miss-expression conditions that were also associated with a tracheal expression pattern and/or have an interesting molecular domain predicted. This list is summarised in Table 9.
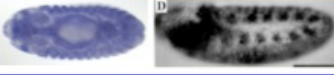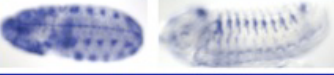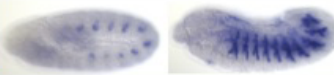
CANDIDATE	EXPRESSION LEVEL (log FC)	CHANGE DIRECTION	GENETIC BACKGROUND	BDGP	PROTEIN DOMAIN
CG11370	-1,52 4,82 3,66	Down Up Up	UAS ttk cels ttk cels ttk embryo		
CG 5873	-2,68 -1,46	Down Down	ttk cels ttk embryo		Peroxidase
NXF2	1,26 1,64	Up Up	ttk cels ttk embryo		Nuclear export factor
CG13188	-1,19	Down	ttk embryo		MAD (Smads)
Tm1	1,07	Up	ttk embryo		Tropomyosin
CG13333	-1,31 -1,23	Down Down	UAS ttk cels UAS ttk embryo		
CG18549	-1,3	Down	ttk cels		DUF 895: Unknown function

Table 9. Selection of genes, which are differentially expressed in our microarray, based on different criteria.

Based on these single-gene selection criteria, seven genes were ranged. Five out of seven are uncharacterised genes named: CG15873, CG1370, CG13333, CG13188 and CG18549. The other two are: *nuclear RNA export factor 2* (*nxf2*) and *tropomyosin 1*(*Tm1*). All of them show interesting tracheal expression patterns according to BDGP or literature.

Chapter II: Analysis of *ttk's* targets

1. CG13188 FUNCTIONAL CHARACTERISATION

1.1. Selection criteria

We selected one of the *ttk* target genes identified in our screen that is referred in FlyBase by the symbol Dmel\CG13188 (FBgn0033668). Two features made this gene an interesting candidate for further functional studies. First, the gene is expressed in the tracheal system (BDGP). Secondly, it encodes, according to the protein family website (Pfam), a protein with a putative Mad homology 2 (MH2) domain typically found at the carboxy terminus of Smad proteins. Interestingly, Smad proteins are the downstream effectors of the Dpp signalling pathway.

1.2. Validation of CG13188 differential expression

The CG13188 locus encodes two alternatively spliced transcripts designated as CG13188-RA (FlyBase ID: FBtr0088039) and CG13188-RB (FlyBase ID: FBtr0088040). We validated the expression change of CG13188 gene variants observed in *ttk* mutant embryos by qPCR (Figure 55). For that, we designed sets of primers pairs according to two different strategies: One set of primers was isoform-specific in order to amplify each alternatively spliced CG13188 gene variants individually. Another set of primers provided no variant-specificity, being common for both transcripts.
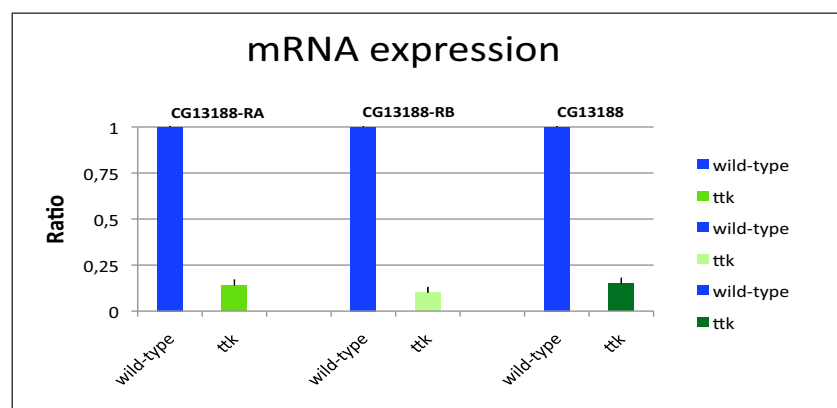
Figure 55. Graphic showing the significant different relative expression of CG13188 gene variants in *ttk* mutants in comparison to wild-type embryos at developmental stages 11-16.

As expected, we found that both CG13188 transcripts were significantly down-regulated in *ttk* mutants in agreement with our whole embryo microarray data.

2. TEMPORAL AND SPATIAL EXPRESSION OF CG131888

2.1. *In situ* hybridisation pattern

One of the interesting features of the candidate CG13188 was the specific tracheal expression pattern reported by BDGP (Figure 56).
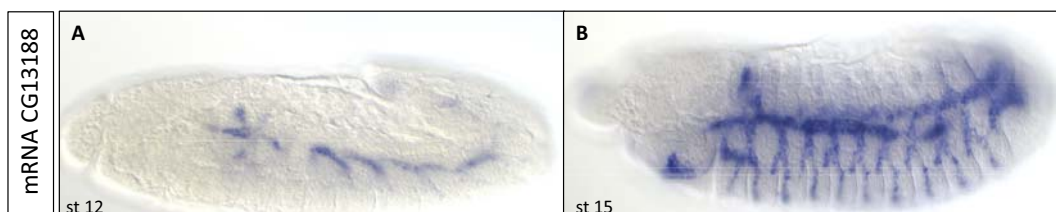
Figure 56. CG13188 *in situ* hybridisation embryonic expression pattern. CG13188 mRNA is first detected at stage 12 in the visceral branches but through development its expression is detected in all the tracheal branches (Adapted from BDGP website).

According to the database, CG13188 gene expression begins to be zygotically transcribed at embryonic stage 12. Its transcript is detected in the cytoplasm of the visceral branches cells but it is excluded from the rest of the tracheal tree (Figure 56A). Then, as development proceeds, the gene is expressed in all tracheal branches (Figure 56B). Moreover, it has been annotated that CG13188 is expressed also in other embryonic tubular organs such as the hindgut and salivary glands. At larval stages it is highly expressed in the tracheal system, central nervous system, hindgut, salivary glands and carcass, whereas in the adult it is expressed at low levels in the hindgut, eye, brain and head.

This tracheal expression pattern suggested a role for CG13188 in tracheal system development and prompted us to study its function.

2.2. Generation of an antibody against CG13188 protein

To further corroborate and refine CG13188 expression, we generated an anti-CG13188 antibody by immunizing rats with a recombinant CG13188-His tag fusion protein (See Materials and Methods). We immunostained wild-type embryos with the generated antibody to define the spatio-temporal and sub-cellular localisation of CG13188 protein (Figure 57).
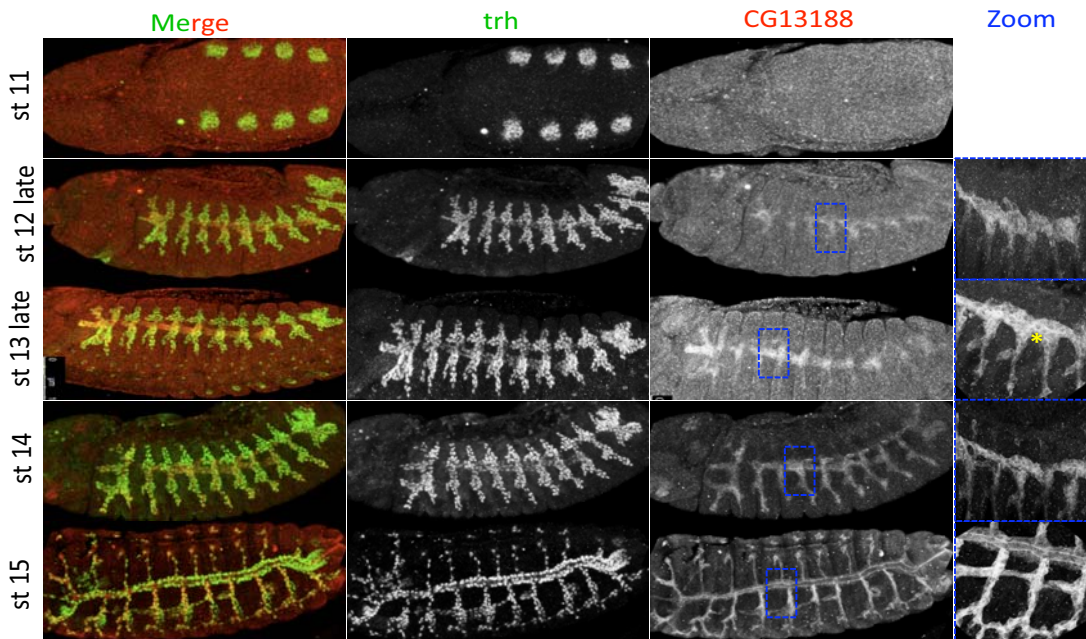
Figure 57. Localisation of CG13188 protein during embryonic tracheal development. Double staining of CG13188-Ab and the nuclear tracheal marker Trachealess (Trh) revealed a dynamic spatial and temporal expression of CG13188 during tracheal development.

We double stained control (yw$^+$) embryos with Trh, which highlight the tracheal cells (marked in green in figure 57) and CG13188 antibody (marked in red in figure 57). The analysis of expression pattern revealed that CG13188 is expressed in the tracheal system in the cytoplasm of mainly, the tracheal visceral cells at stage 12. At stage 13, CG13188 protein starts to be accumulated also in the cytoplasm of transverse connective and ventral branches. At the end of this stage we observed that the protein starts to accumulate apically in the visceral branches (asterisk in figure 57). Expression in the dorsal trunk and dorsal branches start at embryonic stage 14. By stage 15, the apical accumulation of CG13188 in all tracheal cells becomes very clear (zoom images in figure 57).

Our analysis of protein accumulation not only reveals the dynamic and temporal accumulation of CG13188 protein, but also, recapitulates mRNA expression pattern shown in BDGP, as CG13188 protein was detected in those tissues in which CG13188 mRNA was expressed.

2.3. Regulation of CG13188 expression pattern

CG13188 was identified in a microarray analysis for *ttk*. Thus, we first checked in *ttk* mutant embryos how was CG13188 protein expressed. As expected, we noticed differences between control and *ttk* mutant embryos (Figure 58).
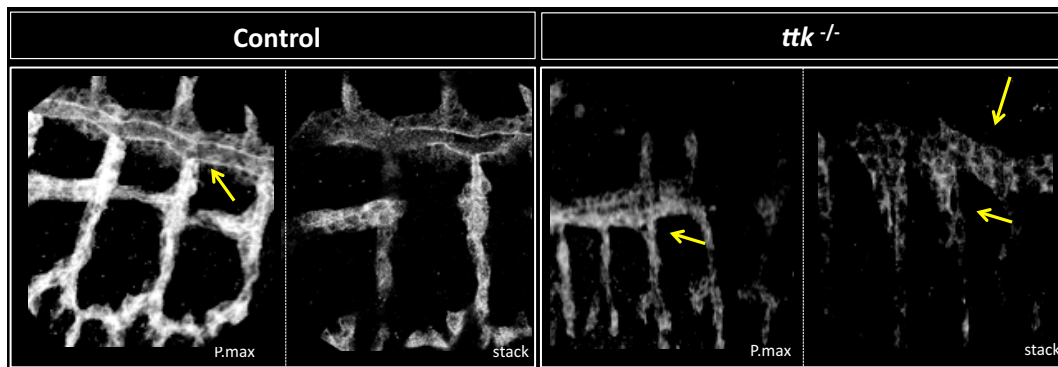
Figure 58. Close view of DT and ventral tracheal branches of late control and *ttk* mutant embryos. Note that CG13188 protein is mis-localised in *ttk* mutant embryos (arrows).

Although the immunostaining analysis did not clearly showed protein levels differences between the control and *ttk* mutant embryos, we observed CG13188 protein sub-cellular localisation defects. Contrary to wild-type embryos, where the protein starts to accumulate apically in the tracheal cells at late embryonic developmental stages, in *ttk* mutant embryos CG13188 protein remained localised mainly in the cytoplasm of all tracheal cells (Figure 58).

The dynamic spatial and temporal expression pattern of CG13188 raised the question of whether it might be dynamically regulated by temporal and spatial specific signalling pathways.

Spalt (Sal) protein has a dynamic expression pattern throughout development. At embryonic stage 11, Sal is found in the dorsal part of the tracheal metameres, the precursors of the DB and the DT. Later, its expression decreases in the non-tracheal cells and become restricted to tracheal cells (Figure 59A). At stage 12, Sal is found in the dorsal parts of all tracheal metameres, corresponding to the outgrowing DTa and DTp as well as in the DB, while no Sal expression is detectable in central and ventral

tracheal structures (Figure 59B). During stage 14 and 15, its expression declines from the dorsal branches, becoming restricted to the DT (Figure 59C).
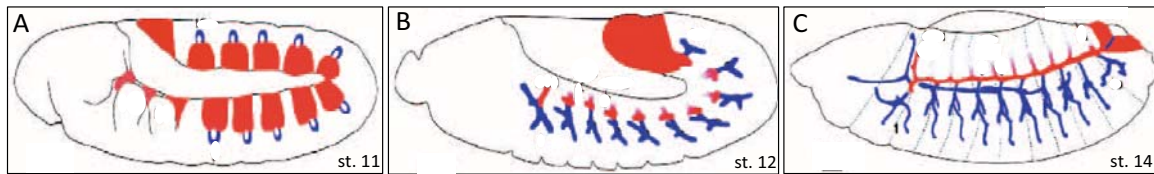
Figure 59. Sal expression during embryonic tracheal system development. Schematic representation of Sal embryonic expression. At stage 10, Sal is found in the dorsal part of the tracheal metameres, the precursors expression associated with the tracheal system is shown in red, while all other tracheal structures are shown in blue (Adapted from Kühnlein and Schuh, 1996).

Therefore, the complementary expression pattern of CG13188 and Sal argues that Sal could be acting as a regulator of CG13188 expression. To investigate this further, we examined the pattern of CG13188 protein accumulation in embryos that mis-expressed Sal (either mutant or over-expression). First, we ectopically expressed Sal in the tracheal system, using a UAS Sal construct with the driver line *btl* Gal4 (Figure 60).
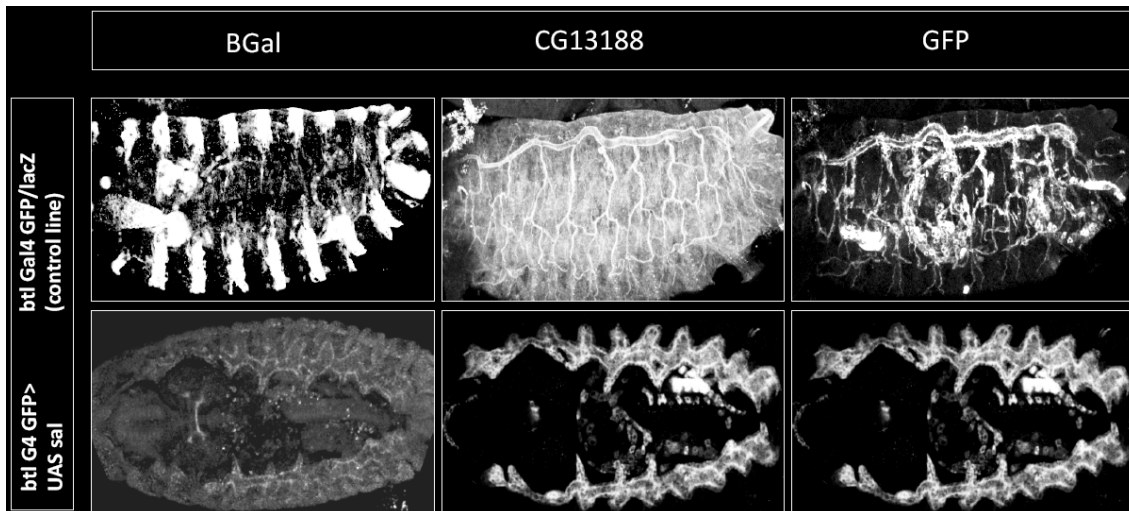
Figure 60. Ectopic expression of Sal in the tracheal system and CG13188 protein accumulation.

We found that CG13188 protein levels are markedly decreased in embryos that over-expressed Sal in all tracheal cells (Figure 60). In addition, as previously described, we observed that the over-expression of Sal confers DT features to the tracheal tree (Chean et al., 1998; Kuhnlein and Schuh, 1996) (Figure 60).

We also analysed the absence of *sal* using a small chromosomal deficiency line (Df (2L) 5 /cyo lacz) over a lacZ balancer, which uncovered both *spalt-major* and *sal* genes (Figure 61).
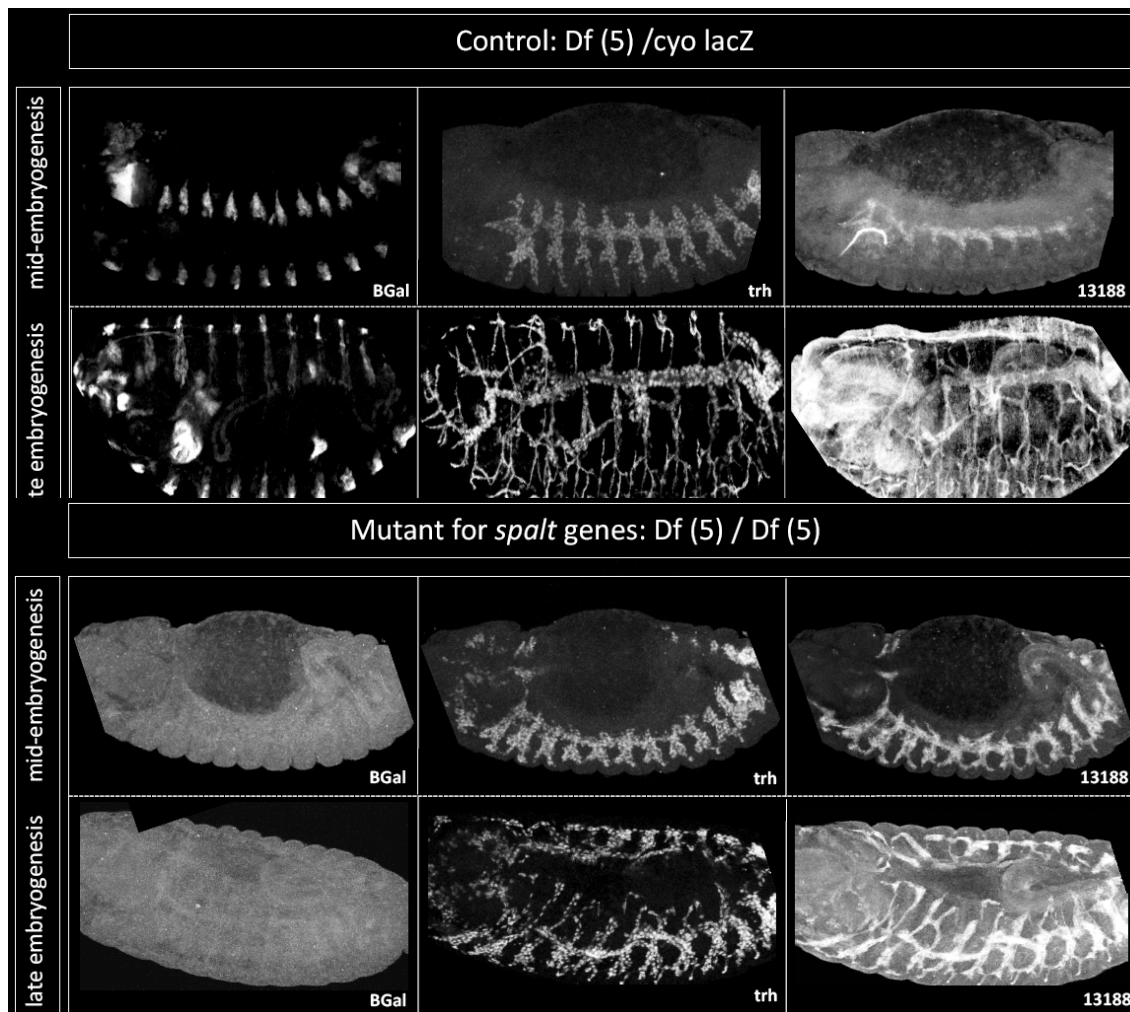
Figure 61. Absence of *sal* in the tracheal system and CG13188 protein accumulation. In homozygous *sal* mutant embryos the spatio-temporal expression pattern of CG13188 protein is lost, as we detected accumulated along the tracheal tree at early stages. Moreover, we detect in *sal* mutants markedly increased levels of CG13188 protein accumulation, as compared to control

In homozygous embryos for the deficiency (distinguished by the absence of β-galactosidase expression), that failed to form a continuous DT branch as described before (Kuhnlein and Schuh, 1996), the spatio-temporal expression pattern of CG13188 is lost. Thus, we found CG13188 expression already at early stages. In addition, we also detected that CG13188 is accumulated at higher levels, as compared to control (Figure 61).

All together these results showed that Sal regulates negatively the expression pattern of CG13188.

Dpp pathway, during tracheal morphogenesis, allows the migration of tracheal cells in the dorso-ventral axis, and is therefore required for the formation of the dorsal and ventral branches (Vincent et al., 1997; Chen et al., 1998). CG13188 expression pattern suggested us that it might be positively regulated by Dpp pathway, prompted us to further investigate whether the activity of CG13188 protein depends on Dpp pathway. Therefore, we tested the over-activation of Dpp signalling in tracheal cells by the expression of an UAS Tkv^{Ac} construct with the driver line *btl*Gal4 (Figure 62).
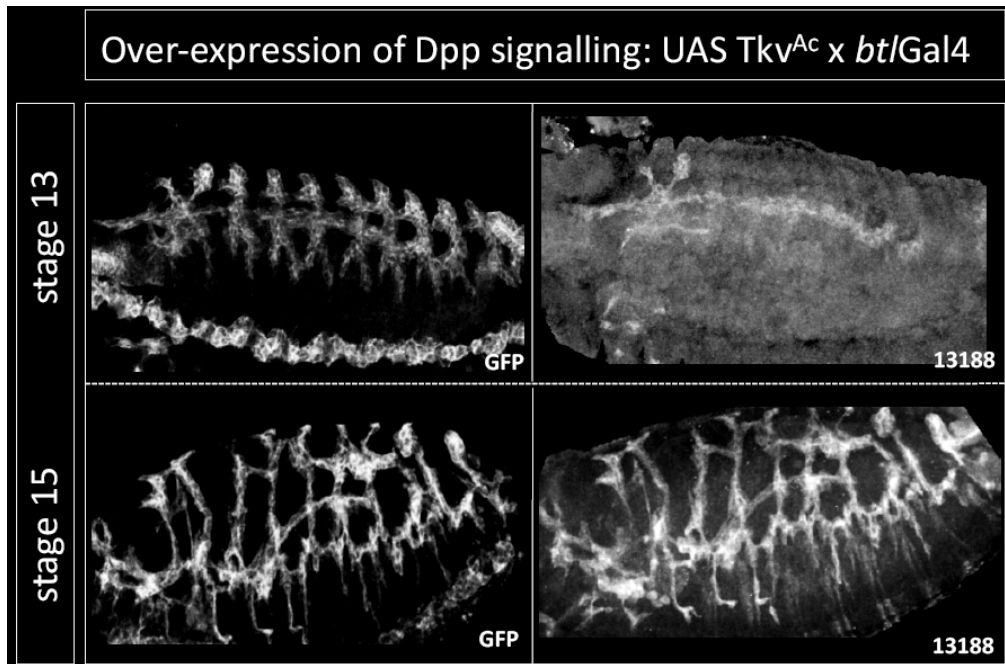
Figure 62. Effect of the over-expression of Dpp signalling in CG13188 protein accumulation during tracheal system development.

This experiment showed no detectable effect of Dpp signalling over-activation on the expression level or sub-cellular localization of CG13188 protein, indicating that Dpp signalling is not required for CG13188 expression (Figure 62).

3. CG13188 MOLECULAR NATURE

3.1. Molecular nature

CG13188 gene encodes, according to the Pfam website (protein family website), a protein with a putative MH2 (Mad homology 2) domain, typically found at the carboxy terminus of Smad proteins. A search in this website identified six proteins that have a MH2 domain similar to the one of CG13188: Mothers against Dpp (Mad), Smad on X (Smox), Daughters against Dpp (Dad), Medea, CG13188 and CG13183. Interestingly, four genes (Mad, Smox, Dad and Medea) out of the six are the known described downstream effectors of Dpp signalling. The other two Smad proteins, CG13188 and CG13183, are uncharacterised. Smad proteins are classified into three classes based on their structure and function (Figure 63):
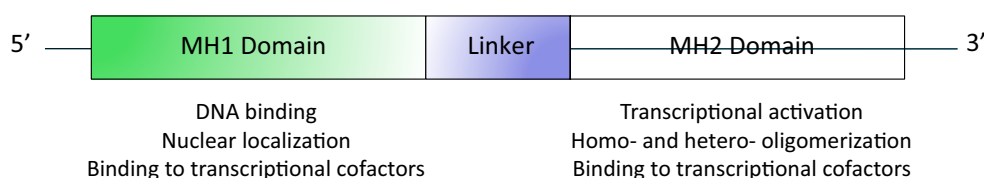
Figure 63. Schematic representation of the typical structure of Smad proteins showing domain regions and known functions. Except for I-Smad, Smad proteins contain two highly conserved domains, Domain 1 and Domain 2, separated by a variable proline-rich linker region (mark in purple). Domain 1 (mark in green) binds DNA sequences and domain 2 (mark in red) acts as a transcriptional activator, homo- and hetero-oligomerization and it binds to transcriptional cofactors.

- Receptor-regulated (R) class: Mad, the founder member of Smad protein family, belongs to this class. These proteins are directly phosphorylated on their carboxi-terminus side in response to TGF-β signalling. Once phosphorylated, R-Smad proteins translocate to the nucleus where they regulate transcription of specific target genes through their interactions with DNA binding proteins or through direct DNA binding.

- Common-mediator (Co) class: Medea belongs to this class. Contrary to R-class, Co-Smads are not regulated by signal dependent phosphorylation although they have both MH1 and MH2 domains. They form a heteromeric nuclear complex with R-Smads in order to be translocated to the nucleus to modify or enhance Dpp signalling.

- Inhibitory (I) class: This subclass of Smads proteins are negative regulators of the pathway. They modulate the signalling by blocking the activity of R-Smads and Co-Smads.

Smad family members have been found only in eumetazoan animals. To understand the evolutionary relationship between these family members, Newfeld lab conducted a phylogenetic analysis (Newfeld and Wisotzkey, 2006). To simplify the analysis but retain its explanatory power, they focused on Smad proteins from organisms in three distinct phyla: human (h), fly (Dm), and nematode (Ce) (Figure 64, marked in red, green and blue respectively).
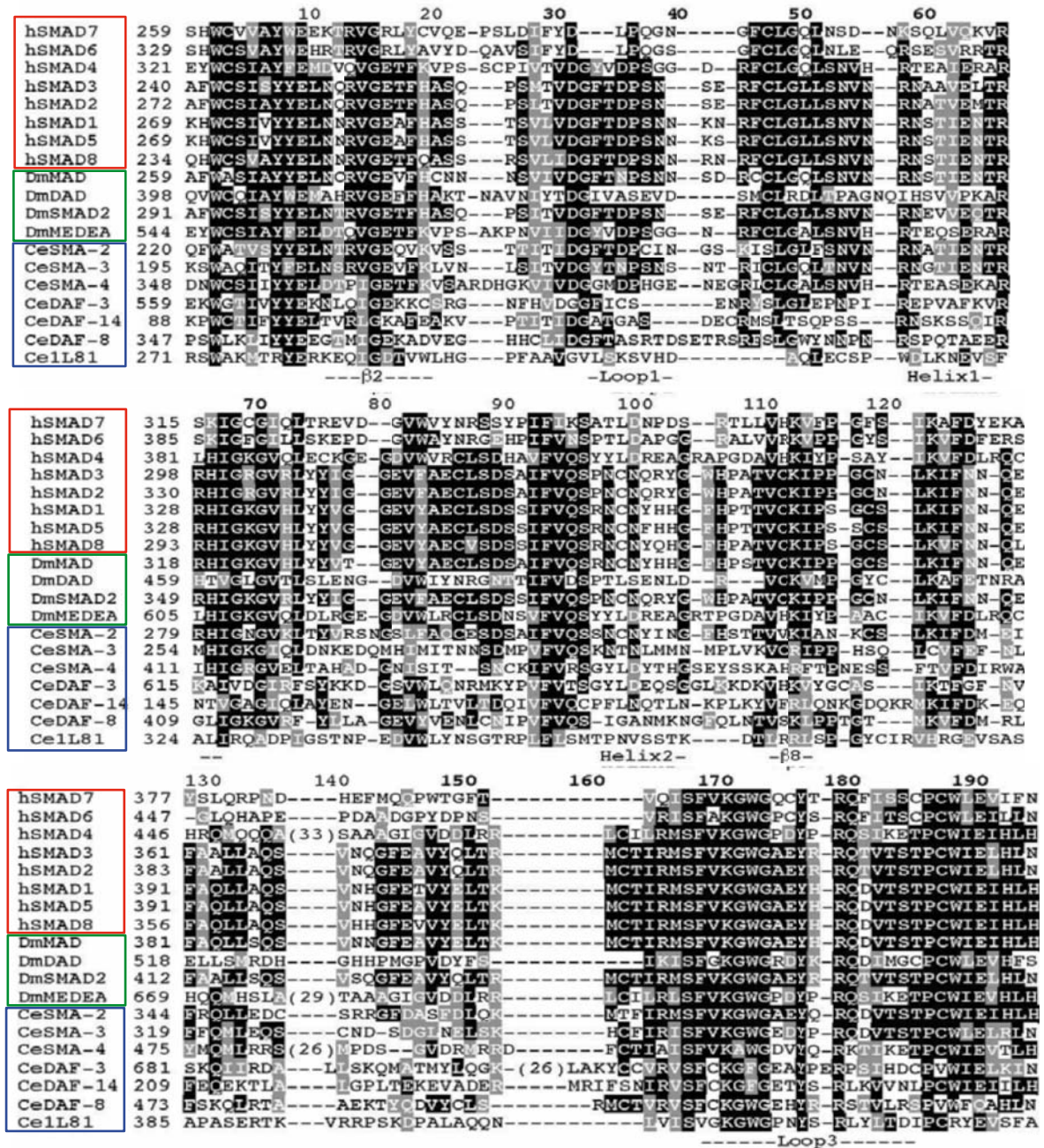
Figure 64. Alignement of Smad family MH2 protein domain from organisms in distinct phyla. Residues were shaded if 40% of them were identical (black) or similar (grey). Numbers above the alignment begin with the first amino acid and run consecutively. Residue number 60 in bold indicates the location of the DNA-binding region. Thus, this domain is highly conserved in all family members with Dad and Ce1L81 the most divergent. The evolutionarily conserved portion of the MH2 domain begins at the invariant Trp261 in Mad and ends at His431 in Mad. The length of the alignment is 222 residues. Bold numbers 30-60 indicate the loop-helix region and 150-190 indicates the helix-bundle region. Several structural features are indicated (Adapted from Newfeld and Wisotzkey, 2006).

The examination of the MH2 alignment between humans, *Drosophila* and *Caenorabditis elegans* revealed that 24% of the amino acid residues are extremely well conserved (at least 17 of the 19 sequences have an identical or similar amino acid at a particular position). Eleven of the 47 highly conserved residues are identical in all sequences and 13 are very well conserved (a similar amino acid residue in all sequences). In addition, the structure of an hSmad MH2 domain reveals three sub-domains (Figure 64). There is a central β-sandwich (b), a loop-helix region near the amino-terminus (loop) and a helix-bundle region (Helix) at the C-terminus that extends into the receptor phosphorylation region.

To test whether the MH2 domain of CG13188 protein is conserved too, we performed a multiple protein sequence alignment between the six *Drosophila* proteins that have this domain using the ClustalW alignment program of Mac Vector software (Figure 65).

```
Mad       WASIAYYELNCRVGEVFHCN--NNSVIVDGFTNPSNNSDRCCLGQLSNVN--RNSTIENT 56
Smox      WCSISYYELNTRVGETFHAS--QPSITVDGFTDPSN-SERFCLGLLSNVN--RNEVVEQT 55
Medea     WCSIAYFELDTQVGETFKVPSAKPNVIIDGYVDPSG-GNRFCLGALSNVH--RTEQSERA 57
CG13188   WAKVIVFERNRRVAKAYARA---PVLTINGSDDGFD-GMRIGLCGFDNPM--RDQKTDEM 54
CG13183   WAKIIVFEKNRRVAKAYARSS---VITINGSKNGFD-GVRIGLNGFDNPM--RDAETKVI 54
Dad       WCQIAYWEMAHRVGEFFHAKTNAVNIYTDG-IVAS-EVDSMCLRDLTPAGNQIHSVVPKA 58
          *..:    :*    :*.: :       :   :*        *  .:

Mad       RRHIGKGVHLYYV-TGEVYAECLSDSAIFVQSRNCNYHHGFHP-STVCKIP-----PGCS 109
Smox      RRHIGKGVRLYYI-GGEVFAECLSDSSIFVQSPNCNQRYGWHP-ATVCKIP-----PGCN 108
Medea     RLHIGKGVQLDLRGEGDVWLRCLSDNSVFVQSYYLDREAGRTPGDAVHKIY-----PAAC 112
CG13188   KRVIGQGVKIKMDDAGNILIRRYAKSNVYVKSTASSPNEETSIGAEILKLPNQALESEKI 114
CG13183   KKSIGDGFKIKMDDTGNIFIKRYGKSSIYVNSTSQG-NEETVIGGDIIQMPQMSLTAATS 113
Dad       RHTVGLGVTLSL-ENGDVWIYNRGNTTIFVDSPTLSENLDR----VCKVMP------GYC 107
          :   :* *. :       *::         ... ::*.*    . .        :

Mad       LKIFN----NQEFAQLLS--------------------QSVNNG--------FEAVYELTKM 139
Smox      LKIFN----NQEFAALLS--------------------QSVSQG--------FEAVYQLTRM 138
Medea     IKVFDLRQCHQQMHSLATNAQAAAAAQAAAVAGVANQQMGGGGRSMTAAAGIGVDDLRRL 172
CG13188   VKLFD----MKKFQSNVN--------------------RELRRA--------YPDRRRLETQ 144
CG13183   ARLFD----MKKFQTNIN--------------------REFART--------YPERGRLERQ 143
Dad       LKAFETN-RAELL--------------------------SMRDHG----------HHPMGPVDY 134
          :  *:         : :               : :

Mad       CTIRMSFVKGWGAEYHRQDVTSTPCWIEIHLHGPLQWLDKVLTQMGSPHNAISSVS---- 195
Smox      CTIRMSFVKGWGAEYRRQTVTSTPCWIELHLNGPLQWLDRVLTQMGSPRLPCSSMS---- 194
Medea     CILRLSFVKGWGPDYPRQSIKETPCWIEVHLHRALQLLDEVLHAMPIDGPRAAA------ 226
CG13188   CLSAVAFVKS------ENDILECPIWVLIVNVVAMDMLKSKLPPVQRPIVDIKNRP---- 194
CG13183   CLSAVSLVKS------NNNLINSPVWILVVNVVAMDMLRSRLQTIPKSLDAMGMRVPLTN 197
Dad       FSIKISFGKGWGRDYKRQDIMGCPCWLEVHFSHLR------------------------- 169
          ::: *.        .: :     * *: :

Mad       --
Smox      --
Medea     --
CG13188   --
CG13183   SS 199
Dad       --
```

Figure 65. *Drosophila* Smad family MH2 domain sequence alignment. Colour code indicates were sequence aligned (ClustalW program).

103

Similarity score between each of the family member analyzed by pairwise is shown in table 10:

Name sequence 1	Length	Name sequence 2	Length	Score
CG13188	201	CG13183	206	56.2189
CG13188	201	SmoX	195	17.4359
CG13188	201	Medea	226	17.4129
CG13188	201	Mad	195	15.3846
CG13188	201	Dad	178	13.4831
Medea	226	Dad	178	27.5281
Medea	226	SmoX	195	41.5385
Medea	226	Mad	195	36.4103
Medea	226	CG13183	206	16.5049
Dad	178	SmoX	195	29.7753
Dad	178	Mad	178	28.0899
Dad	178	CG13183	206	11.7978
SmoX	195	CG13183	206	17.4359
SmoX	195	Mad	195	73.3333
Mad	195	CG13183	206	16.4103

Table 10. Percentage of similarity between *Drosophila* MH2 proteins domain compared. The degree of similarity between two amino acid sequences aligned is shown by a score value. The highest, the more similar they are. Note that CG13188 had the highest alignment with an uncharacterised gene CG13183.

Thus from the obtained outputs, it can be inferred that the MH2 domain of CG13188 has sequence homology with the previously described MH2 domains. Interestingly, it shows the highest similarity highest score in table 10) with an uncharacterised gene named CG13183. To clearly examine the relationship between the MH2 domains analysed, we represented it into a phylogenetic tree (Figure 66).
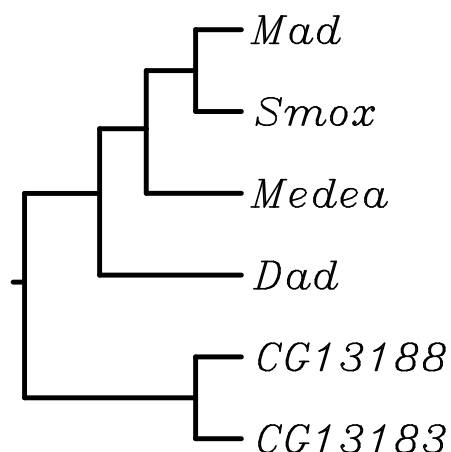
Figure 66. Phylogenetic analysis of *Drosophila* Smad protein family. Phylogenetic tree showing the relationship of amino acid MH2 sequences between the six *Drosophila* Smad proteins. Noted that CG13188 clustered together with another gene, CG13183. Interestingly, both uncharacterised genes clustered closer to Dad than to the other 2 classes of Smads proteins (ClustalW program).

The phylogenetic tree highlighted the three Smad classes described. From this report, we can conclude that the first divergence event separated the lineage that gave rise to tip CG13188 and CG13183 from the lineage that gave rise to tips of the three different Smads classes defined so far.

3.2. CG13188 protein evolutionary conservation

It is assumed that orthologous genes often share functional similarity in different organisms and therefore, functional information can be transferred to different species (Koonin, 2005; Dolinski and Botstein, 2007). To have further information about CG13188, we used the String 9.0 database to search for orthologous (Figure 67).
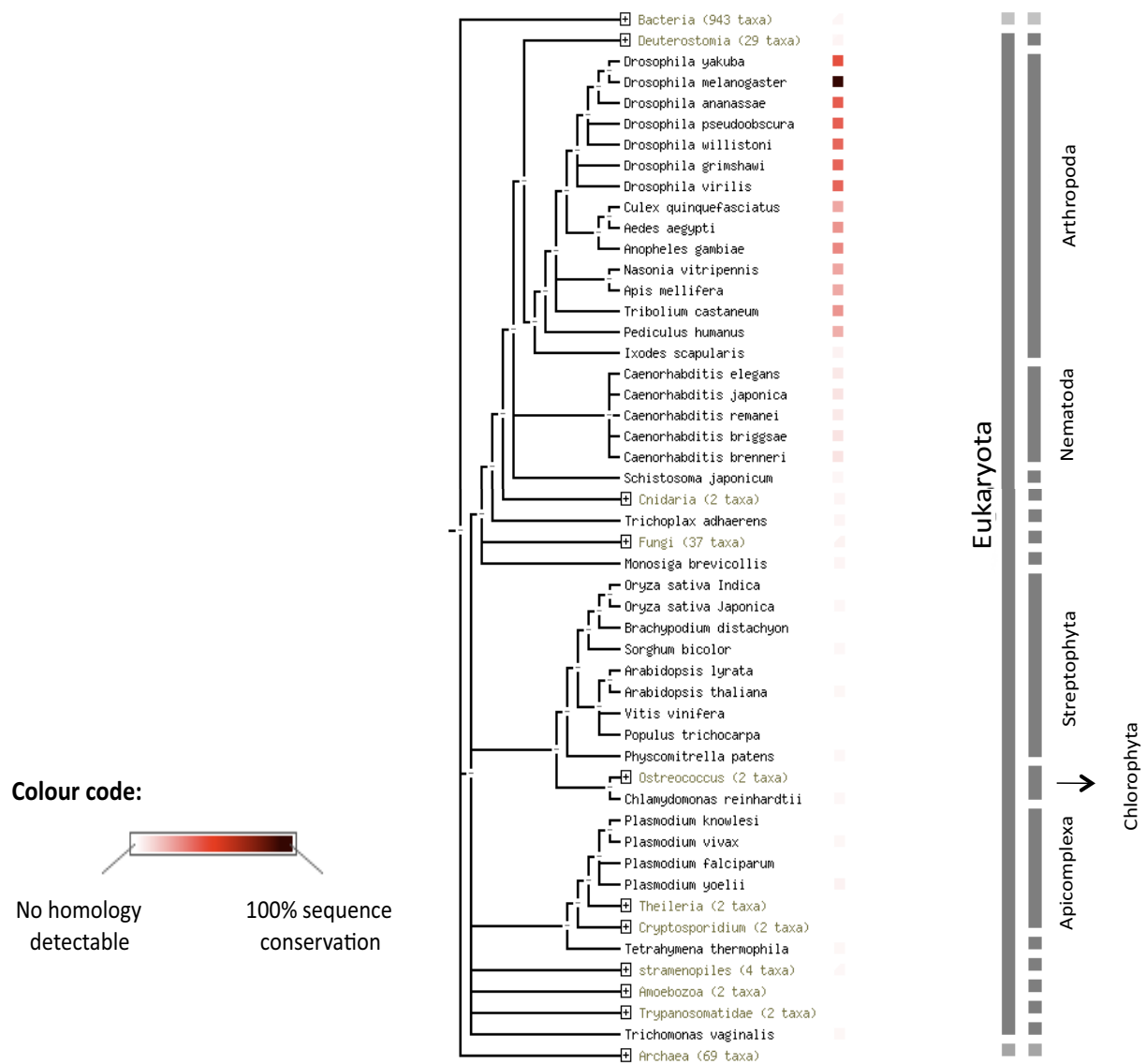
Figure 67. Cladogram showing across eukaryotes different orthologous groups for CG13188 protein.

105

According to the above diagram, CG13188 nucleotide sequence has homology with different *Drosophila* species, non- *Drosophila* dipterans, non-dipterans insects, non-insects arthropods and non-arthropods metazoans. Unfortunately, there is not functional information available for the different orthologous groups proposed that could provide insights into CG13188 function.

4. FUNCTIONAL CHARACTERISATION

We have been and are currently performing a functional characterisation of CG13188 gene during tracheal morphogenesis. To determine its function, we first assayed CG13188 down-regulation in the tracheal system, by RNA interference technology (Kennerdell and Carthew, 1998; Misquitia and Paterson, 1999). We found three different CG13188 RNAi lines available (102370, 32152 and 32153), but we selected one of them, line 102370, to perform our functional analysis because it has no off targets predicted, avoiding therefore the down-regulation of unintended targets. By using the other two lines (31252 and 32153), we corroborated the obtained results as we found comparable phenotypes.

4.1. Analysis of the extent of CG13188 RNAi knockdown

We induced CG13188 down-regulation in the tracheal system by crossing homozygous CG13188 RNAi 102370 flies with flies homozygous for the tracheal driver *btl* Gal4 src GFP, which is fused to the membrane marker src GFP. We first examined the extent effect of the presumed knockdown by qPCR using two sets of primers: isoform-specific and no variant-specificity (Figure 68).
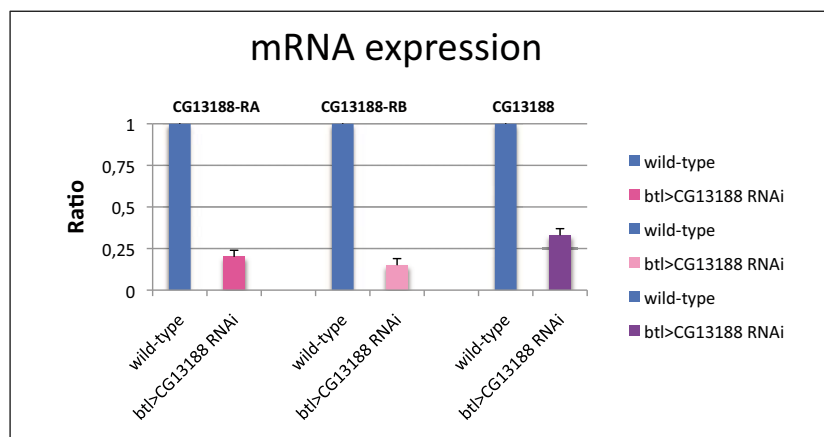
Figure 68. Analysis of the extent of RNAi knockdown by qPCR. Graphic showing the significant different relative expression of CG13188 gene variants in btl>CG1388 RNAi mutant embryos, in comparison to wild-type, at developmental stages 11-16.

We found that the amount of CG13188 mRNA (either RA or RB transcripts) decreased (purple bars in the figure 68), around 70% to 85% in *btl* src GFP>CG13188 RNAi embryos, compared to control embryos (blue bars in figure 68).

To further confirm the decrease of CG13188 protein in *btl* Gal 4 src GFP>CG13188 RNAi embryos, we stained those embryos with CG13188-Ab (Figure 69).
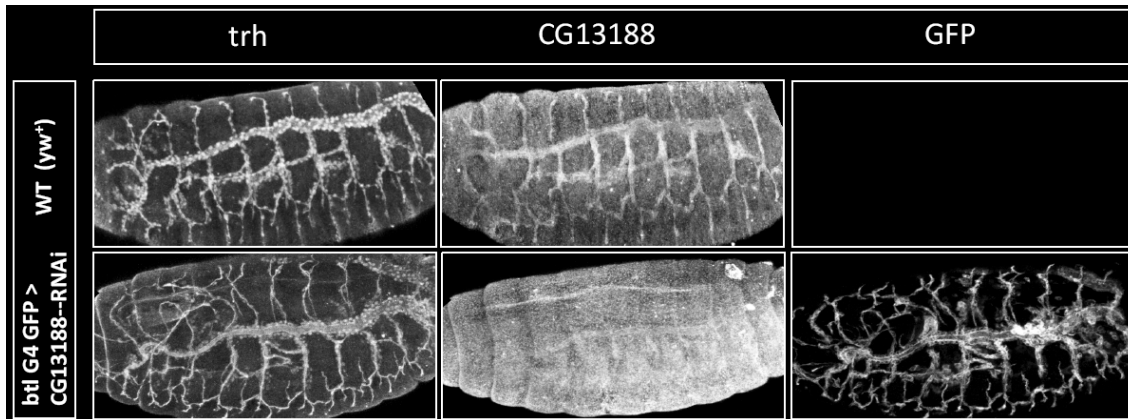
Figure 69. Down-regulation of CG13188 protein in *btl*Gal4>CG13188-RNAi embryos is confirmed by the absence of CG13188-Ab staining detection. Moreover, it confirmed also the specificity of the anti-CG13188 serum generated.

We detected a marked decrease of CG13188 protein expression in the tracheal system of homozygous *btl* Gal 4 src GFP>CG13188 RNAi embryos (Figure 69, lower panel), although the tracheal branches were formed as shown by positive detection of the Trh nuclear marker in the tracheal cells. This experiment also indicated the specificity of the CG13188 generated antibody.

These results showed that the loss-of-function condition generated by the RNAi strategy represents a valuable tool to assess the functional requirements of CG13188 in tracheal morphogenesis. However, as certain levels are still detected, some CG13188 activity might be present.

4.2. Viability test

CG13188 is expressed in tracheal and other tissues. The dynamic pattern of expression raises the question of whether it provides a vital function. To investigate this issue, we performed a viability test.

We used the three different CG13188 RNAi lines available and crossed them to the *btl* Gal4 driver. We observed that all RNAi lines were embryo/larval L1 lethal, suggesting as expected, that CG13188 is required for organism's viability.

4.3. Requirement during tracheal morphogenesis

To analyse the defects of CG13188 down-regulation in the tracheal system, we made use of different available tracheal markers.

4.3.1. Early events of tracheal development occur normally in CG13188-RNAi mutants embryos

As a first approximation to check the general pattern of the tracheal tree and the morphology of tracheal cells, we expressed in the tracheal system a microtubule-associated protein Tau–GFP, using the *btl* Gal4 tracheal driver line, which is expressed in all tracheal cells from invagination onwards, and lines the contour of the cells. At the same time *btl* Gal4 also down-regulated CG13188 levels in the tracheal system (Figure 70).
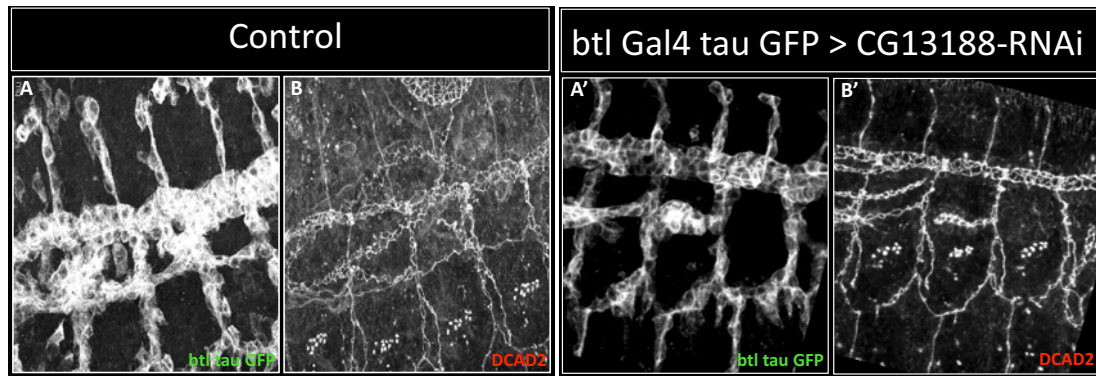
Figure 70. Early events of tracheal development occur normally in CG13188-RNAi mutant embryos.

CG13188-RNAi mutant embryos showed normal branching pattern and branch fusion. In addition, tracheal cells also showed a normal morphology, as highlighted by the tau-GFP marker (Figure 70).

During development, tracheal cells suffer lots of junctional rearrangements and cell shape changes. We analysed in more detail these cellular features in CG13188-RNAi embryos, by staining embryos with an AJ marker, DCAD2 antibody against E-Cadherin. CG13188-RNAi mutants showed normal pattern of apical markers, indicating no obvious defects in cell shape or cell intercalation (Figure 70).

All together these results suggested that CG13188 is not required for the early cellular events that take place during tracheal development.

4.3.2. Late events of tracheal development are defective in CG13188-RNAi mutants embryos

4.3.2.1. Apical ECM formation defects:

From embryonic stages 14-15, CG13188 down-regulation gives rise to particular tracheal defects. When using CBP as a marker to visualise the chitin filament that in wild-type embryos organise inside the lumen, we detected reproducible defects (Figure 71).
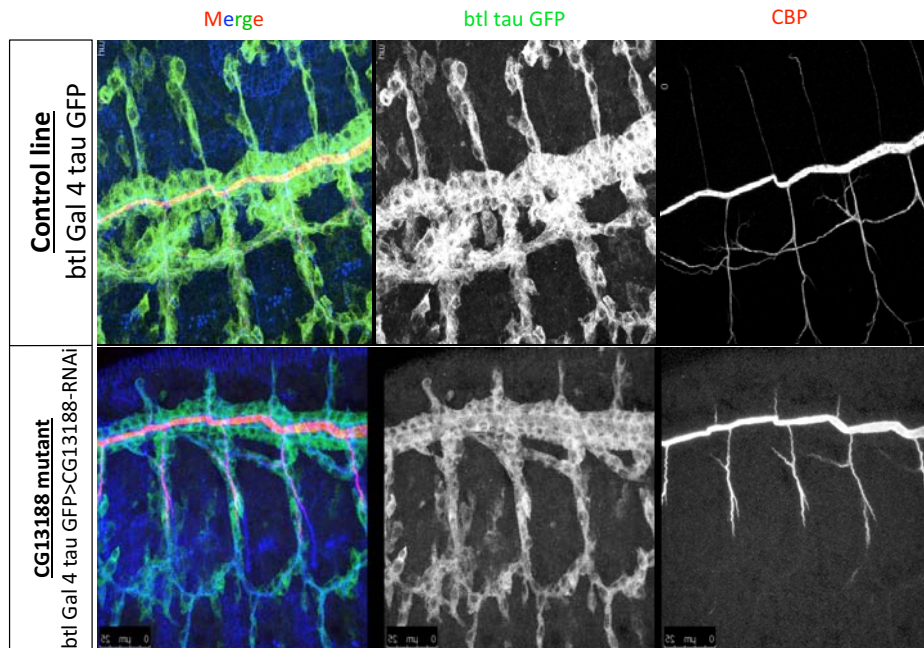
Figure 71. Characterization of the tracheal phenotype of CG13188-RNAi mutant embryos. Close view of four tracheal metameres of late stage control and CG13188-RNAi mutant embryos, stained with CBP to show the lumen (red) and with an anti-GFP antibody to detect the expression of tauGFP in tracheal cells (green), which highlights cell shape. Note the defects of CBP accumulation in mutant embryos in comparison to wild-type.

We observed that in CG13188-RNAi embryos, CBP was only accumulated in the DT and TC branches, whereas the rest of branches did not accumulated CBP or did it only faintly. Consistent with these results of 102370 RNAi, we observed comparable (although milder) defects with the two other RNAi lines (32152 and 32153) tested.

These results suggested the inability of the most dorsal and ventral tracheal cells to accumulate chitin into their luminal space to assemble the chitinous ECM required to guarantee the acquisition of proper tube size and became physiologically functional (Araújo et al., 2005; Devine et al., 2005; Tonning et al., 2005; Moussian et al., 2006; Luschnig et al., 2006).

These experiments suggest that CG13188 has a function in the formation of the chitin cable in specific tracheal branches, particularly in dorsal branches, visceral branches, ganglionic branches and part of the transverse connective. The tracheal branch specific phenotype observed when expressing CG13188 RNAi with *btl* Gal4 could be due to an absence of requirement of this gene for the cable formation in the DT. Alternatively, it could be due to an inefficient down-regulation of CG13188 in the DT domain. In fact, *btl* is expressed at lower levels in the DT region from stage 13-14 (Sutherland et al., 1996), raising the issue that *btl* Gal4 might not be as strong there. To distinguish between these two possibilities, we used a Gal4 driver that is clearly expressed in the DT region, *sal*Gal4.

Thus, we used the LP39 specific tracheal *sal* driver to knockdown CG13188 expression in the DT domain and test therefore, whether CG13188 had a function in that branch (Figure 72).

Control	CG13188 RNAi 102370 x LP39/cyo wg z; UAS GFP		
2A12	2A12	LP39 GFP	Merge
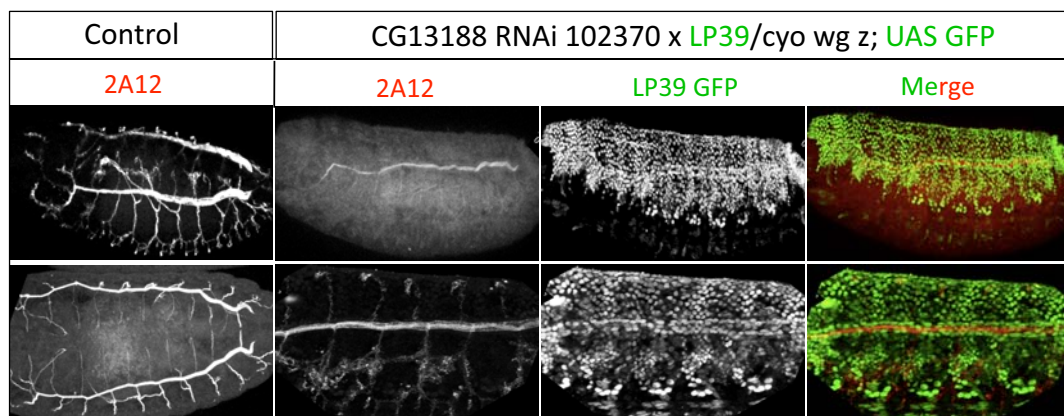
Figure 72. Removal of CG13188 function in Spalt's domain at late embryonic stages, revealed normal accumulation of chitin in this branch (DT) as control embryos.

The continuous down-regulation of CG13188 gene in the DT domain resulted in normal accumulation of chitin in this branch (Figure 72). As expected, the ventral part of the trachea now accumulated CBP (Figure). DBs accumulated certain levels of CBP, although faintly, consistent with the fact that Sal stops being expressed in the DB region.

These results confirm that down-regulation of CG13188 by RNAi produce defective accumulation of luminal material in DB, VB and GB, whereas no clear defects are observed in TC and DT. This observation suggests branch-specific requirements for this gene.

4.3.2.2. Gas filling defects are observed in CG13188-RNAi mutant embryos

At stage 17 of embryogenesis, the chitinous ECM is degraded and protein and liquid are removed from the lumen of the tubes to enable gas filling of the respiratory network. Previous observations by Samakovlis lab have shown that failure during luminal matrix secretion (protein secretion) and/or endocytosis (clearance of the luminal content), disrupt the maturation process, leading to gas filling defects and as a consequence, the tracheal tubes collapse (Tsarouhas et al., 2007).

As CG13188 is involved in the formation of the luminal chitinous cable, we wondered whether CG13188 RNAi embryos were able to successfully reach the last events of tracheal morphogenesis, which is the transition from liquid-to-gas. Thus, we studied this progression *"in vivo"* under a bright field microscope, in *btl* srcGFP > CG13188 RNAi late stage 17 mutant embryos and at first larval stage (L1) (Figure 73).
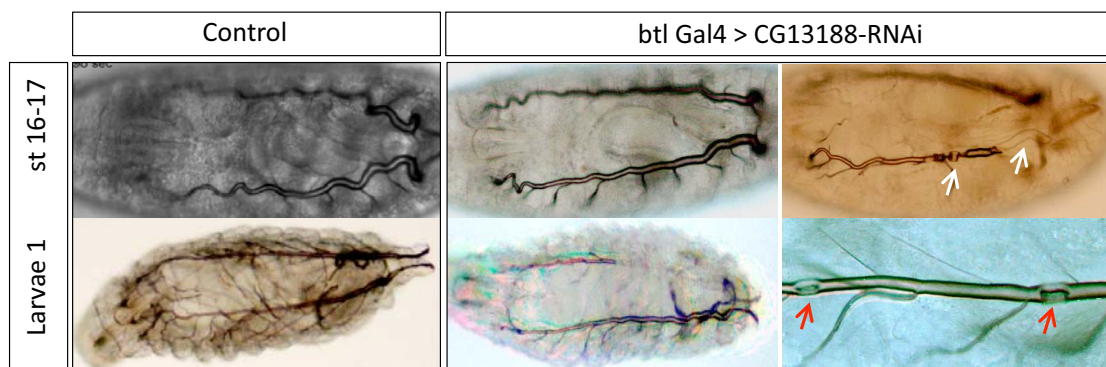
Figure 73. Bright field images showing the defects in liquid clearance and gas filling of btlG4 > CG13188- RNAi living embryos in comparison to wild-type. Note that the refrigence is the result of gas filling. CG13188 RNAi embryos are defective in gas filling of the most dorsal and ventral branches. Interestingly, note the absence of gas filling along the DT (arrows).

As expected, gas filling fails to occur in these mutants. In agreement with the viability test results, CG13188-RNAi mutants dye at late embryogenesis or L1 larvae. In most cases, we observed that air filling failed in dorsal and ventral branches (DB, LTa, LTp, GB, VB and in main cases, TC), where chitin cable was not organised. In addition, we only observed sporadic defects in the DT such as breaks (Figure 73, red arrows) or partial gas filling (Figure73, white arrows).

5. ATTEMPTS TO GENERATE CG13188 MUTANTS

The down-regulation of CG13188 by RNAi in the tracheal system produces a tracheal phenotype. We became interested in studying the complete absence of this gene function. Unfortunately, although one of the strongest advantages of using *Drosophila* as model organism is the huge numbers of mutants fly stocks available, there are no available mutants for all the genes in the *Drosophila* genome. Unfortunately, no mutants for CG13188 have been identified so far. In order to generate CG13188 null mutant alleles, we took advantage of different transposable elements to perform mutagenesis.

5.1. Generation of a small deletion by the FLP-FRT recombination system

PiggyBacs (PBacs) transposons are mobile genetic elements that are useful to generate deletions of flanking genes. PBacs elements excise precisely and its mobilisation occurs with a frequency of approximately 1%. When those elements are excised from a chromosome, a double-stranded break is created. If the ends of such double-stranded break are degraded before repair, a deletion of the genetic material occurs. We attempted to generate small genomic deletions around the CG13188 gene by selecting two compatible P-Bacs elements and using the flip recombinase/FLP recombinase target (FLP/FRT) site-directed recombination system that delete, after the induction of FLP, the region between FRT sites carried on the transposon insertions (Golic and Golic, 1996) (Figure 74).
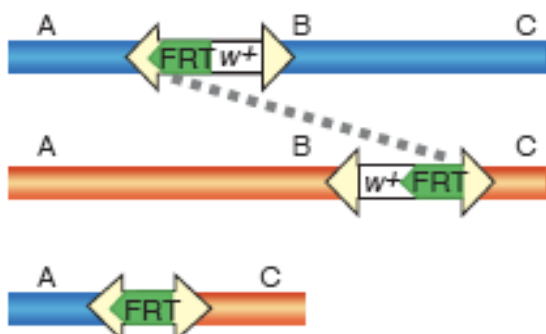
Figure 74. FLP/FRT site-specific recombination mediate chromosomal rearrangements in *Drosophila*. Two fly lines, bearing FRT sites within P elements localized at different positions on the same chromosome, are crossed. Subsequently, FLP recombination creates the desired deletion with well-defined end-points (Adapted from Nature genetics 36, 2004).

We combined the compatibles Exelixis PiggyBac transposons insertion lines available: f03619 and e3069 that closely flank the desired gene to be eliminated, following the scheme below:
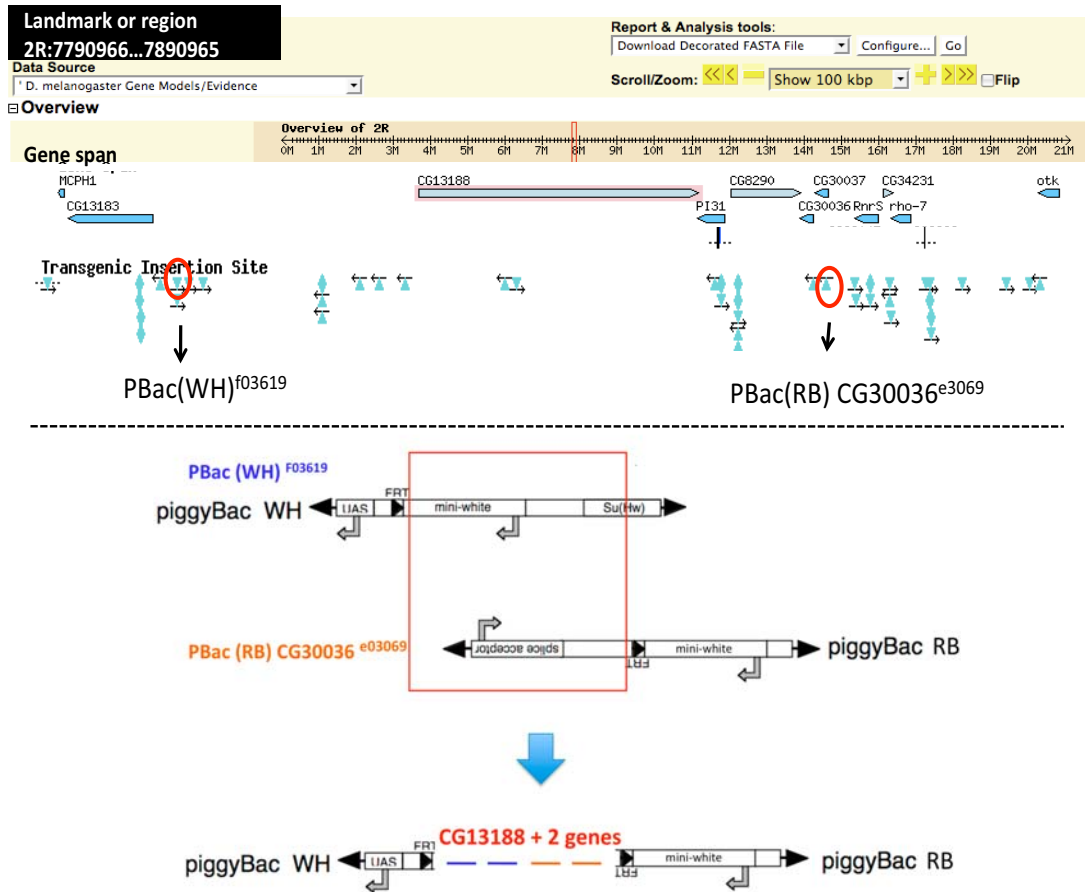
Figure 75. CG13188 locus genome region. Note that transgenic insertion sites used are marked in red (Adapted from Flybase-Genome browser).

The genetic crosses performed to generate a deletion on the desired region of chromosome II are summarised in figure 76:
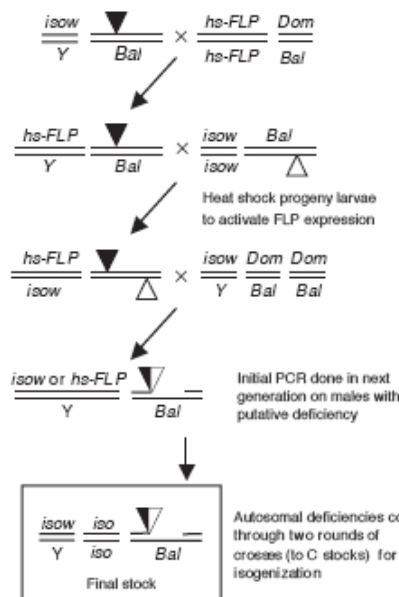
Figure 76. Genetic crosses schemes used to generate deletions on chromosome II (Adapted from Hummel and Klämbt, 2008).

After establishing 200 independent crosses and checking the tracheal phenotype of the lethal and semi-lethal lines obtained, we did not find any expected tracheal phenotype. Thus, we did not succeed in the generation of a CG13188 mutant by this mutagenesis strategy.

5.2. Minos element for imprecise excision (MB08023)

Minos elements are mobile genetic elements, isolated from *Drosophila hydei* that belong to the Tc1/mariner superfamily, that excise imprecisely (Franz and Sakavis, 1991; Arca et al., 1997; Metaxakis et al., 2005). They do not require any host-specific factors for transposition (Finnegan, 1989; Lampe et al., 1996). Thus, we selected a minos transposon inserted in a big intron of CG13188: MB08023 (Figure 77).
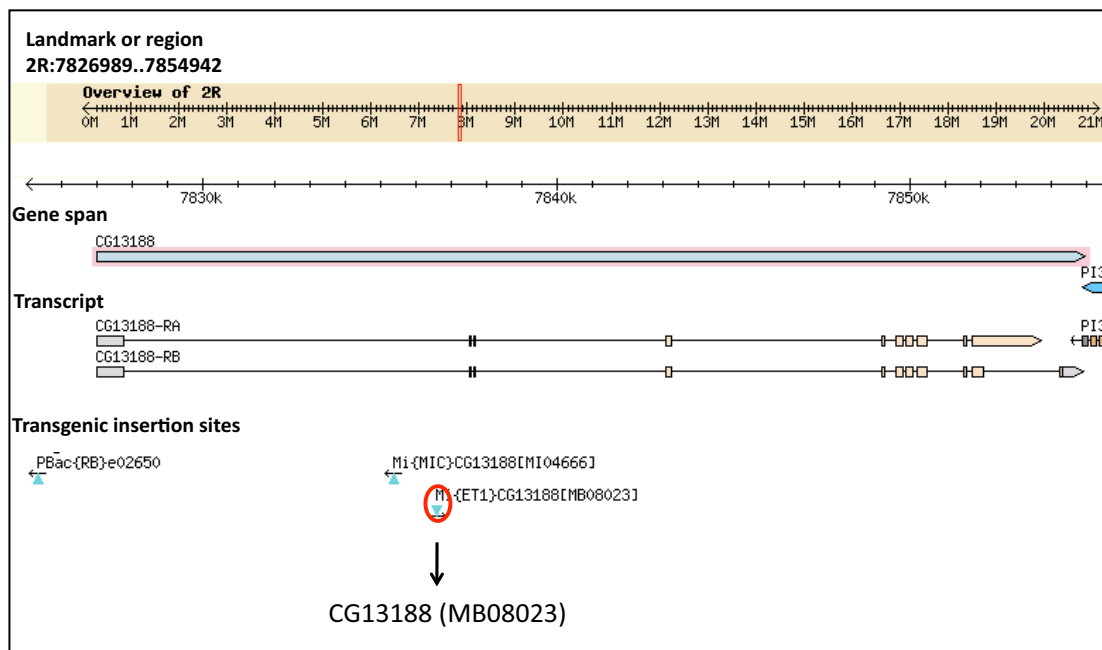
Figure 77. Landmark region of CG13188 gene showing the presence of a minos element inserted in an intronic region (marked in red).

Like most DNA transposons, Minos elements moves in a host genome with a "cut and paste" mechanism, whereby the transposase excises the element from the original site of insertion ("cut") and reinserts it ("paste") into a new locus in a non-replicative manner. For the generation of excision events in the germ line of flies with single Minos insertions, flies homozygous for a MiET1 transposon insertion on the second chromosome were crossed with flies carrying helper chromosome PhsILMiT (cross 1). Two days after setting up the crosses, the flies were transferred to new vials and the old vials were heat-shocked daily for 1 hr in a 37ºC water bath until pupariation. Adults that

114

expressed both the EGFP marker of the transposon and the white marker of the helper chromosome were crossed individually with flies carrying balancer on the second chromosome (cross 2). Progeny with transposon excisions were identified as carrying the balancer but lacking the EGFP and white markers. One such fly was chosen per vial and crossed individually with flies carrying a balancer on the second chromosome over deficiencies covering the region of the initial transposon insertion (cross 3). After checking for the expected tracheal phenotype in 100 lethal or semi-lethal independent excisions events, we did not find any tracheal phenotype.

Discussion

DISCUSSION

Chapter I: Identification of genes that mediate *tramtrack's* function during *Drosophila* tracheal system development

1. General considerations

Branched tubular organs, such as the blood circulatory system, the lung and kidney in mammals, and the tracheal respiratory system in insects, are essential for oxygen and nutrient transport. The tracheal lumen is initially filled with liquid, to help to keep it open during embryonic stages (Manning and Krasnow, 1993). Alterations in the tube maturation process lead to serious pathological conditions, such as the human neonatal respiratory distress syndrome, where premature infants retain liquid in their lungs (which after birth, are still structurally immature) impairing blood oxygenation. This data suggests that liquid secretion and removal are essential and evolutionary conserved steps in airway maturation (O'Brodovich, 1996; Lubarsky and Krasnow, 2003; Wu and Beitel, 2004).

While the early steps of differentiation, lumen formation, and branch patterning begin to be elucidated in several tubular organs (Affolter et al., 2003; Hogan and Kolodziej, 2002), little is known about tubular organ maturation. Part of this knowledge came from genetic screens, which have been very successful at discovering signalling pathways and transcription factors that induce and pattern organs and specify cell fates. However, they have been less successful at identifying the downstream effectors that execute the morphogenetic programs.

Ttk is a widely expressed transcription factor, whose function has been analysed in different tissues (Harrison and Travers, 1990; Badenhorst, 2001; Borghese et al., 2006; Araújo et al., 2007). Our lab described a few years ago that it is also a key factor during *Drosophila* tracheal morphogenesis (Araújo et al., 2007). In particular, it is involved in the establishment of tracheal identities, tracheal cell rearrangements, branch fusion, intracellular tube formation and control of tube size. Thus, due to the wide spectrum of functions performed during tracheal morphogenesis, it exhibits a high degree of pleiotropy that precludes a comprehensive functional characterisation in this specific tissue. Thus, the identification of target genes may help to understand its multiple and complex activities.

2. Microarray design, experimental limitations, data quality and interpretation

In this Thesis we have used a microarray study as a genomic approach to identify both direct and indirect genes acting downstream of *ttk* during tracheal development, with the aim to better dissect *ttk's* tracheal activity. To that end, we combined cell type specific microarrays and compared the results with whole embryo microarrays, with the intention of, through comparing the results from both conditions, reduce the noise generated in the data, maximising the identification of real tracheal targets of *ttk.*

Microarray approaches provide genome wide useful data, which is often associated with experimental noise that could affect the quality and robustness of the results obtained. In order to obtain reliable biological information from our analysis and avoid technological variations, we normalised our data with respect to two groups of invariant genes expression: glycolysis and oxido-phosphorilation (Bilban et al., 2002). By this method, we detected microarray replicates outliers that we filtered out by excluding them for further analysis, eliminating the effect they might have in our data. Although there have been several successful examples of tissue-specific microarrays, cell purification has been since years ago a challenging step (Bryant et al., 1999; Borghese et al., 2006). Nowadays, the novel Pico Profiling method allows obtaining an accurate tissue-specific expression profile from restricted cell populations as small as ten cells (Gonzalez-Roca et al., 2010).

To perform the cell type specific microarrays, we used FACS on cell populations that expressed a fluorescent reporter under the control of the *btl* enhancer (*btl* RFP moe). The *btl* enhancer is widely used in the community for studies of the tracheal system, despite its well-known expression in the ventral midline (Ohshiro and Saigo, 1997) as well as other parts of the embryo. Although it was not possible to isolate a pure tracheal population, we found in the sorted populations similarly strong enrichment for RNAs for primarily tracheal genes (For example, *trachealess*) and the midline marker *single-minded*, but also a strong transcriptional footprint for the amnioserosa and other tissues, for which thus far there was only anecdotal evidence for the activity of the *btl* enhancer. Interestingly, we also found genes expressed in the purified cell population that according to the BDGP gene expression database should not be expressed in the embryo. By comparison to temporal expression profiles from modENCODE, we inferred that many of these are false-negative results of the *"in situ"* hybridisation

experiments.

In addition, due to inherent limitations in high-throughput techniques reliability, genes identified as differentially expressed in microarrays, must be confirmed by an independent gene expression profile method. Although one of the most frequently method used to validate microarray experiments is real-time qPCR, there is no clear agreement between both profiling methods. Some authors believe that in order to confirm microarray data, it is enough an agreement on the direction of fold-change expression (Rajeevan et al., 2001). Moreover, microarray and qPCR techniques differ in many respects, including in the method for reverse transcription, reaction dynamics and the normalization methods applied.

We confirmed by real-time qPCR the directional change in expression of all genes tested, although we saw differences in the magnitude of expression changes. These differences might reflect the sensitivity variance between both techniques. Thus, whereas microarrays allows measuring in one experiment higher number of genes than qPCR, qPCR has been demonstrated to have higher sensitivity as it detects, accurate quantification of fewer genes per reaction (Bio-Rad, 2006).

We also found a few counterintuitive results between the techniques, which were not statistically significant. For example, our previous *in situ* hybridization experiments showed *bnl* to go down in *ttk* mutants (Araújo et al., 2007) while the microarray results could not reproduce this regulation. Further analysis of *bnl* by stage-dependent qPCR validated the transcriptional change observed by *in situ* hybridisation. Moreover, a stage-resolved qPCR analysis helped us to interpret contradictory results between microarray analysis and qPCR experiments, indicating stage-specific modes of Ttk transcriptional control.

Using our criteria to select candidate genes, the screen of Reddy et al. on the S2 *Drosophila* cell line after *ttk* knockdown by RNA interference yielded 1380 candidate genes as compared to 600–800 genes in our ttk^{2D-50} mutant conditions. The larger number of genes is at least in part owed to the fact that their dataset comprises many more replicates and, therefore, allows for a greater number of genes to fulfill the p-value< = 0.05 criterion. Quite reassuringly, however, the degree of overlap between our and their experiments is statistically significant although the absolute overlap between their candidate gene list and our lists is small. For example, the 620 genes down-regulated in S2 cells overlap with 22 of the 246 genes up-regulated in cells after *ttk*

over-expression (p = 9.7×10−4) and 21 of 254 genes down-regulated in our cell population experiments in ttk^{2D-50} mutants (p = 3.3×10−3). The majority of experiments that are expected to be conversely correlated (For example, up in ttk^{2D-50} mutant, down after ttk over-expression, or vice versa) showed significant overlap. However, it should also be noted that in a few cases results emerged that were not intuitive. For example, the overlap of 30 genes up-regulated in both mutant and over-expressing cells (p = 4.7×10−9). It may be assumed that, while the majority of direct or indirect ttk target genes respond appropriately to the experimental situation, the over-expression in particular provokes unexpected responses: the 246 up-regulated genes in cells after ttk over-expression overlap significantly with almost all other experimental conditions. We argue that the mutant situation is likely to represent the biologically better interpretable response, as the over-expression situation may see many more ectopic downstream effects.

Despite technical limitations, we would like to point out that our gene expression catalogue of btl RFP moe positive cells might represent a valuable entry point for further analysis. While the interpretation of the numerical data may not be as straightforward as the *in situ* hybridisation results obtained by the BDGP, the expression values of the purified cell population allow an initial judgment if a gene might be expressed in the trachea or not.

3. The microarray analysis validate previous functional analysis

Ttk plays multiple roles during Drosophila development (Salzberg et al., 1994; Guo et al., 1995; Giesen et al., 1997; Badenhorst et al., 2001; Ramaekers et al., 1997; Badenhorst et al., 2001; Baonza et al., 2002; Althauser et al., 2005; Audibert et al., 2005). In the case of tracheal development we previously observed requirements for Ttk at several steps. Some of these requirements are particularly interesting from the morphogenetic point of view because they involve cellular responses downstream of cell fate specification (Araújo et al.; 2007). Thus, we expected Ttk to control several target genes that impinge directly on cell behaviour, affecting, for instance, the cytoskeletal network, intracellular trafficking or cell junctions. In line with our previous assumptions, we find several Ttk-regulated genes that belong to the GO categories of ''vesicle-mediated transport'', ''cytoskeleton'', or ''plasma membrane''. Very interestingly, we find many genes involved in "Microtubule cytoskeleton", which has been involved in several tracheal events also affected by Ttk activity, like branch fusion,

terminal branch formation, or luminal chitin deposition. Future work will help to determine how Ttk controls microtubule activity and organization, and how this contributes to Ttk phenotype. It is noteworthy that the broadest range of GO terms shared between genes that come up after ttk knockdown in cells and in the *ttk* mutant are involved in 'female gamete generation' (GO:0007292). Ttk has previously been implicated in ovarian follicle development (Althauser et al., 2005; Jordan et al., 2006), and it appears that this function is probably linked to a gene set that may also exhibit broader functionality in the embryonic or cell culture context. This may also be true for an extensive list of genes involved in embryonic axis determination, one of the first functions described for Ttk (Harrison and Travers, 1990). Remarkably, our microarray results confirm previous observations and provide new data for the different Ttk tracheal requirements. For instance, we described that the transcription factor Esg, which plays a pivotal role in fusion cell identity specification (Samakovlis et al., 1996; Tanaka-Matakatsu et al., 1996) is lost when Ttk is over-expressed, but still present in Ttk loss-of-function conditions (Araújo et al.; 2007). The microarray data confirm this regulation, and in addition identifies other genes already shown to directly or indirectly modulate fusion fate as Ttk targets, like *hdc* (Steneberg et al., 1998), CG15252 (Jiang et al., 2007) or *pnt* (Llimargas, 2000. Similarly, we find that *polychaetoid* (*pyd*), which we identified as a Ttk target in *in situ* hybridisation analysis (Araújo et al.; 2007), is differentially expressed in our microarray conditions (it should be noted however that *pyd* is not formally a candidate due to inconsistencies between microarray replicates; in fact only splice variant *pyd*-RE showed a response), explaining in part the requirement of Ttk in tracheal cell intercalation. In addition, it is tempting to speculate about other candidate targets to mediate this function of Ttk in intercalation, like *canoe* (*cno*) for instance, which have been recently shown to act with *pyd* during embryogenesis (Choi et al., 2011).

Finally, it is important to note that besides the organisation and assembly of a transient luminal chitin filament, other mechanisms have also been reported to regulate the size of the tracheal tubes (Schottenfeld et al., 2010). Significantly, we observe that Ttk may be also controlling some of these other mechanisms, like apical secretion through Gef64C (Massarwa et al., 2009), apical cell membrane growth through Mmp1 (Page-McCaw, et al., 2003) or planar cell polarity (Chung et al., 2009). Thus, Ttk would feed into a general and complex program of tube size control being involved in different

mechanisms. Al together, our transcriptome profiling results provided entry points for the investigation of the targets of Ttk regulation in further processes. In particular, they revealed, at least a partial explanation of Ttk's role in tube size regulation.

4. Ttk and Notch interactions

Our microarray data analysis pointed to a regulation of the Notch signalling pathway or its activity by Ttk, likely acting as a negative regulator. These results are in agreement with previously data, which showed Ttk acting as a downstream effector of N activity in the specification of different tracheal identities (Araújo et al., 2007). Indeed, it was showed that Ttk levels depend on N activity in such a way that when N is active, Ttk levels are high, whereas when N is not active, Ttk levels are low. Thus, lower levels of Ttk in tracheal fusion cells due to the inactivity of N were observed (Ikeya and Hayashi, 1999; Llimargas, 2000; Steneberg et al., 1999). Therefore, Ttk acts as a target of N in fusion cell determination. Now, the results of the microarray add an extra level of complexity to the Ttk-N interaction. The observation that in turn Ttk also transcriptionally regulates several N pathway components suggests that Ttk is involved in a feedback mechanism that could play a pivotal role in biasing or amplifying N signalling outcome. In addition, Ttk-N interactions were observed in different developmental contexts, emphasising the importance of such regulations (Guo et al., 1996; Okabe et al., 2001; Ward et al., 2006, Sun et al., 2008; and Mourikis et al., 2010). In addition, a recent report provides evidence of a regulation of N activity by Ttk and proposes a mutually repressive relationship between N and Ttk, which would also involve Ecdysone signalling (Boyle and Berg, 2009). Our results are consistent with many of these observations, indicating that they could represent general molecular mechanisms of morphogenesis. Thus, tracheal cell specification could serve as an ideal scenario to investigate the intricate, and often contradictory, interactions between N and Ttk and the complexity of N signalling.

Chapter II: Analysis of ttk's targets

Identification and selection of a *ttk* target expressed in the tracheal system

We have identified in our *ttk* mis-expression microarray experiments performed, a novel *ttk* target, CG13188, which is expressed in the tracheal system. After validating CG13188 differential expression by qPCR, we selected it for further functional studies.

Firstly, we corroborated and refined CG13188 expression pattern by generating an anti-CG13188 antibody. This protein accumulation analysis not only recapitulated the predicted CG13188 mRNA expression, but also indicated that CG13188 has a dynamic subcellular accumulation during the development of the tracheal system.

We stained *ttk* mutant embryos with the antibody raised against CG13188 to confirm that CG13188 expression levels are, as expected, dependent on the general regulator *ttk*. Interestingly, we saw that *ttk* also controls CG13188 protein localization, as in *ttk* mutant embryos, CG13188 protein did not accumulate apically in the tracheal cells at late embryonic stages, as compared to wild-type. These results suggested on the one hand, that CG13188 in order to perform its function might need to be transported, by an apical sorting mechanism, from the cytoplasm to the apical membrane of the tracheal cells. On the other hand, the CG13188 protein accumulation differences observed could be just a consequence of CG13188 protein levels between the conditions analysed.

CG13188 expression is also controlled by the branch specific regulator *sal*, in a negative manner, as we have seeing that the over-expression of Sal in the tracheal system, caused a markedly decrease of CG13188 protein levels, whereas in the absence of *sal,* we detected a high increased of CG13188 protein levels.

CG13188 is required for the development of the tracheal system

Drosophila tracheal branches have distinct cellular architecture, ranging from multicellular tubes to fine branches. In order to ensure that branches reach their characteristic lengths, apical membrane growth as well as the transient assembly of a luminal chitinous ECM, are required (Hemphala et al., 2003; Devine et al., 2005; Tonning et al., 2005; Luschning et al., 2006). Interestingly, although it has been demonstrated that different branches are formed and elongated by different mechanisms (Samakovlis et al, 1996a; Vincent et al., 1997; Chiara and Hayashi, 2000; Llimargas, 2000; Franch-Marro and Casanova, 2002; Ghabrial et al, 2003), differences between branches regarding maturation events, have not been proposed yet.

The down-regulation of CG13188 in the tracheal system using RNAi technique and several tracheal Gal4 drivers, gave tracheal morphogenesis defects during mid and late embryonic stages. In particular, using several luminal markers, we have seen that from embryonic stage 15, CG13188-RNAi mutants can not accumulate chitin into the luminal space of the most dorsal and ventral tracheal branches. These experiments indicate that CG13188 gene is required to form the chitin luminal cable in a branch specific manner.

Little is known about how tracheal morphological and physiological maturation events are coordinated or connected along embryogenesis. Therefore, although there have not been shown yet experimental evidence that prove a relation between chitin cable formation and gas filling, its correlation has been mainly assumed.

It is known that tracheal tubes in order to become physiologically functional, need to clear the lumen by degrading the chitin filament and the liquid contained (Tsarouhas et al., 2007). One class of genes, whose loss-off-function have been characterized with tracheal gas filling phenotypes, are those implicated in protein clearance by clathrin-mediated endocytosis. Notably, mutations in those genes also result in elongated tracheal phenotypes, suggesting also impairment in tube length control (Behr et al., 2007). Moreover, *serp* and *verm* mutants, which encode for chitin deacytlases proteins that function in tracheal tube length regulation, showed also gas filling defects (Luschnig et al., 2006; Wang et al., 2006).

Another class of proteins that have been reported to function in gas filling are the ENaCs. In vertebrates, ENaC proteins are required to remove the liquid inside the embryonic lung prior to birth (Hummler et al., 1996). In *Drosophila*, there are 16 ENaC genes (also referred as *ppk* genes), 9 of which are expressed in the embryonic tracheal system. Moreover, the down-regulation of several *ppk* genes by RNAi results in larvae gas filling defects. It is thought that the influx of sodium through these channels drives water from the lumen into the epithelial cells, and that degassing of this liquid inflates the trachea (Liu et al., 2003). Besides ENaC, there are other channels known to be also involved in the process, as the sodium-potassium adenosine triphosphatase pump (Na^+/K^+ ATPsa). Interestingly, there are some data suggesting that TGF/BMP pathway may affects the activity of these transporters (Sun et al., 2008).

Tube size and gas filling phenotypes have been detected also exclusively at larvae stages. For instance, mutants for *uif* have correct tracheal morphogenesis and

maturation through embryogenesis, whereas hatched mutants larvae showed crashed and shorter tracheal tubes with gas filling defects (Zhang and Ward, 2010).

In our results, the down-regulation of CG13188 in the tracheal system produced also physiological maturation phenotypes at late embryonic stages. In particular, we have seen in CG13188-RNAi mutants late stage embryos that the branches that did not form the luminal chitinous cable during mid embryogenesis were, in fact, mainly the unique branches that did not gas filled during the maturation process. These observed differences could be dependent on the cellular architecture of the tracheal branches, as CG13188 seem to be mainly required in branches with autocellular AJ. Thus, we suggest on the one hand, the possibility of co-existence of more than one ECM assembly mechanism involved in tracheal tube size control. This novel chitin organisation mechanism might be dependent on branch type. On the other hand, our results might provide a first evidence of a link between chitin cable formation and gas filling tube morphogenesis processes.

Searching on the GENE3D protein database, which provides experimentally defined direct protein-protein interactions (Lees et al., 2012), we have found that CG13188 interact with Sex-lethal and CG11275 proteins. Interestingly, CG11275 gene is assigned, according to this website, to the potassium channel superfamily. In particular, to the potassium voltage-gated channel subfamily A member 1 (also known as Kv1.1), which is a shaker related voltage-gated potassium channel that in humans is encoded by the KCNA1 gene. Mutations in this gene have been shown to be associated with the human myokymia syndrome (Browne et al., 1994). Thus, the possible correlation between CG11275 and CG13188 may open a new direction to investigate the molecular mechanism of CG13188 in gas filling.

It has been recently demonstrated in the *Drosophila* wing that genes encoding for potassium channel proteins are necessary for Dpp production and/or distribution in a temperature dependent manner. Thus, these results connected ion channels and Dpp signalling (Dahal et al., 2012).

In addition, although Ttk regulates transcription, we have found in our microarray data several groups of genes differentially expressed in the Ttk mis-expression conditions analysed, which are classified under GO terms related to ionic intracellular transport, such as GO:0006814 "sodium ion transport", GO: 0015711 "organic anion transport", GO0006812: "cation transport", GO:0005218 "intracellular ligand-gated calcium

channel activity", GO:0015271 "outward rectifier potassium channel activity", GO: 0008273 "potassium:sodium antiporter activity". Thus, it would be interesting to investigate the effects of those genes in gas filling. The use of RNAi lines could serve as a quick approximation to analyse those requirements.

CG13188 molecular nature analysis

We have shown that CG13188 gene putatively encodes a protein with a MH2 domain. This domain is usually found in Smad proteins, which are evolutionarily conserved, and are involved in transducing the TGF-B signalling (Heldin et al, 1997). Upon activation, these proteins directly translocate to the nucleus where they may activate transcription (Datto and Wang, 2000). Therefore, we asked whether CG13188 may acts as a putative dpp transducer during tracheal gas filling. Our preliminary results seem to indicate that it is not the case.

It has been reported that many of the cellular, genetic and molecular mechanisms that underlie the development of different tubular organs in different organisms, are evolutionarily conserved (Metzger and Krasnow, 1999; Gjorevski and Nelson, 2010). We have provided information about the evolutionary conservation of the CG13188 MH2 protein domain, demonstrating that its nucleotide sequence has homology with proteins from different insects, arthropods and non-arthropods organisms. Thus, our preliminary results of CG13188 molecular nature and protein domain conservation show that the organization of the Smad family is more complex than reported, as we have identified two new family members, CG13183 and CG13188.

We intend to carry out a structural-functional analysis through the generation of different forms of CG13188 protein to check it role in the tracheal system. Eventually, and in collaboration with a structural biology laboratory from our Institute, we will analyze the structure of these new proteins.

Future plans

All together our obtained results prompted us to analysis in more detail the role of CG13188 gene during tracheal gas filling, as well as further investigate the role of the TGF-β pathway in the process, and the possibility of CG13188 transducing the pathway.

Conclusions

CONCLUSIONS

1.- The multi-step microarray approach undertaken have identified the transcriptional profile of Ttk's action during *Drosophila* tracheal system development.

2.- The bioinformatics analysis of the microarray outcome performed was validated by an independent quantitative method, strengthening the biological putative value of the data obtained.

3.- The combination of approaches used to analysed the data have provided numerous insights into direct and indirect target genes underlying the broad physiological actions performed by Ttk.

4. - We have identified and confirmed that the group of genes classified under the "chitin metabolism" and "septate junction components" GO terms, mediate Ttk's function in tube size, revealing at least, a partial explanation of Ttk's role in tracheal tube size regulation.

5.- Our results, validating previous functional analysis of Ttk, showed that Ttk is involved in several developmental programmes during tracheal morphogenesis.

6.- Ttk directly regulates the expression of more than half tracheal target genes involved in chitin metabolic processes.

7.- Our results and data validation tests demonstrated that Ttk can perform different stage-specific modes of action, at least, during the development of the tracheal system.

8.- Our microarray analysis is in line with previous observed regulation of the Notch signalling pathway or its activity by Ttk, likely acting as a negative regulator.

9.- Our candidate gene prioritization approach has proved to be a useful toll to identify genes with tracheal requirements (for instance, CG13188).

10.- CG13188 is regulated by *ttk* as observed in the microarray experiments performed and its regulation have been also validated by an independent quantitative method, such as the qPCR.

11.- The dynamic expression of CG13188 during *Drosophila* embryogenesis suggests a developmental function in the tracheal system.

12.- CG13188 protein is spatially, temporally and sub-cellularly regulated, as the generated antibody indicates.

13.- CG13188 expression and protein sub-cellular localisation is regulated by Ttk, whereas Spalt controls negatively its spatial accumulation.

14.- The CG13188 loss-off-function condition generated by the RNAi strategy represents a valuable tool to assess CG13188 tracheal functional requirements.

15.- Down-regulation of CG13188 in trachea is embryo/larvae lethal.

16.- CG13188 encodes for a MH2 protein domain, typically found in Smad proteins. CG13188 MH2 domain presented highest similarity with another uncharacterised protein, CG13183.

17.- Early events of tracheal development occur normally in CG13188-RNAi mutant embryos. In contrast, late events of tracheal development, such as aECM formation and tube maturation, are defective in CG13188-RNAi mutant embryos.

18.- CG13188 has a function in the formation of the chitin cable in specific tracheal branches, particularly in dorsal branches, visceral branches, ganglionic branches and part of the transverse connective

19.- CG13188-RNAi mutant embryos showed tracheal gas filling defects.

Resumen en castellano

RESUMEN DE LA TESIS EN CASTELLANO

INTRODUCCIÓN

Uno de los aspectos más interesantes del campo de la Biología del Desarrollo es entender cómo las células se organizan y coordinan para formar los tejidos y los órganos en los seres vivos (morfogénesis). Muchos órganos que realizan funciones vitales como son el transporte de gases y líquidos en el cuerpo, están formados por estructuras ramificadas tubulares. Ejemplos de órganos tubulares son el pulmón y el sistema vascular en mamíferos, o el sistema traqueal de *Drosophila*.

El desarrollo de un órgano requiere no sólo programas genéticos y mecanismos celulares y moleculares, sino también procesos de maduración, que garantizan la adquisición del tamaño adecuado para su correcta funcionalidad. Por lo tanto, la identificación de los mecanismos que subyacen a la morfogénesis del tubo son una cuestión relevante en el área de la Biología del Desarrollo. Por otra parte, su conocimiento puede tener además implicaciones médicas, ya que hay muchas enfermedades asociadas a defectos en el control del tamaño estructural, como es la enfermedad policística de riñón.

1. MECANISMOS DE TUBULOGÉNESIS

Los tubos se pueden formar mediante diferentes mecanismos morfológicos, dependiendo de la polaridad del tejido al comienzo de la tubulogénesis. Así, hay epitelios prepolarizado y otros en los que la polaridad se establece durante la formación del tubo.

1.1. Envoltura: El tubo se forma por enrollamiento de una porción de un epitelio plano y posterior sellado de sus bordes. Uno de los mecanismos celulares propuestos para conducir la flexión del epitelio es la constricción apical. El tubo neural de muchos vertebrados se forma mediante este mecanismo.

1.2. Gemación: Al igual que el mecanismo anterior, la formación de tubos por gemación generalmente comienza a partir de una lámina epitelial totalmente polarizada. Una porción de la lámina invagina, formándose el nuevo tubo como una extensión directa del tubo original. Es mediante este mecanismo como surgen los tubos durante la morfogénesis de muchos órganos, incluyendo el pulmón de mamíferos y las ramas principales del sistema traqueal de *Drosophila*.

1.3. Cavitación: Las células, que se encuentran formando un cilindro celular, van adquiriendo polaridad, mientras que las células del centro son eliminadas, formándose el lumen. Ejemplos de formación de tubos por cavitación se encuentran en la morfogénesis de la glándula salival y mamaria de mamíferos.

1.4. Vaciamiento del cilindro: Las células, posicionadas en una estructura cilíndrica, remodelan su superficie apical, migran y se agregan, generando así un espacio central (como si vaciarán el centro del cilindro), sin pérdida de células. Los ejemplos incluyen el intestino y sistema nervioso de el pez zebra.

1.5. Vaciamiento de células: El lumen se forma dentro del citoplasma de una única célula abarcando la longitud de la misma (lumen intracelular) y sin presentar uniones adherentes. Este tipo de tubo ha sido descrito en la morfogénesis de la célula excretora de *Caenorhabditis elegans* y en las ramas terminales del sistema traqueal de *Drosophila*.

1.6. Envoltura celular: Mediante este mecanismo también se forman capilares ciegos. Ejemplos han sido descritos en el intestino de *Caenorhabditis elegans*.

1.7. Células de montaje: El tubo se forma como resultado de la migración y cambios morfológicos celulares, acompañados por la especificación de una unión celular adherente. Este mecanismo ha sido descrito en la morfogénesis del corazón de *Drosophila*.

2. SISTEMA TRAQUEAL DE *DROSOPHILA* COMO MODELO DE TUBULOGÉNESIS

El sistema traqueal de *Drosophila* presenta varias características que lo convierten en un excelente modelo para estudiar los mecanismos de formación y regulación del tamaño del tubo. En primer lugar, el sistema traqueal de *Drosophila* consiste en una red de tubos estructuralmente simples, cuyo desarrollo no implica proliferación celular, sino que se basa en la migración de las células y cambios morfológicos. Además, se ha podido observar que muchos de los genes expresados en *Drosophila* tienen su gen ortólogo en organismos vertebrados. De la misma manera, muchos de los mecanismos moleculares y celulares que tienen lugar en la mosca de la fruta han sido conservados a lo largo de la evolución. Por lo tanto, el conocimiento de los principios básicos necesarios para la formación tubular en *Drosophila* no sólo permitirá el conocimiento de mecanismos análogos en vertebrados, sino que ayudarán a

comprender los mecanismos que subyacen enfermedades asociadas a malformaciones de estructuras tubulares durante las etapas embrionarias.

2.1. Función

El sistema traqueal de *Drosophila* es el sistema respiratorio de la mosca. Está compuesto por una red ramificada de tubos epiteliales que transportan oxígeno, facilitando su entrega a todos los tejidos (Ghabrial et al., 2003).

2.2. El desarrollo embrionario del sistema traqueal

2.2.1. Inducción: Veinte grupos de 80-90 células ectodérmicas se diferencian de sus células vecinas y adoptan una morfología específica. Estos grupos de células forman las placodas traqueales. Los factores de transcripción Trachealess (Trh) y Ventral veinless (Vvl) son necesarios para la especificación del destino celular traqueal.

2.2.2. Invaginación: En el estadio 11, las células traqueales empiezan a internalizar de forma ordenada en el embrión.

2.2.3. Ramificación primaria: Seis ramas primarias se forman después de la invaginación. El alargamiento de estas ramas se basa en la migración celular dirigida y reordenamientos celulares. Tres vías de señalización determinan la dirección de la migración y las características particulares de cada rama: Btl se expresa en todas las células traqueales y su ligando Bnl, actúa como un quimioatrayente, dirigiendo la migración celular traqueal (Ribeiro et al., 2002). La vía de Dpp permite la migración de las células traqueales en el eje dorso-ventral. La via de Wg/Wnt permite la migración del DT a lo largo del eje antero-posterior.

2.2.4. Ramificación secundaria: surgen al final de todas las ramas primarias (excepto en el DT) y se caracterizan por su naturaleza unicelular. Las células que dan lugar a ellas expresan marcadores llamados Pantip.

2.2.5. Ramificación terminal: Son largas protuberancias citoplasmáticas constituidos por una sola célula traqueal. Se forman en los extremos de las ramas secundarias y su crecimiento depende de las necesidades de oxígeno de los tejidos.

2.2.6. Fusión de ramas: Es un proceso necesario para interconectar el sistema traqueal, en el que las células de 2 ramas adyacentes (que expresan marcadores de fusión, como *escargot*), mediante cambios en la adhesión celular, morfología y la polaridad, migran hacia la otra.

2.2.7. Maduración: los tubos traqueal para ser fisiológicamente funcionales y alcanzar el tamaño y la forma adecuada, requieren un proceso de maduración.

2.3. Estructura del epitelio traqueal

Las células traqueales están cubiertas de cutícula en su superficie apical o luminal, y de una lámina basal en su superficie basal. Así, su función especializada depende, en parte, de la polaridad apico-basal de las células epiteliales que lo componen. Esta polaridad se evidencia en la localización específica de diferentes complejos de uniones celulares en la membrana lateral. La membrana lateral de las células epiteliales de *Drosophila* se divide en tres dominios, que son, de apical a basal: la zona sub-apical, (SAR), la Zónula Adherente (ZA) y la zona de uniones septadas (SJ). La ZA, cuyo componente principal es la E-cadherina, forma un anillo de adhesión entre las células epiteliales. SJ son específicas de las uniones de invertebrados, cuya función es clave en el mantenimiento de la integridad tisular y en el establecimiento de una barrera de difusión transepitelial. Apical a la ZA, se encuentra la SAR, que tiene un papel organizador en la polarización del epitelio.

2.4. Patrón embrionario traqueal

El patrón embrionario del árbol traqueal es altamente estereotipado, con estructura metamérica y simetría bilateral. Así, cada metámero traqueal consta del tronco dorsal (DT), que es la rama principal y se extiende a lo largo del eje antero-posterior. A partir del DT y perpendiculares a éste, surgen hacia la parte dorsal 10 ramas dorsales (DB). Hacia la parte ventral, 10 conectivos transversales (TC). Los TC conectan el DT con el tronco lateral (LT), tronco paralelo al anterior aunque más fino. Del TC salen las ramas viscerales (VB), que aportan oxígeno al sistema digestivo, la rama del cuerpo graso (FB) y las ramas espiraculares (SB), que llegan hasta la superficie del embrión. Ventrales al LT, surgen las ramas ganglionares (GB) que se extienden hasta el SNC.

2.6. Tipos de ramas traqueales

Cada rama traqueal está formada por un número concreto de células y posee unas dimensiones tubulares características. Análisis estructurales han revelado la existencia de tres tipos de estructuras tubulares en el árbol traqueal:

2.6.1. Tubos de tipo I: Son tubos multicelulares compuestos por células aplanadas, conectadas entre sí por uniones intercelulares, y circundantes al lumen

multicelular que forman. Este tipo de tubo se encuentra, por ejemplo, en el tronco dorsal (DT).

2.6.2. Tubos de tipo II: Se trata también de tubos pluricelulares, pero en este caso son tubos más estrechos que los anteriores. Este tipo de tubos se componen por células traqueales alineadas que se doblan sobre sí mismas y se sellan mediante uniones auto-celulares, envolviendo de esta manera el lumen las células que lo forman. Estos tubos se encuentran en las ramas dorsales (DB), las ramas viscerales (VB) y las ramas ganglionares (GB).

2.6.3. Tubos de tipo III: Este tipo de tubos son tubos ciegos formados por una sola célula carente de uniones auto-celulares. Estas ramas se forman a partir de largas proyecciones citoplasmáticas, en cuyo interior se origina un lumen intracelular. Estos tubos se encuentran en las ramas terminales o traqueolas.

Curiosamente, se ha visto que las ramas de fusion, que conectan los tubos de tipo I y tipo II de metámeros adyacentes para asegurar una red tubular continua, son heterogéneos en su composición. La parte principal de la rama de fusión es un tubo extracelular, mientras que la parte menor de la rama de fusión es intracelular.

3. MADURACIÓN DEL TUBO

Para que el sistema respiratorio lleve a cabo su función correctamente, es necesario que cada rama traqueal adquiera, durante la fase de maduración, un diámetro y longitud específica. Estos dos procesos se regulan independientemente y se producen tanto en las células como en el lumen del sistema traqueal. Se ha relacionado el tamaño de los tubos con modificaciones en la morfología celular, crecimiento de la membrana apical y una reorganización del citoesqueleto sub-apical. Aunque aún no se han identificado diferencias, debido a las características tubulares específicas de cada rama, los mecanismos celulares necesarios para formarlas deberían ser diversos. El proceso de maduración ha sido dividido en varias fases secuenciales e inter-dependientes:

3.1. Secreción: Durante el estadio 14, las células traqueales secretan al lumen los componentes necesarios para el ensamblaje de una matriz extracelular proteica rica en quitina. Este polímero se organiza en fibras/cilindro que acaban ocupando el lumen durante el estadio 15.

3.2. Expansión del diámetro del tubo y restricción de la longitud: Se ha propuesto que la expansión del cilindro de quitina controla el diámetro de las ramas mediante dos acciones simultaneas: la primera es la de promover la dilatación del tubo mecánicamente, y la segunda es la de señalizar a las células traqueales la re-organización de su citoesqueleto con el fin de reajustarse al cambio de diámetro. En el estadio 16, estas mismas fibras de quitina son modificadas, proceso que regula la longitud y la curvatura de las ramas.

 3.3. Eliminación del material sólido luminal y sustitución del líquido luminal por el gas: Finalmente, durante el estadio 17, el haz de quitina es degradado por endocitosis y eliminado de la cavidad luminal antes de rellenarse de gas mediante mecanismos aún no bien entendidos.

4. FUNCIONES DEL FACTOR DE TRANSCRIPCIÓN TRAMTRACK DURANTE EL DESARROLLO EMBRIONARIO DEL SISTEMA TRAQUEAL

4.1. Características generales

Tramtrack (Ttk) es un factor de trancripción que se caracterizó por primera vez mediante una técnica de cribado que pretendía identificar nuevos genes implicados en el proceso de segmentación embrionaria de *Drosophila*. Hasta ahora, las funciones descritas para Ttk han sido relacionadas principalmente con la especificación de destino celular en diversos tejidos.

4.2. Tramtrack regula diferentes procesos morfogenéticos durante el desarrollo del sistema traqueal de *Drosophila*

Interesantemente, un trabajo previo de nuestro laboratorio ha demostrado que Ttk actúa como un gen clave para el desarrollo traqueal. En particular, se observó que Ttk está involucrado durante todo el desarrollo traqueal, en diferentes eventos, como son, la especificación del destino celular traqueal, establecimiento del patrón de ramificación, regulación de los cambios morfológicos en las células, regulación de la formación del lumen intracelular y en el control del tamaño del tubo traqueal. Actualmente, no se entiende completamente cómo Ttk regula todas estas variadas funciones traqueales.

RESULTADOS Y DISCUSIÓN

Capítulo I: Identificación mediante la técnica de microarrays de genes diana de Tramtrack durante el desarrollo del sistema traqueal de *Drosophila*

El objetivo principal de esta Tesis ha sido profundizar en el conocimiento de cómo el factor de transcripción Tramtrack realiza sus múltiples funciones durante el desarrollo del sistema traqueal de *Drosophila*. Así, para identificar su perfil transcripcional y los posibles factores que medien, directa e indirectamente sus funciones, hemos utilizado como aproximación principal la técnica de microarrays.

1. TÉCNICA DE MICROARRAYS PARA IDENTIFICAR EL PERFIL TRANSCRIPCIONAL DE TRAMTRACK EN EL DESARROLLO DEL SISTEMA TRAQUEAL DE *DROSOPHILA*

Ttk, como un factor de transcripción, podría regular la expresión espacio-temporal de miles de genes diferentes que contribuyen al desarrollo y funcionamiento del organismo. Está implicada en una amplia gama de decisiones de desarrollo, que van desde el desarrollo embrionario temprano hasta procesos de diferenciación durante la organogénesis (Harrison y Travers, 1990; Lee y Manley, 1992; Guo et al, 1995; Badenhorst, 2001;. Araújo et al, 2007). Específicamente, estamos interesados en Ttk como actor clave durante el desarrollo traqueal, ya que está involucrado en la creación de identidades traqueales, reordenamientos de las células traqueales, fusión de ramas, en la formación de tubos intracelulares y en el control del tamaño del tubo (Araújo et al., 2007). A fin de separar específicamente la acción traqueal de Ttk de su acción en otros tejidos, e identificar los genes diana directos o indirectos que podrían explicar los diversos fenotipos traqueales observadas en embriones mutantes *ttk*, utilizamos como aproximacíon experimental la técnica de microarrays. Este método cuantifica de forma simultánea y reproducible los niveles de expresión de miles de genes, permitiendo determinar variaciones en la expresión génica de las condiciones biológicas estudiadas.

Así, hemos llevado a cabo experimentos de microarray en embriones homocigotos para mutantes *ttk* y comparado con embriones control, en las etapas embrionarias de 11 a 16. También, hemos realizado el experimento en embriones en los mismos estadios que sobreexpresan *ttk* en el dominio de la línea *btl* Gal4, que incluye el sistema traqueal y la línea media, junto con los controles. Además, hemos combinado estos perfiles de expresión con perfiles de células embrionarias aisladas y enriquecidas en células traqueales.

En primer lugar generamos las líneas de moscas apropiadas (véase Materiales y Métodos para más detalles), las cuales fueron:

- Mutant línea: btl RFP moe ttkD2-50 / TM3 twi-GFP

- Línea control para los experimentos mutantes: btl RFP moe/TM3 twi-GFP.

Estas dos líneas generadas llevan un cromosoma balanceador que presenta la proteína verde fluorescente (GFP), lo que nos permitió distinguir las condiciones homocigotas (por la ausencia de expresión de GFP) de los heterocigotos, tanto de la línea control como del mutante *ttk,* utilizando el citómetro para embriones COPAS.

El experimento de ganancia de función se realizó utilizando el sistema Gal4/UAS (Brand y Perrimon, 1993). En particular, utilizamos la línea viable en homocigosis "*btl* Gal4 UAS tau GFP", para impulsar la expresión del constructo UAS ttk69 en el sistema traqueal, ya que la línea btl Gal4 se expresa principalmente en el sistema traqueal. Tau es una proteína asociada a los microtúbulos y es ideal para mostrar la morfología celular (Butner y Kirschner 1991); Callahan y Thomas, 1994). Por otra parte, esta construcción tiene la proteína Tau, fusionada a GFP, lo que nos permitió detectar la sobreexpresión por la presencia de GFP en las células de la tráquea.

La línea control que utilizamos para este experimento fue la línea recombinante "*btl* RFP moe UAS ttk 69" sin cruzarla con la línea *btl* Gal4.

Además, todas las líneas generadas expresan también la proteína roja fluorescente (RFP) bajo el control del constructo btl Gal4 moe RFP (ver Materiales y métodos para más detalles). Esto permitió aislar las células *btl* positivas utilizando la técnica de FACS.

Tras examinaran "*in vivo*" bajo un microscopio de fluorescencia, la detección de las células *btl* positivas en rojo (debido a la "btl Gal4 RFP moe") y que se distinguían los embriones homocigotos de heterocigotos (por la ausencia o presencia de GFP); comprobamos mediante técnicas de inmunodetección, que los stocks de moscas mutantes generados llevaban las mutaciones deseadas.

A continuación, tras obtener el material biólogico necesario extraíos el ARN de cada muestra en tres réplicas, y las hibridamos en Affymetrix Genoma de Drosophila de 2.0 (véase Materiales y Métodos).

2. Microarray diseño, las limitaciones experimentales, calidad de los datos y la interpretación

En este proyecto se ha utilizado un estudio de microarrays como un enfoque genómico para identificar los genes directos e indirectos que median la función de *ttk* durante el desarrollo traqueal, con el fin de diseccionar mejor la actividad traqueal de *ttk*. A tal fin, combinamos microarrays de células específicas y microarrays de embriones enteros, con la intención de, a través de la comparación de los resultados de ambas condiciones, reducir el ruido generado en los datos, maximizando la identificación de genes diana traqueales de *ttk*.

Con el fin de obtener información biológica fiable de nuestro análisis y evitar variaciones tecnológicas, normalizamos los datos respecto a dos grupos de genes de expresión invariable: glucólisis y oxido-fosforilación (Bilban et al, 2002.). Por este método, hemos detectado réplicas experimentales de microayyars, que no se comportan como tal, por lo que los filtramos por exclusión, para posteriores análisis, eliminando así el efecto que podrían tener sobre nuestros datos. Aunque ha habido varios ejemplos exitosos de microarrays de tejidos específicos, la purificación de un tipo celular específico ha sido desde hace años un reto biológico (Bryant et al, 1999;.. Borghese et al, 2006). Hoy en día, el nuevo método Pico permite obtener gran precisión en perfiles de expresión partiendo de poblaciones celulares muy pequeñas, como son las formadas por tan sólo diez células (González-Roca et al., 2010). Nosotros, para realizar los microarrays específicos de células *btl*, utilizamos FACS, lo que nos premitió detectar y ailsar de entre toda la población celular, las células que expresaban el indicador fluorescente bajo el control del promotor del gen *breathless* (*btl*) (btl RFP moe). Aunque no fue posible aislar una población pura traqueal, encontramos que ésta población estaba enriquecida en genes traqueales (Por ejemplo, *trachealess*), así como también encontramos una fuerte presencia transcripcional para genes de la linía media del embrión, amnioserosa y otros tejidos, que hasta ahora sólo había evidencia anecdótica para la actividad de *btl*. Curiosamente, también encontramos expresión de genes en la población de células, que de acuerdo con la base de datos de expresión génica BDGP, no deberían expresarse en el embrión. En comparación con los perfiles de expresión temporal de modENCODE, inferimos que muchos de ellos son falsos negativos.

Debido a las limitaciones inherentes de los experiemntos, los genes identificados como diferencialmente expresados mediante la técnica de microarrays, deben ser confirmados por un método independiente. Aunque uno de los métodos más utilizados para validar los experimentos de microarrays es qPCR, no existe un acuerdo claro entre los dos métodos. Algunos autores creen que para confirmar los datos de microarrays, basta un acuerdo sobre la dirección del cambio de expresión (Rajeevan et al., 2001). Además, las técnicas de microarrays y qPCR difieren en muchos aspectos, incluyendo en el método para la transcripción reversa, la dinámica de reacción y los métodos de normalización aplicados.

Confirmamos por qPCR el cambio de dirección de expresión de todos los genes testados, aunque hemos visto diferencias en la magnitud del cambio. Estas diferencias podrían reflejar la diferencia de sensibilidad entre ambas técnicas. Así, mientras que los microarrays permiten medir en un único experimento un número mayor de genes que qPCR, se ha demostrado que la qPCR tiene mayor sensibilidad, ya que detecta de modo preciso la cuantificación de un menor número de genes por reacción (Bio-Rad, 2006). También encontramos algunos resultados contra-intuitivos entre las técnicas, los cuales no eran estadísticamente significativos. Por ejemplo, experimentos anteriores de hibridación *in situ* mostraron que el nivel de expresión de *bnl* disminuye en mutantes *ttk* (Araújo et al., 2007), pero no pudimos reproducir en los microarrays este resultado. El análisis adicional de qPCR por estadios embrionarios validó el cambio transcripcional de *bnl* observado en el experimento anterior de hibridación *in situ*. Por otra parte, este tipo de análisis qPCR por estadios, nos ayudó a interpretar los resultados contradictorios entre el microarrays y qPCR.

Usando nuestros criterios de selección de genes candidatos, el trabajo de Reddy y colaboradores, donde estudiaron la disminución de la expresiñon de *ttk* en células S2 de *Drosophila,* produce 1380 genes candidatos, en comparación con los 600-800 genes en que obtenemos en nuestras condiciones mutantes para *ttk*. El mayor número de genes es al menos en parte, debido al hecho de que su conjunto de datos comprende muchos más repeticiones y, por lo tanto, permite a un número mayore de genes cumplir con el criterio de significación (p<= 0,05). Sin embargo, el grado de solapamiento entre nuestros y sus experimentos es estadísticamente significativo, aunque la superposición absolutas entre su lista de genes y las nuestras es pequeña. En los experimentos donde esperamos que los resulatdos sean inversamente correlacionados (Por ejemplo, genes

que disminuyan su expresión en la condición de mutantes *ttk*, y después en la condición de sobre-expresión de *ttk* aumente su expresión o viceversa) fueron significativos. Sin embargo, también hay que señalar que esto no fue observado en unos pocos casos. Se puede suponer que, mientras que la mayoría de los genes diana directos o indirectos de Ttk responden apropiadamente a la situación experimental, la sobre-expresión, en particular, puede provocar resultados inesperados. Así, argumentamos que la situación mutante representa probablemente mejor la respuesta biológicamente interpretables, ya que en la situación de sobre-expresión pueden haber muchos efectos posteriores más ectópicos.

Nuestro análisis proporcionó un censo de genes cuya transcripción depende de Ttk, revelando nuevos aspectos en los mecanismos de acción de Ttk.

3. El análisis por microarrays valida un análisis funcional anterior

Ttk desempeña múltiples funciones durante el desarrollo de *Drosophila* (Salzberg et al, 1994;. Guo et al, 1995;. Giesen et al, 1997;. Badenhorst et al, 2001;. Ramaekers et al, 1997;.. Badenhorst et al, 2001; Baonza et al, 2002;. Althauser et al, 2005;.. Audibert et al, 2005). En el caso del desarrollo traqueal, nuestro laboratorio observó previamente su requerimiento en varios pasos. Algunos de estos requisitos son particularmente interesantes desde el punto de vista morfogenético porque implican respuestas celulares por debajo de la especificación del destino celular (Araújo et al;. 2007). Así, esperamos que Ttk controle varios genes diana que incidan directamente sobre el comportamiento celular, afectando, por ejemplo, al citoesqueleto o al tráfico intracelular. Así, encontramos varios genes regulados por Ttk que pertenecen a las categorías de GO "transporte mediado por vesiculas", "citoesqueleto", o "membrana plasmática". Cabe señalar que la más amplia gama de términos GO compartida entre los experimentos de Reddy y colaboradores y los nuestros están involucrados en la "generación gameto femenino" (GO: 0007292). Ttk ha sido implicado previamente en el desarrollo del folículo ovárico (Althauser et al, 2005;.. Jordan et al, 2006). Esto también puede ser cierto para una lista extensa de genes implicados en la determinación del eje embrionario, una de las primeras funciones descritas para Ttk (Harrison y Travers, 1990). Además, nuestros resultados confirman las observaciones anteriores y proporcionar nuevos datos para los diferentes requerimientos Ttk traqueales. Por ejemplo, hemos descrito que el factor de transcripción Esg, que desempeña un papel fundamental en la especificación de la identidad de la fusión de células (Samakovlis et

al, 1996;.. Tanaka-Matakatsu et al, 1996) se pierde cuando Ttk es sobre-expresado, pero todavía presente TTK en la pérdida de función de las condiciones (Araújo et al;. 2007). Nuestro análisis por microarray confirma esta regulación, e identifica otros genes que, directa o indirectamente modulan la función de Ttk durante el proceso traqueal de fusión, como *headcase* (Steneberg et al., 1998), CG15252 (Jiang et al., 2007) o *pointed* (Llimargas , 2000). De manera similar, encontramos que *polychaetoid*, se expresa diferencialmente en nuestras condiciones de microarrays, que explica en parte la función de Ttk en el proceso de intercalación celular traqueal. Además, es tentador especular acerca de otros candidatos para mediar esta función de Ttk, como *canoe* que ha sido recientemente demostrado que actua con Polychitoid durante la embriogénesis (Choi et al., 2011).

Además, se ha descrito que *ttk* interviene en el proceso de regulación del tamaño del tubo (Araújo et al., 2007). Es importante señalar que además de la organización y montaje de un filamento de quitina luminal transitoria, otros mecanismos también se han reportado para regular el tamaño de los tubos traqueales (Schottenfeld et al., 2010). Significativamente, se observa que Ttk puede ser también el control de algunos de estos otros mecanismos, como la secreción apical a través de Gef64C (Massarwa et al., 2009), el crecimiento celular a través de la membrana apical MMP1 (Page-McCaw, et al., 2003) o de la polaridad planar celular (Chung et al., 2009).

En conjunto, nuestros resultados proporcionan una explicación parcial de Ttk en las diferentes funciones traqueales mencionadas. Además, estos datos pueden considerarse como el punto de partida para la investigación de los genes diana de Ttk en los procesos antes mencionados.

4. IDENTIFICACIÓN DE GENES DIANA DE TTK IMPLICADOS EN EL METABOLISMO DE QUITINA

En un trabajo previo de nuestro laboratorio, se conectó la función de *ttk* con la regulación en el tamaño del tubo (Araújo et al., 2007). Interesantemente, encontramos durante el curso del análisis GO, un montón de genes diferencialmente expresados, que clasificaban bajo el término GO "Metabolismo de quitina". Así, tras validar por qPCR su valor de expresión diferencial observado en los microarrays, y para entender si estos genes podían mediar la función de *ttk* en el control del tamaño del tubo, los seleccionamos para un estudio funcional. La aproximación llevada a cabo consistía en medir (aplicando una modificación de un protocolo previo pubñicado) la longitud de la

rama del DT en embriones mutantes o mediante técnicas RNAi para estos genes y compararlo con la edición de embriones control, y ver estadísticamente si la diferencia era significativa. De este modo, vimos como diferentes genes implicados en el metabolismo de quitina, presentana un fenotipo de ramas traqueales extra-largas.

Además, utilizando lo sdatos disponibles en modENCODE, encontramos que 40 de los 77 genes relacionados con el metabolismo de quitina mostraban sitios de unión para Ttk.

Capítulo II: Analysis of *ttk*'s targets

1. IDENTIFICACIÓN Y SELECCIÓN DE UN GEN DIANA DE *TTK* QUE SE EXPRESA EN EL SISTEMA TRAQUEAL

Hemos identificado en nuestros experimentos por microarrays un nuevo gen diana de *ttk*, CG13188, que se expresa en el sistema traqueal. Después de validar la expresión diferencial de CG13188 mediante qPCR, lo seleccionamos para estudios funcionales.

En primer lugar, corroboramos y refinamos el patrón de expresión de CG13188 mediante la generación de un anticuerpo anti-CG13188 específico. Este análisis, no sólo recapitula el patrón de expresión de ARNm predicho para CG13188 en la web de expresión de BDGP, sino que también indica que la proteína CG13188 se acumula subcelularmente de modo dinámico durante el desarrollo del sistema traqueal.

Al teñir embriones mutantes *ttk* con el anticuerpo producido contra CG13188, confirmamos que los niveles de expresión de CG13188 son, com esperabamos, dependientes del regulador general *ttk*. Curiosamente, hemos visto que también controla *ttk* la localización proteica de CG13188, ya que en embriones mutantes *ttk*, la proteína no se acumulan apicalmente en las células de la tráquea en las últimas etapas embrionarias, en comparación con el de tipo salvaje. Estos resultados sugieren, por una parte, que CG13188 con el fin de realizar su función podría tener que ser transportado desde el citoplasma a la membrana apical de las células tráqueales. Por otra parte, las diferencias en acumulacion de la proteína CG13188 podrían ser simplemente consecuencia de distitos niveles de proteína entre las condiciones analizadas. La expresión de CG13188 también está controlada por el regulador de rama específica *spalt (sal)*, ya que hemos visto que la sobre-expresión de Sal en el sistema traqueal, provoca una marcada disminución de los niveles de la proteína CG13188, mientras que

147

en ausencia de *sal*, detectamos un alto incremento en los niveles de la proteína CG13188.

2. CG13188 ES NECESARIO PARA EL DESARROLLO DEL SISTEMA TRAQUEAL

Las ramas traqueales de *Drosophila* tienen una arquitectura celular distinta, yendo desde tubos multicelulares a las ramas finas. Con el fin de garantizar que las ramas alcanzan su longitud característica, se ha descrito que procesos de crecimiento de la membrana apical, así como el emsamblaje transitoria de un filamento de quitina, se requieren (Hemphala et al, 2003;. Devine et al, 2005;.. Tonning et al, 2005; Luschning et al., 2006). Curiosamente, aunque se ha demostrado que las diferentes ramas se forman y alargan por diferentes mecanismos (Samakovlis et al, 1996a; Vincent et al, 1997;. Chiara y Hayashi, 2000; Llimargas, 2000; Franch-Marro y Casanova, 2002; Ghabrial et al, 2003), diferencias entre las ramas con respecto a eventos de maduración, no se han identificado aún. La disminución de expresion de CG13188 en el sistema traqueal utilizando la técnica de RNAi y varios conductores traqueales Gal4, produjo defectos en la morfogénsis traqueal durante etapas medias y tardías embrionarias. En particular, utilizando varios marcadores luminales, hemos visto que desde la etapa embrionaria 15, los embriones CG13188-RNAi no acumular quitina en el espacio luminal de las ramas traqueales más dorsales y ventrales. Estos experimentos indican que CG13188 es necesario para formar el cable de quitina luminal de una manera rama específica.

Poco se sabe acerca de cómo los eventos morfológicos y fisiológicos durante el proceso de maduración traqueal son coordinadas a lo largo de la embriogénesis. Por lo tanto, aunque no se ha demostrado todavía evidencias experimentaesl que demuestren una relación entre la formación del cable de quitina y el relleno de gas de los tubos, su correlación se ha asumido.

Se sabe que los tubos traqueales para ser fisiológicamente funcionales, necesitan vaciar el lumen, degradando el filamento de quitina y reabsorviendo el líquido contenido (Tsarouhas et al., 2007). Una clase de genes, cuya falta de función se ha caracterizado con fenotipos de llenado de gas, son los implicados en la endocitosis mediada por clatrina. En particular, mutaciones en estos genes también dan lugar a fenotipos de tamaño, ya que presentan tubos traqueales alargados, lo que sugiere también defectos en el control de longitud de tubo (Behr et al., 2007). Además, mutantes para *serp* y *verm*,

que codifican para deacetilasas implicadas en el control del tamaño tubular, presentan también defectos de llenado de gas (Luschnig et al, 2006;.. Wang et al, 2006).

Otra clase de proteínas que han sido reportadas para funcionar en el llenado de gas son los ENaCs. En los vertebrados, las proteínas ENaC se requieren para eliminar el líquido del interior del pulmón embrionario antes del nacimiento (Hummler et al., 1996). En *Drosophila*, existen 16 genes ENAC (también conocidos como genes *ppk*), 9 de los cuales se expresan en el sistema traqueal embrionario. Por otra parte, la disminuciñon de expresión de varios genes *ppk* por la técnica de RNAi, produce defectos de llenado en larvas. Se cree que la afluencia de sodio a través de estos canales conduce el agua desde el interior del tubo hacia las células epiteliales, y que la desgasificación de este líquido infla la tráquea (Liu et al., 2003). Además de los canales ENaC, hay otros canales iónicos que se sabe participan también en el proceso, como es la bomba de sodio-potasio trifosfatasa de adenosina (Na^+/K^+ ATPsa). Curiosamente, existen algunos datos que sugieren que la vía de TGF/BMP afecta a la actividad de estos transportadores (Sun et al., 2008).

En nuestros resultados, la disminución en niveles de expresión de CG13188 en el sistema traqueal produce también fenotipos fisiológicos en las últimas etapas embrionarias, durante el proceso de maduración traqueal. En particular, hemos visto en embriones tardíos CG13188-RNAi que las ramas que no acumulaban quitina luminal durante etapas embrionarias anteriores, eran principalmente las únicas ramas que no se llenaban de gas. Estas diferencias observadas podrían ser dependientes de la arquitectura celular de las ramas traqueales. Por lo tanto, por una parte sugerimos la posibilidad de la coexistencia de más de un mecanismo implicado en la organización de la matriz extracelular necesaria para la adquisión del correcto tamaño de los tubos traqueales. Este mecanismo de organización de quitina podría ser dependiente del tipo de rama. Por otro lado, nuestros resultados proporcionan una primera evidencia de la relación entre la formación del cable de quitina y del proceso de llenad de gas.

En la base de datos de proteínas Gene3D, (Lees et al., 2012), proponen que CG13188 actua con Sex-letal y la proteína CG11275. Curiosamente, el gen CG11275 clasifica de acuerdo con este sitio web, a la superfamilia de canales de potasio. En particular, a la subfamilia de canal de potasio dependiente de voltaje, miembro 1; que en humanos está codificada por el gen KCNA1. Se ha descrito que mutaciones en este gen están asociados al síndrome humano mioquimia, que produce movimientos involuntarios

(Browne et al., 1994). Por lo tanto, la posible correlación entre CG11275 y CG13188 abre un nuevo enfoque para investigar el mecanismo molecular de acción de CG13188 durante el llenado de gas de las tráqueas.

Recientemente, se ha publicado utilzando el ala de *Drosophila* como sistema modelo, que los genes que codifican para las proteínas de canales de potasio son necesarios para la producción y/o distribución de Dpp de manera dependiente de la temperatura. Por lo tanto, estos resultados conectan los canales iónicos con la señalización Dpp (Dahal et al., 2012).

Además, hemos encontrado en nuestros resultados de microarrays varios grupos de genes, diferencialmente expresados en las condiciones analizadas, que se clasifican bajo diferente términos de GO relacionados con el transporte intracelular iónica, como GO 0006814: "ion sodio transporte", GO: 0015711 "transporte de aniones orgánicos", GO0006812:"transporte de cationes ", GO: 0005218: "ligando intracelular actividad de los canales de calcio", GO: 0008273 "potasio: sodio actividad anti-portadora". Por lo tanto, sería interesante investigar los efectos de esos genes en el llenado de gas. El uso de líneas de RNAi podría servir como una aproximación rápida a analizar esos requisitos.

3. ANÁLISIS MOLECULAR DE CG13188

El gen CG13188 codifica para una proteína con un dominio MH2. Este dominio se encuentra normalmente en las proteínas de tipo Smad, que se encuentran conservadas evolutivamente, y están implicadas en la transducción de la vía de señalización de TGF-B. Tras la activación, estas proteínas se translocan al núcleo, donde pueden activar la transcripción de otros genes (Datto y Wang, 2000). Por lo tanto, nos preguntamos si CG13188 pordía actuar como transductor de la vía de Dpp durante el proceso de llenado de gas en las tráqueas. Nuestros resultados preliminares parecen indicar que no es el caso.

Se ha descrito que muchos de los mecanismos celulares, genéticos y moleculares que subyacen al desarrollo de diferentes órganos tubulares en diferentes organismos, están

evolutivamente conservados (Metzger y Krasnow, 1999; Gjorevski y Nelson, 2010). Por lo que nos preguntamos si el dominio MH2 de CG13188 también lo estaría. Así, llevamos a cabo un análisis de comparación de la secuencia nucleótica del dominio MH2 de CG13188 en diferentes organismos. Nuestro análisis indica que el dominio proteico estudiado presenta homología con proteínas de diferentes insectos, artrópodos y organismos no-artrópodos. Además, hemos visto que el dominio proteico de CG13188 presenta homolgía con las otras proteínas Smad de *Drosophila* descritas. En particular, nos ha llamado la atención, encontrar en este análisis que presenta una mayor similitud con otra la proteina codificada por el gen CG13183. Nuestros resultados indican que la organización de la familia proteica Smad es más compleja que lo que se ha reportado hasta la fecha, ya que hemos identificado dos nuevos miembros de la familia, CG13183 y CG13188.

Planes experimentales futuros

Tenemos la intención de llevar a cabo un análisis estructural y funcional, mediante la generación de diferentes formas de la proteína CG13188, para estudiar con mayor profuncidad su implicación y función en el desarrollo del sistema traqueal. Finalmente, y en colaboración con un laboratorio de biología estructural de nuestro Instituto, pretendemos analizar la estructura de estas nuevas proteínas.

References

REFERENCES

Affolter, M., Montagne, J., Walldorf, U., Groppe, J., Kloter, U., LaRosa, M. and Gehring, W.J. (1994). The *Drosophila* SRF homolog is expressed in a subset of tracheal cells and maps within a genomic region required for tracheal development. *Development* **120**, 743-753.

Affolter, M., Bellusci, S., Itoh, N., Shilo, B., Thiery, J.P. and Werb, Z. (2003). Tube or not tube. Remodeling epithelial tissues by branching morphogenesis. *Dev. Cell* **4,** 11-18.

Althauser, C., Jordan, K.C., Deng, W.M. and Ruohola-Baker, H. (2005). Fringe-dependent *notch* activation and tramtrack function are required for specification of the polar cells in *Drosophila* oogenesis. *Dev. Dyn.* **232**, 1013-1020.

Ashburner, M. (1989). *Drosophila: A laboratory handbook. Cold Spring Harbor Laboratory Press, Cold Spring Harbor, NY.*

Araújo, S., Aslam, H., Tear, G. and Casanova, J. (2005). *mummy/cystic* encodes an enzyme required for chitin and glycan synthesis, involved in trachea, embryonic cuticle and CNS development- Analysis of its role in *Drosophila* tracheal morphogenesis. *Dev. Biol.* **288**, 179-193.

Araújo, S., Cela, C. and Llimargas, M. (2007). Tramtrack regulates different morphogenetic events during *Drosophila* tracheal development. *Development* **134**, 3665-3676.

Audibert, A., Simon, F. and Gho, M. (2005). Cell cycle diversity involves differential regulation of Cyclin E activity in the *Drosophila* bristle cell lineage. *Development* **132**, 2287-2297.

Bachmann, A., Draga, M., Grawe, F. and Knust, E. (2008). On the role of the MAGUK proteins encoded by *Drosophila varicose* during embryonic and postembryonic development. *BMC Dev. Biol.* 8:55.

Badenhorst, P. (2001). *Tramtrack* controls glial number and identity in the *Drosophila* embryonic CNS. *Development* **128,** 4093-410.

Baer, M.M., Chanut-Delalande, H. and Affolter, M. (2009). Cellular and molecular mechanisms underlying the formation of biological tubes. *Curr. Top Dev. Biol.* **89**, 137-62.

Baer, M.M., Bilstein, A., Caussinus, E., Csiszar, A., Affolter, M. And Leptin, M. (2010). The role of apoptosis in shaping the tracheal system in the *Drosophila* embryo. *Mech Dev*.**127**, 28-35.

Baonza, A., Murawsky, C.M., Travers, A.A. and Freeman, M. (2002). Pointed and Tramtrack69 establish an EGFR-dependent transcriptional switch to regulate mitosis. *Nat. Cell Biol*. **4**, 976-980.

Bardwell, V.J. and Treisman, R. (1994). The POZ domain: a conserved protein-protein interaction motif. *Genes Dev.* **8**, 1664-1677.

Barrett, T., Troup, D.B., Wilhite, S.E., Ledoux, P., Evangelista, C., et al. (2011). NCBI GEO: archive for functional genomics data sets–10 years on. *Nucleic Acids Res*. **39**, 1005-1010.

Behr, M., Riedel, D. and Schuh, R. (2003). The claudin-like *megatrachea* is essential in septate junctions for the epithelial barrier function in *Drosophila. Dev Cell* **5**, 611-620.

Behr, M., Wingen, C., Wolf, C., Schuh, R. and Hoch, M. (2007). Wurst is essential for airway clearance and respiratory-tube size control. *Nat Cell Biol.* **9**, 847-853.

Beitel, G.J and Krasnow, M.A. (2000). Genetic control of epithelial tube size in *Drosophila* tracheal system. *Development* **127**, 3271-3281.

Bilban, M., Buehler, L., Head, S., Desoye, G. and Quaranta, V. (2002). Normalizing DNA Microarray Data. *Curr. Issues Mol. Biol*. **4**, 57-64.

References

Bio-Rad Laboratories (2006). Real-Time PCR Applications Guide.

Borghese, L., Fletcher, G., Mathieu, J., Atzberger, A., Eades, W., Cagan, R.L. and Rørth, R. (2006). Systematic analysis of the transcriptional switch inducing migration of border cells. *Dev. Cell* **10**, 497-508.

Boube, M., Llimargas, M. and Casanova, J. (2000). Cross-regulatory interactions among tracheal genes support a co-operative model for the induction of tracheal cell fates in the *Drosophila* embryo. *Mech. Dev.* **91**, 271-278.

Boube, M., Martin-Bermudo, M.D, Brown, N.H. and Casanova, J. (2001). Specific tracheal migration is mediated by complementary expression of cell surface proteins. *Genes Dev.* **15**, 1554-1562.

Boyle, M.J. and Berg, C.A. (2009). Control in time and space: Tramtrack69 cooperates with Notch and Ecdysone to repress ectopic fate and shape changes during *Drosophila* egg chamber maturation. *Development* **136**, 4187-4197.

Bradshaw, R.A. (1989). Protein translocation and turnover in eukaryotic cells. *Trends Biochem. Sci.* **14**, 276-279.

Brand, A.H. and Perrimon, N. (1993). Targeted gene expression as a means of altering cell fates and generating dominant phenotypes. *Development* **118,** 401-415.

Bryant, Z., Subrahman, L., Tworoger, M., Latray, L., Chun-Rong, L., Meng-Jin, L., Ger-Van, D. and Ruohola-Baker, H. (1999). Characterization of differentially expressed genes in purified *Drosophila* follicle cells: Toward a general strategy for cell type-specific developmental analysis. *Proc. Natl. Acad. Sci. USA* **96**, 5559-5564.

Brodu, V. and Casanova, J. (2006). The RhoGAP crossveinless-c links *tracheales* and EGFR signaling to cell shape remodeling in *Drosophila* tracheal invagination. *Genes Dev.* **20,** 1817-1828.

Brown, J.L., Sonoda, S., Ueda, H., Scott M.P. and Wu, C. (1991). Repression of the *Drosophila fushi tarazu* (*ftz*) segmentation gene. *EMBO J.* **10**, 665-674.

Brown, S., Hu, N. and Hombria, J.C. (2001). Identification of the first invertebrate interleukin JAT/STAT receptor, the *Drosophila* gene *domeless*. *Curr. Biol.* **11**, 1700-1705.

Browne, D.L., Gancher, S.T., Nutt, J.G., Brunt, E.R., Smith, E.A., Kramer, P. and Litt, M. (1994). Episodic ataxia/myokymia syndrome is associated with point mutations in the human potassium channel gene, KCNA1. *Nat. Genet.* **8**, 136-140.

Buechner, M. (2002). Tubes and the single *C. elegans* excretory cell. *Trends Cell Biol.* **10**, 479-484.

Buck, J. And Keister, M. (1955). Further studies of gas-filling in the insect tracheal system. *J. Exp. Bio.* **32**, 681-691.

Buechner, M. (2002). Tubes and the single *C. elegans* excretory cell. *Trends Cell Biol.* **12**, 479-84.
Butuer, K.A., and Kirschner, M.W. (1991). Tau protein binds to microtubules through a flexible array of distributed weak sites. *J. Cell Biol*. **115,** 717-730.

Cabernard, C. and Affolter, M. (2005). Distinct roles for two receptor tyrosine kinases in epithelial branching morphogenesis in *Drosophila*. *Dev Cell* **9**, 831-842.

Campos-Ortega, J.A and Hartestein, V. (1985). The embryonic development of *Drosophila melanogaster. Springer-Verlag, Berlín.*

Chapman, R.F. (1982). The Insects. Structure and function. Cambridge, Massachusetts*: Harvard University Press*

Chen, C.K., Kühnlein, R.P., Eulenberg, K.G., Vincent, S., Affolter, M. and Schuh, R. (1998). The transcription factors KNIRPS and KNIRPS RELATED control cell migration and branch morphogenesis during *Drosophila* tracheal development. *Development* **125**, 4959-4968.

Chen, H.W., Chen, X., Oh, S.W., Marinissen, M.J., Gutkind, J.S and Hou, S.X. (2002). *mom* identifies a receptor for the *Drosophila* JAK/STAT signal transduction pathway and encodes a protein distanly related to the mammalian cytokine receptor family. *Genes Dev.* **16**, 388-398.

Chihara, T. and Hayashi, S. (2000) Control of tracheal tubulogenesis by *Wingless* signaling. *Development* **127**, 4433-4442.

Choi, W., Jung, K.C., Nelson, K.S., Bhat, M.A., Beitel, G.J., et al. (2011) The single *Drosophila* ZO-1 protein Polychaetoid regulates embryonic morphogenesis in coordination with Canoe/afadin and Enabled. *Mol. Biol. Cell* **22**, 2010–2030.

Chung, S.Y. and Andrew, D.J. (2008) The formation of epithelial tubes. *Journal of Cell Science* **121**, 3501-3504.

Chung, S, Vining, M.S., Bradley, P.L., Chan, C-C., Wharton, K.A., Jr., et al. (2009) Serrano (sano) functions with the planar cell polarity genes to control tracheal tube length. *PLoS Genet 5*: e1000746. doi:10.1371/journal.pgen.1000746.

Chung, S.Y., Chavez, C. and Andrew, D.J. (2011). Trachealess (Trh) regulates all tracheal genes during *Drosophila* embryogenesis. *Dev. Biol*. **360**, 160-172.

Colas, J.F., and Schoenwolf, G.C. (2001). Towards a cellular and molecular understanding of neurulation. *Dev. Dyn.* **221**, 117–145.

Dahal, G.R., Rawson, J., Gassaway, B., Kwok, B., Tong, Y., Ptácek, L.J. and Bates, E. (2012). An inwardly rectifying K+ channel is required for patterning. *Development* **139**, 3653-3664.

Datto, M. and Wang, X.F. (2000). The Smads: Transcriptional regulation and mouse models. *Cytokine Growth Factor Rev.* **1**1, 37-48.

De Celis, J.F, Llimargas, M. and Casanova, J., (1995). *Ventral veinles*, the gene encoding the CF1 transcription factor, links positional information and cell differentiation during embryonic and imaginal development in *Drosophila*. *Development* **121**, 3405-3416.

Devine, W.P., Lubarsky, B., Shaw, K., Luschnig, S., Messina, L. and Krasnow, M.A. (2005). Requirement for chitin biosynthesis in epithelial tube morphogenesis. *Proc. Natl. Acad. Sci.* U S A **102**, 17014-17019.

Dhorian, P., Albagli, O., Lin, J.R., Ansieaus, S., Quief, S., Leutzs, A., Kerkcaert, J.P., Evans, R.M., and Leprince, D. (1997). Corepressor SMRT binds the BTB/POZ repressing domain of the LAZ3yBCL6 oncoprotein. *Proc. Natl. Acad. Sci.* USA **94**, 10762-10767.

Finnegan, D.J. (1989). Eukaryotic transposable elements and genome evolution. *Trends Genet.* **5**, 103-107.

Förster, D., Armbruster, K. and Luschnig, S. (2010). Sec24-dependent secretion drives cell-autonomous expansion of tracheal tubes in *Drosophila*. *Curr Biol*. **20**, 62-68.

Förster, D. and Luschnig, S. (2012). Src42A-dependent polarized cell shape changes mediate epithelial tube elongation in *Drosophila*. *Nat Cell Biol*. **14**, 526-534.

Förster, T.D. and Woods, H.A. (2012). Mechanisms of tracheal filling in insects. *Biol Rev Camb Philos Soc*. doi: 10.1111.

Franch-Marro, X. and Casanova, J. (2002). spalt-induced specification of distinct dorsal and ventral domains is required for *Drosophila* tracheal patterning. *Dev. Biol.* 250, 374-382.

References

Franz, G. and Savakis, C. (1991). Minos, a new transposable element from *Drosophila hydei*, is a member of the Tc-1 like family of transposons. *Nucleic Acids Res.* **19**, 6646.

Gentleman, R.C., Carey, V.J., Bates, D.M., Bolstad, B., Dettling, M., et al. (2004). Bioconductor: open software development for computational biology and bioinformatics. *Genome Biol* **5**: R80.

Gervais, L. and Casanova, J. (2011). The *Drosophila* homologue of SRF acts as a boosting mechanism to sustain FGF-induced terminal branching in the tracheal system. *Development* **138**, 1269-1274.

Gervais, L., Lebreton, G. and Casanova, J. (2012). The making of a fusion branch in the *Drosophila* trachea. *Dev. Biol.* **362**, 187-193.

Ghabrial, A., Luschnig, S., Metzstein, M.M., and Krasnow, M.A. (2003). Branching morphogenesis of the *Drosophila* tracheal system. *Annu. Rev. Cell Dev. Biol.* **19,** 623–647.

Giesen, K., Hummel, T., Stollewerk, A., Harrison, S., Travers, A. and Klämbt, C. (1997). Glial development in the *Drosophila* CNS requires concomitant activation of glial and repression of neuronal differentiation genes. *Development.* **124**, 2307-2316.

Giniger, L., Jan, L.Y. and Jan, Y.N. (1993). Specifying the path of the intersegmental nerve of the *Drosophila* embryo: A role for *Delta* and *Notch*. *Development* **117**, 431-440.

Gjorevski, N. and Nelson, C.M. (2010). Branch formation during organ development. *Wiley Interdiscip Rev Syst Biol Med* **2**, 734-741.

Glazer, L. and Shilo, B.Z. (1991). The *Drosophila* FGF-R homolog is expressed in the embryonic tracheal system and appears to be required for directed tracheal cell extension. *Genes Dev.* **5**, 697-705.

Gonzalez-Roca, E., Garcia-Albeniz, X., Rodriguez-Mulero, S., Gomis, R.R., Kornacker, K., et al. (2010). Accurate expression profiling of very small cell populations. PLoS ONE **5**(12): e14418.

Golic, K.G. and Golic, M.M. (1996). Engineering the *Drosophila* genome: chromosome rearrangements by design. *Genetics* **144**, 1693-1711.

Guha, A., Lin, L. and Kornberg, T.B. (2005). Organ renewal and cell divisions by differentiated cells in *Drosophila*. *Proc Natl Acad Sci U S A.* **105**, 10832-10836.

Guillemin, K., Groppe, J., Ducker, K., Treisman, R., Hafen, E., Affolter, M. and Krasnow, M.A. (1996). The *pruned* gene encodes the *Drosophila* serum response factor and regulates cytoplasmic outgrowth during terminal branching of the tracheal system. *Development* **122**, 1353-1362.

Gumbiner, B.M. (1992). Epithelial morphogenesis. *Cell* **69**, 385-387.

Guo, M., Bier, E., Jan, L.H. and Jan, Y.N (1995). *tramtrack* acts downstream of *numb* to specify distinct daughter cell fates during asymmetric cell divisions in the *Drosophila* PNS. *Neuron* **14**, 913-925.

Guo, M., Jan, L.Y. and Jan, Y.N. (1996) Control of daughter cell fates during asymmetric division: interaction of Numb and Notch. *Neuron* **17**, 27-41.

Hacohen, N., Kramer, S., Sutherland, D., Hiromi, Y. and Krasnow, M.A. (1998). *sprouty* encodes a novel antagonist of FGF signalling that patterns apical branching of the *Drosophila* airways. *Cell* **92**, 253-263.

Haigo, S.L., Hildebrand, J.D., Harland, R.M. and Wallingford, J.B. (2003). Shroom induces apical constriction and is required for hingepoint formation during neural tube closure. *Curr Biol.* **13**, 2125-2137.

Harlow, E. and Lane, D. (1989). Using antibodies: a laboratory manual. *Ed. Cold Spring Harbor (New York).*

Harrison, S.D. and Travers, A.A. (1990). The *tramtrack* gene encodes a *Drosophila* finger protein that interacts with the ftz transcriptional regulatory region and shows a novel embryonic expression pattern. *EMBO J.* **9**, 207-216.

Hartestein, V. (1993). Atlas of *Drosophila* development. *Cold Spring Harbor Laboratory Press.*

Hartenstein, K., Sinha, P., Mishra, A., Schenkel, H., Török, I. And Mechler, B.M. (1997). The *congested-like tracheae* gene of *Drosophila melanogaster* encodes a member of the mitochondrial carrier family required for gas-filling of the tracheal system and expansion of the wings after eclosion. *Genetics* **147**, 1755-1768.

Heldin, C.H., Miyazono, K. and Ten-Dijke, P. (1997). TGF-b signalling from cell membrane to nucleus through SMAD proteins. *Nature* **390**, 465-471.

Hemphala, J., Uv, A., , Cantera, R., Bray, S., and Samakovlis1, C. (2003). Grainy head controls apical membrane growth and tube elongation in response to Branchless/FGF signalling. *Development* **130**, 249-258.

Hogan, B.L. and Kolodziej, P.A. (2002). Organogenesis: Molecular mechanisms of tubulogenesis. *Nat. Rev. Genet.* **3**, 513-523.

Huang, D.C. and Strasser, A. (2000). BH3-Only proteins-essential initiators of apoptotic cell death. *Cell* **103**, 839-842.

Hummel, T. and Klämbt, C. (2008). Book of *Drosophila* methods and protocols. Chapter 6: P-elements mutagenesis.

Hummler, E., Barker, P., Gatzy, J., Beermann, F., Verdumo, C., Schmidt, A., Boucher, R., Rossier, B.C. (1996). Early death due to defective neonatal lung liquid clearance in alpha-ENaC-deficient mice. *Nat. Genet*. **12**, 325-328.

Ikeya ,T. and Hayashi, S. (1999) Interplay of Notch and FGF signaling restricts cell fate and MAPK activation in the *Drosophila* trachea. Development *126, 4455-4463*.

Isaac, D.D and Andrew, D.J. (1996.) Tubulogenesis in *Drosophila*: a requirement for the *trachealess* gene product. *Gene dev.* **10**, 103-117.

Jarecki, J., Johnson, E. and Krasnow, M.A. (1999). Oxygen regulation of airway branching in *Drosophila* is mediated by *branchless* FGF. *Cell* **99**, 211-220.

Jayaram, S.A., Senti, K.A., Tiklová, K., Tsarouhas, V., Hemphälä, J. and Samakovlis, C. (2008). COPI vesicle transport is a common requirement for tube expansion in *Drosophila. PLoS One* **3**(4):e1964.

Jiang, L. and Crews, S.T. (2003). The *Drosophila dysfusion* basic helix-loop-helix (bHLH)-PAS gene controls tracheal fusion and levels of the *trachealess* bHLH-PAS protein. *Mol. Cell. Biol.* **23**, 5625-5637.

Jiang, L., Rogers, S.L. and Crews, S.T. (2007) The *Drosophila* Dead end Arf-like3 GTPase controls vesicle trafficking during tracheal fusion cell morphogenesis. *Dev Biol.* **311**, 487-499.

Jiang, L., Pearson, J.C. and Crews, S.T. (2010). Diverse modes of *Drosophila* tracheal fusion cell transcriptional regulation. *Mech. Dev.* **127**, 265-280.

Jordan, K.C., Schaeffer, V., Fischer, K.A., Gray, E.E. and Ruohola-Baker, H. (2006) Notch signaling through tramtrack bypasses the mitosis promoting activity of the JNK pathway in the mitotic-to endocycle transition of Drosophila follicle cells. *BMC Dev Biol.* **6**:16.

Kaplan, J. and Calame, K. (1995). The ZiN/POZ domain of ZF5 is required for both transcriptional activation and repression. *Nucl. Ac. Res.* **25**, 1108-1116.

References

Kennerdell, J.R., and Carthew, R.W. (1998) Use of dsRNA-mediated genetic interference to demonstrate that *frizzled* and *frizzled 2* act in the wingless pathway. *Cell* **95**, 1017-1026.

Kerman, B.E., Chesire, A.M and Andrew, D.J. (2006). From fate to function: the *Drosophila* trachea and salivary gland as models for tubulogenesis. *Differentiation* **74**, 326-348.

Knust, E. (2002). Regulation of epithelial cell shape and polarity by cell-cell adhesion. *Mol Membr Biol.* **19**, 113-120.

Knust, E. and Bossinger, O. (2002). Composition and formation of intercellular junctions in epithelial cells. *Science* **298**, 1955-1959.

Kobayashi, A.H., Yamagiwa, H., Hoshino, A., Muto, K. and Sato (2000). A combinatorial code for gene expression generated by transcription factor Bach2 and MAZR (MAZ-related factor) through the BTB/POZ domain.. *Mol. Cell. Biol.* **20**, 1733-1746.

Kuhnlein, R.P. and Schuh, R. (1996). Dual function of the region-specific homeotic gene *spalt* during *Drosophila* tracheal system development. *Development* **122**, 2215-2223.

Lampe, D.J., Churchill, M.E.A. and Robertson, H.M. (1996). A purified mariner transposase is sufficient to mediate transposition *in vitro*. *EMBO J.* **15**, 5470-5479.

Laplante, C., Paul, S.M., Beitel, G.J. and Nilson, L.A. (2010). Echinoid regulates tracheal morphology and fusion cell fate in *Drosophila*. *Dev. Dyn.* **239**, 2509-2519.

Laprise, P., Paul, S.M., Boulanger, J., Robbins, R.M., Beitel, G.J. and Tepass, U. (2010). Epithelial polarity proteins regulate *Drosophila* tracheal tube size in parallel to the luminal matrix pathway. *Curr. Biol.* **20**, 55-61.

Lee, S. and Kolodziej, P.A. (2002). The plakin Short Stop and the RhoA GTPase are required for E-cadherin-dependent apical surface remodeling during tracheal tube fusion. *Dev.* **129**, 1509-1520.

Lee, M., Lee, S., Zadeh, A.D. and Kolodziej, P.A. (2003). Distinct sites in E-cadherin regulate different steps in *Drosophila* tracheal tube fusion. *Dev.* **130**, 5989-5999.

Lees, J., Yeats, C., Perkins, J., Sillitoe, I., Rentzsch, R., and Orengo, C. (2012). Gene3D: a domain-based resource for comparative genomics, functional annotation and protein network analysis. *Nucleic Acids Res.* **40**, 465-471.

Lehmann, F.O. (2001). Matching spiracle opening to metabolic need during flight in *Drosophila*. *Science* **30**, 1926-1929.

Letizia, A., Sotillos, S., Campuzano, S. and Llimargas, M. (2010). Regulated Crb accumulation controls apical constriction and invagination in *Drosophila* tracheal cells. *J. Cell. Sci.* **124**, 240-251.

Liu, L., Johnson, W.A., and Welsh, M.J. (2003). *Drosophila* DEG/ENaC *pickpocket* genes are expressed in the tracheal system, where they may be involved in liquid clearance. *Proc. Natl. Acad. Sci. U S A* **100,** 2128-2133.

Llimargas, M. and Casanova, J. (1997). *ventral veinless*, a POU domain transcription factor, regulates different transduction pathways required for tracheal branching in *Drosophila*. *Development* **124**, 3273-3281.

Llimargas, M. and Casanova, J. (1999). EGF signalling regulates cell invagination as well as cell migration during formation of tracheal system in *Drosophila*. *Dev. Genes Evol*. **209**, 174-179.

Llimargas, M. (2000). *Wingless* and its signalling pathway have common and separable functions during tracheal development. *Development* **127**, 4407-4417.

Llimargas, M. and Lawrence, PA. (2001). Seven Wnt homologues in *Drosophila*: a case study of the developing tracheae. *Proc Natl Acad Sci. U S A* **98**, 14487-14492.

Llimargas, M., Strigini, M., Katidou, M., Karagogeos, D. and Casanova, J. (2004). Lachesin is a component of a septate junction-based mechanism that controls tube size and epithelial integrity in the *Drosophila* tracheal system. *Development* **131**, 181-190.

Locke, M. (2001). The Wigglesworth Lecture: Insects for studying fundamental problems in Biology. *J. of Insect Physiol.* **47**, 495-507.

Loukeris, T.G., Livadaras, I., Arca, B., Zabalou, S. and Savakis, C. (1995). Gene transfer into the medfly, *Ceratitis capitata*, with a *Drosophila hydei* transposable element. *Science* **170**, 2002-2005.

Lubarsky, B. and Krasnow, M.A (2003). Tube morphogenesis: making and shaping biological tubes. *Cell* **112**, 19-28.

Luschnig, S., Batz, T., Armbruster, K. and Krasnow, M.A. (2006). *Serpentine* and *vermiform* encode matrix proteins with quitin binding and deacetylation domains that limit tracheal tube length in *Drosophila. Curr. Biol.* **16**, 186–194.

Lyne, R., Smith, R., Rutherford, K., Wakeling, M., Varley, A., et al. (2007). FlyMine: an integrated database for *Drosophila* and *Anopheles* genomics. *Genome Biol*. **8:** R129

Manning, G. and Krasnow, M.A. (1993). Development of the *Drosophila* tracheal system. In The Development of *Drosophila. Cold Spring Harbor, New York: Cold Spring Harbor Laboratory Press 1,* 609-685.

Martin, D., Zusman, S., Li, X., Williams, E.L., Khare, N., DaRocha, S., Chiquet-Ehrismann, R. and Baumgartner, S. (1999). wing blister, a new *Drosophila* laminin alpha chain required for cell adhesion and migration during embryonic and imaginal development. *J Cell Biol.* **145**, 191-201.

Massarwa, R., Schejter, E.D. and Shilo, B.Z. (2009). Apical secretion in epithelial tubes of the *Drosophila* embryo is directed by the Formin-family protein Diaphanous. *Dev. Cell* **16**, 877-888.

Matusek, T., Djiane, A., Jankovics, F., Brunner, D., Mlodzik, M. And Mihály, J. (2005). The *Drosophila* formin DAAM regulates the tracheal cuticle pattern through organizing the actin cytoskeleton *Development* **133**, 957-966.

Medioni, C., Astier, M., Zmojdzian, M., Jagla, K. and Sémériva, M. (2008). Genetic control of cell morphogenesis during *Drosophila* melanogaster cardiac tube formation. *J. Cell Biol*. **182**, 249-261.

Melnick, M. and Jaskoll, T. (2000). Mouse submandibular gland morphogenesis: a paradigm for embryonic signal processing. *Crit. Rev. Oral Biol. Med.* **11**, 199-215.

Metaxakis, A., Oehler, S., Klinakis A. and Savakis, S. (2005). Minos as a genetic and genomic tool in *Drosophila melanogaster*. *Genetics* **171**, 571-581.

Metzger, R.J. and Krasnow, M.A. (1999). Genetic control of branching morphogenesis. *Science* **284**, 1635-1639.

Misquitta, L. and Paterson, B.M. (1999). Targeted disruption of gene function in *Drosophila* by RNA interference (RNAi): a role for *nautilus* in embryonic somatic muscle formation. *Proc. Natl. Acad. Sci. USA* **96**, 1451-1456.

modENCODE Consortium et al. (2010). Identification of functional elements and regulatory circuits by *Drosophila* modENCODE.. *Science* **330**, 1787-1797.

Mourikis, P., Lake, R.J., Firnhaber, C.B. and DeDecker, B.S. (2010). Modifiers of notch transcriptional activity identified by genome-wide RNAi. *BMC Dev. Biol.* **10**: 107. doi:10.1186/1471-213X-10-107.

References

Moussian B., Schwarz, H., Bartoszewski S. and Nusslein-Volhard, C. (2005). Involvement of chitin in exoskeleton morphogenesis in *Drosophila melanogaster. J. Morphol.* **264**, 117-130.

Moussian, B., Tång, E., Tonning, A., Helms, S., Schwarz, H., Nüsslein-Volhard, C. and Uv, A (2006). *Drosophila* Knickkopf and Retroactive are needed for epithelial tube growth and cuticle differentiation through their specific requirement for chitin filament organization. *Development* **133**, 163-171.

Nelson, K.S., Furuse, M. and Beitel, G.J. (2010). The *Drosophila* claudin *kune-kune* is required for septate junction organization and tracheal tube size control. *Genetics* **185,** 831-839.

Newfeld, S.J. and Wisotzkey, R.G. (2006). Molecular Evolution of Smad Proteins. *Genetics* **174**, 1299-1313.

Nishimura, M., Inoue, Y. and Hayashi, S. (2007). A wave of EGFR signaling determines cell alignment and intercalation in the *Drosophila* tracheal placode *Development* **134**, 4273-4282.

O'Brodovich, H.M. (1996). Immature epithelial Na+ channel expression is one of the pathogenetic mechanisms leading to human neonatal respiratory distress syndrome. *Proc. Assoc. Am. Physicians* **108**, 345-355.

Okabe, M., Imai, T., Kurusu, M., Hiromi, Y. and Okano, H. (2001). Translational repression determines a neuronal potential in *Drosophila* asymmetric cell division. *Nature* **411**, 94-98.

Ohshiro, T. and Saigo, K. (1997). Transcriptional regulation of *breathless* FGF receptor gene by binding of TRACHEALESS/dARNT heterodimers to three central midline elements in *Drosophila* developing trachea. *Development* **124,** 3975-3986.

Page-McCaw, A., Serano, J., Sante, J.M. and Rubin, G.M. (2003). *Drosophila* matrix metalloproteinases are required for tissue remodelling, but not embryonic development. *Dev. Cell* 4, 95-106.

Paul, S.M., Ternet, M., Salvaterra, P.M. and Beitel, G.J. (2003). The Na+/K+ ATPase is required for septate junction function and epithelial tube-size control in the *Drosophila* tracheal system. *Development* **130**, 4963-4974.

Paul, S.M., Palladino, M.J. and Beitel, G.J. (2007). A pump-independent function of the Na,K-ATPase is required for epithelial junction function and tracheal tube-size control. *Development* **134**, 147-155.

Rajeevan,S.M., Ranamukhaarachchi, D.G., Vernon, D.S. and Unger, E.R. (2001). Use of real-time quantitative PCR to validate the results of cDNA array and differential display PCR technologies. *Methods* **25,** 443-451.

Ramaekers, G., Usui, K., Usui, A., Ramaekers, A., Ledent, V., Ghysen, A. and Dambly-Chaudière, C. (1997). Lineage and fate in *Drosophila*: Role of the gene *tramtrack* in sense organ development. *Dev. G. and Evo.* **207**, 97-106.

Rasmussen, J.P., English, K., Tenlen, J.R. and Priess, J.R. (2008). Notch signalling and morphogenesis of single-cell tubes in the *C. elegans* digestive tract. *Dev. Cell* **14**, 559-569.

Read, D. and Manley, J.L. (1992). Alternatively spliced transcripts of the *Drosophila tramtrack* gene encode zinc finger proteins with distinct DNA binding specificities. *EMBO J.* **11**, 1035-1044.

Reddy, B.A., Bajpe, P.K., Bassett, A., Moshkin, Y.M., Kozhevnikova, E., Bezstarosti, K., Demmers, J.A., Travers, A.A. and Verrijzer, C.P. (2010). *Drosophila* transcription factor Tramtrack69 binds MEP1 to recruit the chromatin remodeler NuRD. *Mol. Cell. Biol.* **30**, 5234-5244.

Ribeiro, C., Neumann, M. and Affolter, M. (2004). Genetic control of cell intercalation during tracheal morphogenesis in *Drosophila. Curr. Biol.* **14**, 2197-2207.

Ryder, E., Ashburner, M., Bautista-Llacer, R., Drummond, J., Webster, J., Johnson, G., et al. (2007). The DrosDel deletion collection: a *Drosophila* genome wide chromosomal deficiency resource. *Genetics* **177**, 615-629.

Salzberg, A., D'Evelyn, D., Schulze, K.L., Lee, J.K., Strumpf, D., Tsai, L. and Bellen, H.J. (1994). Mutations affecting the pattern of the PNS in *Drosophila* reveal novel aspects of neuronal development. *Neuron* **13**, 269-287.

Samakovlis, C., Hacohen, N., Manning, G., Sutherland, D.C., Guillemin, K. and Krasnow, M.A. (1996a). Development of the *Drosophila* tracheal system occurs by a series of morphologically distinct but genetically coupled branching events. *Development* **122**, 1395-1407.

Samakovlis, C., Manning, G., Steneberg, P., Hacohen, N., Cantera, R. and Krasnow, M.A. (1996b). Genetic control of epithelial tube fusion during *Drosophila* tracheal development. *Development* **122**, 3531-3536.

Santiago-Martínez, E., Soplop, N.H., Patel, R. and Kramer, S.G. (2008). Repulsion by Slit and Roundabout prevents Shotgun/E-cadherin-mediated cell adhesion during *Drosophila* heart tube lumen formation. *J. Cell Biol.* **182**, 241-248.

Scholz, H., Deatrick, J., Klaes, A. and Klambt, C. (1993). Genetic dissection of *pointed*, a *Drosophila* gene encoding two ETS-related proteins. *Genetics* **135**, 455-468.

Schottenfeld, J., Song, Y. and Ghabrial, A.S. (2010). Tube continued: morphogenesis of the *Drosophila* tracheal system. *Curr. Opin. Cell Biol.* **22**, 633-639.

Shaye, D.D, Casanova, J. and Llimargas, M. (2008). Modulation of intracellular trafficking regulates cell intercalation in the *Drosophila* trachea. *Nat. Cell Biol*. **10**, 964-970.

Shiga, Y., Tanaka-Matakatsu, M. and Hayashi, S. (1996). A nuclear GFP/ beta-galactosidase fusion protein as a marker for morphogenesis in living *Drosophila. Dev. Growth Diff.* **38**, 99-106.

St Johnston, D. (2002). The art and design of genetic screens: *Drosophila melanogaster*. *Nat. Rev. Genetics* **3,** 176-188.

Stark, C., Breitkreutz, B.J., Chatr-Aryamontri, A., Boucher, L., Oughtred, R., et al. (2011). The BioGRID Interaction Database: 2011 update. *Nucleic Acids Res.* **39**, 698-704.

Steneberg, P., Englund, C., Kronhamn, J., Weaver, T.A. and Samakovlis, C. (1998). Translational readthrough in the *hdc* mRNA generates a novel branching inhibitor in the *Drosophila* trachea. *Genes Dev*. **12**, 956-967.

Steneberg, P., Hemphala, J. and Samakovlis, C. (1999). *Dpp* and *Notch* specify the fusion cell fate in the dorsal branches of the *Drosophila* trachea. *Mech Dev*. **87**, 153-163.

Sun, J., Chen, H., Chen, C., Whitsett, J.A., Mishina, Y., Bringas, P., Jr., Ma, J.C., Warburton, D. and Shi, W. (2008). Prenatal lung epithelial cell-specific abrogation of Alk3-bone morphogenetic protein signaling causes neonatal respiratory distress by disrupting distal airway formation. *Am. J. Pathol.* **172**, 571-582.

Sun, J., Smith, L., Armento, A. and Deng W.M. (2008). Regulation of the endocycle/gene amplification switch by Notch and ecdysone signalling. *J. Cell Biol.* **182**, 885-896.

Sutherland, D., Samakovlis, C., and Krasnow, M.A. (1996). *branchless* encodes a *Drosophila* FGF homolog that controls tracheal cell migration and the pattern of branching. *Cell* **87**, 1091-1101.

Swanson, L.E and Beitel, G.J. (2006). Tubulogenesis: an inside job. *Curr. Biol.* **16**, 51-53.

References

Tanaka-Matakatsu, M., Uemura, T., Oda, H., Takeichi, M. and Hayasi, S. (1996). Cadherin-mediated cell adhesion and cell motility in *Drosophila* trachea regulated by the transcription factor Escargot. *Development* **122**, 3697-3705.

Tanaka, H., Takasu, E., Aigaki, T., Kato, K., Hayashi, S. and Nose, A. (2004). Formin3 is required for assembly of the F-actin structure that mediates tracheal fusion in *Drosophila*. *Dev. Biol.* **274**, 413-425.

Tepass, U., Tanentzapf, G., Ward, R., and Fehon, R. (2001). Epithelial cell polarity in *Drosophila*. *Annu. Rev. Genet.* **35**, 747-784.

Thermo Fisher Scientific (2010). Off-Target Effects: Disturbing the silence of RNA interference (RNAi). *Thermo Fisher Scientific Teach review.*

Tomancak, P., Berman, B.P., Beaton, A., Weiszmann, R. and Kwan, E. (2007). Global analysis of patterns of gene expression during *Drosophila* embryogenesis. *Genome Biol* **8**, R145.

Tonning, A., Hemphala, J., Tang, E., Nannmark, U., Samakovlis, C. and Uv, A. (2005). A transient luminal chitinous matrix is required to model epithelial tube diameter in the *Drosophila* trachea. *Dev. Cell* **9**, 423-430.

Tsarouhas, V., Senti, K., Jayaram, S.A., Tiklova, K., Hemphala, Y., Adler,J., and Samakovlis1, C. (2007). Sequential pulses of apical epithelial secretion and endocytosis drive airway maturation in *Drosophila. Dev. Cell* **13**, 214-225.

Urbano, J.M., Torgler, C.N., Molnar, C., Tepass, U., López-Varea, A., Brown, N.H., De Celis, J.F. and Martín-Bermudo, M. (2009). *Drosophila* laminins act as key regulators of basement membrane assembly and morphogenesis. *Development* **136**, 4165-4176.

Uv, A., Cantera, R. and Samakovlis, C. (2003). Drosophila tracheal morphogenesis: intricate cellular solutions to basic plumbing problems. *Trends Cell Bio.* **13**, 301-309.

Vincent, S., Ruberte, E., Grieder, N.C., Chen, C.K., Haerry, T., Schuh, R. and Affolter, M. (1997). DPP controls tracheal cell migration along the dorsoventral body axis of the *Drosophila* embryo. *Development* **124**, 2741-2750.

Wang, P., Ding, F., Chiang, H., Thompson, R.C., Watson, S.J., et al. (2002). ProbeMatchDB: a web database for finding equivalent probes across microarray platforms and species. *Bioinformatics* **18**, 488-489.

Wang, X., Bo, J., Bridges, T., Dugan, K.T., Pan, T., Chodosh, L.A. and Montell, D.J. (2006). Analysis of cell migration using whole-genome expression profiling of migratory cells in the *Drosophila* ovary. *Dev. Cell* **10**, 483-495.

Wang, S., Jayaram, S.A., Hemphala, J., Senti, K.A., Tsarouhas, V., Jin, H. and Samakovlis, C. (2006). Septate junction dependent luminal deposition of chitin deacetylases restricts tube elongation in the *Drosophila* trachea. *Curr. Biol.* **16**, 180-185.

Ward, E.J., Zhou, X., Riddiford, L.M., Berg, C.A. and Ruohola-Baker, H. (2006). Border of Notch activity establishes a boundary between the two dorsal appendage tube cell types. *Dev. Biol,* **297**, 461-470.

Weaver, M. and Krasnow, M.A. (2008). Dual origin of tissue-specific progenitor cells in *Drosophila* tracheal remodeling. *Science* **321,** 1496-1499.

Weigmann, K., Klapper, R., Strasser, T., Rickert, C., Technau, G., Jackle, H., Janning, W. and Klambt, C. (2003). FlyMove: A new way to look at development of *Drosophila. Trends Genet* **19**, 310-311.

Wen, Y., Nguyen, D., Li, Y. and Lai, Z.C. (2000**).** The N-terminal BTB/POZ domain and C-terminal sequences are essential for Tramtrack69 to specify cell fate in the developing *Drosophila* eye. *Genetics* **156**, 195-203.

Wilk, R., Weizman, I. and Shilo, B.Z. (1996). t*rachealess* encodes a bHLH-PAS protein that is an inducer of tracheal cell fates in *Drosophila. Genes Dev.* **10**, 93-102.

Wingen,C., Aschenbrenner, A.C., Stumpges, B., Hoch, M. and Behr, M. (2009). The Wurst protein: A novel endocytosis regulator involved in airway clearance and respiratory tube size control. *Cell Adhesion and Migration* **3**, 14-18.

Wu, V.M. and Beitel, G.J. (2004). A junctional problem of apical proportions: epithelial tube-size control by septate junctions in the *Drosophila* tracheal system. *Curr. Opin. Cell Biol*.**16**, 493-499.

Wu, V.M., Schulte, J., Hirschi, A., Tepass, U. and Beitel, G.J. (2004). Sinuous is a *Drosophila* claudin required for junction organization and epithelial tube size. *J. Cell Biol*. **164**, 313-323.

Xiong, W.C and Montell, C. (1993). *tramtrack* is a transcriptional repressor required for cell fate determination in the *Drosophila* eye. *Genes Dev.* **6**, 1085-1096.

Younossi-Hartestein, A. and Hartestein, V. (1993). The role of the tracheae and musculature during pathfinding of *Drosophila* embryonic sensory axons. *Dev. Biology* **158**, 430-447.

Zhang, L. and Ward, R.E 4th. (2009). *uninflatable* encodes a novel ectodermal apical surface protein required for tracheal inflation in *Drosophila*. *Dev Biol.* **336**, 201-212.

Zollman, S., Godt, D., Privé, G.G., Couderc, J.L. and Laski, F.A. (1994). The BTB domain, found primarily in zinc finger proteins, defines an evolutionarily conserved family that includes several developmentally regulated genes in *Drosophila*. *Proc. Natl. Acad. Sci.* U.S.A. **91**, 10717-10721.

Annex I

PLoS one

Tramtrack Is Genetically Upstream of Genes Controlling Tracheal Tube Size in *Drosophila*

Barbara Rotstein[1], David Molnar[2], Boris Adryan[2]*, Marta Llimargas[1]*

1 Institut de Biologia Molecular de Barcelona, CSIC, Barcelona, Spain, 2 Department of Genetics, Cambridge Systems Biology Centre, University of Cambridge, Cambridge, United Kingdom

Abstract

The *Drosophila* transcription factor Tramtrack (Ttk) is involved in a wide range of developmental decisions, ranging from early embryonic patterning to differentiation processes in organogenesis. Given the wide spectrum of functions and pleiotropic effects that hinder a comprehensive characterisation, many of the tissue specific functions of this transcription factor are only poorly understood. We recently discovered multiple roles of Ttk in the development of the tracheal system on the morphogenetic level. Here, we sought to identify some of the underlying genetic components that are responsible for the tracheal phenotypes of Ttk mutants. We therefore profiled gene expression changes after Ttk loss- and gain-of-function in whole embryos and cell populations enriched for tracheal cells. The analysis of the transcriptomes revealed widespread changes in gene expression. Interestingly, one of the most prominent gene classes that showed significant opposing responses to loss- and gain-of-function was annotated with functions in chitin metabolism, along with additional genes that are linked to cellular responses, which are impaired in *ttk* mutants. The expression changes of these genes were validated by quantitative real-time PCR and further functional analysis of these candidate genes and other genes also expected to control tracheal tube size revealed at least a partial explanation of Ttk's role in tube size regulation. The computational analysis of our tissue-specific gene expression data highlighted the sensitivity of the approach and revealed an interesting set of novel putatively tracheal genes.

Introduction

Transcription factors play critical roles in all aspects of development. They control the gene batteries that lead to cellular events such as proliferation, cell fate specification and differentiation, cell migration, cell morphological changes and apoptosis. Given this wide spectrum of functions, very often transcription factors exhibit a high degree of pleiotropy that hinders a comprehensive functional characterisation in a given tissue or developmental stage. Thus, identifying the plethora of target genes regulated by transcription factors is key to disentangling their multiple and complex activities. Nowadays, the combination of genome-wide approaches with cell type- or stage-specific isolation provides a powerful strategy to understand how the function of transcription factors is mediated.

Our previous work indicated that the transcription factor Ttk plays multiple relevant roles in the formation of the *Drosophila* tracheal system [1]. For a more mechanistic view, in the present work we aimed to map the downstream mediator targets of *ttk* during embryogenesis with a particular emphasis in the developing tracheal system. Ttk is a zinc-finger transcription factor widely used during the development of a number of different organ systems [2–15], with a pivotal role in many different morphoge-

netic events. In the trachea, we observed that Ttk is not only required for tracheal cell identity specification, but in addition it enables several morphogenetic changes, including the cell rearrangements of tube formation, and the proper setting of tube sizes [1]. Thus Ttk may govern a complex hierarchy of downstream mediators that execute cellular changes in tracheal development. We aimed to identify these downstream targets using microarray transcriptome profiling. This enabled us to find direct and indirect transcriptional targets, including those which are difficult to identify in traditional mutant screens due to pleiotropy and/or functional redundancy. To identify targets specific to the tracheal system, and to separate the specifically tracheal action of Ttk from action on other target systems, we combined whole-embryo expression profiles with transcription profiles of embryonic cell isolates, which were enriched for tracheal cells by fluorescence-activated cell sorting (FACS).

In this work we compared microarray expression profiles of wild-type embryos with different *ttk* mutant conditions, as well as expression profiles of tracheal cell isolates from both wild-type and mutant embryos. This analysis provided an *in vivo* census of genes whose transcription responds to Ttk loss-of-function or over-expression. Several of these genes have predicted Ttk binding sites in their regulatory regions, which make them candidates for direct

regulation. To validate our experimental approach, we further analysed effects on the mechanism of tube size regulation, as we established the role of Ttk in this process before [1]. The size control of tracheal tubes is complex and involves several molecular mechanisms. It has been shown earlier that the transient assembly of a chitin filament inside the tracheal tubes, and epithelial septate junctions (SJs) play critical roles in the process (reviewed in [16–18]). Our current analysis of microarray data from whole embryos and isolated cells pointed to changes in the expression of chitin metabolism and SJ-related genes in *ttk* mutants, which were confirmed by quantitative real-time PCR (qPCR) profiling. In further tests we found that several of these targets are functionally required in tube size control. Thus we could confirm the involvement of Ttk in tube size regulation, and connect Ttk regulation to several downstream genes, which are involved in the control of tube size.

Our results provide entry points for the investigation of the targets of Ttk regulation in further processes. The results also show that our method of cell enrichment is a powerful tool in the search for transcription factor targets.

Results

Microarray analysis of ttk mis-expression mutants

In order to identify direct or indirect Ttk target genes that could explain the diverse tracheal phenotypes seen in mutant embryos, we pursued RNA profiling experiments on embryos that are homozygous for the mutant *ttk*[D2-50] allele and control embryos at developmental stages 11 to 16. Furthermore we profiled embryos

of the same age range that over-express *ttk* in the domain of the *btl*-GAL4 driver line, which includes the tracheal system and the midline, together with controls. All embryos, mutants and controls, expressed a membrane tethered RFP under the control of the *btl* enhancer from the Red Fluorescent Protein-moesin (btl-enh-RFP-moe) construct. This enabled a FACS strategy, which enabled us to obtain a cell population that was enriched for tracheal cells that were then subject to microarray gene expression analysis. The genotypes of these embryos and cells are detailed in Figure 1.

RNA was extracted in three biological replicates from each experimental group, with the exception of the experiments on the sorted cell populations in the over-expression group, where only two replicates were performed. The samples were hybridised to Affymetrix *Drosophila* Genome 2.0 Arrays. Following a rigorous protocol for quality control (see Text S1 and Figure S1), we decided to exclude one experiment from the embryo control for the mutant situation, one from embryo mutant, one from cell mutant. All experiments for the over-expression situation could be used. The microarray dataset is available from the Gene Expression Omnibus (http://www.ncbi.nlm.nih.gov/geo/) database under accession code GSE30239.

Two parameters primarily determine the number of candidate genes that can be obtained from a microarray experiment: the expected expression change (as indicated by the fold change in signal) and the reliability for this observation (implied in the p-value in the comparison between two different groups, under consideration of the noise structure within each of these groups). We therefore explored the parameter space from $\log_2$ fold change

Figure 1. Experimental conditions, fly stocks and genotypes analysed in this study. The sample genotype and tracheal phenotype refer to the experimental condition that was analysed by microarray gene expression profiling. The tracheal pattern was visualised by the accumulation of chitin in the lumen using CBP. Immunostainings show projections of confocal sections of embryos of the indicated genotypes at embryonic stage 16 in lateral or dorsolateral views. In this and all figures anterior is to the left and dorsal is up. Scale bar 100 µm.
doi:10.1371/journal.pone.0028985.g001

(logFC) 0.7 to 4 in increments of 0.1 between 0.7 and 1.5, and larger increments above 1.5, along with the p-value at 0.001, 0.005, 0.01 and 0.05 (Supplementary Table S1). For further analysis, we opted to define primary candidate genes as those with a logFC>=1 (translating to an at least two-fold expression change) at a p-value<=0.05. This parameter set identified 761 candidates in the mutant cell experiment and 676 genes in the mutant embryo experiment, with an overlap of 182 genes (24%). The identical parameter set was used for the over-expression experiments, identifying 322 genes in cells and 397 genes in embryos, with an overlap of 72 genes (22%).

The *btl* gene is expressed both in the tracheal system and in the ventral midline [19]. Manual inspection of the btl-enh-RFP-moe construct further confirmed detectable levels of expression in various other cell types (e.g. lateral ectoderm, endoderm, amnioserosa, others) (data not shown). The employed cell sorting strategy relied on the appropriate expression of marker fluorescence, and furthermore, cell sorting can be highly subjective to choosing appropriate gate settings (Figure S2). It was therefore unclear whether the sorted cell population was enriched for tracheal cells. We assessed the merit of the cell sorting strategy using a computational approach, making use of the high-throughput *in situ* hybridisation database at the BDGP [20]. We binned the signal intensity data from the control cell population in steps of approximately 0.5 (covering the dynamic range of 0 to16 of the microarray), and for each bin determined from the genes with BDGP information what fraction was known to be expressed in the tracheal system or midline, ubiquitously expressed, expressed elsewhere in the embryo, or not expressed (Figure S3). Surprisingly, we found a large number of genes that are supposedly not expressed in embryogenesis, accounting for almost half of the genes detected in the sorted cell population. While signal amplification issues in the pre-processing and detection of our microarray data are possible and may lead to considerable signals also for non-existent mRNA, it cannot be ruled out that a good proportion of the *in situ*-negative genes are indeed expressed. Of the group of genes known to be expressed during the relevant stages of embryogenesis, about half are expressed in the midline and/or trachea (and probably elsewhere), while the other half should not be present if our preparations were pure. Using two different normalization strategies to account for the differences in the RNA sources and microarray experiments, we found that the tracheal marker gene *trachealess* shows a two-fold enrichment in the sorted cell population in comparison to whole embryos, while e.g. a marker for mesoderm (*twist*) is reduced to about one third (Table S2 and Table S3). These results also hold for the over-expression experiments. In summary, while it was not possible to isolate a pure population of tracheal cells, we were confident that these experiments still provide valuable information for candidate gene prioritisation.

The *in vivo* transcriptome confirms in vitro results and is backed by known biology

Recently, Reddy et al. published an expression profile of the S2 *Drosophila* cell line after *ttk* knockdown by RNA interference [21]. Using our criteria for candidate genes, their screen yielded 1,380 candidate genes. Although the absolute overlap between their candidate gene list and our lists is small, the degree of overlap between these experiments is statistically significant (Table 1) indicating that similar trends were detected in both datasets (see Discussion for a more detailed comparison).

We were also interested in genome-wide trends in gene expression that are probably better reflected on a functional rather than per-gene level. For each gene list in Table 1 we

calculated Gene Ontology (GO) over-representation statistics. The variety of functional classes that show over-representation in these gene lists was diverse, with no clearly defined general function for Ttk action (Supplementary Table S4). While the analysis of the S2 data confirmed previously detected GO terms involved in developmental processes [21], our mutant data revealed not immediately conclusive terms such as up-regulation of genes involved in 'oocyte axis specification' (GO:0007309) or 'G-protein coupled receptor protein signaling pathway' (GO:0007186), while no GO over-representation could be identified for genes down-regulated in the mutant. Equally remarkable, there was very little overlap in GO terms between the different experiments, 'cell fate commitment' (GO:0045165) being one of them that was shared between the S2 cell-based experiments and the genes down-regulated in embryos after *ttk* over-expression. Interestingly, as our work had previously implied a connection between Ttk function and cuticle formation [1], we found a range of GO terms involved in the 'chitin metabolic process' being over-represented amongst the genes up-regulated after Ttk over-expression in embryos.

Identification of putative Ttk target genes involved in chitin metabolism

In order to prioritize target genes for further validation, we visually inspected scatter plots in which we plotted the logFC in whole embryos versus our enriched (tracheal) cell population for both mutant and over-expression experiments (Figure 2A). As can be seen, the majority of genes cluster around the origin of the plots (i.e. coordinate 0;0), indicating they are not affected by the mis-expression condition. Importantly, the majority of genes with clear expression changes lie on the diagonal of the plot, indicating that direction and amplitude are the same for embryos and sorted cells, though this trend is less pronounced in the over-expression situation. We restricted the display to genes that were involved in GO biological processes with at least 50 annotated genes, with a closer look at those terms previously flagged as significantly enriched, one GO term at a time (File S1). As already suggested in the gene expression analysis of cell isolates, this analysis also showed a footprint of nervous system development. A large variety of GO terms implicated in central and peripheral nervous system development displayed converse expression behaviour in mutant and over-expression conditions. However, as we were particularly interested in genes involved in the tracheal system, genes annotated for functions in chitin metabolism (known to be involved in tracheal tube size control) came to our immediate attention, because in many cases they show inverse regulation in the mutant and over-expression situation, and consistently showed significant absolute logFC values (Figure 2B).

We therefore picked a few of the genes highlighted in this process for further validation of our microarray results.

Chitin metabolic genes show tube length phenotypes consistent with *ttk* mis-expression

We previously described that *ttk* plays a role in controlling tracheal tube size [1]. Thus, we selected genes differentially expressed in our *ttk* experimental assays that participate in chitin metabolism and SJ organization (as identified by annotation with GO:0005918, 'septate junction') as they are involved in tube size control (review in [16–18]).

To validate the expression changes of these putative *ttk* targets obtained in the microarray experiment we performed quantitative real-time PCR analysis. The results confirmed the directional change in the levels of expression of all genes we tested (Table 2). Nine genes assigned to the GO term 'chitin metabolism' were

Table 1. Overlap in candidate gene lists from different transcriptomes.

	FlyMine genes	S2 mutant		UAS, cells		UAS, embryos		mutant, cells		mutant, embryos	
		down	up	down	up	down	up	down	up	down	up
		620	760	96	246	73	326	254	515	220	422
S2 cells down	620	-	1	1	22 (**9.7×10^{-4}**)	3	7	21 (**3.3×10^{-3}**)	14	16 (**2.5×10^{-2}**)	18
up	760	-	-	5	12	2	9	10	79 (**<10^{-16}**)	13	35 (**8.4×10^{-3}**)
UAS, cells down	96	-	-	-	0 (**<10^{-16}**)	21 (**<10^{-16}**)	2	7 (**4.5×10^{-4}**)	13 (**1.6×10^{-5}**)	4 (**2.0×10^{-2}**)	7 (**1.0×10^{-2}**)
up	246	-	-	-	-	0	51 (**<10^{-16}**)	17 (**9.4×10^{-7}**)	30 (**4.7×10^{-9}**)	14 (**1.2×10^{-5}**)	21 (**9.6×10^{-6}**)
UAS, embryos down	73	-	-	-	-	-	0	4 (**1.2×10^{-2}**)	10 (**9.3×10^{-5}**)	1	2
up	326	-	-	-	-	-	-	18 (**1.3×10^{-5}**)	23 (**1.6×10^{-3}**)	10 (**1.8×10^{-2}**)	7
mutant, cells down	254	-	-	-	-	-	-	-	0	35 (**<10^{-16}**)	0
up	515	-	-	-	-	-	-	-	-	4	143 (**<10^{-16}**)
mutant, embryos down	220	-	-	-	-	-	-	-	-	-	-
up	422	-	-	-	-	-	-	-	-	-	-

The table shows the number of candidate genes observed under each experimental condition. The degree of overlap is shown in absolute numbers, overlaps with statistically significant p-values are highlighted in bold. Note that the FlyMine list comparison tool considers splits and merges in gene models, which explains the slight offset between Table 1 and Table S1.

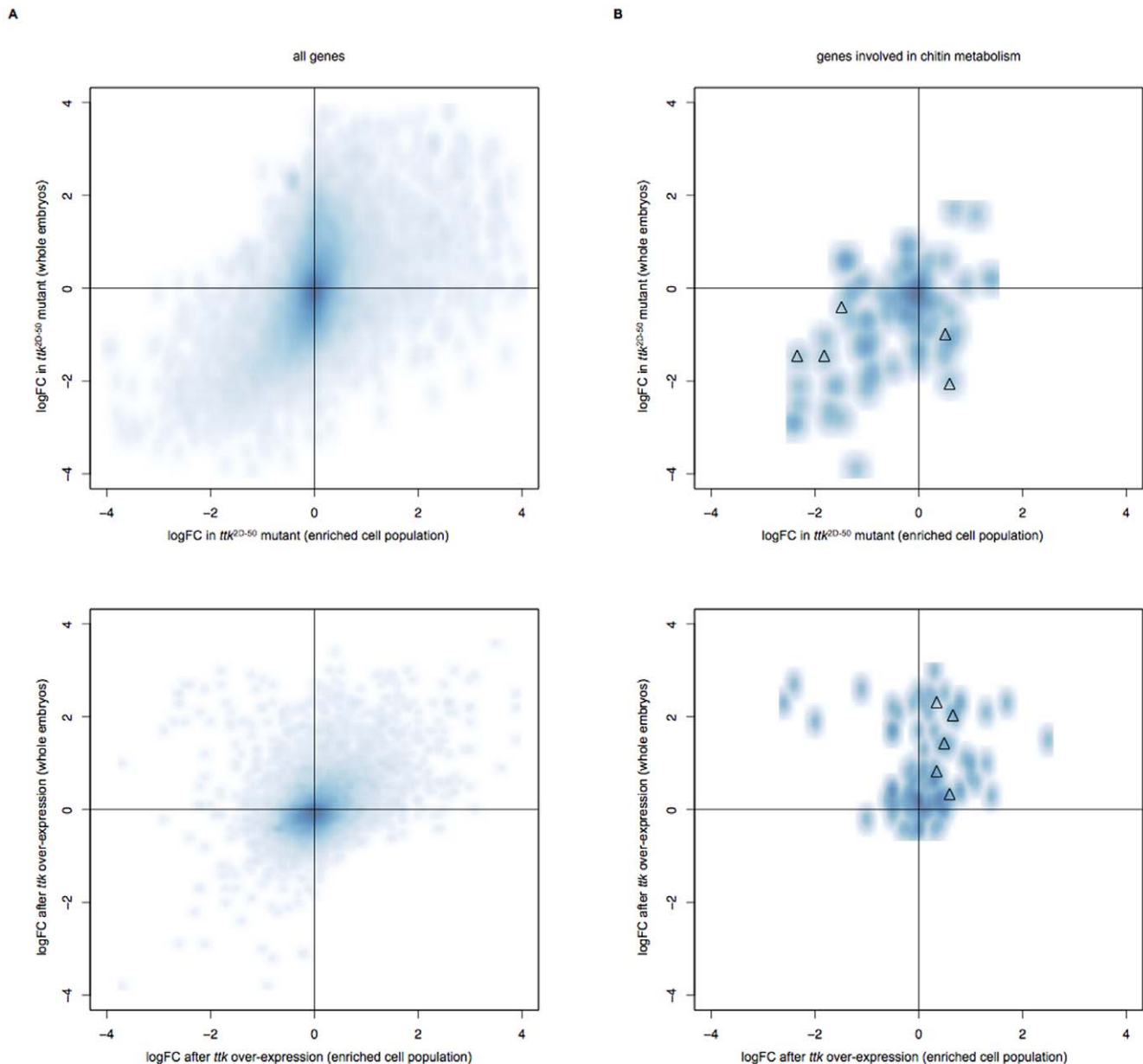doi:10.1371/journal.pone.0028985.t001

Figure 2. Gene expression changes in *ttk* mis-expression experiments. (A) Upper panel: *ttk*^D2-50 mutant; lower panel: *ttk* over-expression. The density plots show the expression changes of all genes on the microarray, in direct comparison of the enriched cell population (along the x-axis) to whole embryos (along the y-axis). Most genes do not change in expression (darker shade of blue around 0;0). If genes respond to *ttk* mutation, the change follows the same trend in embryos and sorted cells (roughly describing a diagonal), however there are outliers that behave counter-intuitively. Similar results can be observed after ttk over-expression. (B) The same plot as in (A), but restricted to genes annotated with GO term "chitin metabolism". In contrast to all genes, the expression changes are much more pronounced and suggest a systematic response to *ttk* mis-expression. Triangles indicate genes further investigated in the course of this study.
doi:10.1371/journal.pone.0028985.g002

analyzed. We confirmed the expected gain or loss of RNA abundance in eight candidate genes in mutant embryo conditions. Furthermore, we validated the directional change of six of them in *ttk* over-expression experiments. Remarkably, our qPCR experiments confirmed minor transcriptional changes (absolute logFC<1) for several candidate *ttk* target genes. Three genes annotated with 'septate junction' were also analysed by qPCR. Also here, the qPCR results confirmed the transcriptional changes and the direction in the change that were observed in the microarray analysis. This established that our microarray data can be used as a reliable platform for further downstream analysis.

To understand whether these *ttk* targets can mediate, at least in part, the function of *ttk* in tube size regulation we performed a functional analysis. We either expressed UAS-inducible RNAi in the tracheal system using the *btl*-GAL4 driver or used available loss-of-function alleles to down-regulate the activity of eleven selected *ttk* targets. We scored the tube size phenotype by staining embryos with chitin binding probe (CBP), a marker that allows visualizing the luminal chitin filament, which can be used as a read-out for tube length. We obtained normalized measures of dorsal trunk length and compared each mutant condition to an internal control. We found that five out of the eleven genes tested

Table 2. Validation of microarray candidates by quantitative PCR.

	ttk^{D2-50} embryos				ttk over-expression embryos			
Gene name	Microarray log FC	p-value	qPCR FC	p-value	Microarray log FC	p-value	qPCR FC	p-value
Cht2	**−1.47** ↓	1.65E⁻⁰¹	**−5.5** ↓	<0.05	0.22	**2.53E⁻⁰²**	**2.4** ↑	<0.05
Cht5	**−1.27** ↓	**2.64E⁻⁰²**	**−10.0** ↓	<0.05	**0.85** ↑	**1.60E⁻⁰⁴**	**2.1** ↑	<0.05
Cda4	**−2.03** ↓	1.59E⁻⁰¹	**−5.3** ↓	<0.05	−0.02	9.36E⁻⁰¹	**−1.5** ↓	<0.05
Cpr78Cb	**−2.08** ↓	**3.20E⁻⁰²**	**−15.0** ↓	<0.05	0.65	3.37E⁻⁰¹	ND	
Idgf3	**−1.96** ↓	**2.53E⁻⁰²**	**−2.5** ↓	<0.05	0.29	5.91E⁻⁰¹	ND	
Cht9	−0.61	2.58E⁻⁰¹	ND		**2.41** ↑	**0.00E⁺⁰⁰**	**4.7** ↑	<0.05
CG7715	**−1.46** ↓	2.68E⁻⁰¹	**−15.6** ↓	<0.05	**1.42** ↑	**4.44E⁻⁰²**	**2.9** ↑	<0.05
CG8460	**1.67** ↑	**1.79E⁻⁰²**	**5.4** ↑	<0.05	0.18	8.11⁻⁰²	ND	
Idgf1	−0.70	2.83E⁻⁰¹	**−9.00** ↓	<0.05	**2.00** ↑	**2.83E⁻⁰²**	**10.0** ↑	<0.05
dlg1	**1.57** ↑	**9.15E⁻⁰³**	**1.61** ↑	<0.05	−0.015	1.03E⁻⁰¹	ND	
Scrib	0.50	5.00E⁻⁰¹	ND		**1.57** ↑	**3.35E⁻⁰³**	**1.3** ↑	<0.05
vari	**−1.35** ↓	**4.91E⁻⁰²**	**−6.6** ↓	<0.05	−0.015	2.32E⁻⁰¹	ND	
Hdc	**2.55** ↑	**3.78E⁻⁰²**	**10.0** ↑	<0.05	0.25	1.00E⁻⁰¹	ND	
sc	**1.86** ↑	9.75E⁻⁰²	**1.6** ↑	<0.05	**−1.29** ↓	**4.36E⁻⁰²**	**−2.8** ↓	<0.05
ac	**1.21** ↑	3.12E⁻⁰¹	**−2.6** ↓	<0.05	**−1.80** ↓	**4.88E⁻⁰²**	**−2.0** ↓	<0.05
H	**2.27** ↑	**4.83E⁻⁰²**	**1.5** ↑	<0.05	−0.15	2.34E⁻⁰¹	ND	

Values obtained in the microarray and qPCR validation experiments performed on selected genes identified by microarray analysis in ttk mutant and ttk overexpression in whole embryo conditions, at developmental stages 11–16. qPCR analysis was performed using aliquots of cDNA pools prepared for microarray analysis. Note the correlation in the levels and direction of change between the two sets of experiments.
doi:10.1371/journal.pone.0028985.t002

exhibited a tube size phenotype. Interestingly, the mutant situations achieved by loss-of-function alleles (the cases of vari and dlg1) proved positive. 4 out of 10 candidates tested by RNAi expression produced a tube size effect (Cda4, Cpr78Cb, Scrib, dlg1) indicating expected [22] or non-previously described requirements of these genes in controlling the growth of the tracheal tubes (Figure 3). The tracheal expression of RNAi lines of another 6 candidates did not result in tube size defects, indicating that either the gene is not involved in tube size regulation or that the strength of the interfering lines are not sufficient to generate a visible effect.

Together these results identify several direct or indirect target genes for ttk involved in chitin metabolism or SJ organization that mediate Ttk activity during tube size regulation.

Tramtrack feeds into various developmental programmes in the tracheal system

Our previous work further found an involvement of Ttk in the fusion cell fate and a potential interaction with the Notch signaling cascade [1]. We examined genes with described functions in the fusion process (branch fusion, open tracheal system; GO:0035147) and the Dysfusion target gene CG15252 [23] for transcriptional changes in our microarray dataset (Supplementary Table S6). A key transcription factor gene (escargot) and headcase and CG15252 showed a significant transcriptional response in the enriched cell population after ttk over-expression (logFCs of −1.2, 1.1 and 2.3, respectively; all at p<0.02 or less). We observed changes in the same direction in mutant embryos (logFC>2.5 for hdc) that we could positively validate by qPCR (Table 2).

In a computational analysis of the genetic interaction network in Drosophila, we were searching for interacting gene pairs where both partners show a transcriptional response in either our or the S2 microarray datasets (data not shown). Interestingly, we found a local cluster of genes that are either targets of the Notch

downstream effector Su(H) (HLHmdelta, scute, achaete, E(spl), HLHm4) or known interactors of the transcription complex (Hairless), or factors downstream of H function (e.g. Bearded). Importantly, many of these genes show significantly decreased expression in the over-expression situation, and increased expression in the mutant situation, which could be confirmed by qPCR (Table 2). While the role and mechanism of Ttk in the regulation of these Notch target genes is not clear, this may provide a first explanation of our previous observations (see Discussion).

Stage-specific effects of Ttk regulation

Our microarray analysis and the validations of several candidates by qPCR generated results not always easy to interpret. For instance, we previously described a regulation of branchless (bnl) and mummy (mmy) by in situ hybridisation [1] that we could not confirm in our microarray experimental data. In addition, many genes showed unidirectional transcriptional responses (either up or down) to Ttk mis-expression conditions (either mutant or over-expression). For instance, the expression of cda4 goes down in both mutant and over-expression conditions. Furthermore, we also found some inconsistencies in the mode of transcriptional regulation (either up or down) between the microarray data and the qPCR experiments, as in the case of ac (see Table 2). While over-compensation effects of the genetic interaction network could possibly explain these counterintuitive behaviors, another possibility is that Ttk itself exhibits different time-specific roles (e.g. first activating, then repressing), which cannot be resolved in our samples. We therefore selected three genes (bnl, cda4 and ac) and probed their expression profile by stage-resolved qPCR. We performed qPCR experiments on Ttk mutant embryos and compared to their controls at stages 11 to 13 and at stages 14 to 16 (Table S7). We observed a downregulation of cda4 and bnl at
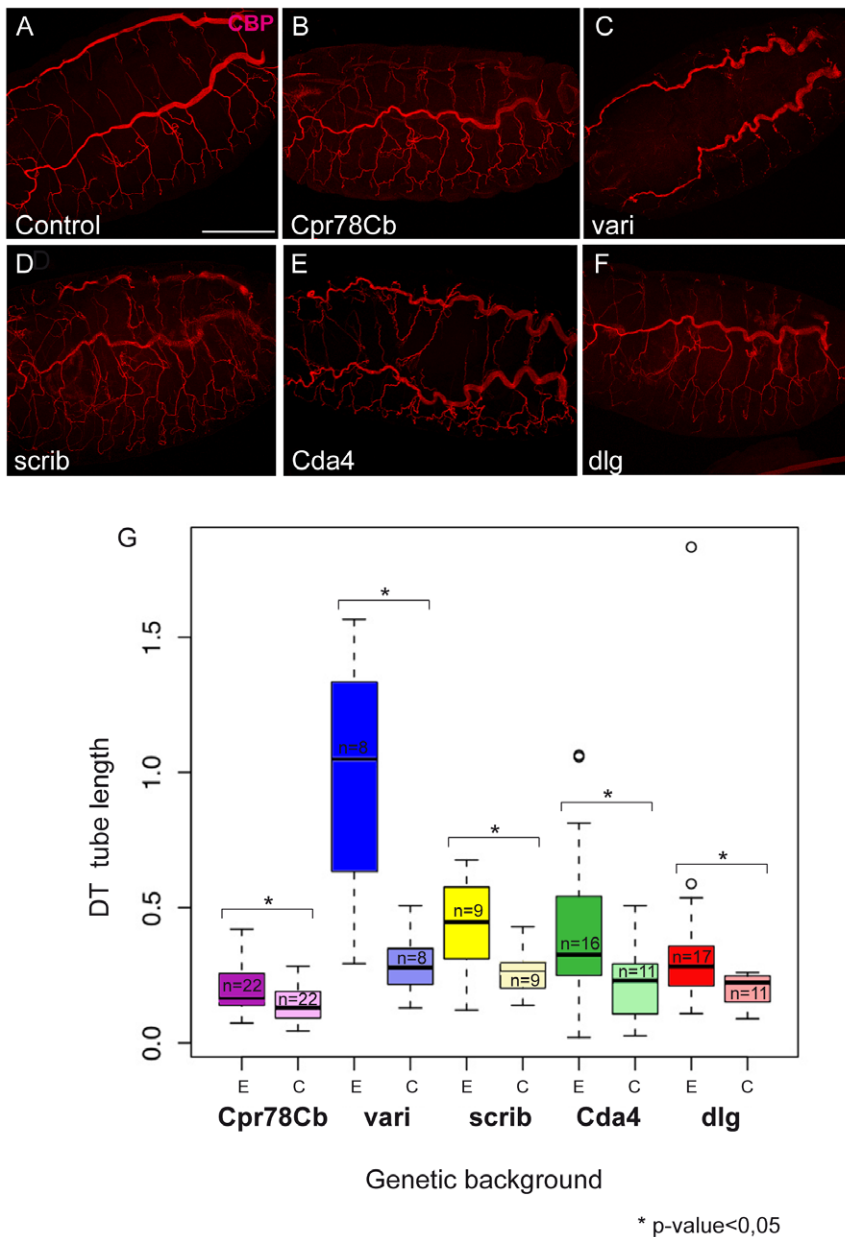
Figure 3. Analysis of the effect of putative *ttk* targets on tube length. (A–F) Projections of confocal sections showing dorso-lateral views of embryos at embryonic stage 16, labelled to visualise the chitin filament with CBP. Anterior is to the left and dorsal is up in all panels. The RNAi lines or loss-of-function alleles used were the following: (B) Cpr78Cb: RNAi 107767; (C) vari[3953]; (D) Scrib RNAi; (E) Cda4: RNAi 36106; (F) dlg1: RNAi 1076. RNAi lines were driven with *btl*-GAL4 UAS-tau-GFP. Note the enlarged DTs in embryos from B to F as compared to A (control). (G) Histogram showing tracheal tube lengths. For each gene we compared the experimental situation that we called E to its internal control that we called C. E corresponds to the loss-of-function situation, either RNAi expressed with *btl*-GAL4 UAS-tau-GFP, or the homozygote mutant in the case of loss-of-function alleles. C corresponds to heterozygote embryos in the case of loss-of-function alleles or to the RNAi line alone. n indicates the number of embryos that were measured. The differences in length between the experimental and control conditions are significant at p<0.05. Scale bar 100 μm.
doi:10.1371/journal.pone.0028985.g003

the different stages tested, in agreement with our previous observations. Interestingly, we found that *ac* is regulated differently by Ttk at early or late embryonic stages, indicating that Ttk can exert different stage-specific modes of action.

Tramtrack might directly regulate the expression of tracheal target genes

The broad range of biological functions could be either direct or indirect consequences of Ttk's role as a transcription factor. An initial step towards asserting this question is a look at genome-wide

binding profiles of Ttk, and to see whether our candidate genes are positioned in the vicinity of Ttk binding sites. The modENCODE project [24] has recently published such data for *Drosophila* embryos between stages 1–15, thereby capturing a significant proportion of tracheal development. While many caveats apply in the interpretation from whole-embryo data at this broad time frame, the manual inspection of our candidate genes suggests that the majority of them possess significant Ttk binding (Figure 4). This direct input from Ttk concerns genes involved in chitin metabolism (Figure 4A), septate junction formation (Figure 4C and
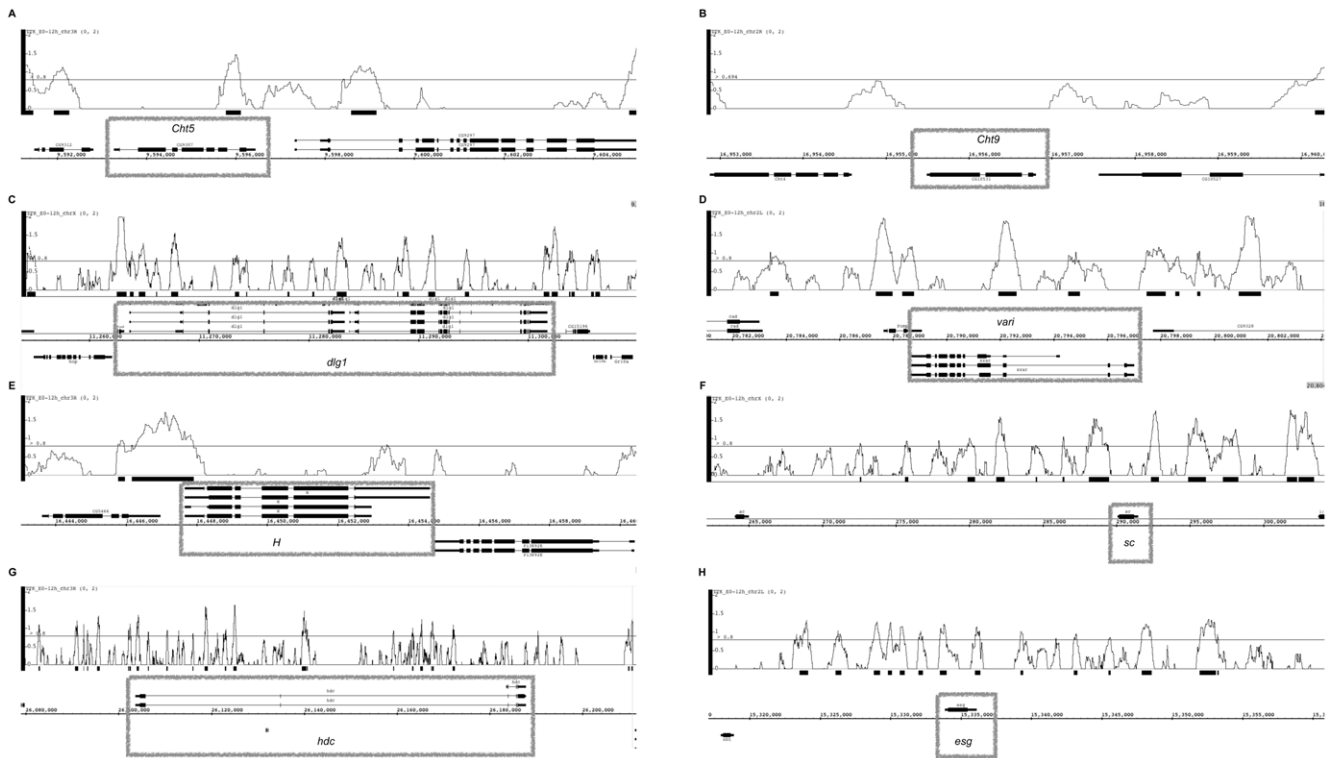
Figure 4. Chromatin immunoprecipitation (ChIP) enrichment for Ttk as determined by modENCODE. Panels (A–H) show ChIP profiles along the chromosomal axis for candidate genes (boxed) obtained by gene expression profiling. We assume measurable enrichment at lg2(0.8), or 1.5-fold enrichment over background levels (indicated by the gray horizontal line. Genes plotted above the coordinate line are encoded on the plus-strand, and those below the coordinate line are on the minus-strand. It is noteworthy that Ttk enrichment does not necessarily occur near the 5′-end of these genes, but can also occur in intronic regions as frequently seen also for transcription factors.
doi:10.1371/journal.pone.0028985.g004

4D), Notch signaling (Figure 4E and 4F) and fusion cell fate (Figure 4G and 4H). It is noteworthy that Ttk binding is not a default, and that some of our candidate genes do not show significant binding during embryonic development, e.g. *Cht9* (Figure 4B) or *m4* (data not shown). In respect to the apparent importance of Ttk in the regulation of genes involved in chitin metabolic processes, we performed a global analysis of Ttk binding using the modENCODE data (Figure S4). We found that 40 of 77 chitin metabolic genes showed Ttk ChIP enrichment$\geq =$lg2(1). Within this group of genes with Ttk enrichment, there is a higher proportion of genes with absolute logFC$\geq =1$ as transcriptional response in at least one of the experimental conditions probed with our microarrays (70% versus 51%), although this difference is not statistically significant (χ^2 test, p = 0.11). The observation that about half of the genes without Ttk enrichment show a transcriptional response suggests that Ttk may indirectly moderate their expression via yet unknown additional regulators. However, the result of many target genes having Ttk enrichment also suggests that Ttk mediates its function not only as a coordinator of other transcriptional regulators, but feeds in directly to the target genes immediately involved in the cellular response. It remains to be shown whether this role requires additional cofactors, or is primarily dependent on Ttk binding.

Discussion

The study of transcriptional regulators involved in *Drosophila* tracheal development has thus far primarily focused on their characterisation on the morphological level. While tracheal phenotypes were reported for many transcription factors and their developmental role was assessed on the cellular level (see [25] for review), we still lack a deeper understanding why certain factors yield particular phenotypes, mostly for the lack of putative target genes. In the present paper, we used transcriptional profiling to show that mis-regulation of the transcription factor Ttk feeds into a variety of previously known tracheal regulatory processes. While it is not possible to infer whether this input is direct with Ttk activating or repressing the respective target genes, or indirect due to effects mediated by additional regulators, this analysis provides a first step to understand the molecular basis of the morphological abnormalities that can be seen in *ttk* mutant embryos [1]. We previously showed that Ttk has immediate impact on several tracheal morphogenetic events such as tube size regulation, cell rearrangements or intracellular lumen formation. Here, we provide first evidence that the effect on tube size is to a large degree dependent on genes we find transcriptionally downstream of Ttk (see further below).

Microarray data quality, experimental limitations and interpretation

We used microarray gene expression profiling to identify putative targets of Ttk-dependent gene regulation. Data reproducibility in microarray experiments is typically a function of the number of replicates that are afforded. Given the number of experimental conditions we wanted to study, we compromised on a rather small number of replicates (three per condition attempted, in some cases only two were successful). Therefore, taking a rather conservative approach in the data analysis, we concentrated on genes with significant changes in gene expression as response to

Ttk mis-regulation. Quite reassuringly, we found that the expression changes of most genes better our p-value cutoff (p<0.05) could be confirmed in our qPCR validation experiments. This implies that there may be many more transcriptional changes that we were not able to detect due to stringent cutoffs. There were a few counterintuitive results, which however were not statistically significant. For example, our previous *in situ* hybridization experiments showed *bnl* to go down in *ttk* mutants [1] while the microarray results could not reproduce this regulation. However, the variation for this gene between individual microarray replicates is large (resulting in a p-value≫0.5), meaning that the measurement for this gene is unreliable. Further analysis of *bnl* by stage-dependent qPCR validated the transcriptional change observed by *in situ* hybridisation. Interestingly, a stage-resolved qPCR analysis also helped to interpret contradictory results between microarray analysis and qPCR experiments, as it indicated stage-specific modes of Ttk transcriptional control.

We sought to obtain tissue-specific gene expression profiles to discern Ttk-responses that are general and those that are probably specific to the tracheal system. We therefore generated expression profiles from FACS-sorted cell populations that expressed a fluorescent reporter under the control of the *btl* enhancer (btl-enh-RFP-moe). The *btl* enhancer is widely used in the community for studies of the tracheal system, despite its well-known expression in the ventral midline [26] as well as other parts of the embryo. Importantly, we find similarly strong enrichment for RNAs for primarily tracheal genes (e.g. *trachealess*) and the midline marker *single-minded*, but also a strong transcriptional footprint for the amnioserosa and other tissues, for which thus far there was only anecdotal evidence for the activity of the *btl* enhancer. We therefore conclude that non-visual analyses of the tracheal system should therefore avoid the *btl* enhancer if tracheal specificity is desired. Interestingly, we also found genes expressed in the purified cell population that according to the BDGP gene expression database should not be expressed in the embryo. By comparison to temporal expression profiles from modENCODE (data not shown), we inferred that many of these are false-negative results of the *in situ* hybridisation experiments. Despite technical limitations, we would like to point out that our gene expression catalogue of btl-enh-RFP-moe positive cells might represent a valuable entry point for further analysis. While the interpretation of the numerical data may not be as straightforward as the *in situ* hybridisation results obtained in high-throughput by the BDGP, the expression values of the purified cell population allow an initial judgment if a gene might be expressed in the trachea or not.

Although not pure, our analysis indicates that the expression profiles of the sorted cell population are at least enriched for tracheal targets and therefore very useful. Using our parameter combination to identify "significantly changed" transcripts after Ttk mis-expression, we determined an overlap of about 25% between the whole embryo versus the purified cell population datasets. Can this degree of overlap be expected? While one may naively expect a higher degree of overlap as the molecular mechanisms of transcription factor function should be conserved, we argue that a versatile transcription factor such as Ttk likely depends on a wide range of different co-factors to exhibit its different functions. We therefore argue that the observed degree of overlap in the transcriptional response reflects the different transcriptional background (of active genes) of whole embryos and sorted cells. In addition, the assayed cell population accounts for an estimated 5–10% of the whole embryonic cell mass, and transcriptional changes in these cells may therefore be too dilute to be picked up in the whole-embryo expression profile. Furthermore, variations due to technical reasons may also account for,

although minor, differences in the transcriptome profiles. We observe cases were the transcriptional response is opposite in whole embryos and cells. Again, this is probably due to different co-regulators that dictate the directionality of an expression change. Although Ttk is widely believed to act as transcriptional repressor [3,5,9,14], the analysis of genome-wide binding data has suggested alternative roles for many transcription factors, and a recent theoretical study implies that most transcription factors may act in different directions [27].

Using our criteria to select candidate genes, the screen of Reddy et al. on the S2 *Drosophila* cell line after *ttk* knockdown by RNA interference [21] yielded 1,380 candidate genes as compared to 600–800 genes in our *ttk*$^{2D-50}$ mutant conditions. The larger number of genes is at least in part owed to the fact that their dataset comprises many more replicates and, therefore, allows for a greater number of genes to fulfill the p-value<=0.05 criterion. Quite reassuringly, however, the degree of overlap between our and their experiments is statistically significant although the absolute overlap between their candidate gene list and our lists is small (Table 1). For example, the 620 genes down-regulated in S2 cells overlap with 22 of the 246 genes up-regulated in cells after *ttk* over-expression (p = 9.7×10^{-4}) and 21 of 254 genes down-regulated in our cell population experiments in *ttk*$^{2D-50}$ mutants (p = 3.3×10^{-3}). The majority of experiments that are expected to be conversely correlated (e.g. up in *ttk*$^{2D-50}$ mutant, down after *ttk* over-expression, or vice versa) show significant overlap. However, it should also be noted that in a few cases results emerged that were not intuitive, e.g. the overlap of 30 genes up-regulated in both mutant and over-expressing cells (p = 4.7×10^{-9}). It may be assumed that, while the majority of direct or indirect Ttk target genes respond appropriately to the experimental situation, the over-expression in particular provokes unexpected responses: the 246 up-regulated genes in cells after *ttk* over-expression overlap significantly with almost all other experimental conditions. We argue that the mutant situation is likely to represent the biologically better interpretable response, as the over-expression situation may see many more ectopic downstream effects.

The microarray analysis validate previous functional analysis

Ttk plays multiple roles during *Drosophila* development. In the case of tracheal development we previously observed requirements for Ttk at several steps. Some of these requirements are particularly interesting from the morphogenetic point of view because they involve cellular responses downstream of cell fate specification [1]. Thus, we expected Ttk to control several target genes that impinge directly on cell behaviour, affecting, for instance, the cytoskeletal network, intracellular trafficking or cell junctions. In line with our previous assumptions, we find several Ttk-regulated genes that belong to the GO categories of "vesicle-mediated transport", "cytoskeleton", or "plasma membrane" (Table S6). Very interestingly, we find many genes involved in the Microtubule cytoskeleton, which has been involved in several tracheal events also affected by Ttk activity, like branch fusion, terminal branch formation, or luminal chitin deposition [28–32]. Immunostainings with several microtubule markers further indicate that the microtubule network is not properly organized in Ttk mutants (ML, unpublished data). Future work will help to determine how Ttk controls microtubule activity and organization, and how this contributes to Ttk phenotype. It is noteworthy that the broadest range of GO terms shared between genes that come up after *ttk* knockdown in cells and in the *ttk* mutant are involved in 'female gamete generation' (GO:0007292). Ttk has previously been implicated in ovarian follicle development [12,33], and it

appears that this function is probably linked to a gene set that may also exhibit broader functionality in the embryonic or cell culture context. This may also be true for an extensive list of genes involved in embryonic axis determination, one of the first functions described for Ttk [2].

Remarkably, our microarray results confirm previous observations and provide new data for the different Ttk tracheal requirements. For instance, we described that the transcription factor Esg, which plays a pivotal role in fusion cell identity specification [34,35] is lost when Ttk is over-expressed, but still present in Ttk loss-of-function conditions [1]. The microarray data confirm this regulation, and in addition identifies other genes already shown to directly or indirectly modulate fusion fate as Ttk targets, like *hdc* [36], CG15252 [28], or *pnt* [37]. Similarly, we find that *polychaetoid* (*pyd*), which we identified as a Ttk target in *in situ* hybridisation analysis [1], is differentially expressed in our microarray conditions (it should be noted however that *pyd* is not formally a candidate due to inconsistencies between microarray replicates; in fact only splice variant *pyd*-RE shows a response), explaining in part the requirement of Ttk in tracheal cell intercalation. In addition, it is tempting to speculate about other candidate targets to mediate this function of Ttk in intercalation, like *canoe* (*cno*) for instance, which have been recently shown to act with *pyd* during embryogenesis [38].

We have focused on the role of Ttk in tube size to validate our experimental approach. To date, several factors have been shown to control tube growth, the septate junctions (SJs) and a transient intraluminal chitin filament being two key elements (review in [16–18]). Among Ttk-regulated genes in our screen we have identified several with known or potential functions in chitin metabolism (included in the GO term 'chitin metabolism') and SJ organisation. We confirmed by qPCR the predicted transcriptional regulation observed in the microarray analysis. Remarkably, the functional requirement of some of these genes in tube size regulation could also be confirmed in our or other's experiments. Our functional approach based on the expression in the tracheal tissue of RNAi lines of chitin metabolism and SJ organisation targets of Ttk identified 40% of these genes as modulators of tube size. For instance, we identify such a role in the chitin-binding protein Cda4 which might act as a chitin deacetylase. However, we did not observe an effect on tube size using RNAi lines of several genes with expected roles in this process, like for instance *Cht2* (BR and ML, unpublished data), which has been shown to generate tube size defects upon overexpression [39]. The lack of effect of several RNAi lines tested indicate that either the downregulation of the gene does not affect the control of tube size (because the gene is not required or due to functional redundancy), or that the strength of the interfering lines is not sufficient to generate a visible effect. Further experiments would be required to distinguish between these two possibilities. Nevertheless, the fact that some RNAi lines produce extra long tracheal tubes already establishes the link between Ttk and (at least some) tracheal tube size genes. Finally, it is important to note that besides the organisation and assembly of a transient luminal chitin filament other mechanisms have also been reported to regulate the size of the tracheal tubes (reviews in [18]). Importantly, we observe that Ttk may be also controlling some of these other mechanisms, like apical secretion through Gef64C [40], apical cell membrane growth through Mmp1 [41] or planar cell polarity through ft [42] (Supplementary Table S6). Thus, Ttk would feed into a general and complex program of tube size control involving different mechanisms.

Altogether our results validate previous functional analysis and identify several targets that we show or we propose can mediate the different activities of Ttk during tracheal development.

Ttk and Notch interactions

Our microarray analysis pointed to a regulation of the Notch signalling pathway or its activity by Ttk, likely acting as a negative regulator. On the other hand, we had previously observed that Ttk acts as a downstream effector of N activity in the specification of different tracheal identitites [1]. Indeed, we showed that Ttk levels depend on N activity in such a way that when N is active, Ttk levels are high, whereas when N is not active, Ttk levels are low. Thus, we observed lower levels of Ttk in tracheal fusion cells due to the inactivity of N there [37,43,44]. Therefore, Ttk acts as a target of N in fusion cell determination. Now, the results of the microarray add an extra level of complexity to the Ttk-N interaction. The observation that in turn Ttk also transcriptionally regulates several N pathway components suggests that Ttk is involved in a feedback mechanism that could play a pivotal role in biasing or amplifying N signalling outcome.

Interactions between Ttk and N have been observed in different developmental contexts, emphasising the importance of such regulations. Several examples illustrate the regulation, either positive or negative, of Ttk expression by N activity [45–49]. In addition, a recent report provides evidence of a regulation of N activity by Ttk and proposes a mutually repressive relationship between N and Ttk which would also involve Ecdysone signalling [15]. Our results are consistent with many of these observations, indicating that they could represent general molecular mechanisms of morphogenesis. Thus, tracheal cell specification could serve as an ideal scenario to investigate the intricate, and often contradictory, interactions between N and Ttk and the complexity of N signaling.

Materials and Methods

Drosophila stocks

In this work we use the loss-of-function allele ttk^{D2-50} balanced over a TM3 Twi-GFP balancer, which allows the identification of mutant embryos by the absence of fluorescence. All gain-of-function experiments were performed using the GAL4/UAS system [50]. All the *Drosophila* stocks used are described in FlyBase. We used a transgenic line containing the btl-enh-RFP-moe insertion [51] that enables the visualization of the shape of all *btl* positive cells *in vivo*. We generated recombinants carrying btl-enh-RFP-moe and the *ttk* mutant conditions, in particular: btl-enh-RFP-moe ttk^{D2-50}/TM3 Twi-GFP for the mutant, and btl-enh-RFP-moe UAS-*ttk69* for the over-expression condition. We used *btl*-GAL4 UAS-tau-GFP [52] to drive *ttk* over-expression.

Embryo and cell sorting strategy

To obtain homogeneous-as-possible embryos for RNA extraction, we devised a two-step sorting strategy for first embryos and then cells. In order to enrich the embryo collection for embryos undergoing tracheal development, we allowed flies to lay eggs for 7,40 hr at 25°C, and subsequently let the embryos age for another 5,20 hr at 25°C. This enabled us to maximize the number of embryos at the appropriate developmental stages 11–16.

Embryos were first dechorionated and washed 3× with PBS-Triton (0.1%). They were then collected into an Eppendorff with cold Schneider's medium (S2) (GIBCO). We used a COPAS PLUS Embryo Sorter (Union Biometrica) following the manufacturer's recommendations to obtain homozygous mutants that were characterised by the absence of balancer-GFP. The appropriate embryo population was selected according to their extinction/absortion profile. The gated population was analysed and sorted according to the lack of GFP expression (blue excitation, green

emission). Manual examination confirmed the success of this sorting step.

For several rounds, pools of 600–1000 sorted embryos were homogenised in cold S2 medium in a crystal douncer (KONTES Gerresheimer) with three strokes without rotating the pestle. Thereafter, 60 µl of trypsin-EDTA 9X (SIGMA) was added to 1.5 ml of S2 medium and shaken for 15 minutes at room temperature to the homogenised embryonic sample. 5 µl of Hoechst-33342 nuclear marker per 600–1000 embryos was added to the trypsinisation reaction. Subsequently, the reaction was stopped with a 1:1 PBS:BSA buffer.

Ultimately, dissociated cells were sorted using a FacsAria SORP sorter (Beckton Dickinson, San Jose, California). Excitation of the sample was done using a blue (488 nm) laser for forward-scatter (FSC) and GFP green fluorescence; green (532 nm) laser for RFP fluorescence, and a UV laser for Hoechst-33342 fluorescence. A combination of excitation wavelengths was used to distinguish autofluorescence from fats from actual cells. Those enriched for RFP (by their expression of the btl-enh-RFP-moe construct) were selected according to their forward-scatter/side-scatter (SSC) signal. The Hoechst-33342 signal was used to eliminate debris and broken cells. The gating strategy is shown in Figure S2.

RNA extraction

Total RNA from pools of about 1,000 embryos from the four genotypes (control, ttk^{D2-50} mutant, btl-GAL4; btl-enh-RFP-moe and btl-GAL4; btl-enh-RFP-moe UAS-ttk69) was extracted using the GibcoBRL Trizol protocol. RNA extraction from the purified cell samples from the four genotypes were performed using the RNeasy QIAGEN RNA Extraction Kit, starting with 100,000 isolated cells of each condition. RNA was quantified using the Nanodrop ND-1000 spectrophotometer (Fisher Scientific) and integrity was evaluated on the Bioanalyzer 2100 (Agilent) using the RNA 6000 Nano Kit.

Microarray experiments

We pooled multiple RNA collections from different cell sorting runs from the same week to minimise the variation inherent among collections and to obtain adequate RNA from each genotype. 5 ng total RNA per sample was processed using the isothermal amplification SPIA Biotin System (NuGEN Technologies, Inc.).

2.2 µg of cDNA from each genotype and for each sample condition were hybridized to GeneChip 2.0 *Drosophila* Genome Arrays (Affymetrix, Santa Clara, CA) in triplicate. The Functional Genomics Core Facility at the IRB provided all the reagents, equipment and expertise for hybridisation and scanning.

Raw microarray data has been deposited in the MIAME compliant GEO database, series GSE30239.

Computational analysis

Raw microarray data were processed in *R* and Bioconductor [53] using the Brainarray ENSEMBL Custom v12 CDF mapping [54]. For further details on normalisation and scaling see GEO [55] data series GSE30239. All other data analysis was performed using custom-written Perl scripts, using BDGP gene expression database (March 2007) [20] and BioGrid genetic interactions (early 2011) [56] for comparison. Gene lists were managed in FlyMine [57] and analysed for Gene Ontology-enrichment using their implementation of the hypergeometric test with Benjamini-Hochberg multiple testing correction. The Ttk chromatin immunopurification data was obtained from the modENCODE website and visualised using the Integrated Genome Browser (http://bioviz.org/igb/).

Quantitative real time qPCR

Equal amounts of total RNA of embryos at stages 11 to 16 from each condition and genotype were used to synthesise complementary cDNA by random-hexamer-priming (RevertAid H Minus First Strand cDNA Synthesis FERMENTAS Kit) in triplicate. A LightCycler 480 Real-Time PCR System and the SYBR Green PCR Master Mix (Roche) were used to amplify cDNAs. Relative quantities were normalized to expression of CG13167, a mitochondrial ATPase that showed stable expression throughout all experimental conditions. All PCR reactions were carried out in triplicate in 20 µl reaction volumes containing 2 µl cDNA template. Samples were analyzed using the LightCycler 480 Real-Time PCR System software (Roche). All PCR primers were designed using the MacVector 11.1 software, aimed to amplify a product size of 75–150 bp, and are listed in Supplementary Table S5. Expression changes were deemed significant at $p < 0.05$.

Stage-specific qPCR

To compare the expression profile of embryos at different stages, we collected embryos at stages 11 to 13 and embryos at stages 14 to 16. For the collection of the younger embryos we allowed flies to lay eggs for 5,20 hr at 25°C and subsequently allowed embryos to develop for another 5 hr at 25°C. For the older embryo collection we allowed flies to lay eggs for 5,20 hr at 25°C and subsequently allowed embryos to develop for another 10,20 hr at 25°C.

Embryos were dechorionated and sorted by absence of GFP using the COPAS PLUS Sorter to obtain the homozygous mutants and control embryos. Total RNA from pools of about 1,000 embryos from each genotype (control and ttk^{D2-50} mutant) at each developmental stage was extracted using the GibcoBRL Trizol standard protocol. RNA was quantified using the Nanodrop ND-1000 spectrophotometer (Fisher Scientific).

Equal amounts of total RNA were used to synthesise complementary cDNA by random-hexamer-priming (RevertAid H Minus First Strand cDNA Synthesis FERMENTAS Kit) in triplicate, to perform and analyse the qPCR experiments as we describe above.

Immunohistochemistry

Embryos were stained following standard protocols. Immunostainings were performed on embryos fixed in 4% formaldehyde for 20′. The following primary antibodies were used: anti-GFP, 1:600 (Molecular Probes and Roche) and anti-βGal, 1:600 (Cappel and Promega). Cy2 and Cy3-conjugated secondary antibodies (Jackson ImmunoResearch) were used at 1:300 in PBT+0.5%BSA. Chitin was visualised with Chitin-binding protein CBP (NEB) at 1:500. Confocal images were obtained with a Leica TCS-SPE system. Images were imported into Adobe Photoshop and assembled into figures using the Adobe Illustrator software.

Tube length measurements

Drosophila embryos from mid-late stage 16 and stage 17 were stained with CBP and GFP to visualise their tracheal system. Digital micrographs of dorsal trunks were used to measure their length adapting a previously published method [22]. The significance of tracheal length differences between controls, RNAi knockdown mutants and the available loss-of-function alleles, measured in ImageJ, was determined using Wilcoxon's test in *R*.

Supporting Information

Figure S1 Quality control plots. Microarray quality control before normalization. Panel (A) shows histograms and panel (B)

shows box plots, each grouped by experiment. The outcomes of cell sorting experiments are generally close to the corresponding whole-embryo outcomes. The MA plots in panel (C) indicate that the arrays are well comparable within each experiment.
(TIF)

Figure S2 Gating strategy for FACS-assisted cell sorting. Examples for the isolation of RFP positive cells from a whole embryo cell suspension. Regions are drawn to include the population of interest. (Panel 1) Data for mutant control cell suspension. (1A) Region in A is drawn and placed to include most of the events that exhibit similar SSC and FSC values. (1B) P5 region is drawn and placed to include live cells with only 2C DNA content, which are the cells at G0/G1 cell cycle phase. (1C) P4 region is drawn and placed to distinguish RFP-positive from RFP-negative cells with respect to relative cell size and fluorescence. (Panels 2–4) show equivalent plots. (Panel 2) Data for ttk^{D2-50} mutant cell suspension. (Panel 3) Data for control UAS-experiment cell suspension. (Panel4) Data for UAS-$ttk69$ cell suspension.
(TIF)

Figure S3 Spatial gene expression representation in microarray signal categories. Spatial gene expression pattern representation in different microarray signal strength categories. Gene expression profiles from enriched cell populations for the control group in the (A) mutant and (B) over-expression are shown. Within the signal intensity histogram (x-axis: bins of $\log_2$ signal strength, y-axis: number of genes), the proportion of genes falling into one of four different spatial gene expression categories is shown: genes with tracheal or midline expression (red), genes with ubiquitous expression (blue), genes with expression elsewhere (light gray), genes not expressed according to the BDGP *in situ* database (dark gray).
(TIF)

Figure S4 Cluster diagram of genes involved in chitin metabolic processes. Genes are clustered according to the gene expression changes in response to Ttk-mis-expression (from bottom to top: over-expression in cells, over-expression in embryos, mutant cells and mutant embryos) as well as Ttk occupancy in the modEN-CODE dataset (ChIP enrichment$> = \lg2(1)$ over the gene body +/ -1 kb; blue indicates occupancy and yellow non-occupancy).
(PDF)

Table S1 Number of putative candidate genes after *ttk* mis-expression.
(XLS)

Table S2 Comparison of raw signal intensities for selected marker genes.
(XLS)

Table S3 Expression enrichment in FACS-sorted cell populations.
(XLS)

Table S4 Over-represented Gene Ontology categories.
(XLS)

Table S5 Real-time PCR primer sequences for target validation.
(DOC)

Table S6 Selected Gene Ontology terms with putative involvement in tracheal development, and genes with that annotation which are mis-regulated either in our microarray dataset or in S2 cells.
(XLS)

Table S7 Analysis of stage-specific regulation by quantitative PCR.
(DOC)

Text S1 Quality control of microarrays.
(DOC)

File S1 Archive (gzip2 compressed tar ball format) with 82 PDF files showing scatter plots for GO biological process terms with more than 50 annotated genes. Legend analogous to Figure 2.
(BZ2)

Acknowledgments

Author Contributions

Conceived and designed the experiments: BR DM BA ML. Performed the experiments: BR DM BA ML. Analyzed the data: BR DM BA ML. Wrote the paper: BR DM BA ML.

References

1. Araújo SJ, Cela C, Llimargas M (2007) Tramtrack regulates different morphogenetic events during Drosophila tracheal development. Development 134: 3665–3676. doi:10.1242/dev.007328.
2. Harrison SD, Travers AA (1990) The tramtrack gene encodes a Drosophila finger protein that interacts with the ftz transcriptional regulatory region and shows a novel embryonic expression pattern. EMBO J 9: 207–216.
3. Brown JL, Sonoda S, Ueda H, Scott MP, Wu C (1991) Repression of the Drosophila fushi tarazu (ftz) segmentation gene. EMBO J 10: 665–674.
4. Read D, Manley JL (1992) Alternatively spliced transcripts of the Drosophila tramtrack gene encode zinc finger proteins with distinct DNA binding specificities. EMBO J 11: 1035–1044.
5. Brown JL, Wu C (1993) Repression of Drosophila pair-rule segmentation genes by ectopic expression of tramtrack. Development 117: 45–58.
6. Guo M, Bier E, Jan LY, Jan YN (1995) tramtrack acts downstream of numb to specify distinct daughter cell fates during asymmetric cell divisions in the Drosophila PNS. Neuron 14: 913–925.
7. Lai ZC, Li Y (1999) Tramtrack69 is positively and autonomously required for Drosophila photoreceptor development. Genetics 152: 299–305.
8. Badenhorst P (2001) Tramtrack controls glial number and identity in the Drosophila embryonic CNS. Development 128: 4093–4101.
9. Chen Y-J, Chiang C-S, Weng L-C, Lengyel JA, Liaw G-J (2002) Tramtrack69 is required for the early repression of tailless expression. Mech Dev 116: 75–83.

10. Baonza A, Murawsky CM, Travers AA, Freeman M (2002) Pointed and Tramtrack69 establish an EGFR-dependent transcriptional switch to regulate mitosis. Nat Cell Biol 4: 976–980. doi:10.1038/ncb887.
11. French RL, Cosand KA, Berg CA (2003) The Drosophila female sterile mutation twin peaks is a novel allele of tramtrack and reveals a requirement for Ttk69 in epithelial morphogenesis. Dev Biol 253: 18–35.
12. Althauser C, Jordan KC, Deng W-M, Ruohola-Baker H (2005) Fringe-dependent notch activation and tramtrack function are required for specification of the polar cells in Drosophila oogenesis. Dev Dyn 232: 1013–1020. doi:10.1002/dvdy.20361.
13. Audibert A, Simon F, Gho M (2005) Cell cycle diversity involves differential regulation of Cyclin E activity in the Drosophila bristle cell lineage. Development 132: 2287–2297. doi:10.1242/dev.01797.
14. Siddall NA, Hime GR, Pollock JA, Batterham P (2009) Ttk69-dependent repression of lozenge prevents the ectopic development of R7 cells in the Drosophila larval eye disc. BMC Dev Biol 9: 64. doi:10.1186/1471-213X-9-64.
15. Boyle MJ, Berg CA (2009) Control in time and space: Tramtrack69 cooperates with Notch and Ecdysone to repress ectopic fate and shape changes during Drosophila egg chamber maturation. Development 136: 4187–4197. doi:10.1242/dev.042770.
16. Wu VM, Beitel GJ (2004) A junctional problem of apical proportions: epithelial tube-size control by septate junctions in the Drosophila tracheal system. Curr Opin Cell Biol 16: 493–499. doi:10.1016/j.ceb.2004.07.008.

17. Swanson LE, Beitel GJ (2006) Tubulogenesis: an inside job. Curr Biol 16: R51–53. doi:10.1016/j.cub.2006.01.008.

18. Schottenfeld J, Song Y, Ghabrial AS (2010) Tube continued: morphogenesis of the Drosophila tracheal system. Curr Opin Cell Biol 22: 633–639. doi:10.1016/j.ceb.2010.07.016.

19. Glazer L, Shilo BZ (1991) The Drosophila FGF-R homolog is expressed in the embryonic tracheal system and appears to be required for directed tracheal cell extension. Genes Dev 5: 697–705.

20. Tomancak P, Berman BP, Beaton A, Weiszmann R, Kwan E, et al. (2007) Global analysis of patterns of gene expression during Drosophila embryogenesis. Genome Biol 8: R145. doi:10.1186/gb-2007-8-7-r145.

21. Reddy BA, Bajpe PK, Bassett A, Moshkin YM, Kozhevnikova E, et al. (2010) Drosophila transcription factor Tramtrack69 binds MEP1 to recruit the chromatin remodeler NuRD. Mol Cell Biol 30: 5234–5244. doi:10.1128/MCB.00266-10.

22. Laprise P, Paul SM, Boulanger J, Robbins RM, Beitel GJ, et al. (2010) Epithelial polarity proteins regulate Drosophila tracheal tube size in parallel to the luminal matrix pathway. Curr Biol 20: 55–61. doi:10.1016/j.cub.2009.11.017.

23. Jiang L, Pearson JC, Crews ST (2010) Diverse modes of Drosophila tracheal fusion cell transcriptional regulation. Mech Dev 127: 265–280. doi:10.1016/j.mod.2010.03.003.

24. Roy S, Ernst J, Kharchenko PV, Kheradpour P, Negre N, et al. (2010) Identification of functional elements and regulatory circuits by Drosophila modENCODE. Science 330: 1787–1797. doi:10.1126/science.1198374.

25. Ghabrial A, Luschnig S, Metzstein MM, Krasnow MA (2003) Branching morphogenesis of the Drosophila tracheal system. Annu Rev Cell Dev Biol 19: 623–647. doi:10.1146/annurev.cellbio.19.031403.160043.

26. Ohshiro T, Saigo K (1997) Transcriptional regulation of breathless FGF receptor gene by binding of TRACHEALESS/dARNT heterodimers to three central midline elements in Drosophila developing trachea. Development 124: 3975–3986.

27. Bauer DC, Buske FA, Bailey TL (2010) Dual-functioning transcription factors in the developmental gene network of Drosophila melanogaster. BMC Bioinformatics 11: 366. doi:10.1186/1471-2105-11-366.

28. Jiang L, Rogers SL, Crews ST (2007) The Drosophila Dead end Arf-like3 GTPase controls vesicle trafficking during tracheal fusion cell morphogenesis. Dev Biol 311: 487–499. doi:10.1016/j.ydbio.2007.08.049.

29. Gervais L, Casanova J (2010) In vivo coupling of cell elongation and lumen formation in a single cell. Curr Biol 20: 359–366. doi:10.1016/j.cub.2009.12.043.

30. Lee M, Lee S, Zadeh AD, Kolodziej PA (2003) Distinct sites in E-cadherin regulate different steps in Drosophila tracheal tube fusion. Development 130: 5989–5999. doi:10.1242/dev.00806.

31. Kakihara K, Shinmyozu K, Kato K, Wada H, Hayashi S (2008) Conversion of plasma membrane topology during epithelial tube connection requires Arf-like 3 small GTPase in Drosophila. Mech Dev 125: 325–336. doi:10.1016/j.mod.2007.10.012.

32. Brodu V, Baffet AD, Le Droguen P-M, Casanova J, Guichet A (2010) A developmentally regulated two-step process generates a noncentrosomal microtubule network in Drosophila tracheal cells. Dev Cell 18: 790–801. doi:10.1016/j.devcel.2010.03.015.

33. Jordan KC, Schaeffer V, Fischer KA, Gray EE, Ruohola-Baker H (2006) Notch signaling through tramtrack bypasses the mitosis promoting activity of the JNK pathway in the mitotic-to-endocycle transition of Drosophila follicle cells. BMC Dev Biol 6: 16. doi:10.1186/1471-213X-6-16.

34. Tanaka-Matakatsu M, Uemura T, Oda H, Takeichi M, Hayashi S (1996) Cadherin-mediated cell adhesion and cell motility in Drosophila trachea regulated by the transcription factor Escargot. Development 122: 3697–3705.

35. Samakovlis C, Manning G, Steneberg P, Hacohen N, Cantera R, et al. (1996) Genetic control of epithelial tube fusion during Drosophila tracheal development. Development 122: 3531–3536.

36. Steneberg P, Englund C, Kronhamn J, Weaver TA, Samakovlis C (1998) Translational readthrough in the hdc mRNA generates a novel branching inhibitor in the drosophila trachea. Genes Dev 12: 956–967.

37. Llimargas M (1999) The Notch pathway helps to pattern the tips of the Drosophila tracheal branches by selecting cell fates. Development 126: 2355–2364.

38. Choi W, Jung K-C, Nelson KS, Bhat MA, Beitel GJ, et al. (2011) The single Drosophila ZO-1 protein Polychaetoid regulates embryonic morphogenesis in coordination with Canoe/afadin and Enabled. Mol Biol Cell 22: 2010–2030. doi:10.1091/mbc.E10-12-1014.

39. Tonning A, Hemphälä J, Tång E, Nannmark U, Samakovlis C, et al. (2005) A transient luminal chitinous matrix is required to model epithelial tube diameter in the Drosophila trachea. Dev Cell 9: 423–430. doi:10.1016/j.devcel.2005.07.012.

40. Massarwa R, Schejter ED, Shilo B-Z (2009) Apical secretion in epithelial tubes of the Drosophila embryo is directed by the Formin-family protein Diaphanous. Dev Cell 16: 877–888. doi:10.1016/j.devcel.2009.04.010.

41. Page-McCaw A, Serano J, Santé JM, Rubin GM (2003) Drosophila matrix metalloproteinases are required for tissue remodeling, but not embryonic development. Dev Cell 4: 95–106.

42. Chung S, Vining MS, Bradley PL, Chan C-C, Wharton KA, Jr., et al. (2009) Serrano (sano) functions with the planar cell polarity genes to control tracheal tube length. PLoS Genet 5: e1000746. doi:10.1371/journal.pgen.1000746.

43. Steneberg P, Hemphälä J, Samakovlis C (1999) Dpp and Notch specify the fusion cell fate in the dorsal branches of the Drosophila trachea. Mech Dev 87: 153–163.

44. Ikeya T, Hayashi S (1999) Interplay of Notch and FGF signaling restricts cell fate and MAPK activation in the Drosophila trachea. Development 126: 4455–4463.

45. Guo M, Jan LY, Jan YN (1996) Control of daughter cell fates during asymmetric division: interaction of Numb and Notch. Neuron 17: 27–41.

46. Okabe M, Imai T, Kurusu M, Hiromi Y, Okano H (2001) Translational repression determines a neuronal potential in Drosophila asymmetric cell division. Nature 411: 94–98. doi:10.1038/35075094.

47. Ward EJ, Zhou X, Riddiford LM, Berg CA, Ruohola-Baker H (2006) Border of Notch activity establishes a boundary between the two dorsal appendage tube cell types. Dev Biol 297: 461–470. doi:10.1016/j.ydbio.2006.05.021.

48. Sun J, Smith L, Armento A, Deng W-M (2008) Regulation of the endocycle/gene amplification switch by Notch and ecdysone signaling. J Cell Biol 182: 885–896. doi:10.1083/jcb.200802084.

49. Mourikis P, Lake RJ, Firnhaber CB, DeDecker BS (2010) Modifiers of notch transcriptional activity identified by genome-wide RNAi. BMC Dev Biol 10: 107. doi:10.1186/1471-213X-10-107.

50. Brand AH, Perrimon N (1993) Targeted gene expression as a means of altering cell fates and generating dominant phenotypes. Development 118: 401–415.

51. Cabernard C, Affolter M (2005) Distinct roles for two receptor tyrosine kinases in epithelial branching morphogenesis in Drosophila. Dev Cell 9: 831–842. doi:10.1016/j.devcel.2005.10.008.

52. Cela C, Llimargas M (2006) Egfr is essential for maintaining epithelial integrity during tracheal remodelling in Drosophila. Development 133: 3115–3125. doi:10.1242/dev.02482.

53. Gentleman RC, Carey VJ, Bates DM, Bolstad B, Dettling M, et al. (2004) Bioconductor: open software development for computational biology and bioinformatics. Genome Biol 5: R80. doi:10.1186/gb-2004-5-10-r80.

54. Wang P, Ding F, Chiang H, Thompson RC, Watson SJ, et al. (2002) ProbeMatchDB–a web database for finding equivalent probes across microarray platforms and species. Bioinformatics 18: 488–489.

55. Barrett T, Troup DB, Wilhite SE, Ledoux P, Evangelista C, et al. (2011) NCBI GEO: archive for functional genomics data sets–10 years on. Nucleic Acids Res 39: D1005–1010. doi:10.1093/nar/gkq1184.

56. Stark C, Breitkreutz B-J, Chatr-Aryamontri A, Boucher L, Oughtred R, et al. (2011) The BioGRID Interaction Database: 2011 update. Nucleic Acids Res 39: D698–704. doi:10.1093/nar/gkq1116.

57. Lyne R, Smith R, Rutherford K, Wakeling M, Varley A, et al. (2007) FlyMine: an integrated database for Drosophila and Anopheles genomics. Genome Biol 8: R129. doi:10.1186/gb-2007-8-7-r129.